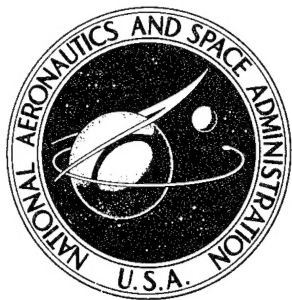
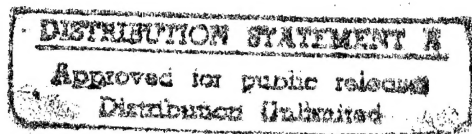


NASA CONTRACTOR
REPORT

NASA CR-1856



NASA CR-1856



19960607 116

THE KINETICS OF CRYSTALLIZATION
OF MOLTEN BINARY AND TERNARY
OXIDE SYSTEMS AND THEIR APPLICATION
TO THE ORIGINATION OF
HIGH MODULUS GLASS FIBERS

by J. F. Bacon

Prepared by
UNITED AIRCRAFT CORPORATION
East Hartford, Conn. 06108
for

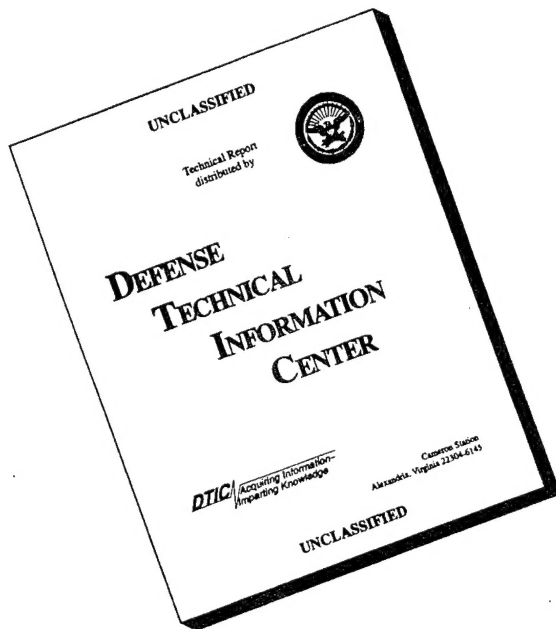
DTIC QUALITY INSPECTED 3

NATIONAL AERONAUTICS AND SPACE ADMINISTRATION • WASHINGTON, D. C. • NOVEMBER 1971

58H9105

1. Report No. NASA CR-1856	2. Government Accession No.	3. Recipient's Catalog No.	
4. Title and Subtitle THE KINETICS OF CRYSTALLIZATION OF MOLTEN BINARY AND TERNARY OXIDE SYSTEMS AND THEIR APPLICATION TO THE ORIGINATION OF HIGH MODULUS GLASS FIBERS		5. Report Date November 1971	
7. Author(s) J. F. Bacon		6. Performing Organization Code	
9. Performing Organization Name and Address United Aircraft Corporation Research Laboratories East Hartford, Connecticut 06108		8. Performing Organization Report No. K910939-4	
12. Sponsoring Agency Name and Address National Aeronautics and Space Administration Washington, D. C. 20546		10. Work Unit No.	
		11. Contract or Grant No. NASW-1301 and NASW-2013	
		13. Type of Report and Period Covered Contractor Report	
		14. Sponsoring Agency Code	
15. Supplementary Notes			
16. Abstract Emphasis on the consideration of glass formation as a kinetic process made it possible to think of glass compositions different from those normally employed in the manufacture of glass fibers. Approximately 450 new glass compositions were prepared and three dozen of these compositions have values for Young's modulus measured on bulk specimens greater than nineteen million pounds per square inch. Of the new glasses about a hundred could be drawn into fibers by mechanical methods at high speeds. The fiber with which we have the most experience has a Young's modulus measured on the fiber of 18.6 million pounds per square inch and has been prepared in quantity as a monofilament (to date more than 150 million lineal feet of 0.2 to 0.4 mil fiber have been produced). This fiber has also been successfully incorporated both in epoxy and polyimide matrices. The epoxy resin composite has shown a modulus forty percent better than that achievable using the most common grade of competitive glass fiber, and twenty percent better than that obtainable with the best available grade of competitive glass fiber. Other glass fibers of even higher modulus have been developed but we have very little experience with these as yet. The method of producing modulus from glass composition due to C. J. Phillips has been extended.			
17. Key Words (Suggested by Author(s)) Glass, Composition, Kinetics of Crystallization, Viscosity, Modulus, Strength, Fiberizing Characteristics		18. Distribution Statement Unclassified - Unlimited	
19. Security Classif. (of this report) Unclassified	20. Security Classif. (of this page) Unclassified	21. No. of Pages 310	22. Price* \$6.00

DISCLAIMER NOTICE



THIS DOCUMENT IS BEST
QUALITY AVAILABLE. THE
COPY FURNISHED TO DTIC
CONTAINED A SIGNIFICANT
NUMBER OF PAGES WHICH DO
NOT REPRODUCE LEGIBLY.

FOREWORD

This document constitutes the final report for the work under Contract numbers NASW-1301 and NASW-2013. The NASA contract monitor for this program was James J. Gangler of NASA/OART Washington Headquarters.

James F. Bacon was program manager. Other UARL personnel participated as follows. Dr. Robert B. Graf carried out the crystal growth measurements and research mentioned in the earlier section of this report. Dr. George Layden initiated the strength investigations and was responsible for most of the strength instrumentation and data mentioned in this report. Drs. Daniel Scola, Roscoe Pike, and Mr. Richard Novak have prepared and evaluated the composites of UARL glass fiber with the resins described in the report.

Mr. Kenneth Fowler of Panametrics, Inc., a division of Esterline Corporation, carried out the dynamic modulus fiber measurements and Panametrics furnished us permission to use Figs. 63, 64, and 65. Dr. David H. Pfister, Technical Director, Testing Division, Lowell Institute of Technology, carried out the many static fiber modulus measurements. Messrs. A. W. LaDue and Leo E. Stadler of the Hartford Division of the Emhart Corporation made many other physical property measurements.

SUMMARY

The research contracts on the kinetics of crystallization of molten binary and ternary oxide systems have concentrated on those systems likely to form complex three-dimensional crystal structures and which, in addition, have higher than usual values of elastic moduli. Ten such systems studied include cordierite-beryl-rare earth oxide systems, cordierite systems with calcia substituted for magnesia, cordierites in which calcia is substituted for alumina, fluoborate optical glass systems, Morey's glasses from acid forming elements, calcia-alumina glasses of the type pioneered by the National Bureau of Standards and further developed by the Bausch and Lomb Optical Company, calcia-yttria glasses, calcia-alumina-silicate glasses, "invert" analog glass systems, and two-phase systems with controllable microstructure. A total of 466 glasses were formed from these ten systems.

The glasses melted were characterized as fully as possible. For this purpose density of the glass, viscosity, in some cases its electrical conductivity, fiberizability, Young's modulus, strength, estimated liquidus and working range, and its rate of nucleation and of crystal growth as determined optically were all employed at one time or another. To make such characterization studies possible a microfurnace was designed to permit microscopic observations of crystals growing in molten oxides; an enlarged platform furnace usable in air at temperatures up to 1800°C was constructed which, when used in conjunction with a 20 cm³ platinum crucible with properly shaped nozzle, made possible the production of mechanically drawn glass fibers; equipment for continuously monitoring the electrical conductivity of molten oxide systems was devised and used to study the crystallization kinetics of molten oxide systems, a sonic apparatus for measuring Young's modulus of bulk samples was developed, and a tester and test system for the evaluation of the strength of pristine glass fibers was developed. Since the measured value of Young's modulus proved to be very nearly independent of forming conditions, processing variables and small inclusions such moduli measurements were used as the principal method of evaluating new glass compositions. Such measurements were greatly expedited and markedly lowered in cost by establishing a procedure in which samples suitable for modulus measurements could be easily formed by drawing the molten oxide mixture into fused silica tubes using a hypodermic syringe to supply controlled suction.

Characterization studies of these types yielded an unexpected dividend when it was discovered that rare-earth oxides markedly decreased the rate of crystallization of molten oxide systems belonging to the alumina-magnesia-silica field and made the largest contribution per mol percent to Young's modulus of any of the types of oxides studied. The work on the cordierite-rare earth oxide-beryl systems was further simplified when it was found possible to calculate Young's modulus for such systems from a knowledge of their composition in mol percent by the methods of C. J. Phillips (Ref. 1) and the additional experimental data of UARL. Characterization procedures also furnished the directions in which to make compositional modifications to produce glasses of improved workability, higher specific modulus, and higher absolute modulus.

Kinetics research, composition exploration, and characterization procedures indicated three systems of molten oxides that seemed most promising. Invert analog glass systems gave compositions with values for Young's modulus of 22.75, 22.00, 21.6, and 20.9 million psi for bulk samples and with specific moduli as high as 197 to 200 million inches. Cordierite-rare earth oxide-beryllia system compositions were found with values for Young's modulus of 21.1, 20.9, 20.6, and 20.3 million psi and specific moduli of 184 to 197 million inches for bulk samples. A promising new direction resulted when the barest of research efforts on two phase systems resulted in a system whose modulus could be changed from ten million psi to fifteen million psi by heat treatment while the fiber was being drawn at moderate speeds.

Of the four hundred and sixty-six glass compositions investigated, about one hundred could be drawn into glass fibers using mechanical drawing apparatus. One of the more outstanding high modulus beryllia containing glasses developed at UARL is the glass composition UARL 344. Intensive investigation of this composition showed that it could be readily fiberized and fibers can be continuously drawn at high rates of speed and restarted at will. Over 100,000,000 feet of these fibers have been drawn through an orifice of 0.038 in. diameter at orifice temperatures from 1260°C to 1310°C, with heads of molten glass from 3/8 in. to 1 1/2 in., and at winding speeds of 4000 to 8000 ft/min (the top speed on our winder). The glass fibers processed under these conditions show excellent properties. Diameters vary from 0.2 to 0.4 mils with a Young's modulus of 18.6 million psi, a specific modulus of 157 million inches, and strengths which, in twenty-two consecutive measurements, averaged 772,000 psi and ranged from 600,000 to 1,000,000 psi with a few extreme values discarded.

A limited evaluation of the UARL 344 glass fiber in a resin matrix has been very encouraging and indicated a unidirectional longitudinal modulus as high as twelve million psi, shear strengths as high as 16,000 psi and tensile strengths (unsized) of 270,000 psi. UARL scientists calculate for a 70 vol % glass fiber-resin matrix $\pm 45^\circ$ alignment, that the results will be:

<u>Fiber</u>	<u>Density lbs/in³</u>	<u>Modulus million psi</u>	<u>Specific Modulus ten million inches</u>
E	0.0776	3.27	4.21
S	0.0762	4.12	5.41
UARL 344	0.0951	6.08	6.39

In bulk form, the properties of UARL 344 are also excellent. Bulk samples have a Young's modulus of 20.3 million psi and a specific modulus of 168 million inches. The value of 20.3 million psi for this glass is higher than that of any other available glass or glass ceramic.

This research also led to five patent applications and three papers presented at scientific society meetings. Abstracts for all of these are included in this report.

TABLE OF CONTENTS

	<u>Page</u>
INTRODUCTION	1
ORIGINATION OF NEW GLASS COMPOSITIONS	2
Concepts of Mechanisms by Which Some Crystalline Materials Might Become Glass Polymers	2
Low Atomic Number Oxide Components are Primary Though Not the Only Choice	5
Selection of Glass Systems Investigated	6
Systematic Modifications of Glass Systems Investigated	91
CHARACTERIZATION OF THE NEW EXPERIMENTAL GLASSES I	103
Density Measurements	103
Electrical Conductivity Measurements	103
Viscosity Measurements	110
Direct Optical Measurement of Kinetics of Crystallization	134
Role of Lanthana in Kinetics of Crystallization of UARL Cordierite Based Glasses	164
Estimation of Liquidus and Working Range	176
Evaluation of Glass Forming Characteristics and Fiberizability on UARL Experimental Glasses	177
CHARACTERIZATION OF THE EXPERIMENTAL GLASSES II. YOUNG'S MODULUS FOR BULK SPECIMENS	182
Young's Modulus Measured on Bulk Samples of Glass	182
CHARACTERIZATION OF EXPERIMENTAL GLASSES III. YOUNG'S MODULUS FOR GLASS FIBERS	221
The Uselessness of Data Based on Hand-Drawn Fibers	221
Mechanical Drawing of Glass Fibers from An Orifice	221
Young's Modulus Measurements	224
Strength Measurements on Pristine Glass Fibers	236
Preliminary Experiments	236
Fiber Capture	241
Fiber Testing	241
Measurement of Fiber Diameter	246
Experimental Results	246

TABLE OF CONTENTS (Cont'd)

	<u>Page</u>
EVALUATION OF EPOXY RESIN-GLASS FIBER COMPOSITES MADE WITH UARL GLASS FIBERS	261
Preliminary Research on Sizing UARL Glass Fibers, Especially UARL 344	261
Comments on Composite Preparation and Properties	261
Polyimide-Fiber Glass Composites	267
Improvement in Specific Modulus of Epoxy-Glass Fiber Composites as Fiber Modulus Increases	271
Comparative Evaluation of UARL 344 Glass Fiber-Epoxy Resin Impact Specimens	271
PRELIMINARY MANUFACTURING RESEARCH	275
Multihole (6-hole) Bushing Operations	278
CONCLUSIONS	281
REFERENCES	283
ABSTRACTS OF THREE PAPERS PRESENTED DURING THE CONTRACTUAL PERIOD . . .	291
Studies of the Young's Modulus of Magnesia-Alumina-Silica- Rare Earth Glass Systems with Respect to their Composition and Crystallization Kinetics	291
Recent Developments of High Modulus Glass Fibers	292
The Origination and Testing of New High-Modulus Glass Fibers . . .	293
SUMMARY OF PATENT APPLICATIONS	295

LIST OF FIGURES

<u>Fig. No.</u>		<u>Page</u>
1	Structure of Beryl	3
2	Postulated Structure of Glass Formed When Cordierite Rings Open	4
3	Structure in Glass	76
4	Structure in Glass	77
5	Structure in Glass	78
6	Structure in Glass	79
7	Structure in Glass	80
8	Structure in Glass	81
9	Structure in Glass	82
10	Structure in Glass	83
11	Structure in Glass	84
12	Structure in Glass	85
13	Structure in Glass	86
14	Structure in Glass	87
15	Structure in Glass	88
16	Structure in Glass	89
17	Super-Kanthal Hair-Pin Kiln Used for Melting Oxide Mixtures	102
18	Tungsten Crucible Conductivity Cell	107
19	Temperature Tungsten Resistance Furnace	108
20	Log Ohmmeter	109
21	Large Tungsten Spindle Used for High Temperature Viscosity Measurement	112

LIST OF FIGURES (Cont'd)

<u>Fig. No.</u>		<u>Page</u>
22	Brookfield Viscometer and Constant Temperature Bath Used for Calibration	113
23	Calibration Data for Large Tungsten Spindle, Brookfield Viscometer, and Standard Oil "P" from N.B.S.	116
24	Extrapolated Calibration Curve for N.B.S. Viscosity Standard "P"	117
25	Brookfield Viscometer Installed on Tungsten Furnace for High Temperature Viscosity Measurements	119
26	Experimentally Determined Viscosity-Temperature Relations	120
27	Experimentally Determined Viscosity-Temperature Relations	121
28	Experimentally Determined Viscosity-Temperature Relations	122
29	Experimentally Determined Viscosity-Temperature Relations	123
30	Experimentally Determined Viscosity-Temperature Relations	124
31	Experimentally Determined Viscosity-Temperature Relations	125
32	Experimentally Determined Viscosity-Temperature Relations	126
33	Experimentally Determined Viscosity-Temperature Relations	127
34	Experimentally Determined Viscosity-Temperature Relations	128
35	Viscosity-Temperature Curves for Owens-Corning "E" Glass Compared to UARL 344 Glass	135
36	Close-Up of Micro-Furnace with Heat Shields Removed	137
37	Micro-Furnace and Associated Equipment in Position for Use	138
38	Effect of Temperature on the Rate of Growth of Cordierite Crystals	140
39	Sapphirine Crystals in Molten Glass at 1222°C	142
40	Sapphirine Crystals in Glass	143
41	Cordierite Crystals in Glass	145

LIST OF FIGURES (Cont'd)

<u>Fig. No.</u>		<u>Page</u>
42	Cordierite Crystals in Glass	146
43	Effect of Temperature Upon the Rate of Growth of Cordierite in Batch 64	148
44	Effect of Temperature Upon the Rate of Growth of Cordierite in Batch 63	149
45	Viscosity-Temperature Curves for Three Glasses	153
46a	Representative Growth Curves for Cordierite, The Increase of Crystal Length with Time	154
46b	Effect of Temperature Upon the Rate of Growth of Cordierite in Batch 62	155
47	Effect of Temperature Upon the Rate of Growth of Devitrite	159
48	Effect of Temperature Upon the Rate of Growth of Devitrite after Swift	162
49	Effect of Rare-Earth Additives on Temperature-Growth Rate Curve of Cordierite	163
50	Light Photomicrographs Showing the Approximate Locations of Beam Scan Analyses	165
51a	Electron Beam Scan Analysis of Area 1 as Indicated in Fig. 50	167
51b	Electron Beam Scan Analysis of Area 2 as Indicated in Fig. 50	168
52	Schematic Representation of the Paths Scanned by the Electron Beam	169
53a - f	Lanthanum Distribution Scans Across Path Shown Schematically in Fig. 52	170 - 175
54	Sonic Equipment Assembled for Measurement of Young's Modulus	183
55	Improved Apparatus for Measurement of Young's Modulus	185
56	Preparation of Samples for Modulus Measurement	187

LIST OF FIGURES (Cont'd)

<u>Fig. No.</u>		<u>Page</u>
57	Rod Casting Syringe and Examples of Glass Rods	188
58	Cross-Sections of Hand-Drawn Glass Fibers Showing the Least and the Most Departure from Circular Cross-Section Compared to a Platinum Wire	222
59	Platform Kiln in Use for Mechanically Drawing Glass Fibers	223
60	Pronounced Decrease in Size and Improvement in Circularity of Machine Drawn Fibers	225
61	Pronounced Decrease in Size and Improvement in Circularity of Machine Drawn Fibers	226
62	Relationships Existing Between Sound Velocity and Modulus	229
63	Experimental Arrangement for Making Thin-Line Ultrasonic Determinations of Dynamic Elastic Moduli	230
64	Line Construction for Thin-Line Ultrasonic Measurement of Elastic Moduli of Fibrous Materials	232
65	Ultrasonic Pulse-Echo Signals from Single Glass Fiber	233
66	Strength of Glass Fiber	239
67	E-Glass Tear Drops	240
68	Fiber Capture Shears	242
69	Improved Fiber Capture Device	243
70	Tensile Tester Developed at UARL	244
71	Calibration Curve for Tensile Test Apparatus	245
72	Virgin Strength of E-Glass Fibers	250
73	Strength of E-Glass Fibers Taken Off Winding Drum	251
74	Method of Damping Tensile Test Specimen	252
75	Strength of Pristine E Glass Fibers	253

LIST OF FIGURES (Cont'd)

<u>Fig. No.</u>		<u>Page</u>
76	Paper Tab Fiber Mounting System	255
77	Strength of Experimental Glass Fibers	256
78	Typical Inclusions in Fibers	257
79	Crystal Grown in UAC 126 Glass at 1200°C for 20 Minutes	259
80	UARL 344 Fiber Glass-Epoxy Resin Composites	268
81	High Modulus Glass Reinforced Polyimide Composite	270
82	Improvement in the Specific Modulus of Epoxy-50% Glass Fibers Composite as Modulus of Glass Fiber is Increased	272
83	Notched Charpy Impact Sample UARL 344 Fiber Glass-Epoxy Composite	274
84	Evolution of UARL Design for Single-Hole Bushing	276
85	Final Design UARL Platinum-Rhodium Bushing	277
86	UARL Design 6-Hole Platinum-Rhodium Bushing	279
87	6 UARL 344 Glass Fibers are Simultaneously Drawn from Experimental 6-Hole Bushing	280

LIST OF TABLES

<u>Table No.</u>		<u>Page</u>
I	New Experimental Glass Batches Actual Ingredients in Grams	7
II	New Glass Compositions in Weight %	30
III	Experimental Glass Composition in Mol Percent	51
IV	Composition in Mol % of Borate-Series Glasses	94
V	New Compositional Guide for Beryllia Containing Glasses	98
VI	Compositional Guideposts for the Development of Non-toxic (no BeO) Improved High Modulus Glasses	100
VII	Summary of All Density Determinations for Bulk Specimens of UARL Experimental Glasses	104
VIII	Calibration of Large Tungsten Spindle in N.B.S. Standard Oil "P"	114
IX	Extrapolated and Certificate Values of Viscosity for N.B.S. Viscosity Standard Oil. "P"	118
X	Experimental Determination of Viscosity Individual Runs	129
XI	Summary of Experimental Viscosity Determinations	133
XII	Rate of Growth of Cordierite in Batch 1	139
XIII	Rate of Growth of Cordierite in Batch 64	147
XIV	Rate of Growth of Cordierite in Batch 63	150
XV	Comparative Rates of Cordierite Growth In Several Glasses	151
XVI	Growth Data for Cordierite in Batch 62	156
XVII	X-ray Diffraction Data for Devitrites	158
XVIII	Growth Rate Data for Devitrite in Soda-Lime-Aluminosilicate Glass	160
XIX	Liquidus Temperature and Working Characteristics of Several UARL Invert Analog Glasses	178

LIST OF TABLES (Cont'd)

<u>Table No.</u>		<u>Page</u>
XX	Glass Forming Characteristics of Selected Rare-Earth and Cordierite Based Glasses and Two Calcium-Silica Glasses	181
XXI	Comparison of Young's Modulus of As-Cast and Annealed Glass Bars	190
XXII	Comparative Results of Sonic and Transverse Rupture Tests on Bulk Glass Rods	191
XXIII	Reproducibility of Values of Young's Modulus Measured on Rods Aspirated Directly from Melt	192
XXIV	Values of Young's Modulus for Several Cordierite-Rare Earth Glasses	197
XXV	Calculation of Molar Modulus Coefficients by Method of C. J. Phillips-Magnesia Contribution	199
XXVI	The Use of Known Molar Modulus Coefficients to Obtain a Corrected Phillips Coefficient for Beryllia	200
XXVII	Calculation of Young's Modulus from the Composition by C. J. Phillips Method	202
XXVIII	Calculation of Young's Modulus from the Composition by C. J. Phillips Method	203
XXIX	Using Known Molar Modulus Coefficients to Obtain Similar Coefficients for Zinc and Zirconia	204
XXX	Summary of All Experimentally Determined Molar Modulus Coefficients	205
XXXI	Comparison of Calculated and Experimentally Determined Moduli	206
XXXII	Discrepancies Resulting When Young's Modulus for Calcium Aluminate Glasses are Calculated by C. J. Phillips Factors Derived from Silica Glass Systems	207
XXXIII	Use of Phillips Type Calculations to Evaluate Literature Claims on High Modulus Glasses	208
XXXIV	Best Glasses to Date from Cordierite-Rare Earth and Cordierite-Beryl-Rare Earth Systems	211

LIST OF TABLES (Cont'd)

<u>Table No.</u>		<u>Page</u>
XXXV	Summary of All Values for Young's Modulus Measured on Circular Rods Formed Directly from Melt	212
XXXVI	Summary Extended, All Values for Young's Modulus Measured on Square Rods Cut from Plates by Optical Equipment	216
XXXVII	Best Glasses to Date from Invert Analog Systems	218
XXXVIII	Circularity Checks on Mechanically Drawn Glass Fibers	227
XXXIX	Typical Standard Deviations Found in Static Tensile Measurements of Young's Modulus of Glass Fibers	228
XL	Comparative Results on Glass Fibers of One Composition Evaluated by Static and Dynamic Methods	234
XLI	Young's Modulus for the More Promising Mechanically Drawn Glass Fibers	235
XLII	Values of Young's Modulus on Mechanically Drawn Fibers of UARL Experimental Glasses As Determined by Measurements Either on Tensile Test Equipment or Thin-Line Ultrasonics	237
XLIII	Strength Data	247
XLIV	Assessment of Strength of UARL 344 Glass Fiber	260
XLV	Glass Fiber 2256-0820 Epoxy Resin Composites	262
XLVI	UARL 344 Glass Fiber-Epoxy Resin Laminates - Effect of UARL Glass Finish	263
XLVII	UARL 344 Glass Fiber-Epoxy Resin Laminates - Effect of UARL Glass Finish	264
XLVIII	Shear Strength Retention of UARL 344 Glass-Epoxy Resin Composites	265
XLIX	RS-6228 Polyimide/Glass Reinforced Composites	269

INTRODUCTION

In connection with its proposals which resulted in NASA contracts NASW-1301 and NASW-2013, UARL had first pursued the technical literature concerned with high strength, high modulus glass fibers. The extent of this literature representing as it does 75 to 100 man years of research effort is only partially indicated by references 2 through 40. From the thousands of experimental glass compositions investigated, a plateau seemed to have been reached with the development of a glass fiber with an average Young's modulus of 14.64 million psi and an average tensile strength of about 800,000 psi.

The vast extent of the prior art needed to achieve this plateau made it obvious that a further direct brute force assault on the problem of attaining a still higher modulus, higher strength glass fiber could only yield marginal improvements. It was clearly indicated that a better understanding of glass formation was necessary for any hope of success. A consideration of glass formation as a kinetic process guided the preparation by UARL of candidate glasses selected from silicate and nonsilicate compositions that tend to form complex three-dimensional crystal structures such as rings or chains or layers. In turn, this belief in glass formation as a rate controlled process led to the systematic investigation of the rates of crystallization of selected binary and ternary oxides and the effects of oxide additives on these rates of crystallization. The report that follows shows the consequences of this philosophy.

The examination of this literature also showed UARL the necessity of extreme precautions in making meaningful measurements of the properties of glass fibers since in many cases elastic moduli were reported by one laboratory that differed by as much as a factor of 1.6 or more from the moduli reported by other laboratories for almost identical compositions or from moduli calculated by the method of C. J. Phillips (Ref. 1) for that composition. As this report will show, such discrepancies frequently arise from basing moduli measurements on hand-drawn fibers and assuming them to be circular in cross section although any actual microscopic examination of such fibers usually shows them to have a greatly flattened elliptical cross section.

ORIGINATION OF NEW GLASS COMPOSITIONS

All investigators working in the field of glass research quickly become convinced that in spite of the existence of many thousands of oxide systems, the formation of a glass from a molten oxide system is a rare event. But if one will consider the viewpoint of Douglas (Ref. 41), a world renowned glass chemist, that the possibility of glass formation perhaps rests almost entirely with the kinetics of crystallization of molten binary and ternary oxide systems, then perhaps the chance of glass formation may be made a little less rare. This should be especially true if one puts together molten oxides in such proportions that the only crystalline phases likely to form will be many-atom three-dimensional structures. The formation of such complicated crystal structures examined from the point of view of the number of atomic collisions that must take place for their synthesis can only be considered a time-consuming step and one which may possibly be defeated by antinucleating agents and/or rapid cooling.

Concepts of Mechanisms by Which Some Crystalline Materials Might Become Glass Polymers

R. J. Charles writing in the Scientific American (Ref. 42) speaks of "glass-forming materials which when crystallized often take the form of spiral chains in a hexagonal array (selenium, tellurium) or nests of eight-member rings (sulfur). When such ring structures are heated in a melt, the rings tend to open and link up into extended chains. If the melt is quickly cooled, the rings do not have time to re-form and a glass results. Glasses are also readily produced from spiral-chain arrays."

An example of the type of structure which UARL is considering in this report and that may be considered both multi-atom and three-dimensional is beryl, $\text{Be}_3\text{Al}_2\text{Si}_6\text{O}_{18}$, for which a two-dimensional representation due to Wells (Ref. 43) is shown in Fig. 1. This molecule requires that 29 atoms meet in a common location for its formation and its crystal structure possess rings of ions arranged in sheets with their planes parallel and with the metal ions lying between the sheets with their planes parallel and with the metal ions lying between the sheets and binding the rings together (Ref. 43). In all of these structures discrete ions such as $\text{Si}_3\text{O}_9^{6-}$ and $\text{Si}_6\text{O}_{18}^{12-}$ form the basis of the cyclic silicon-oxygen complex when it is allowed to form. Figure 2 represents the postulated structure for a glass possessing a remanent ring silicate structure left from the original cordierite structure when the oxide has first been heated to the melting temperature where the rings can open and rejoin to form long chains and the melt is then cooled so rapidly that this structure is frozen and the material remains glossy.

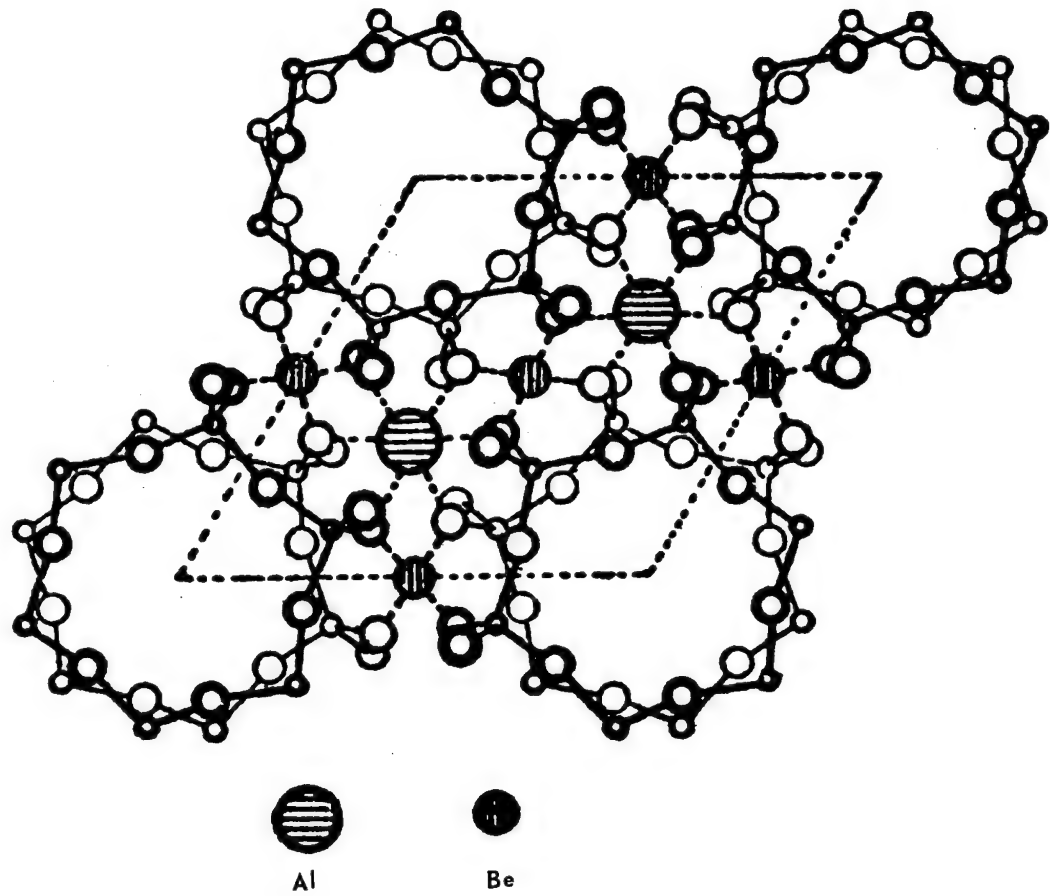


FIGURE 1. STRUCTURE OF BERYL

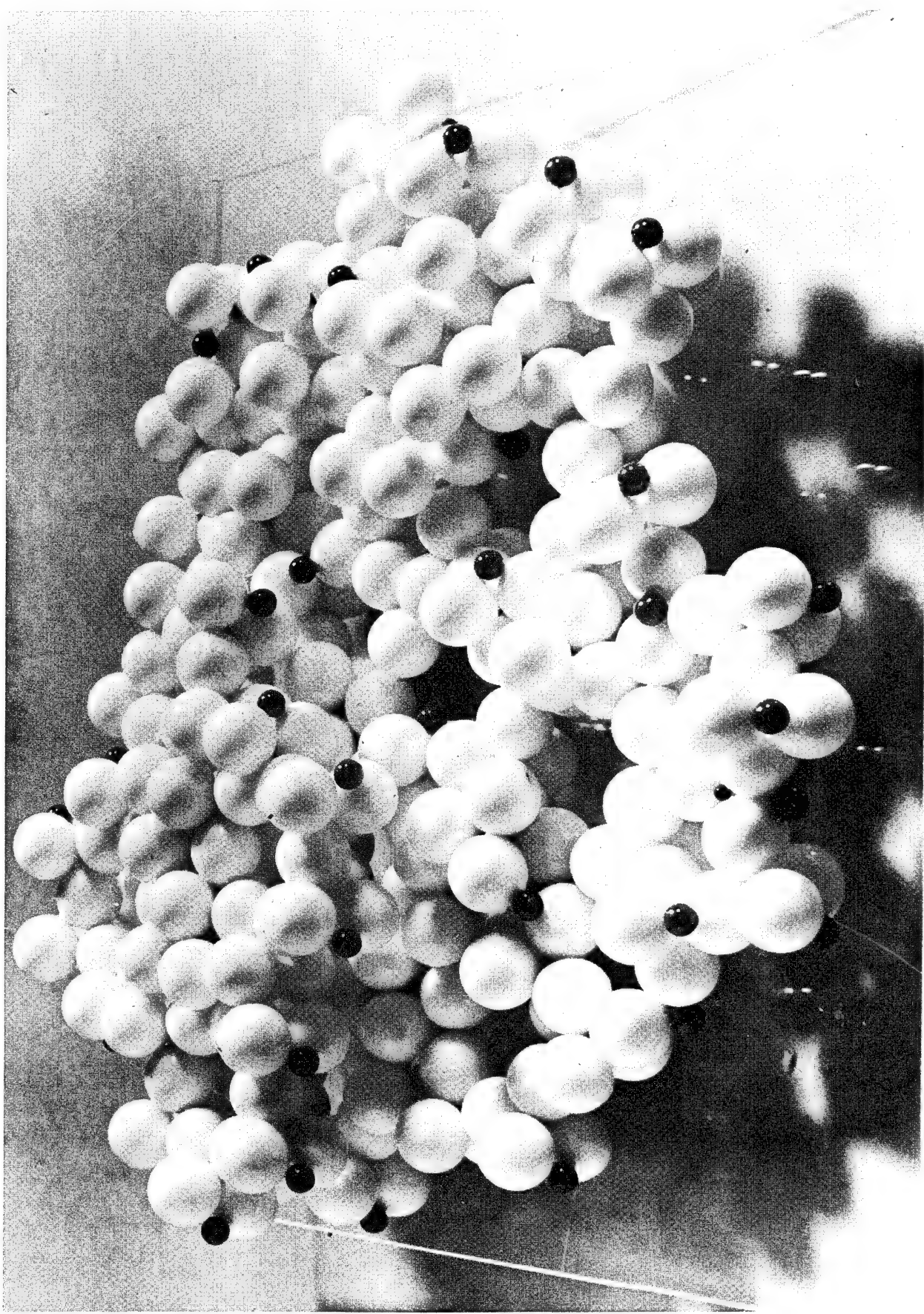


FIGURE 2. POSTULATED STRUCTURE OF GLASS FORMED WHEN CORDIERITE RINGS OPEN

Low Atomic Number Oxide Components are Primary
Though Not the Only Choice

Since the ultimate long-range objective of this program is the attainment of high-modulus, high-strength-to-density continuous vitreous fibers, research will be largely concentrated on complex molecules composed of low atomic number oxides such as those shown in the tabulation below (Ref. 44).

Moduli-Density Values for Several Low Atomic Number Oxides

<u>Oxide</u>	<u>Young's Modulus (10^6 psi)</u>	<u>Density (gms/cm3)</u>	<u>Maximum Strength (5% strain-10^6 psi)</u>	<u>Modulus Density Ratio 10^6 psi/gms/cm3</u>
Al ₂ O ₃	76	4.0	3.8	19
BeO	51	3.0	2.6	17
MgO	35	3.5	1.8	10
SiO ₂	10.5	2.2	0.53	5
MgO Al ₂ O ₃	35	3.6	1.8	10
TiO ₂	41	4.26	2.06	9.6

For this reason, specific molecular systems considered have been silicates (since silica is the best known glass former) such as cordierite, Al₃Mg₂(Si₅Al)₁₈, known to have a ring crystal structure with ions arranged in sheets but not a layer structure (Ref. 43); benitoite, BaTiSi₃O₉, likewise a complex three-dimensional structure (Ref. 43); and beryl, Be₃Al₂Si₆O₁₈, a ring structure like that of cordierite. The low value for silica in contrast to the other oxides indicates that the percentage of silica in such a glass must be held at a minimum if high moduli are to be achieved. The major constituent, silica, which provides the glass structure and the desired viscosity characteristics, can be regarded as a necessary evil and the positive direction for modulus improvement clearly lies in using no more silica than necessary and so leads to the consideration of invert analog glasses as we show in a later section.

Although low atomic number oxides are the most promising ingredients for high modulus glass fibers, they are not the only allowable constituents. In our earlier report (Ref. 45), we showed that based on UARL experimental data and the method of calculation introduced by C. J. Phillips (Ref. 1) contributions per mol % to Young's modulus of several of the heavier elements were high:

<u>Oxide</u>	<u>Contribution to Young's Modulus per mol % (kilobars)</u>
SiO ₂	7.3
Al ₂ O ₃	12.1
CaO	12.6
Li ₂ O	7.0
B ₂ O ₃	7.2

<u>Oxide</u>	<u>Contribution to Young's Modulus per mol % (kilobars)</u>
ZnO	1.72 and rising with increasing R ₂ O
TiO ₂	13.3
BeO	19.0
ZrO ₂	18.9
MgO	12.0 and rising with decreasing R ₂ O & SiO ₂ to 14.8
Ce ₂ O ₃	18.6
Y ₂ O ₃	24.3
La ₂ O ₃	22.4

The judicious use of several of these heavier oxides is obviously to be considered in cases where they improve the viscosity, surface tension, working range and other characteristics contributing to fiberizability.

Selection of Glass Systems Investigated

The compositions of the glass systems investigated are shown in Table I in terms of the number of grams used of each actual ingredient, in Table II in weight percent, and in Table III in mol percent. These glass compositions can be discussed in terms of ten types or glass fields as indicated below.

Cordierite-beryl rare earth systems. - A glass field in which UARL has carried out extensive research is that of the cordierite glass system to which rare earths have been added as major constituents. As discussed in our introductory remarks, cordierite or Mg₂Al₄Si₅O₁₈ is a three-dimensional ring former and as shown in a later section of this report rare earth additions such as lanthana, ceria and yttria actively delay the onset of devitrification in glass systems of the cordierite composition field. At the same time the rare earth oxides greatly increase the values for Young's modulus of the cordierite glasses. These glasses, therefore, contain major amounts of rare-earth oxides and may or may not also contain beryllia. In addition to the rare earths, zirconia has been found to have similar beneficial results and may be substituted for or added in addition to the rare earth oxide constituent.

Tables I, II, and III contain many glasses formed from the cordierite-rare earth constituents. Typical glasses of this type are UARL 125, 304, 337, 323, 344, 345, and 363. Table XXXV shows that UARL 125 with no toxic ingredients has a Young's modulus of 16.1 million psi and a specific modulus of 161 million inches. Corresponding numbers for other nontoxic cordierite-base glasses are UARL 304 with 19.2 and 147; UARL 337, 20.9 and 147; UARL 363 with 19.3 and 150.5. With beryllia added to the cordierite base, UARL 323 shows a Young's modulus of 18.4 million psi and a specific modulus of 184 million inches; UARL has values of 20.3 and 168; UARL gives 21.1 and 174.5. These results together with results for glasses such as UARL 416 through 423 indicate clearly that the cordierite-rare earth oxide with or without beryllia forms a very encouraging approach to the problem of finding a new high modulus high strength glass fiber.

Table I
New Experimental Glass Batches
Actual Ingredients in Grams

<u>Actual Ingredient</u>	<u>1*</u>	<u>2</u>	<u>3</u>	<u>5</u>	<u>8</u>	<u>9</u>
Silica	198.0	---	88.5	88.5	---	50.0
Alumina	120.0	---	---	---	---	---
Magnesium Carbonate (basic)	180.0	---	---	---	---	---
Zirconia	---	75.0	---	---	---	---
Titanium Dioxide	---	200.0	141.5	141.5	50.0	---
Tantalum Oxide	---	225.0	---	---	50.0	50.0
Barium Carbonate	---	---	355.0	355.0	---	---
	<u>10</u>	<u>12</u>	<u>20</u>	<u>22</u>	<u>23</u>	<u>25</u>
Silica	30.0	88.5	---	75.0	---	250.0
Alumina	---	---	---	---	100.0	175.0
Magnesium Carbonate (basic)	---	---	---	---	---	80.0
Zirconia	20.0	---	---	---	---	---
Titanium Dioxide	20.0	141.5	---	50.0	---	---
Tantalum Oxide	30.0	---	146.0	75.0	---	---
Barium Carbonate	---	355.0	---	---	---	---
Lanthanum Oxalate	---	---	427.0	---	---	---
Thoria	---	---	83.5	---	---	---
Fused Boric Acid	---	---	83.0	---	---	---
Zirconium Carbonate	---	---	---	61.5	123.0	---
Beryllium Carbonate	---	---	---	---	---	80.0
	<u>26</u>	<u>27</u>	<u>28</u>	<u>29</u>	<u>30</u>	<u>31</u>
Silica	360.5	310.0	138.0	177.5	360.5	310.0
Alumina	4.3	4.0	142.0	145.5	4.3	4.0
Zirconium Carbonate	58.0	117.8	75.2	77.4	58.0	117.8
Beryllium Carbonate	---	---	---	75.9	---	---
Sodium Carbonate	144.4	119.7	---	---	144.4	119.7
Rutile	1.0	---	---	---	1.0	---
Calcium Carbonate	---	4.36	68.7	47.3	---	4.36
Potassium Carbonate	---	14.6	---	---	---	14.6
Cerium Oxide	---	---	51.0	47.5	---	---
	---	---	72.0	---	---	---

* Also batches 4, 6, 7, 11, 13, 14, 15, 16, 17, 18, 19, 21, 24

Table I (Cont'd)

<u>Actual Ingredient</u>	<u>32</u>	<u>33</u>	<u>34</u>	<u>35</u>	<u>36</u>	<u>37</u>
Silica	---	---	---	---	149.0	149.0
Alumina	---	---	---	---	90.0	90.0
Magnesium Carbonate (basic)	---	---	---	---	135.0	135.0
Zirconia	---	50.0	---	25.0	---	---
Lanthanum Oxalate	---	409.0	---	217.0	---	---
Zirconium Carbonate	---	---	---	---	---	75.0
Beryllium Carbonate	---	---	---	---	135.0	---
Boric Anhydride	260.0	120.0	---	---	---	---
Calcium Fluoride	240.0	30.0	180.0	20.0	---	---
Boric Acid (H_3BO_3)	---	---	346.5	142.0	---	---
	<u>38</u>	<u>39</u>	<u>40</u>	<u>41</u>	<u>42</u>	<u>43</u>
Silica	149.0	149.0	149.0	176.0	176.0	176.0
Alumina	90.0	90.0	90.0	---	---	---
Magnesium Carbonate (basic)	135.0	135.0	135.0	---	---	---
Barium Carbonate	---	---	---	57.2	31.2	57.2
Calcium Carbonate	---	---	---	78.5	42.82	78.5
Potassium Carbonate	---	---	---	75.4	34.99	75.5
Lithium Carbonate	123.5	---	---	---	---	---
Zinc Oxide	---	37.5	---	---	---	---
Cerium Oxalate	---	---	135.0	---	---	---
Lead Carbonate	---	---	---	57.6	57.6	57.6
Titanium Nitrate	---	---	---	---	92.0	18.4
Strontium Carbonate	---	---	---	62.7	34.2	62.7
	<u>44</u>	<u>44A</u>	<u>45</u>	<u>46</u>	<u>46B</u>	<u>47</u>
Silica	176.0	176.0	200.0	325.0	267.0	300.0
Barium Carbonate	57.2	57.2	65.0	45.5	95.25	48.5
Calcium Carbonate	78.5	78.5	89.20	62.4	47.75	66.9
Potassium Carbonate	75.5	75.5	85.75	60.0	77.2	64.3
Strontium Carbonate	62.7	62.7	71.25	49.8	70.50	53.4
Rutile	48.0	24.0	---	35.0	---	50.0
Titanium Dioxide	---	24.0	---	---	38.15	---

Table I (Cont'd)

<u>Actual Ingredient</u>	<u>47B</u>	<u>48</u>	<u>48B</u>	<u>49</u>	<u>49B</u>	<u>50</u>
Silica	241.75	250.0	190.75	240.0	183.5	225.0
Barium Carbonate	100.3	65.0	126.3	63.3	124.2	71.5
Calcium Carbonate	50.3	88.8	63.3	87.0	61.3	98.2
Potassium Carbonate	80.2	85.8	83.4	83.5	99.1	94.2
Strontium Carbonate	74.2	71.25	93.6	69.4	90.5	78.4
Rutile	---	50.0	---	65.0	---	---
Titanium Dioxide	53.5	---	50.65	---	65.25	55.0
	<u>50B</u>	<u>51</u>	<u>51B</u>	<u>52</u>	<u>52B</u>	<u>53</u>
Silica	168.0	190.0	139.75	190.0	130.0	175.0
Barium Carbonate	136.2	67.2	126.3	67.2	143.5	84.5
Calcium Carbonate	68.2	92.2	63.3	92.2	71.3	115.8
Potassium Carbonate	110.3	88.5	102.5	88.5	116.3	111.4
Strontium Carbonate	100.7	73.6	93.7	73.6	106.3	92.6
Rutile	---	103.3	---	103.3	---	65.0
Titanium Dioxide	54.55	---	103.30	---	76.75	---
	<u>53B</u>	<u>54</u>	<u>54A</u>	<u>54B</u>	<u>55</u>	<u>55A</u>
Silica	125.65	170.0	175.0	123.2	170.0	175.0
Barium Carbonate	149.0	71.5	71.5	132.2	71.5	71.5
Calcium Carbonate	77.75	98.2	98.2	66.6	98.2	98.2
Potassium Carbonate	125.3	94.3	94.3	107.2	94.3	94.3
Strontium Carbonate	114.6	78.4	78.4	97.7	78.4	78.4
Rutile	---	110.0	---	---	---	---
Titanium Dioxide	62.0	---	105.0	105.9	---	---
Zirconia	---	---	---	---	110.0	117.81

Table I (Cont'd)

	<u>55B</u>	<u>56</u>	<u>57</u>	<u>58</u>	<u>59</u>	<u>60</u>
Silica	110.8	382.5	---	---	---	12.5
Barium Carbonate	118.5	---	---	---	---	10.0
Calcium Carbonate	59.4	---	---	15.15	---	---
Potassium Carbonate	96.4	---	---	---	---	25.0
Strontium Carbonate	87.8	---	---	---	---	15.0
Titanium Dioxide	---	---	---	---	---	---
Zirconia	165.0	---	---	---	---	2.5
Lithium Carbonate	---	185.5	---	---	---	---
Phosphorus Pentoxide	---	5.0	---	---	---	---
Zinc Carbonate	---	57.75	---	---	---	---
Alumina	---	---	276.5	491.5	---	17.5
Zirconium Carbonate	---	---	250.5	---	---	---
Lanthanum Oxalate	---	---	---	407.0	434.0	---
Tantalum Oxide	---	---	---	146.0	55.0	---
Thorium Dioxide	---	---	---	83.5	30.0	---
Boric Acid	---	---	---	147.5	195.5	---
Tungsten Oxide	---	---	---	---	---	11.7
Zirconium Dioxide	---	---	---	---	---	50.0
	<u>61</u>	<u>62</u>	<u>63</u>	<u>64</u>	<u>65</u>	<u>66</u>
Silica	---	258.0	258.0	258.0	258.0	258.0
Alumina	15.0	125.0	125.0	125.0	125.0	125.0
Zirconium Carbonate	---	---	---	---	---	28.0
Lanthanum Oxalate	293.0	---	54.0	---	---	---
Tantalum Oxide	80.0	---	---	---	---	---
Thorium Dioxide	80.0	---	---	---	---	---
Boric Acid	212.0	---	---	---	---	---
Tungsten Oxide	10.0	---	---	---	---	---
Zirconium Dioxide	60.0	---	---	---	---	---
Magnesium Carbonate (basic)	---	192.0	192.0	192.0	192.0	192.0
Cerium Oxalate	---	54.0	---	---	---	---
Yttrium Oxalate	---	---	---	67.0	---	---
Samarium Oxalate	---	---	---	---	53.5	---
	<u>67</u>	<u>68</u>	<u>69</u>	<u>70</u>	<u>71</u>	<u>72</u>
Silica	258.0	258.0	283.0	258.0	250.0	250.0
Alumina	125.0	150.0	125.0	100.0	125.0	112.5
Magnesium Carbonate (basic)	192.0	192.0	192.0	192.0	261.5	157.0
Tantalum Oxide	25.0	---	---	---	---	---
Yttrium Oxalate	---	---	---	134.0	---	---
Cerium Oxalate	---	---	---	---	---	135.0

Table I (Cont'd)

<u>Actual Ingredient</u>	<u>73</u>	<u>74</u>	<u>75</u>	<u>76</u>	<u>77</u>	<u>78</u>
Silica	250.0	258.0	310.0	310.0	310.0	460.0
Alumina	62.5	75.0	---	---	---	---
Magnesium Carbonate (basic)	157.0	192.0	---	---	---	---
Yttrium Oxalate	134.0	191.0	---	---	---	---
Cerium Oxalate	135.0	---	---	---	---	---
Sodium Carbonate	---	---	153.9	111.11	68.4	---
Calcium Carbonate	---	---	178.4	223.0	267.6	---
Titanium Oxalate	---	---	---	---	---	80.0
	<u>79</u>	<u>80</u>	<u>81</u>	<u>82</u>	<u>83</u>	<u>84</u>
Silica	155.0	20.4	160.0	235.0	255.0	---
Alumina	---	---	---	180.0	---	210
Magnesium Carbonate (basic)	---	31.4	10.45	109.83	104.14	---
Yttrium Oxalate	120.5	315.6	201.0	---	---	---
Cerium Oxalate	---	---	---	---	32.25	---
Sodium Carbonate	---	---	17.1	4.28	---	---
Calcium Carbonate	428.0	261.6	321.0	---	115.96	349
Boric Acid	106.5	---	---	---	---	---
Ferric Oxide	---	---	35.0	---	---	---
Zirconium Carbonate	---	---	---	22.44	11.22	28
Beryllium Carbonate	---	---	---	---	121.0	---
Titania (not Rutile)	---	---	---	---	40.0	---
Lithium Carbonate	---	---	---	---	37.1	---
Barium Carbonate	---	---	---	---	---	65
Magnesium Oxide	---	---	---	---	---	25
	<u>85</u>	<u>86</u>	<u>87</u>	<u>88</u>	<u>89</u>	<u>90</u>
Calcium Carbonate	384	384	349	384	384	250
Alumina	235	235	---	---	---	---
Barium Carbonate	---	---	65	---	---	---
Magnesium Oxide	25	25	25	25	25	100
Zirconium Carbonate	---	28	28	---	28	28
Tantalum Oxide	25	---	---	25	---	---
Yttrium Oxalate	---	---	562	625	625	625

Table I (Cont'd)

<u>Actual Ingredient</u>	<u>91</u>	<u>92</u>	<u>93</u>	<u>94</u>	<u>95</u>	<u>96</u>
Calcium Carbonate	178	89.5	250	268	295	295
Alumina	---	---	210	---	---	185
Barium Carbonate	---	---	65	65	---	---
Magnesium Oxide	140	190	25	25	25	25
Zirconium Carbonate	28	28	28	28	28	28
Yttrium Oxalate	625	625	---	562	562	---
Silica	---	---	50	40	50	50
	<u>97</u>	<u>98</u>	<u>99</u>	<u>100</u>	<u>101</u>	<u>102</u>
Silica (SiO_2)	261.5	209.5	158.8	120.5	120.5	221.0
Alumina (Al_2O_3)	47.80	58.1	67.4	76.0	122.7	92.0
Potassium Carbonate	75.5	92.4	107.5	120.7	102.5	---
Lithium Carbonate	---	---	---	---	---	66.7
Calcium Carbonate	47.1	57.1	66.3	74.5	63.0	90.3
Strontium Carbonate	69.2	77.1	97.6	110.0	93.0	---
Zinc Carbonate	---	---	---	---	---	113.6
Barium Carbonate	93.7	113.7	134.3	148.7	125.5	---
Magnesia (MgO)	---	---	---	---	---	36.25
	<u>103</u>	<u>104</u>	<u>105</u>	<u>106</u>	<u>107</u>	<u>108</u>
Silica (SiO_2)	213.5	191.5	181.0	136.0	229.5	281.5
Alumina (Al_2O_3)	88.0	79.5	---	---	---	---
Yttrium Oxalate	---	---	442.0	509.0	378.0	305.0
Potassium Carbonate	---	126.0	---	---	---	---
Lithium Carbonate	64.3	---	54.4	62.0	46.1	37.1
Calcium Carbonate	86.7	77.7	73.7	84.5	62.5	50.4
Strontium Carbonate	127.5	115.5	---	---	---	---
Zinc Carbonate	---	---	92.1	105.4	78.4	63.1
Magnesia (MgO)	34.85	31.35	29.6	33.9	25.15	20.3
	<u>109</u>	<u>110</u>	<u>111</u>	<u>112</u>	<u>113</u>	<u>114</u>
Silica (SiO_2)	116.5	256	224	224	167.75	187.0
Alumina (Al_2O_3)	---	175	221.2	221.2	123.0	138.0
Yttrium Oxalate	703.0	---	---	---	---	360.5
Lithium Carbonate	43.5	---	---	---	---	---
Calcium Carbonate	60.9	---	---	---	---	---
Zinc Carbonate	76.4	---	---	53.40	34.25	38.4
Magnesia (MgO)	24.55	---	---	---	---	---
Basic Magnesia Carbonate	---	137.2	130.3	---	379	---
Cerium Oxalate	---	---	---	---	---	---

Table I (Cont'd)

<u>Actual Ingredient</u>	<u>115</u>	<u>116</u>	<u>117</u>	<u>118</u>	<u>119</u>	<u>120</u>
Silica (SiO_2)	138.0	136.5	149.0	113.5	165.5	146.5
Alumina (Al_2O_3)	140	138.5	48.75	---	54.25	---
Magnesia (MgO)	40.75	40.35	35.45	27	39.40	34.85
Cerium Oxalate	389.5	---	677	773	---	---
Yttrium Oxalate	---	492	---	---	644	853
	<u>121</u>	<u>122</u>	<u>123</u>	<u>124</u>	<u>125</u>	<u>126</u>
Silica (SiO_2)	104.1	69.8	101.0	104.5	178.5	165.5
Alumina (Al_2O_3)	96.0	83.75	92.5	95.75	181.5	127.5
Magnesia (MgO)	26.6	23.0	25.75	26.70	52.75	30.95
Cerium Oxalate	588	774	---	---	---	---
Yttrium Oxalate	---	---	---	---	---	460
Samarium Oxalate	---	---	602	---	---	---
Zirconium Carbonate	---	---	---	---	98.1	---
Lanthanum Oxalate	---	---	---	592	---	---
	<u>127</u>	<u>128</u>	<u>129</u>	<u>130</u>	<u>131</u>	<u>132</u>
Silica	230	275	193	225	270.5	185.0
Alumina	64.5	44.5	87.8	63.1	43.6	83.6
Magnesia (MgO)	51.0	35.0	74.1	---	---	---
Calcium Carbonate	---	---	---	128.3	74.1	164.0
Yttrium Oxalate	384.0	393.0	382	375	388	372.0
	<u>133</u>	<u>134</u>	<u>135</u>	<u>136</u>	<u>137</u>	<u>138</u>
Silica	229.5	244.5	258.0	242.5	223.0	173.15
Alumina	64.8	69.0	125.5	119.75	108.35	96.75
Magnesia (MgO)	25.65	---	92.0	88.1	79.85	71.15
Calcium Carbonate	62.8	---	---	---	---	---
Yttrium Oxalate	384	409.0	---	---	---	---
Beryllium Carbonate	---	74.5	---	---	---	---
Lanthanum Oxalate	---	---	55.7	106.9	192.3	346.0

Table I (Cont'd)

<u>Actual Ingredient</u>	<u>139</u>	<u>140</u>	<u>141</u>	<u>142</u>	<u>143</u>	<u>144</u>
Silica	114.15	167.25	107.75	153.5	111.5	33.6
Alumina	76.75	83.6	72.25	87.35	109.5	165.0
Magnesia (MgO)	56.55	66.35	49.25	18.25	24.1	---
Calcium Carbonate	---	---	---	144.5	179.5	279
Yttrium Oxalate	---	---	---	361	360	337
Lanthanum Oxalate	547	332	514	---	---	---
Cerium Oxalate	---	41.6	64.3	42.1	42.2	39.4
	<u>145</u>	<u>146</u>	<u>147</u>	<u>148</u>	<u>149</u>	<u>150</u>
Yttrium Oxalate	404	390	---	---	---	---
Lanthanum Oxalate	---	---	417	402	---	---
Cerium Oxalate	47.8	45.6	41.7	40.2	40.7	39.5
Samarium Oxalate	---	---	---	---	431.0	418
Silica	160.5	155	142.0	130.3	139.0	134.5
Calcium Carbonate	71.2	106.7	112.5	94.2	115.3	98.0
Magnesia (MgO)	51.1	42.85	45.2	37.95	35.4	37.15
Zirconium Carbonate	9.22	8.94	8.15	7.93	---	---
Titania (not Rutile)	26.3	25.75	23.6	22.8	23.0	22.35
Lithium Carbonate	24.7	21.2	21.8	21.04	21.2	20.62
Alumina	---	32.9	---	24.1	---	23.45
	<u>151</u>	<u>152</u>	<u>153</u>	<u>154</u>	<u>155</u>	<u>156</u>
Silica	216.5	193.5	194.6	189.0	179.0	248.5
Alumina	45.2	40.6	40.6	39.9	43.4	103.3
Magnesia	107.3	95.9	96.3	93.6	88.85	123.2
Yttrium Oxalate	351.5	---	---	---	---	---
Lanthanum Oxalate	---	368.0	---	---	---	---
Cerium Oxalate	---	---	364.0	---	---	---
Samarium Oxalate	---	---	---	380.0	---	---
Tantalum Oxide	---	---	---	---	188.0	---
Chromium Oxide	---	---	---	---	---	25.45
	<u>157</u>	<u>158</u>	<u>159</u>	<u>160</u>	<u>161</u>	<u>162</u>
Silica	239.0	195.0	244.0	219.0	219.0	193.5
Alumina	57.75	27.45	47.75	42.75	42.75	40.6
Magnesia	118.4	96.75	80.0	71.85	71.85	95.9
Rare Earth Oxalate 381	---	---	---	---	368.0	368.0
Yttrium Oxalate	---	198.5	343.0	---	---	---
Lanthanum Oxalate	---	232.0	---	358.5	---	---
Vanadium Oxide	85.0	---	---	---	---	---

Table I (Cont'd)

<u>Actual Ingredient</u>	<u>163</u>	<u>164</u>	<u>165</u>	<u>166</u>	<u>167</u>	<u>168</u>
Silica	193.5	193.5	187.0	208.0	157.5	176.1
Alumina	81.2	---	43.2	157.0	82.3	92.6
Magnesia	95.9	95.9	31.8	49.5	32.35	36.15
Rare Earth Oxalate 381	185.0	600.0	---	---	---	---
Yttrium Oxalate	---	---	396.0	---	---	343.0
Cerium Oxalate	---	---	---	---	359.0	---
Calcium Carbonate	---	---	78.7	---	---	---
Lithium Carbonate	---	---	27.5	---	---	---
TiO ₂ (not Rutile)	---	---	29.6	---	---	---
Vanadium Pentoxide	---	---	---	85.35	60.0	67.0
	<u>169</u>	<u>170</u>	<u>171</u>	<u>172</u>	<u>173</u>	<u>174</u>
Silica	129.7	131.0	158.5	99.25	96.8	155.8
Alumina	100.5	21.6	26.05	64.75	63.2	85.8
Magnesia	38.35	31.3	37.25	25.25	24.7	29.8
Yttrium Oxalate	468.0	---	618.0	---	---	445.0
Cerium Oxalate	---	597.0	---	452.0	---	---
Vanadium Pentoxide	56.6	38.5	46.4	46.85	45.6	62.2
Samarium Oxalate	---	---	---	---	575.0	---
	<u>175</u>	<u>176</u>	<u>177</u>	<u>178</u>	<u>179</u>	<u>180</u>
Silica	223.5	215.5	109.5	158.9	104.0	103.4
Alumina	31.3	23.6	47.3	57.0	45.0	56.45
Magnesia	49.6	34.0	54.1	62.9	47.8	22.35
Calcium Carbonate	---	---	---	---	---	166.2
Yttrium Oxalate	371.0	382.0	---	---	---	334.2
Cerium Oxalate	---	---	---	39.4	62.2	38.9
Vanadium Pentoxide	55.9	34.5	46.95	56.5	44.6	80.6
Lanthanum Oxalate	---	---	525.0	317.0	498.0	---

Table I (Cont'd)

	<u>181</u>	<u>182</u>	<u>183</u>	<u>184</u>	<u>185</u>	<u>186</u>
Silica	31.1	148.0	145.8	128.0	130.0	128.7
Alumina	105.5	---	30.9	---	27.6	---
Magnesia	---	47.2	40.3	42.1	36.0	41.3
Calcium Carbonate	259.5	86.2	54.6	77.2	48.8	81.1
Yttrium Oxalate	314.0	372.0	367.0	---	---	---
Lithium Carbonate	---	22.7	22.3	20.3	20.0	19.8
Cerium Oxalate	36.65	43.5	42.8	38.8	38.7	37.9
Vanadium Pentoxide	84.9	56.0	55.2	50.0	49.2	48.9
Samarium Oxalate	---	---	---	---	---	401.0
Lanthanum Oxalate	---	---	---	389.0	382.0	---
Zirconium Carbonate	---	8.45	8.39	7.55	7.37	---
Titania	---	24.6	24.3	21.9	21.6	21.5
	<u>187</u>	<u>188</u>	<u>189</u>	<u>190</u>	<u>191</u>	<u>192</u>
Silica	125.9	193.5	174.3	170.7	174.4	174.3
Alumina	26.7	40.4	36.5	35.9	36.6	36.5
Magnesia	34.8	79.7	72.1	70.7	72.2	72.2
Calcium Carbonate	65.4	---	---	---	---	---
Yttrium Oxalate	---	313.0	---	---	---	---
Cerium Oxalate	37.1	---	332.0	---	---	---
Samarium Oxalate	391.0	---	---	343.0	---	---
Lanthanum Oxalate	---	---	---	---	330.0	---
Vanadium Pentoxide	47.6	70.75	64.0	62.8	64.0	64.0
Titania	21.0	---	---	---	---	---
Lithium Carbonate	19.25	---	---	---	---	---
Rare Earth Oxalate	---	---	---	---	---	331.0
	<u>193</u>	<u>194</u>	<u>195</u>	<u>196</u>	<u>197</u>	<u>198</u>
Silica	173.0	---	---	---	---	---
Alumina	36.8	---	---	---	---	---
Magnesia	67.0	---	---	---	---	---
Yttrium Oxalate	175.8	---	---	248.5	282.0	374.0
Lanthanum Oxalate	204.7	222.5	268.5	---	---	---
Vanadium Pentoxide	63.5	---	43.9	47.7	54.0	---
Thoria	---	40.0	54.4	59.8	67.0	60.0
Barium Carbonate	---	57.5	75.5	82.0	92.8	77.2
Fused B ₂ O ₃	---	110.0	143.8	156.3	177.0	150.0
Tantalum Pentoxide	---	65.0	76.2	82.7	---	90.0
Zirconium Carbonate	---	---	---	---	28.65	---

Table I (Cont'd)

<u>Actual Ingredient</u>	<u>199</u>	<u>200</u>	<u>201</u>	<u>202</u>	<u>203</u>	<u>204</u>
Silica	---	165.5	165.7	154.7	212.6	201.3
Alumina	---	78.2	78.1	73.0	---	---
Magnesia	---	66.1	66.0	61.7	101.2	97.6
Yttrium Oxalate	414.0	208.0	207.5	---	499.0	478.0
Lanthanum Oxalate	---	243.0	---	226.0	---	---
Cerium Oxalate	---	---	241.5	227.5	---	46.8
Barium Carbonate	89.7	---	---	---	---	---
Thoria	76.8	---	---	---	---	---
Fused B ₂ O ₃	174.0	---	---	---	---	---
Zirconium Carbonate	28.8	---	---	---	---	---
	<u>205</u>	<u>206</u>	<u>207</u>	<u>208</u>	<u>209</u>	<u>210</u>
Silica	176.4	185.0	164.1	193.0	172.5	154.8
Alumina	---	83.9	80.8	87.8	81.9	73.2
Magnesia	83.7	---	68.3	74.1	69.2	61.8
Yttrium Oxalate	---	372.0	502.0	382.0	367.0	---
Lanthanum Oxalate	478.0	---	---	---	---	378.0
Cerium Oxalate	52.9	---	---	---	84.8	75.9
Calcium Carbonate	---	164.2	---	---	---	---
	<u>211</u>	<u>212</u>	<u>213</u>	<u>214</u>	<u>215</u>	<u>216</u>
Silica	381.0	321.0	197.0	323.0	224.0	33.0
Alumina	---	---	13.6	55.0	---	173.0
Magnesia	---	---	---	123.0	22.6	---
Barium Carbonate	154.0	257.0	---	---	35.3	---
Lanthanum Oxalate	---	---	627.0	---	---	---
Calcium Carbonate	---	---	---	---	287.0	515.0
Titania (not Rutile)	---	---	---	---	73.0	---
Zirconium Carbonate	---	---	---	---	46.6	---

Table I (Cont'd)

<u>Actual Ingredient</u>	<u>217</u>	<u>218</u>	<u>219</u>	<u>220</u>	<u>221</u>	<u>222</u>
Silica	---	63.3	32.4	16.8	---	---
Alumina	178.5	156.3	186.0	192.3	201.5	---
Magnesia	---	---	13.0	13.4	14.0	---
Calcium Carbonate	528.0	458.0	376.0	388.0	406.0	---
Barium Carbonate	32.2	31.8	16.7	17.2	18.0	---
Sodium Carbonate	---	---	41.6	42.9	44.8	---
Potassium Carbonate	---	---	14.2	14.6	15.3	---
Lanthanum Oxalate	---	---	14.1	14.5	15.2	361.0
Ferric Oxide	---	---	6.5	6.7	1.75	---
Tantalum Oxide	---	---	---	---	---	111.0
Fused Boric Oxide	---	---	---	---	---	167.0
Thoria	---	---	---	---	---	111.0
	<u>223</u>	<u>224</u>	<u>225</u>	<u>226</u>	<u>227</u>	<u>228</u>
Lanthanum Oxalate	---	302.0	---	458.0	---	---
Tantalum Oxide	119.0	70.0	77.8	140.0	186.5	76.8
Fused Boric Oxide	174.2	100.0	111.1	---	---	---
Thoria	119.3	140.0	148.1	---	---	---
Zirconium Carbonate	---	---	---	33.8	45.2	---
Titania (not Rutile)	---	---	---	60.0	79.9	423.3
Lithium Nitrate	---	50.0	55.6	---	---	---
Yttrium Oxalate	221.0	---	288.0	---	520.0	---
	<u>229</u>	<u>230</u>	<u>231</u>	<u>232</u>	<u>233</u>	<u>234</u>
Lanthanum Oxalate	---	361.0	---	---	---	---
Tantalum Oxide	225.0	111.0	---	---	---	---
Fused Boric Oxide	---	167.0	---	---	---	---
Zirconium Carbonate	84.4	111.0	---	---	---	---
Titania (not Rutile)	200.0	---	---	---	---	---
Silica	---	---	160.0	173.5	203.5	161.25
Alumina	---	---	94.65	81.85	91.9	59.5
Magnesia	---	---	96.35	69.15	77.8	70.6
Yttrium Oxalate	---	---	402.0	364.0	204.5	366.0
Cerium Oxalate	---	---	---	85.0	---	164.5
Vanadia	---	---	---	---	50.7	---

Table I (Cont'd)

<u>Actual Ingredient</u>	<u>235</u>	<u>236</u>	<u>237</u>	<u>238</u>	<u>239</u>	<u>240</u>
Silica	201.0	157.2	175.8	185.0	122.5	114.7
Alumina	68.1	92.9	99.4	104.6	138.5	126.7
Magnesia	80.9	73.4	78.6	82.7	117.7	110.2
Yttrium Oxalate	403.0	367.0	394.0	206.5	205.0	---
Cerium Oxalate	---	85.7	---	---	97.0	314.0
Vanadia	---	---	---	51.3	---	---
	<u>241</u>	<u>242</u>	<u>243</u>	<u>247</u>	<u>248</u>	<u>249</u>
Silica	114.9	33.2	24.4	197.0	172.0	147.3
Alumina	129.9	156.2	123.5	100.2	108.4	116.5
Magnesia	110.3	---	8.2	39.7	42.9	46.0
Yttrium Oxalate	---	---	305.0	---	---	---
Cerium Oxalate	---	155.3	143.0	---	---	---
Lanthanum Oxalate	314.0	155.0	---	---	---	---
Cobaltous Carbonate	---	35.4	32.5	---	---	---
Calcium Carbonate	---	256.0	214.0	98.7	106.5	114.0
Lithium Carbonate	---	16.4	---	72.6	78.3	84.2
Zirconium Carbonate	---	---	28.1	---	---	---
Zinc Carbonate	---	---	---	122.5	133.5	143.0
	<u>250</u>	<u>251</u>	<u>252</u>	<u>253</u>	<u>254</u>	<u>255</u>
Silica	195.5	193.6	192.0	97.6	158.1	136.6
Alumina	99.35	98.6	97.5	132.5	---	---
Lithium Carbonate	48.0	23.6	35.6	95.9	53.5	50.4
Calcium Carbonate	97.5	96.5	144.0	130.5	79.2	68.2
Zinc Carbonate	122.0	121.0	121.3	163.2	98.7	85.3
Magnesia	52.35	64.8	38.7	52.4	31.9	27.5
Yttrium Oxalate	---	---	---	---	476.0	---
Lanthanum Oxalate	---	---	---	---	---	479.0
	<u>256</u>	<u>257</u>	<u>258</u>	<u>259</u>	<u>260</u>	<u>261</u>
Silica	147.7	128.5	262.0	254.5	310.0	310.0
Alumina	74.9	65.4	112.0	109.0	75.0	92.5
Lithium Carbonate	54.6	47.4	---	---	---	---
Zinc Carbonate	92.2	80.3	---	---	---	---
Magnesia	29.7	25.9	60.5	59.0	---	47.5
Yttrium Oxalate	446.0	442.0	---	---	---	---
Calcium Carbonate	---	---	81.2	---	206.0	89.2
Calcium Fluoride	---	---	20.0	78.0	---	---

Table I (Cont'd)

<u>Actual Ingredient</u>	<u>262</u>	<u>263</u>	<u>264</u>	<u>265</u>	<u>266</u>	<u>267</u>	<u>268</u>
Boric Acid (fused)	---	---	29.4	---	---	---	---
Barium Carbonate	---	---	153.2	---	---	---	---
Titanium Dioxide	---	---	359.0	---	---	---	---
Sodium Carbonate	---	---	9.4	---	---	---	---
Silica	345.5	175.5	---	128.5	122.3	168.8	114.8
Alumina	105.0	56.5	---	65.4	124.3	133.5	109.3
Magnesia	13.5	7.35	---	25.9	49.4	52.8	43.0
Beryllium Carbonate	75.6	---	---	---	---	69.0	---
Lanthanum Oxalate	---	542.0	---	442.0	---	---	---
Zinc Carbonate	---	---	---	80.3	154.0	---	143.6
Lithium Carbonate	---	---	---	47.4	90.6	98.0	79.2
Calcium Carbonate	---	---	---	---	122.5	131.2	107.2
Zirconium Carbonate	---	---	---	---	---	---	53.0
	<u>269</u>	<u>270</u>	<u>271</u>	<u>272</u>	<u>273</u>	<u>274</u>	<u>275</u>
Silica	76.3	107.0	97.4	85.8	177.0	132.3	183.0
Alumina	90.5	58.1	52.9	---	120.4	134.7	51.6
Lithium Carbonate	65.8	79.2	72.2	63.5	87.2	97.3	---
Calcium Carbonate	88.9	106.8	97.3	85.5	118.0	---	---
Magnesia	35.8	43.1	39.2	34.6	47.6	53.4	---
Yttrium Oxalate	---	301.0	---	---	---	---	---
Lanthanum Oxalate	---	---	319.5	615.0	---	---	358.0
Beryllium Carbonate	---	---	---	44.9	113.2	69.5	78.8
Zinc Carbonate	118.8	134.3	122.2	---	---	158.0	70.2
Zirconium Carbonate	44.0	---	---	---	---	---	---
Cerium Oxalate	224.3	---	---	---	---	---	---
	<u>276</u>	<u>277</u>	<u>278</u>	<u>279</u>	<u>280</u>	<u>281</u>	<u>282</u>
Silica	202.0	129.7	---	---	---	---	---
Alumina	57.2	44.0	---	---	---	---	---
Lithium Carbonate	46.6	33.1	123.5	61.8	---	---	---
Lanthanum Oxalate	395.0	303.0	---	---	---	---	---
Beryllium Carbonate	87.5	67.0	---	---	---	---	---
Cerium Oxalate	---	305.0	---	---	---	---	---
SiO ₂	---	---	325	325	333.3	275	150
Boric Acid Fused	---	---	---	---	243	222	444
Barium Carbonate	---	---	---	---	---	128.5	128.5
TiO ₂ (not Rutile)	---	---	100	---	---	---	---
Zirconium Carbonate	---	---	---	112.4	---	---	---
Calcium Carbonate	---	---	44.6	---	---	---	---
Zinc Carbonate	---	---	---	38.6	---	---	---
Sodium Carbonate	---	---	---	42.8	48.6	---	---

Table I (Cont'd)

<u>Actual Ingredient</u>	<u>283</u>	<u>284</u>	<u>285</u>	<u>286</u>	<u>287</u>	<u>288</u>
Silica	92.4	92.4	79.9	96.5	63.4	80.2
Aluminum Oxide	50.2	50.2	65.1	65.5	64.4	65.4
Lithium Carbonate	68.2	68.2	47.2	45.6	46.7	47.4
Calcium Carbonate	12.3	12.3	----	----	----	----
Zinc Carbonate	116.0	61.7	80.0	80.6	78.9	40.3
Magnesium Oxide	37.2	37.3	25.8	25.9	25.5	25.9
Boric Acid (fused)	80.0	79.7	99.0	66.1	130.2	98.8
Lanthanum Oxalate	309.5	303.5	442.0	439.0	436.0	440.0
Cerium Oxalate	21.9	21.7	----	----	----	----
Zirconium Carbonate (nominal)	17.7	17.8	----	----	----	----
Titanium Dioxide	----	----	----	----	----	----
Cupric Carbonate	----	55.2	----	----	----	41.1
Yttrium Oxalate	----	----	----	----	----	----
Cupric Oxide	----	----	----	----	----	----
Rare Earth Oxalate	----	----	----	----	----	----
Cobaltous Carbonate	----	----	----	----	----	----
	<u>289</u>	<u>290</u>	<u>291</u>	<u>292</u>	<u>293</u>	<u>294</u>
Silica	79.5	104.2	90.5	79.9	104.7	63.4
Aluminum Oxide	64.8	56.6	73.9	65.2	56.8	57.4
Lithium Carbonate	46.9	74.2	53.5	47.2	61.9	78.2
Calcium Carbonate	----	----	----	----	104.3	105.4
Zinc Carbonate	79.5	126.0	90.6	79.9	104.7	132.4
Magnesium Oxide	25.6	42.0	29.2	25.8	33.7	42.6
Boric Acid (fused)	58.9	128.9	112.0	98.5	77.5	86.9
Lanthanum Oxalate	435.0	293.0	----	439.0	----	----
Cerium Oxalate	----	----	----	----	----	----
Zirconium Carbonate (nominal)	----	----	----	----	----	----
Titanium Dioxide	----	----	----	----	----	----
Cupric Carbonate	40.6	----	----	----	----	----
Yttrium Oxalate	----	----	438.0	----	294.5	297.4
Cupric Oxide	----	----	----	----	----	----
Rare Earth Oxalate	----	----	----	----	----	----
Cobaltous Carbonate	----	----	----	----	----	----

Table I (Cont'd)

<u>Actual Ingredient</u>	<u>295</u>	<u>296</u>	<u>297</u>	<u>298</u>	<u>299</u>	<u>300</u>	<u>301</u>
Silica	83.6	84.4	107.3	97.5	99.8	132.7	97.3
Aluminum Oxide	56.7	57.2	58.2	52.9	54.1	----	52.8
Lithium Carbonate	77.2	77.6	79.1	72.1	73.4	97.1	71.8
Calcium Carbonate	34.7	70.5	107.2	97.5	99.7	132.5	97.3
Zinc Carbonate	130.8	132.0	71.5	65.2	----	166.3	121.8
Magnesium Oxide	42.1	42.4	43.2	39.3	40.2	53.4	39.2
Boric Acid (fused)	128.9	86.7	----	----	122.8	163.8	----
Lanthanum Oxalate	----	----	----	320.0	328.0	----	----
Cerium Oxalate	----	----	----	----	----	----	----
Zirconium Carbonate (nominal)	----	----	----	----	----	----	----
Titanium Dioxide	----	----	----	----	----	----	----
Cupric Carbonate	----	----	----	----	----	----	----
Yttrium Oxalate	295.0	297.0	305.0	----	----	----	----
Cupric Oxide	----	----	39.7	36.2	----	----	----
Rare Earth Oxalate	----	----	----	----	----	----	322.0
Cobaltous Carbonate	----	----	----	----	----	----	----
	<u>302</u>	<u>303</u>	<u>304</u>	<u>305</u>	<u>306</u>	<u>307</u>	<u>308</u>
Silica	102.2	104.8	133.0	133.0	134.0	106.0	107.7
Aluminum Oxide	55.4	56.8	96.6	96.7	97.0	57.6	58.4
Lithium Carbonate	40.3	77.2	----	----	----	67.6	79.5
Calcium Carbonate	102.2	55.8	----	----	----	105.8	107.2
Zinc Carbonate	127.8	131.0	79.2	76.5	40.0	70.7	54.0
Magnesium Oxide	41.1	42.2	76.4	----	77.0	42.7	43.4
Boric Acid (fused)	----	----	----	----	----	----	----
Lanthanum Oxalate	----	----	----	----	----	----	----
Cerium Oxalate	----	----	----	----	----	----	----
Zirconium Carbonate (nominal)	----	----	----	----	----	----	----
Titanium Dioxide	----	----	----	----	----	----	----
Cupric Carbonate	----	----	----	----	----	----	----
Yttrium Oxalate	288.0	295.0	381.0	384.4	384.0	299.0	303.0
Cupric Oxide	38.9	38.8	----	25.2	----	39.4	28.6
Rare Earth Oxalate	----	----	----	----	----	----	----
Cobaltous Carbonate	----	----	----	----	51.0	22.7	46.1

Table I (Cont'd)

<u>Actual Ingredient</u>	<u>309</u>	<u>310</u>	<u>311</u>	<u>312</u>	<u>313</u>
Silica	170.9	146.7	124.1	102.8	82.1
Aluminum Oxide	64.5	74.6	84.2	93.1	100.2
Lithium Carbonate	46.7	54.2	60.9	67.2	72.4
Calcium Carbonate	-----	-----	-----	-----	-----
Zinc Carbonate	-----	-----	-----	-----	-----
Magnesium Oxide	-----	-----	-----	-----	-----
Beryllium Carbonate	83.1	80.4	77.4	74.7	71.7
Yttrium Oxalate	-----	-----	-----	-----	-----
Lanthanum Oxalate	446	473	499	522	551
Cerium Oxalate	-----	-----	-----	-----	-----
Zirconium Carbonate (nom.)	-----	-----	-----	-----	-----
Cupric Oxide	-----	-----	-----	-----	-----
	<u>314</u>	<u>315</u>	<u>316</u>	<u>317</u>	<u>318</u>
Silica	140.0	147.0	141.9	142.6	238
Aluminum Oxide	71.3	62.3	60.2	60.5	134.6
Lithium Carbonate	52.0	45.2	43.7	43.9	-----
Calcium Carbonate	-----	61.2	-----	-----	-----
Zinc Carbonate	-----	-----	74.0	-----	-----
Magnesium Oxide	58.7	24.7	23.8	23.9	106.4
Beryllium Carbonate	-----	32.2	31.0	31.2	46.2
Yttrium Oxalate	-----	-----	-----	-----	-----
Lanthanum Oxalate	453	430	415	418	-----
Cerium Oxalate	-----	-----	-----	-----	-----
Zirconium Carbonate (nom.)	-----	-----	-----	-----	-----
Cupric Oxide	-----	-----	-----	47.2	-----

Table I (Cont'd)

<u>Actual Ingredient</u>	<u>319</u>	<u>320</u>	<u>321</u>	<u>322</u>	<u>323</u>
Silica	155.5	202.6	141.0	178.0	195.4
Aluminum Oxide	88.0	114.7	89.6	129.7	142.0
Lithium Carbonate	----	----	----	----	68.6
Calcium Carbonate	----	----	----	----	----
Zinc Carbonate	----	----	----	106.0	----
Mangesium Oxide	69.5	90.6	70.9	102.4	112.3
Beryllium Carbonate	----	----	----	45.3	48.7
Yttrium Oxalate	----	----	531	----	----
Lanthanum Oxalate	404	----	----	----	----
Cerium Oxalate	----	----	----	----	----
Zirconium Carbonate (nom.)	----	104	----	----	----
Cupric Oxide	----	----	----	----	----
	<u>324</u>	<u>325</u>	<u>326</u>	<u>327</u>	<u>328</u>
Silica	161.9	124.4	144.8	189.7	88.0
Aluminum Oxide	109.7	70.3	81.9	62.0	49.7
Lithium Carbonate	79.3	51.2	59.6	45.0	36.1
Calcium Carbonate	----	----	----	----	----
Zinc Carbonate	134.7	86.6	100.7	76.4	61.2
Magnesium Oxide	86.8	55.6	64.7	48.9	39.4
Beryllium Carbonate	47.1	36.2	42.2	----	----
Yttrium Oxalate	----	417	----	368	294
Lanthanum Oxalate	----	----	----	----	344
Cerium Oxalate	----	----	----	----	----
Zirconium Carbonate (nom.)	----	----	111.4	84.4	----
Cupric Oxide	----	----	----	----	88.2

Table I (Cont'd)

<u>Actual Ingredient</u>	<u>330</u>	<u>331</u>	<u>332</u>	<u>333</u>	<u>334</u>	<u>335</u>
Silica	129.2	148.8	123.8	142.1	117.9	124.3
Aluminum Oxide (C.P.)	67.4	77.5	64.7	74.0	85.8	90.4
Magnesium Oxide (C.P.)	---	---	53.4	60.9	67.8	---
Yttrium Oxalate	---	460	---	439	---	---
Lanthanum Oxalate	466	---	447	---	395	416
Beryllium Carbonate	98.3	113	---	---	---	121.8
Zinc Carbonate (C.P.)	82.9	95.4	79.6	91.0	70.2	74.2
	<u>336</u>	<u>337</u>	<u>338</u>	<u>339</u>	<u>340</u>	<u>341</u>
Silica	140.7	107.6	93.8	98.5	106.2	109.5
Aluminum Oxide (C.P.)	102.5	91.2	79.3	83.5	72.2	61.9
Magnesium Oxide (C.P.)	---	72.1	62.8	---	56.8	48.9
Yttrium Oxalate	405	450	---	---	421	---
Lanthanum Oxalate	---	---	459	480	---	428
Beryllium Carbonate	143.1	---	---	116.9	75.3	42.7
Zinc Carbonate (C.P.)	84.2	93.3	81.3	85.5	88.4	75.9
Lithium Carbonate (C.P.)	---	---	---	---	52.2	45.0
	<u>342</u>	<u>343</u>	<u>344</u>	<u>345</u>	<u>346</u>	<u>347</u>
Silica	127.4	111.6	181.0	156.9	78.0	190.9
Aluminum Oxide (C.P.)	71.9	63.1	102.3	105.9	66.0	53.9
Magnesium Oxide (C.P.)	28.4	24.9	40.5	---	26.1	---
Yttrium Oxalate	427	---	405	418	391	---
Lanthanum Oxalate	---	435	---	---	---	371
Zirconium Carbonate(nominal)	---	---	---	---	89.8	---
Beryllium Carbonate	100.7	88.1	71.8	148.0	92.2	113.3
Zinc Carbonate (C.P.)	88.2	77.5	---	---	81.1	66.5
Lithium Carbonate (C.P.)	52.1	45.6	---	---	47.9	---
	<u>348</u>	<u>349</u>	<u>350</u>	<u>351</u>	<u>352</u>	<u>353</u>
Silica	182.9	190.9	144.7	209.5	94.0	111.5
Aluminum Oxide (C.P.)	51.8	53.9	133.1	108.3	63.9	62.0
Magnesium Oxide (C.P.)	---	---	52.7	42.8	35.4	25.1
Yttrium Oxalate	---	---	---	---	378	374
Lanthanum Oxalate	357	---	---	---	---	---
Zirconium Carbonate(nominal)	70.0	---	---	---	86.7	85.7
Beryllium Carbonate	108.3	113.3	174.5	137.5	45.7	44.0
Zinc Carbonate (C.P.)	---	66.5	---	---	78.4	77.7
Lithium Carbonate (C.P.)	---	---	96.2	78.4	41.2	45.8
Calcium Carbonate (C.P.)	---	---	130.8	106.2	---	---
Cerium Oxalate	---	371	---	---	---	---
					<u>354</u>	

Table I (Cont'd)

<u>Actual Ingredient</u>	<u>355</u>	<u>356</u>	<u>357</u>	<u>358</u>	<u>359</u>	<u>360</u>
Silica (SiO_2)	138.9	157.0	128.1	146.7	137.6	153.0
Alumina (Al_2O_3)	72.4	82.4	66.8	76.5	71.8	79.8
Magnesia (MgO)	57.9	65.2	52.7	60.4	56.8	63.1
Yttrium Oxalate	358	---	91.2	378	355	394
Zirconium Acetate	---	220	---	---	---	---
Cerium Oxalate	125.3	142.6	---	---	---	---
Rare Earth Oxalate	---	---	385	---	---	---
Zinc Carbonate	44.5	50.7	41.2	47.0	---	49.2
Lithium Carbonate	26.2	28.8	24.1	27.4	21.6	28.9
Vanadium Pentoxyde	---	---	---	34.2	---	---
Zinc Tungstate	---	---	---	---	92.8	---
Cobaltous Carbonate	---	---	---	---	---	31.4
	<u>361</u>	<u>362</u>	<u>363</u>	<u>364</u>	<u>365</u>	<u>366</u>
Silica (SiO_2)	148.1	152.2	154.0	182.1	144.5	159.0
Alumina (Al_2O_3)	77.0	80.0	80.2	95.2	75.4	82.4
Magnesia (MgO)	60.9	62.9	63.5	75.2	59.5	---
Beryllium Carbonate	---	---	---	55.3	26.4	120.5
Yttrium Oxalate	382	393	396	---	372	---
Zirconium Acetate	---	---	---	---	---	268.0
Cerium Oxalate	---	---	---	164.5	130.3	143.3
Zinc Carbonate	47.5	48.8	---	58.5	---	76.5
Lithium Carbonate	27.9	28.8	29.1	34.4	27.3	---
Ferric Oxide	30.2	---	---	---	---	---
Fused Boric Acid	---	---	48.7	---	---	---
Copper Oxide	---	15.6	15.7	---	---	---
	<u>367</u>	<u>368</u>	<u>369</u>	<u>370</u>	<u>371</u>	<u>372</u>
Silica (SiO_2)	154.8	149.7	150.8	147.7	150.0	128.7
Alumina (Al_2O_3)	80.8	78.2	78.8	77.2	78.3	67.2
Magnesia (MgO)	31.9	15.5	---	---	10.3	---
Beryllium Carbonate	117.5	114	114.7	112.3	114.3	97.9
Yttrium Oxalate	396	385	389	382	387	---
Lanthanum Oxalate	---	---	---	---	---	77.3
Cerium Oxalate	93.2	90.1	90.7	88.8	90.3	---
Rare Earth Oxalate	---	---	---	---	---	388
Zinc Carbonate	---	47.9	---	47.5	32.2	82.7
Calcium Carbonate	---	---	77.2	37.7	25.5	---

Table I (Cont'd)

<u>Actual Ingredient</u>	<u>373</u>	<u>374</u>	<u>375</u>	<u>376</u>	<u>377</u>	<u>378</u>
Silica (SiO_2)	153.9	151.3	83.8	66.7	56.4	110.0
Alumina (Al_2O_3)	80.3	84.0	34.2	33.9	33.9	46.7
Magnesia (MgO)	---	---	35.9	35.7	35.7	49.1
Beryllium Carbonate	104.2	122.3	---	---	---	---
Yttrium Oxalate	396	416	---	---	---	---
Zirconium Acetate	---	---	---	---	---	298.0
Lanthanum Oxalate	---	---	471	474	467	---
Cerium Oxalate	92.6	---	---	---	---	---
Zinc Carbonate	---	51.8	54.9	55.6	54.8	76.5
Lithium Carbonate	29.0	30.4	48.6	49.2	48.9	67.3
Fused Boric Acid	---	---	62.1	96.0	116.2	94.2
Copper Oxide	---	11.0	---	---	---	---
Calcium Carbonate	39.4	---	67.2	66.5	66.5	91.8
	<u>379</u>	<u>380</u>	<u>381</u>	<u>382</u>	<u>383</u>	<u>384</u>
Silica (SiO_2)	99.9	91.5	111.2	107.2	111.2	82.2
Alumina (Al_2O_3)	21.2	---	23.4	22.8	23.6	17.5
Magnesia (MgO)	44.6	40.8	49.7	47.9	49.7	36.7
Zirconium Acetate	272	248	303	291	302	---
Lanthanum Oxalate	146	278	---	---	---	---
Zinc Carbonate	69.6	63.3	77.1	74.2	77.2	57.0
Lithium Carbonate	61.2	56.1	62.1	65.7	68.4	50.4
Fused Boric Acid	85.8	78.2	95.5	92.2	95.5	70.3
Calcium Carbonate	83.0	74.8	92.5	89.2	92.7	68.5
Copper Oxide	---	---	18.5	---	---	---
Titanium Oxide (not rutile)	---	---	---	---	18.6	---
Beryllium Carbonate	---	---	---	---	---	17.4
Ferric Oxide	---	---	---	35.7	---	---
Rare Earth Oxalate	---	---	---	---	---	483
	<u>385</u>	<u>386</u>	<u>387</u>	<u>388</u>	<u>389</u>	<u>390</u>
Silica (SiO_2)	9.6	8.3	53.1	87.3	96.7	76.9
Alumina (Al_2O_3)	338.9	263.5	---	---	39.4	39.2
Lithium Carbonate	37.8	32.4	52.1	53.5	57.1	56.7
Calcium Carbonate	188.3	145.8	265.0	72.7	77.2	76.5
Zinc Carbonate	32.2	27.6	44.4	---	64.4	64.2
Magnesia (MgO)	10.3	8.9	7.2	29.3	41.4	41.3
Fused Boric Acid	---	---	63.1	74.7	71.6	110.9
Lanthanum Oxalate	---	154.7	248.7	---	---	---
Titanium Oxide (not rutile)	---	---	14.1	19.4	---	---
Beryllium Carbonate	---	---	306.5	84.2	---	---
Ferric Oxide	---	35.2	---	---	---	---
Rare Earth Oxalate	---	---	---	513	---	---
Yttrium Oxalate	---	---	---	---	466	463

Table I (Cont'd)

<u>Actual Ingredient</u>	<u>391</u>	<u>392</u>	<u>393</u>	<u>394</u>	<u>395</u>	<u>396</u>
Silica (SiO_2)	65.1	81.0	79.1	87.6	72.3	194
Alumina (Al_2O_3)	39.0	37.4	61.0	67.6	61.4	108.7
Lithium Carbonate	50.2	45.2	44.2	39.2	73.0	52.8
Calcium Carbonate	76.3	61.2	---	---	---	---
Zinc Carbonate	63.9	76.8	75.1	58.4	75.2	---
Magnesia (MgO)	41.0	37.0	48.2	80.2	48.6	43.3
Fused Boric Acid	133.7	83.1	81.5	90.0	74.1	---
Zirconium Acetate	---	79.9	97.5	---	196.0	351
Copper Oxide	---	---	---	10.3	---	---
Yttrium Oxalate	462	443	443	400	362	433
	<u>397</u>	<u>398</u>	<u>399</u>	<u>400</u>	<u>401</u>	<u>402</u>
Silica (SiO_2)	192.3	92.5	90.8	94.9	91.4	90.2
Alumina (Al_2O_3)	203.8	50.3	48.9	---	49.5	49.0
Lithium Carbonate	61.6	45.2	30.7	46.5	22.3	22.1
Calcium Carbonate	---	80.0	60.2	94.8	72.7	54.2
Zinc Carbonate	80.5	---	54.1	47.5	---	---
Magnesia (MgO)	---	31.6	38.7	40.7	48.9	48.4
Fused Boric Acid	---	106.5	103.6	109.6	104.9	103.9
Copper Oxide	---	---	---	---	9.65	9.6
Titanium Oxide (not rutile)	---	---	---	---	---	14.4
Yttrium Oxalate	---	523	507	536	512.5	506
	<u>403</u>	<u>404</u>	<u>405</u>	<u>406</u>	<u>407</u>	<u>408</u>
Silica (SiO_2)	87.3	88.1	153.3	124.3	190.8	164.8
Alumina (Al_2O_3)	47.4	47.8	73.3	59.9	54.0	58.9
Lithium Carbonate	21.4	21.4	2.72	2.22	---	---
Calcium Carbonate	34.8	37.2	---	---	---	---
Magnesia (MgO)	46.7	47.2	---	---	---	---
Fused Boric Acid	100	57.1	---	---	---	---
Lanthanum Oxalate	---	---	---	648.5	---	412
Copper Oxide	9.2	9.3	---	---	---	---
Titanium Oxide (not rutile)	13.9	14.1	---	---	---	---
Beryllium Carbonate	---	17.8	73.5	60.2	143.6	132.5
Ferric Oxide	27.8	28.1	---	---	---	---
Yttrium Oxalate	490	495	682	---	---	---
Zinc Carbonate	---	---	---	---	66.3	73.5
Rare Earth Oxalate	---	---	---	---	372	---

Table I (Cont'd)

<u>Actual Ingredient</u>	<u>409</u>	<u>410</u>	<u>411</u>	<u>412</u>	<u>413</u>	<u>414</u>
Silica (SiO_2)	129.3	159.4	159.8	122.8	213.9	146.2
Alumina (Al_2O_3)	67.4	90.2	90.3	78.1	60.5	61.9
Zinc Carbonate	82.7	---	---	---	74.2	76.1
Magnesia (MgO)	---	35.7	35.7	30.9	---	---
Lanthanum Oxalate	465	---	415	539	---	428
Beryllium Carbonate	124.3	80.0	80.0	69.3	161.0	165.3
Rare Earth Oxalate	---	417	---	---	---	---
Yttrium Oxalate	---	---	---	---	358	---

415

Silica (SiO_2)	158.2
Lithium Carbonate	62.9
Calcium Carbonate	85.3
Magnesia (MgO)	34.3
Beryllium Carbonate	153.5
Yttrium Oxalate	518

Table II
New Glass Compositions in Weight %

<u>Actual Ingredient</u>	<u>1</u>	<u>2</u>	<u>3</u>	<u>4</u>	<u>5</u>	<u>20</u>
SiO ₂	49.15	---	17.7	49.15	---	---
Al ₂ O ₃	29.57	---	---	29.57	---	---
MgO	21.28	---	---	21.28	---	---
B ₂ O ₃	---	---	---	---	---	16.6
La ₂ O ₃	---	---	---	---	---	37.5
ZrO ₂	---	15	---	---	---	---
TiO ₂	---	45	28.3	---	50	---
Ta ₂ O ₅	---	40	---	---	50	29.2
BaO	---	---	54.6	---	---	---
ThO ₂	---	---	---	---	---	16.7
	<u>22</u>	<u>23</u>	<u>24</u>	<u>25</u>	<u>26</u>	<u>27</u>
SiO ₂	30	---	60	50	72.1	62.0
Al ₂ O ₃	---	50	30	35	0.85	0.8
CaO	---	---	---	---	---	0.5
MgO	---	---	10	7.5	---	---
ZrO ₂	20	50	---	---	10.33	21.0
TiO ₂	20	---	---	---	0.21	---
BeO	---	---	---	7.5	---	---
Ta ₂ O ₅	30	---	---	---	---	---
K ₂ O	---	---	---	---	---	2.3
Na ₂ O	---	---	---	---	16.89	14.0
	<u>28</u>	<u>29</u>	<u>32</u>	<u>33</u>	<u>34</u>	<u>35</u>
SiO ₂	27.6	35.5	---	---	---	---
Al ₂ O ₃	28.4	29.1	---	---	---	---
CaO	6.5	5.3	48	8.0	48	8.0
B ₂ O ₃	8.6	9.5	52	31.9	52	31.9
La ₂ O ₃	---	---	---	50.3	---	50.3
ZrO ₂	13.4	13.8	---	10.0	---	10.0
BeO	---	6.9	---	---	---	---
Ce ₂ O ₃	14.4	---	---	---	---	---

Table II (Cont'd)

<u>Actual Ingredient</u>	<u>40</u>	<u>41</u>	<u>42</u>	<u>43</u>	<u>44</u>	<u>45</u>
SiO ₂	45.2	44	44	40	44	50
Al ₂ O ₃	27.3	---	---	---	---	---
Li ₂ O	---	---	6	11	---	---
CaO	---	11	---	---	11	12.5
MgO	8.39	---	---	---	---	---
TiO ₂	---	---	20	4	12	---
Ce ₂ O ₃	19.2	---	---	---	---	---
PbO	---	12	12	12	---	---
K ₂ O	---	11	6	11	11	12.5
SrO	---	11	6	11	11	12.5
BaO	---	11	6	11	11	12.5
	<u>46B</u>	<u>47B</u>	<u>48B</u>	<u>49B</u>	<u>50B</u>	<u>51B</u>
SiO ₂	53.4	48.35	38.15	36.7	33.6	27.95
CaO	5.37	5.64	7.11	6.87	7.65	7.11
TiO ₂	7.63	10.7	10.13	13.05	10.91	20.66
K ₂ O	9.00	9.35	11.94	11.55	12.87	11.92
SrO	9.90	10.4	13.13	12.7	14.15	13.15
BaO	14.65	15.43	19.45	19.1	20.95	19.43
	<u>52B</u>	<u>53B</u>	<u>54B</u>	<u>55B</u>	<u>56</u>	<u>57</u>
SiO ₂	26.0	25.13	24.64	22.16	76.5	---
Al ₂ O ₃	---	---	---	---	---	55.3
Li ₂ O	---	---	---	---	15.0	---
CaO	8.08	8.71	7.43	6.67	---	---
ZnO	---	---	---	---	7.5	---
ZrO ₂	---	---	---	29.40	---	44.7
TiO ₂	15.35	12.40	21.18	---	---	---
K ₂ O	13.55	14.65	12.5	11.23	---	---
SrO	14.90	16.07	13.72	12.32	---	---
BaO	22.10	22.93	20.35	18.25	---	---
P ₂ O ₅	---	---	---	---	1.0	---

Table II (Cont'd)

<u>Actual Ingredient</u>	<u>58</u>	<u>59</u>	<u>60</u>	<u>61</u>	<u>62</u>	<u>63</u>
SiO ₂	---	---	2.5	---	51.67	51.67
Al ₂ O ₃	98.3	---	3.5	3	25.0	25.0
Li ₂ O	---	---	0.2	---	---	---
CaO	1.7	---	---	---	---	---
MgO	---	---	---	---	18.33	18.33
B ₂ O ₃	---	16.6	22.0	24	---	---
La ₂ O ₃	---	37.5	40	27	---	5.0
ZrO ₂	---	---	2.0	12	---	---
TiO ₂	---	---	3.0	---	---	---
Ta ₂ O ₅	---	29.2	11	16	---	---
ThO ₂	---	16.7	6	16	---	---
SrO	---	---	3.5	---	---	---
BaWO ₃	---	---	6.3	2	---	---
Ce ₂ O ₃	---	---	---	---	5.0	---
	<u>64</u>	<u>65</u>	<u>66</u>	<u>67</u>	<u>68</u>	<u>69</u>
SiO ₂	51.67	51.67	51.67	51.67	51.67	56.67
Al ₂ O ₃	25	25	25	25	30	25
MgO	18.33	18.33	18.33	18.33	18.33	18.33
Y ₂ O ₃	5.0	---	---	---	---	---
Sm ₂ O ₃	---	5.0	---	---	---	---
ZrO ₂	---	---	5.0	---	---	---
Ta ₂ O ₅	---	---	---	5.0	---	---
	<u>70</u>	<u>71</u>	<u>72</u>	<u>73</u>	<u>74</u>	<u>75</u>
SiO ₂	51.67	50	50	50	51.67	62
Al ₂ O ₃	20	25	22.5	12.5	15	---
CaO	---	---	---	---	---	20
MgO	18.33	25	15	15	18.33	---
Y ₂ O ₃	10	---	---	10	15	---
Ce ₂ O ₃	---	---	12.5	12.5	---	---
Na ₂ O	---	---	---	---	---	0.18

Table II (Cont'd)

<u>Actual Ingredient</u>	<u>76</u>	<u>77</u>	<u>78</u>	<u>79</u>	<u>80</u>	<u>81</u>
SiO ₂	62	62	92	31	6.8	32
CaO	25	30	---	48	48.9	36
MgO	---	---	---	---	5.0	1
B ₂ O ₃	---	---	---	12	---	---
TiO ₂	---	---	8	---	---	---
Y ₂ O ₃	---	---	---	9.0	39.3	15
Na ₂ O	0.13	0.8	---	---	---	2
Fe ₂ O ₃	---	---	---	---	---	7
	<u>82</u>	<u>83</u>	<u>97</u>	<u>98</u>	<u>99</u>	<u>100</u>
SiO ₂	47	51.0	52.3	41.9	31.75	24.1
Al ₂ O ₃	36	---	9.56	11.62	13.48	15.2
Li ₂ O	---	3.0	---	---	---	---
CaO	---	13.0	5.27	6.4	7.42	8.36
MgO	10.5	9.0	---	---	---	---
ZrO ₂	4	2.0	---	---	---	---
TiO ₂	---	8.0	---	---	---	---
BeO	---	11.0	---	---	---	---
Ce ₂ O ₃	0.5	---	---	---	---	---
K ₂ O	---	---	8.82	10.77	12.57	14.05
SrO	---	---	9.71	10.83	13.7	15.43
BaO	---	---	14.4	17.5	20.65	22.84
	<u>101</u>	<u>102</u>	<u>103</u>	<u>104</u>	<u>105</u>	<u>106</u>
SiO ₂	24.1	44.2	42.7	38.3	36.2	27.2
Al ₂ O ₃	24.53	18.4	17.6	15.9	---	---
Li ₂ O	---	5.39	5.2	---	4.4	5.02
CaO	7.07	10.11	9.7	8.75	8.26	9.47
ZnO	---	14.65	---	---	11.97	13.7
MgO	---	7.25	6.97	6.27	5.92	6.78
Y ₂ O ₃	---	---	---	---	33.2	38.0
K ₂ O	---	---	---	14.7	---	---
SrO	13.05	---	17.9	16.2	---	---
BaO	19.3	---	---	---	---	---

Table II (Cont'd)

<u>Actual Ingredient</u>	<u>107</u>	<u>108</u>	<u>109</u>	<u>110</u>	<u>111</u>	<u>112</u>
SiO ₂	45.9	56.3	23.3	51.2	44.8	44.8
Al ₂ O ₃	---	---	---	35.0	44.3	44.3
Li ₂ O	3.73	3.0	3.64	---	---	---
CaO	7.01	5.66	6.82	---	---	---
ZnO	10.15	8.2	9.91	---	---	---
MgO	5.03	4.06	4.91	13.85	10.68	10.68
Y ₂ O ₃	28.2	22.3	52.5	---	---	---
	<u>113</u>	<u>114</u>	<u>115</u>	<u>116</u>	<u>117</u>	<u>118</u>
SiO ₂	33.35	37.4	27.6	27.3	27.2	22.7
Al ₂ O ₃	24.6	27.6	28.0	27.7	8.43	---
MgO	6.85	7.68	8.15	8.07	6.77	5.4
Y ₂ O ₃	---	27.2	---	36.8	---	---
Ce ₂ O ₃	35.25	---	36.2	---	57.6	72.0
	<u>119</u>	<u>120</u>	<u>121</u>	<u>122</u>	<u>123</u>	<u>124</u>
SiO ₂	33.1	29.3	20.82	13.95	20.2	20.95
Al ₂ O ₃	10.85	---	19.2	16.75	18.5	19.15
MgO	7.88	6.97	5.32	4.6	5.15	5.34
La ₂ O ₃	---	---	---	---	---	54.5
Y ₂ O ₃	48.2	63.8	---	---	---	---
Ce ₂ O ₃	---	---	54.7	72.0	---	---
Sm ₂ O ₃	---	---	---	---	56.2	---
	<u>125</u>	<u>126</u>	<u>127</u>	<u>128</u>	<u>129</u>	<u>130</u>
SiO ₂	35.7	33.1	46.0	55.0	38.62	45.0
Al ₂ O ₃	36.3	25.5	12.9	8.9	17.55	12.62
CaO	---	---	---	---	---	14.4
MgO	10.53	6.19	10.2	7.0	14.82	---
ZrO ₂	17.55	---	---	---	---	---
Y ₂ O ₃	---	35.4	28.6	29.4	29.06	28.0

Table II (Cont'd)

<u>Actual Ingredient</u>	<u>131</u>	<u>132</u>	<u>133</u>	<u>134</u>	<u>135</u>	<u>136</u>
SiO ₂	54.1	37.0	45.9	48.9	51.6	48.5
Al ₂ O ₃	8.72	16.73	12.96	13.8	25.1	23.95
CaO	8.31	18.43	7.15	---	---	---
MgO	---	---	5.13	---	18.4	17.62
La ₂ O ₃	---	---	---	---	5.15	9.85
BeO	---	---	---	6.78	---	---
Y ₂ O ₃	29.0	27.8	28.7	30.6	---	---
	<u>137</u>	<u>138</u>	<u>139</u>	<u>140</u>	<u>141</u>	<u>142</u>
SiO ₂	44.6	34.63	22.83	33.45	21.55	30.7
Al ₂ O ₃	21.67	19.35	15.35	18.72	14.45	17.47
MgO	15.97	14.23	11.31	13.27	9.85	3.65
La ₂ O ₃	88.9	31.83	50.4	30.75	47.6	---
CaO	---	---	---	---	---	16.22
Y ₂ O ₃	---	---	---	---	---	26.9
Ce ₂ O ₃	---	---	---	3.87	5.98	3.91
	<u>143</u>	<u>144</u>	<u>145</u>	<u>146</u>	<u>147</u>	<u>148</u>
SiO ₂	22.3	6.71	32.1	31.0	28.4	27.45
Al ₂ O ₃	21.9	33.0	---	6.58	---	5.82
Li ₂ O	---	---	2.0	1.92	1.76	1.7
CaO	20.08	31.3	14.23	11.89	12.6	10.55
MgO	4.82	---	10.22	8.57	9.04	7.59
La ₂ O ₃	---	---	---	---	38.5	37.2
ZrO ₂	---	---	1.64	1.59	1.45	1.41
TiO ₂	---	---	5.33	5.15	4.72	4.56
Y ₂ O ₃	26.95	25.2	30.15	29.1	---	---
Ce ₂ O ₃	3.92	3.67	4.52	4.23	3.87	3.74
	<u>149</u>	<u>150</u>	<u>151</u>	<u>152</u>	<u>153</u>	<u>154</u>
SiO ₂	27.8	26.9	48.3	38.7	38.8	37.8
Al ₂ O ₃	---	5.69	9.04	8.12	8.12	7.92
Li ₂ O	1.72	1.67	---	---	---	---
CaO	12.95	10.98	---	---	---	---
MgO	8.84	7.43	21.45	19.18	19.25	18.73
La ₂ O ₃	---	---	---	34.0	---	---
TiO ₂	4.6	4.47	---	---	---	---
Y ₂ O ₃	---	---	26.28	---	---	---
Ce ₂ O ₃	3.79	3.67	---	---	33.8	---
Sm ₂ O ₃	40.3	39.0	---	---	---	35.5

Table II (Cont'd)

<u>Actual Ingredient</u>	<u>155</u>	<u>156</u>	<u>157</u>	<u>158</u>	<u>159</u>	<u>160</u>
SiO ₂	35.9	49.7	47.8	39.0	48.8	43.8
Al ₂ O ₃	8.68	20.66	11.55	5.49	9.55	8.55
MgO	17.77	24.64	23.68	19.35	16.0	14.37
La ₂ O ₃	---	---	---	21.38	---	33.2
Y ₂ O ₃	---	---	17.0	14.85	25.62	---
Ta ₂ O ₅	37.6	---	---	---	---	---
Cr ₂ O ₃	---	5.09	---	---	---	---
	<u>165</u>	<u>166</u>	<u>167</u>	<u>168</u>	<u>169</u>	<u>170</u>
SiO ₂	37.4	41.6	31.55	35.22	25.94	26.2
Al ₂ O ₃	9.64	31.4	16.46	18.52	20.1	4.32
Li ₂ O	2.22	---	---	---	---	---
CaO	8.83	---	---	---	---	---
MgO	6.35	9.9	6.47	7.23	7.67	6.25
TiO ₂	5.92	---	---	---	---	---
Y ₂ O ₃	29.6	---	---	25.63	35.0	---
V ₂ O ₅	---	17.07	12.0	13.4	11.32	55.5
Ce ₂ O ₃	---	---	33.41	---	---	7.7
	<u>171</u>	<u>172</u>	<u>173</u>	<u>174</u>	<u>175</u>	<u>176</u>
SiO ₂	31.7	19.85	19.35	31.15	44.7	53.1
Al ₂ O ₃	5.21	12.95	12.63	17.16	6.25	4.71
MgO	7.55	5.05	4.93	5.85	9.91	6.8
Y ₂ O ₃	46.2	---	---	33.3	27.75	28.5
V ₂ O ₅	9.28	9.37	9.12	12.44	11.18	6.9
Ce ₂ O ₃	---	52.0	---	---	---	---
Sm ₂ O ₃	---	---	53.8	---	---	---
	<u>177</u>	<u>178</u>	<u>179</u>	<u>180</u>	<u>181</u>	<u>182</u>
SiO ₂	21.9	31.78	20.8	20.68	6.22	29.6
Al ₂ O ₃	9.46	11.4	8.99	11.29	21.1	---
Li ₂ O	---	---	---	---	---	1.84
CaO	---	---	---	18.65	29.1	9.66
MgO	10.82	12.58	9.56	4.47	---	9.43
La ₂ O ₃	48.37	29.18	46.0	---	---	---
ZrO ₂	---	---	---	---	---	1.51
TiO ₂	---	---	---	---	---	4.92
Y ₂ O ₃	---	---	---	25.0	23.4	27.8
V ₂ O ₅	9.39	11.3	8.92	16.12	16.97	11.2
Ce ₂ O ₃	---	3.67	5.78	3.64	3.4	4.04

Table II (Cont'd)

<u>Actual Ingredient</u>	<u>183</u>	<u>184</u>	<u>185</u>	<u>186</u>	<u>187</u>	<u>188</u>
SiO ₂	29.15	25.6	26.0	25.93	25.18	38.7
Al ₂ O ₃	6.18	---	5.52	---	5.34	8.08
Li ₂ O	1.81	1.64	1.61	1.6	1.56	---
CaO	6.12	8.63	5.46	9.07	7.33	---
MgO	8.06	8.41	7.19	8.26	6.96	15.93
La ₂ O ₃	---	35.78	35.26	---	---	---
ZrO ₂	1.49	1.35	1.33	---	---	---
TiO ₂	4.85	4.39	4.32	4.3	4.19	---
Y ₂ O ₃	27.4	---	---	---	---	23.42
V ₂ O ₅	11.03	10.0	9.84	9.77	9.52	14.15
Ce ₂ O ₃	3.98	3.6	3.55	3.52	3.43	---
Sm ₂ O ₃	---	---	---	37.5	36.58	---
	<u>189</u>	<u>190</u>	<u>191</u>	<u>192</u>	<u>193</u>	<u>194</u>
SiO ₂	34.85	34.13	34.87	34.85	34.6	---
Al ₂ O ₃	7.3	7.17	7.32	7.3	7.26	---
MgO	14.42	14.13	14.43	14.43	13.4	---
B ₂ O ₃	---	---	---	---	---	30.0
La ₂ O ₃	---	---	30.62	---	18.95	28.0
Y ₂ O ₃	---	---	---	---	13.15	---
BaO	---	---	---	---	---	12.0
Ce ₂ O ₃	30.8	---	---	---	---	---
Sm ₂ O ₃	---	32.06	---	---	---	---
V ₂ O ₅	12.8	12.55	12.8	12.8	12.7	---
R ₂ O ₃	---	---	---	30.8	---	---
ThO ₂	---	---	---	---	---	12.0
Ta ₂ O ₅	---	---	---	---	---	18.0
	<u>195</u>	<u>196</u>	<u>197</u>	<u>198</u>	<u>199</u>	<u>200</u>
SiO ₂	---	---	---	---	---	33.1
Al ₂ O ₃	---	---	---	---	---	15.64
MgO	---	---	---	---	---	13.22
B ₂ O ₃	28.75	31.25	35.4	30.0	34.8	---
La ₂ O ₃	24.66	---	---	---	---	22.46
Y ₂ O ₃	---	18.57	21.06	28.0	31.0	15.57
BaO	11.6	12.62	14.27	12.0	13.97	---
V ₂ O ₅	8.77	9.53	10.79	---	---	---
R ₂ O ₃	10.88	11.85	13.4	12.0	15.35	---
Ta ₂ O ₅	15.23	16.53	---	18.0	---	---
ZrO ₂	---	---	5.22	---	5.11	---

Table II (Cont'd)

<u>Actual Ingredient</u>	<u>201</u>	<u>202</u>	<u>203</u>	<u>204</u>	<u>205</u>	<u>206</u>
SiO ₂	33.13	30.93	42.52	40.26	34.28	37.0
Al ₂ O ₃	15.62	14.6	---	---	---	16.77
CaO	---	---	---	---	---	18.4
MgO	13.2	12.33	20.24	19.52	16.63	---
La ₂ O ₃	---	20.94	---	---	44.2	---
Y ₂ O ₃	15.53	---	37.25	35.92	---	27.8
Ce ₂ O ₃	22.6	21.13	---	4.35	4.92	---
	<u>207</u>	<u>208</u>	<u>209</u>	<u>210</u>	<u>211</u>	<u>212</u>
SiO ₂	32.82	38.62	34.5	30.96	76.2	64.1
Al ₂ O ₃	16.16	17.55	16.37	14.63	---	---
MgO	13.66	14.82	---	12.36	---	---
Y ₂ O ₃	37.54	29.06	27.4	---	---	---
Li ₂ O	---	---	13.84	---	---	---
La ₂ O ₃	---	---	---	35.01	---	---
Ce ₂ O ₃	---	---	7.89	7.05	---	---
BaO	---	---	---	---	23.95	35.95
	<u>213</u>	<u>214</u>	<u>215</u>	<u>216</u>	<u>217</u>	<u>218</u>
SiO ₂	39.35	64.6	41.2	6.6	---	10.0
Al ₂ O ₃	2.72	10.97	---	48.6	47.0	42.0
CaO	---	---	27.6	44.8	43.0	38.0
MgO	---	24.55	2.8	---	---	---
La ₂ O ₃	58.0	---	---	---	---	---
ZrO ₂	---	---	8.3	---	---	---
TiO ₂	---	---	14.6	---	---	---
BaO	---	---	5.5	---	10.0	10.0
	<u>222</u>	<u>223</u>	<u>224</u>	<u>225</u>	<u>226</u>	<u>227</u>
B ₂ O ₃	33.4	35.84	20.0	22.22	---	---
La ₂ O ₃	22.2	---	28.0	---	42.0	---
ZrO ₂	---	---	---	---	6.0	7.98
TiO ₂	---	---	---	---	12.0	15.97
Y ₂ O ₃	---	16.53	---	21.56	---	38.85
Ta ₂ O ₅	22.2	23.8	14.0	15.55	28.0	37.3
ThO ₂	22.2	23.86	28.0	29.62	---	---
LiNO ₃	---	---	10.0	11.12	---	---

Table II (Cont'd)

<u>Actual Ingredient</u>	<u>228</u>	<u>229</u>	<u>230</u>	<u>231</u>	<u>232</u>	<u>233</u>
La ₂ O ₃	---	---	30.6	---	---	---
ZrO ₂	---	15.0	---	---	---	---
TiO ₂	84.65	40.0	---	---	---	---
Ta ₂ O ₅	15.35	45.0	20.35	---	---	---
ZrCO ₃	---	---	18.35	---	---	---
LaOx	---	---	30.7	---	---	---
SiO ₂	---	---	---	32.0	34.7	40.7
Al ₂ O ₃	---	---	---	18.93	16.37	18.38
MgO	---	---	---	19.27	13.85	15.55
Y ₂ O ₃	---	---	---	30.0	27.18	25.42
Ce ₂ O ₃	---	---	---	---	7.9	---
	<u>234</u>	<u>235</u>	<u>236</u>	<u>237</u>	<u>238</u>	<u>239</u>
SiO ₂	32.25	40.2	31.43	35.15	37.0	24.5
Al ₂ O ₃	11.9	13.62	18.58	19.88	20.92	27.7
MgO	14.13	16.17	14.68	15.12	16.53	23.53
Y ₂ O ₃	26.4	30.15	27.4	29.36	25.68	15.35
Ce ₂ O ₃	15.35	---	7.98	---	---	8.92
	<u>240</u>	<u>241</u>	<u>242</u>	<u>243</u>	<u>247</u>	<u>248</u>
SiO ₂	22.92	22.95	6.64	4.85	39.4	34.4
Al ₂ O ₃	25.93	25.95	31.23	24.7	20.04	21.67
Li ₂ O	---	---	1.33	---	5.88	6.34
CaO	---	---	28.64	23.95	11.04	11.93
ZnO	---	---	---	---	15.97	17.3
MgO	22.03	22.05	---	1.63	7.93	8.58
La ₂ O ₃	---	29.05	14.4	---	---	---
ZrO ₂	---	---	---	4.98	---	---
Y ₂ O ₃	---	---	---	22.8	---	---
Ce ₂ O ₃	29.2	14.5	---	13.25	---	---
CoO	---	---	3.31	3.03	---	---
	<u>249</u>	<u>250</u>	<u>251</u>	<u>252</u>	<u>253</u>	<u>254</u>
SiO ₂	29.46	39.1	38.75	38.4	19.52	31.62
Al ₂ O ₃	23.3	19.87	19.71	19.5	26.5	---
Li ₂ O	6.82	3.88	1.93	2.88	7.76	4.73
CaO	12.78	10.92	10.83	16.1	14.57	8.85
ZnO	18.57	15.85	15.7	15.57	21.14	12.82
MgO	9.19	10.47	12.96	7.73	10.47	6.37
Y ₂ O ₃	---	---	---	---	---	35.64

Table II (Cont'd)

<u>Actual Ingredient</u>	<u>255</u>	<u>256</u>	<u>257</u>	<u>258</u>	<u>259</u>	<u>260</u>
SiO ₂	27.32	29.53	25.7	52.4	50.9	62.0
Al ₂ O ₃	---	14.98	13.07	22.4	21.8	15.0
Li ₂ O	4.08	4.41	3.84	---	---	---
CaO	7.64	---	---	9.1	---	23.0
ZnO	11.08	11.97	10.43	12.1	---	---
MgO	5.5	5.94	5.18	---	11.8	---
Y ₂ O ₃	44.35	33.25	---	---	---	---
La ₂ O ₃	---	---	41.8	---	---	---
CaF ₂	---	---	---	4.0	15.6	---
	<u>261</u>	<u>262</u>	<u>263</u>	<u>264</u>	<u>266</u>	<u>267</u>
SiO ₂	62.0	69.1	37.1	---	24.46	33.75
Al ₂ O ₃	18.5	21.0	11.3	---	24.85	26.7
Li ₂ O	---	---	---	---	7.33	7.83
CaO	10.0	---	---	---	13.73	14.65
ZnO	---	---	---	---	19.95	---
MgO	9.5	2.7	1.47	---	9.87	10.55
B ₂ O ₃	---	---	---	2.4	---	---
La ₂ O ₃	---	---	50.2	---	---	---
ZrO ₂	---	---	---	---	---	9.43
TiO ₂	---	---	---	58.44	---	---
BeO	---	7.2	---	---	---	6.55
BaO	---	---	---	37.9	---	---
Na ₂ O	---	---	---	0.71	---	---
	<u>268</u>	<u>269</u>	<u>270</u>	<u>271</u>	<u>272</u>	<u>273</u>
SiO ₂	22.96	15.25	21.4	19.48	17.15	35.4
Al ₂ O ₃	21.86	18.1	11.62	10.57	---	24.07
Li ₂ O	6.4	5.31	6.4	5.83	5.13	7.06
CaO	12.0	9.96	11.98	10.92	9.6	13.23
ZnO	18.67	15.47	17.42	15.83	---	---
MgO	8.63	7.16	8.62	7.84	6.92	9.52
La ₂ O ₃	---	---	---	29.55	56.9	---
ZrO ₂	7.82	---	---	---	---	---
BeO	---	---	---	---	4.28	10.8
Y ₂ O ₃	---	---	22.54	---	---	---
Ce ₂ O ₃	20.85	---	---	---	---	---

Table II (Cont'd)

<u>Actual Ingredient</u>	<u>274</u>	<u>275</u>	<u>276</u>	<u>277</u>	<u>283</u>	<u>284</u>
SiO ₂	26.46	36.6	40.4	25.93	18.47	18.48
Al ₂ O ₃	26.93	10.35	11.43	8.79	10.03	10.03
Li ₂ O	7.91	---	3.35	2.68	5.52	5.52
CaO	---	---	---	---	1.38	1.38
ZnO	21.52	---	---	---	15.03	8.02
MgO	10.67	---	---	---	7.44	7.45
B ₂ O ₃	---	---	---	---	9.00	9.0
La ₂ O ₃	---	33.1	36.55	28.05	28.07	28.13
ZrO ₂	---	12.48	---	---	3.15	3.16
BeO	6.62	7.52	8.31	6.38	---	---
Ce ₂ O ₃	---	---	---	---	2.04	2.02
CeO ₂	---	---	---	28.27	---	---
CuO	---	---	---	---	---	6.86
	<u>285</u>	<u>286</u>	<u>287</u>	<u>288</u>	<u>289</u>	<u>290</u>
SiO ₂	15.97	19.3	12.67	16.03	15.9	20.84
Al ₂ O ₃	13.01	13.09	12.87	13.07	12.95	11.31
Li ₂ O	3.82	3.84	3.78	3.83	3.8	6.21
ZnO	10.37	10.43	10.27	5.22	10.32	16.93
MgO	5.15	5.18	5.09	5.17	5.12	8.39
B ₂ O ₃	11.1	7.43	14.66	11.15	6.63	14.48
La ₂ O ₃	40.75	40.75	40.35	40.7	40.3	---
CuO	---	---	---	5.11	5.06	---
Y ₂ O ₃	---	---	---	---	---	21.93
	<u>291</u>	<u>292</u>	<u>293</u>	<u>294</u>	<u>295</u>	<u>296</u>
SiO ₂	18.1	15.98	20.93	12.68	16.71	16.87
Al ₂ O ₃	14.77	13.04	11.36	11.47	11.33	11.43
Li ₂ O	4.33	3.82	5.01	6.32	6.24	6.28
CaO	---	---	11.72	11.83	3.89	7.87
ZnO	11.77	10.37	13.58	17.19	16.98	17.12
MgO	5.83	5.15	6.74	8.52	8.42	8.48
B ₂ O ₃	12.6	11.12	8.73	9.79	14.52	9.76
La ₂ O ₃	---	40.6	---	---	---	---
Y ₂ O ₃	32.7	---	22.03	22.22	22.0	22.2

Table II (Cont'd)

<u>Actual Ingredient</u>	<u>297</u>	<u>298</u>	<u>299</u>	<u>300</u>	<u>301</u>	<u>302</u>
SiO ₂	21.45	19.5	19.95	26.54	19.45	30.44
Al ₂ O ₃	11.63	10.58	10.82	---	10.56	11.08
Li ₂ O	6.39	5.82	5.94	7.92	5.8	3.25
CaO	12.0	10.92	11.17	14.86	10.9	11.43
ZnO	9.29	8.45	---	21.58	15.82	16.6
MgO	8.63	7.86	8.03	10.18	7.84	8.22
B ₂ O ₃	---	---	13.83	18.45	---	---
La ₂ O ₃	---	29.64	30.33	---	---	---
CuO	7.94	7.23	---	---	---	7.57
Re ₂ O ₃	---	---	---	---	29.8	---
Y ₂ O ₃	22.6	---	---	---	---	21.48
	<u>303</u>	<u>304</u>	<u>305</u>	<u>306</u>	<u>307</u>	<u>308</u>
SiO ₂	20.95	26.6	26.6	26.73	21.2	21.53
Al ₂ O ₃	11.36	19.32	19.35	19.4	11.52	11.68
Li ₂ O	6.25	---	---	---	5.48	6.43
CaO	6.26	---	---	---	11.88	12.04
ZnO	17.02	10.28	5.14	5.17	9.18	7.0
MgO	8.43	15.28	15.3	15.37	8.54	8.67
CuO	7.76	---	5.03	---	7.87	5.71
Y ₂ O ₃	22.05	28.53	28.97	28.7	22.34	22.65
CoO	---	---	---	4.76	2.12	4.3
	<u>309</u>	<u>310</u>	<u>311</u>	<u>312</u>	<u>313</u>	<u>314</u>
SiO ₂	34.17	29.33	24.81	20.55	16.41	28.0
Al ₂ O ₃	12.89	14.93	16.83	18.62	20.04	14.25
Li ₂ O	3.78	4.38	4.93	5.44	5.87	4.19
MgO	---	---	---	---	---	11.74
La ₂ O ₃	41.25	43.77	46.15	48.31	50.9	41.9
BeO	7.91	7.63	7.37	7.12	6.83	---
	<u>315</u>	<u>316</u>	<u>317</u>	<u>318</u>	<u>319</u>	<u>320</u>
SiO ₂	29.4	28.37	28.52	47.6	31.1	40.52
Al ₂ O ₃	12.45	12.03	12.09	26.92	17.59	22.93
Li ₂ O	3.65	3.53	3.55	---	---	---
CaO	6.85	---	---	---	---	---
ZnO	---	9.6	---	---	---	---
MgO	4.93	4.76	4.78	21.27	13.9	18.12
La ₂ O ₃	39.8	38.4	38.63	---	37.46	---
ZrO ₂	---	---	---	---	---	18.45
CuO	---	---	9.43	---	---	---
BeO	3.06	2.95	2.97	4.4	---	---

Table II (Cont'd)

<u>Actual Ingredient</u>	<u>321</u>	<u>322</u>	<u>323</u>	<u>324</u>	<u>325</u>	<u>326</u>
SiO ₂	28.2	35.6	39.07	32.37	24.87	28.95
Al ₂ O ₃	17.92	25.93	28.4	21.94	14.05	16.38
Li ₂ O	---	---	5.53	6.43	4.13	4.81
ZnO	---	13.77	---	17.5	11.23	13.08
MgO	14.17	20.47	22.46	17.35	11.12	12.93
ZrO ₂	---	---	---	---	---	19.79
BeO	---	4.24	4.64	4.48	3.45	4.02
Y ₂ O ₃	39.77	---	---	---	31.16	---
	<u>327</u>	<u>328</u>	<u>329</u>	<u>330</u>	<u>331</u>	<u>332</u>
SiO ₂	21.94	17.6	15.27	25.83	29.76	24.75
Al ₂ O ₃	12.4	9.94	12.95	13.48	15.5	12.93
Li ₂ O	3.64	2.92	3.8	---	---	---
ZnO	9.9	7.94	10.32	10.76	12.37	10.33
MgO	9.78	7.87	10.22	---	---	10.67
ZrO ₂	14.98	---	15.63	---	---	---
Y ₂ O ₃	27.5	22.05	28.66	---	34.4	---
La ₂ O ₃	---	31.8	---	43.15	---	41.32
BeO	---	----	3.18	6.89	7.93	---
	<u>333</u>	<u>334</u>	<u>335</u>	<u>336</u>	<u>337</u>	<u>338</u>
SiO ₂	28.41	23.58	24.86	28.13	21.52	18.75
Al ₂ O ₃	14.8	17.15	18.07	20.5	18.23	15.86
ZnO	11.82	9.12	9.63	10.92	12.13	10.57
MgO	12.48	13.56	---	---	14.42	12.55
La ₂ O ₃	---	36.58	38.53	---	---	42.35
BeO	---	---	8.87	10.05	---	---
Y ₂ O ₃	32.8	---	---	30.28	33.63	---
	<u>339</u>	<u>340</u>	<u>341</u>	<u>342</u>	<u>343</u>	<u>344</u>
SiO ₂	19.7	21.23	21.9	25.48	22.32	36.2
Al ₂ O ₃	16.7	14.4	12.38	14.38	12.61	20.46
Li ₂ O	---	4.22	3.64	4.22	3.7	---
ZnO	11.1	11.47	9.87	11.47	10.07	---
MgO	---	11.36	9.78	5.68	4.98	8.1
La ₂ O ₃	44.45	---	39.56	---	40.25	---
BeO	8.19	5.28	3.04	7.05	6.18	5.03
Y ₂ O ₃	---	31.82	---	31.87	---	30.24

Table II (Cont'd)

<u>Actual Ingredient</u>	<u>345</u>	<u>346</u>	<u>347</u>	<u>348</u>	<u>349</u>	<u>350</u>
SiO ₂	37.38	15.6	38.18	36.58	50.0	28.93
Al ₂ O ₃	21.17	13.2	10.78	10.35	8.3	26.62
Li ₂ O	---	3.88	---	---	---	7.78
ZnO	---	10.53	8.61	---	8.3	---
MgO	---	5.22	---	---	---	10.53
La ₂ O ₃	---	---	34.37	33.06	---	---
ZrO ₂	---	15.95	---	12.47	---	---
BeO	10.38	6.48	7.94	7.61	25.0	12.03
Y ₂ O ₃	31.26	29.25	---	---	---	---
Ce ₂ O ₃	---	---	---	---	8.3	---
CaO	---	---	---	---	---	14.63
	<u>351</u>	<u>352</u>	<u>353</u>	<u>354</u>	<u>355</u>	<u>356</u>
SiO ₂	44.9	18.8	22.3	25.7	27.78	31.4
Al ₂ O ₃	21.65	12.77	12.63	12.45	14.48	16.48
Li ₂ O	6.36	3.74	3.71	3.66	2.12	2.41
CaO	11.88	---	---	---	---	---
ZnO	---	10.19	10.08	9.95	5.78	6.58
MgO	8.56	7.08	5.01	2.47	11.57	13.03
ZrO ₂	---	15.43	15.27	15.06	---	16.6
BeO	9.66	3.13	3.09	3.06	---	---
Y ₂ O ₃	---	28.28	27.96	27.6	26.77	---
Ce ₂ O ₃	---	---	---	---	11.66	13.27
	<u>357</u>	<u>358</u>	<u>359</u>	<u>360</u>	<u>361</u>	<u>362</u>
SiO ₂	25.62	29.33	27.52	30.6	29.62	30.43
Al ₂ O ₃	13.35	15.3	14.36	15.96	15.4	16.0
Li ₂ O	1.95	2.24	1.75	2.34	2.26	2.33
ZnO	5.32	6.1	5.0	6.37	6.16	6.34
MgO	10.53	12.08	11.35	12.62	12.18	12.57
CuO	---	---	---	---	---	3.11
Fe ₂ O ₃	---	---	---	---	6.04	---
Y ₂ O ₃	7.39	28.25	26.55	29.48	28.5	29.35
Rare Earth	35.83	---	---	---	---	---
V ₂ O ₃	---	6.83	---	---	---	---
CoO	---	---	---	2.94	---	---

Table II (Cont'd)

<u>Actual Ingredient</u>	<u>363</u>	<u>364</u>	<u>365</u>	<u>366</u>	<u>367</u>	<u>368</u>
SiO ₂	30.8	36.42	28.9	31.8	30.95	29.93
Al ₂ O ₃	16.04	19.03	15.08	16.48	16.15	15.61
Li ₂ O	2.35	2.78	2.21	---	---	---
ZnO	---	7.58	---	9.91	---	6.23
MgO	12.7	15.03	11.89	---	6.37	3.09
B ₂ O ₃	5.48	---	---	---	---	---
ZrO ₂	---	---	---	20.05	---	---
CuO	3.14	---	---	---	---	---
BeO	---	3.89	1.85	8.47	8.25	7.98
Y ₂ O ₃	29.65	---	27.85	---	29.86	28.83
Ce ₂ O ₃	---	15.3	12.14	13.35	8.65	8.38
	<u>369</u>	<u>370</u>	<u>371</u>	<u>372</u>	<u>373</u>	<u>374</u>
SiO ₂	30.16	29.53	30.0	25.73	30.77	32.25
Al ₂ O ₃	15.76	15.43	15.65	13.43	16.05	16.8
CaO	8.67	4.24	2.87	---	4.42	---
ZnO	---	6.16	4.17	10.72	---	6.72
MgO	---	---	2.06	---	---	---
BeO	8.06	7.888	8.0	6.87	8.21	8.59
Y ₂ O ₃	29.08	28.53	28.93	---	29.67	31.08
Ce ₂ O ₃	8.44	8.27	8.39	---	8.61	---
Li ₂ O	---	---	---	---	2.35	2.46
La ₂ O ₃	---	---	---	7.16	---	---
CuO	---	---	---	---	---	2.19
R.E. Mix	---	---	---	36.06	---	---
	<u>376</u>	<u>377</u>	<u>378</u>	<u>379</u>	<u>380</u>	<u>381</u>
SiO ₂	13.33	11.28	22.0	19.98	18.29	22.24
Al ₂ O ₃	6.78	6.78	9.33	4.24	---	4.67
Li ₂ O	3.97	3.96	5.46	4.96	4.54	5.03
CaO	7.45	7.43	10.27	9.32	8.52	10.38
ZnO	7.21	7.19	9.92	9.01	8.25	10.02
MgO	7.13	7.13	9.82	8.92	8.16	9.93
B ₂ O ₃	10.8	13.09	10.62	9.65	8.82	10.73
La ₂ O ₃	43.9	43.18	---	13.53	24.77	---
ZrO ₂	---	---	22.55	20.48	18.75	22.82
CuO	---	---	---	---	---	3.69

Table II (Cont'd)

<u>Actual Ingredient</u>	<u>382</u>	<u>383</u>	<u>384</u>	<u>385</u>	<u>386</u>	<u>388</u>
SiO ₂	21.44	22.24	16.43	1.92	1.65	17.46
Al ₂ O ₃	4.55	4.72	3.49	67.78	52.69	---
Li ₂ O	5.32	5.53	4.08	3.06	2.63	4.33
CaO	10.0	10.38	7.66	21.16	16.35	8.14
ZnO	9.67	10.03	7.4	4.17	3.59	---
MgO	9.57	9.93	7.33	2.06	1.77	5.86
B ₂ O ₃	10.36	10.73	7.92	---	---	---
La ₂ O ₃	---	---	---	---	14.35	---
ZrO ₂	21.96	22.78	---	---	---	---
TiO ₂	---	3.71	---	---	---	3.88
BeO	---	---	0.85	---	---	4.23
Fe ₂ O ₃	7.13	---	---	---	7.03	---
Re ₂ O ₃	---	---	44.83	---	---	47.65
	<u>389</u>	<u>390</u>	<u>391</u>	<u>392</u>	<u>393</u>	<u>394</u>
SiO ₂	19.33	15.37	13.01	16.19	15.82	17.52
Al ₂ O ₃	7.87	7.83	7.79	7.48	12.2	13.52
Li ₂ O	4.61	4.58	4.06	3.66	3.58	3.17
CaO	8.66	8.6	8.56	6.87	---	---
ZnO	8.37	8.32	8.29	9.96	9.73	7.58
MgO	8.28	8.25	8.2	7.4	9.64	16.03
B ₂ O ₃	8.07	12.46	15.07	9.38	9.16	10.14
ZrO ₂	---	---	---	6.03	7.36	---
CuO	---	---	---	---	---	2.06
Y ₂ O ₃	34.86	34.64	34.53	33.15	32.42	29.93
	<u>395</u>	<u>396</u>	<u>397</u>	<u>398</u>	<u>399</u>	<u>400</u>
SiO ₂	14.45	38.78	38.46	18.49	18.0	18.98
Al ₂ O ₃	12.27	21.73	40.75	10.05	9.78	---
Li ₂ O	3.6	4.28	4.98	3.68	2.51	3.78
CaO	---	---	---	8.97	6.73	10.63
ZnO	9.78	---	---	---	5.85	6.16
MgO	9.69	8.66	16.09	7.92	7.73	8.13
B ₂ O ₃	8.37	---	---	11.99	11.69	12.33
ZrO ₂	14.8	26.48	---	---	---	---
Y ₂ O ₃	27.13	---	---	38.93	37.88	39.96

Table II (Cont'd)

<u>Actual Ingredient</u>	<u>401</u>	<u>402</u>	<u>403</u>	<u>404</u>	<u>405</u>	<u>406</u>
SiO ₂	18.27	18.04	17.45	17.62	30.65	24.85
Al ₂ O ₃	9.9	9.8	9.47	9.56	14.65	11.97
Li ₂ O	1.81	1.79	1.74	1.74	0.22	0.18
CaO	8.16	6.06	3.9	1.97	---	---
MgO	9.77	9.67	9.33	9.43	---	---
B ₂ O ₃	11.82	11.7	11.32	11.42	---	---
La ₂ O ₃	---	---	---	---	---	60.14
CuO	1.93	1.91	1.34	1.86	---	---
TiO ₂	---	2.87	2.78	2.82	---	---
BeO	---	---	---	0.88	3.6	2.94
Fe ₂ O ₃	---	---	5.55	5.61	---	---
Y ₂ O ₃	38.26	37.93	36.7	37.03	51.1	---
	<u>407</u>	<u>408</u>	<u>409</u>	<u>410</u>	<u>411</u>	<u>412</u>
SiO ₂	38.16	30.95	25.85	31.87	31.95	24.55
Al ₂ O ₃	10.79	11.97	13.48	18.03	18.06	15.62
ZnO	8.61	9.55	10.73	---	---	---
MgO	---	---	---	7.13	7.14	6.18
La ₂ O ₃	---	38.2	43.11	---	38.45	49.9
BeO	7.93	7.33	6.88	4.42	4.43	3.83
Re ₂ O ₃	34.6	---	---	38.72	---	---
	<u>413</u>	<u>414</u>	<u>415</u>	<u>416</u>	<u>417</u>	<u>418</u>
SiO ₂	42.78	29.24	31.63	37.2	39.24	38.9
Al ₂ O ₃	12.09	12.38	---	16.84	22.22	21.95
Li ₂ O	---	---	5.09	1.24	1.31	1.29
CaO	---	---	9.55	---	---	---
ZnO	9.64	9.89	---	---	---	---
MgO	---	---	6.85	8.32	8.78	8.69
La ₂ O ₃	---	39.65	---	---	---	---
BeO	8.89	9.11	8.5	5.16	5.45	6.47
Y ₂ O ₃	26.78	---	38.47	31.06	23.05	22.75

Table II (Cont'd)

<u>Actual Ingredient</u>	<u>419</u>	<u>420</u>	<u>421</u>	<u>422</u>	<u>423</u>	<u>424</u>
SiO ₂	34.2	34.55	35.68	34.78	34.07	31.6
Al ₂ O ₃	20.73	16.73	14.4	13.28	13.0	21
Li ₂ O	1.2	1.23	1.27	2.16	0.85	---
CaO	---	---	---	---	---	15.9
ZnO	---	3.34	---	---	3.46	---
MgO	8.19	8.28	11.38	10.5	10.29	10.5
ZrO ₂	---	---	---	---	---	10.5
BeO	5.08	5.13	5.31	6.51	6.38	10.5
Y ₂ O ₃	30.62	30.87	31.94	32.66	32.0	---
	<u>425</u>	<u>426</u>	<u>427</u>	<u>428</u>	<u>429</u>	<u>430</u>
SiO ₂	52.4	13.58	17.20	12.42	12.71	24.64
Al ₂ O ₃	14.3	23.00	13.12	13.55	13.85	8.37
Li ₂ O	---	4.12	4.71	5.74	4.52	---
CaO	---	12.68	11.34	13.27	12.71	---
ZnO	---	---	---	---	---	6.67
MgO	20.9	9.11	5.76	9.52	6.09	---
B ₂ O ₃	---	---	9.95	6.19	6.31	---
La ₂ O ₃	---	---	---	---	---	26.73
BeO	12.4	5.65	5.72	5.92	9.82	6.16
Y ₂ O ₃	---	31.92	32.30	33.40	34.07	---
Nd ₂ O ₃	---	---	---	---	---	27.62
	<u>431</u>	<u>432</u>	<u>433</u>	<u>434</u>	<u>435</u>	<u>436</u>
SiO ₂	25.44	31.87	33.33	33.75	31.85	32.00
Al ₂ O ₃	8.64	10.82	10.92	11.22	13.82	13.89
Li ₂ O	---	---	---	---	2.43	2.44
CaO	---	---	---	---	1.52	1.53
ZnO	---	---	---	---	6.64	6.67
MgO	3.42	7.72	7.82	8.00	5.48	5.49
La ₂ O ₃	27.61	34.55	36.05	36.65	---	---
CuO	---	---	---	---	2.16	---
TiO ₂	---	---	---	---	---	2.10
BeO	6.36	7.96	8.13	8.20	5.09	5.12
Y ₂ O ₃	---	---	---	---	30.62	30.79
Nd ₂ O ₃	28.50	7.14	3.56	1.78	---	---

Table II (Cont'd)

<u>Actual Ingredient</u>	<u>437</u>	<u>438</u>	<u>439</u>	<u>440</u>	<u>441</u>	<u>442</u>
SiO ₂	32.30	23.50	33.13	32.66	31.48	34.00
Al ₂ O ₃	14.01	13.74	14.38	14.18	21.86	---
Li ₂ O	2.46	2.41	2.53	2.49	2.40	2.60
CaO	1.54	1.51	1.58	6.25	1.50	1.63
ZnO	6.73	6.57	---	---	---	11.82
MgO	5.56	5.43	9.10	5.62	5.41	9.37
B ₂ O ₃	---	9.38	---	---	---	---
CuO	---	2.14	2.24	2.22	2.14	2.31
BeO	5.12	5.06	5.29	5.22	5.03	5.45
Fe ₂ O ₃	4.39	---	---	---	---	---
Y ₂ O ₃	31.08	30.43	31.86	31.44	30.26	32.82
	<u>443</u>	<u>444</u>	<u>445</u>	<u>446</u>	<u>447</u>	<u>448</u>
SiO ₂	33.55	31.06	31.27	33.05	19.60	19.42
Al ₂ O ₃	---	13.52	13.62	8.64	---	---
Li ₂ O	2.46	2.38	2.39	2.53	3.92	2.70
CaO	6.42	7.45	1.50	1.58	10.97	10.88
ZnO	11.65	8.64	6.52	6.89	10.62	8.41
MgO	5.77	---	10.77	7.96	7.99	7.82
B ₂ O ₃	---	---	---	---	11.82	11.70
CuO	2.28	2.11	2.12	2.24	---	2.06
TiO ₂	---	---	---	---	---	2.07
BeO	5.37	4.98	1.67	5.29	---	---
Y ₂ O ₃	32.36	29.95	30.20	31.88	35.38	35.02
	<u>449</u>	<u>450</u>	<u>451</u>	<u>452</u>	<u>453</u>	<u>454</u>
SiO ₂	19.50	18.87	31.15	23.83	30.72	29.68
Al ₂ O ₃	---	7.67	---	---	---	7.62
Li ₂ O	2.72	2.62	3.91	2.99	2.54	2.45
CaO	10.92	6.33	10.89	8.41	10.82	6.28
ZnO	4.24	4.09	10.64	6.51	4.20	4.06
MgO	10.47	10.12	7.89	6.05	10.74	10.15
B ₂ O ₃	11.77	11.37	---	---	---	---
CuO	2.06	2.00	---	1.59	2.60	2.52
TiO ₂	3.12	3.05	---	2.40	3.91	3.78
Y ₂ O ₃	35.24	34.03	35.42	27.10	34.90	33.76

Table II (Cont'd)

<u>Actual Ingredient</u>	<u>455</u>	<u>456</u>	<u>457</u>	<u>458</u>	<u>459</u>	<u>460</u>
SiO ₂	23.36	22.85	23.05	22.70	20.68	20.38
Li ₂ O	6.96	6.82	6.88	4.51	5.75	5.26
CaO	13.07	12.80	8.61	12.70	10.79	9.87
ZnO	18.98	18.57	18.70	18.42	15.68	14.33
MgO	9.40	6.13	9.28	9.12	8.32	7.10
B ₂ O ₃	10.82	15.90	15.98	15.76	7.66	12.25
Y ₂ O ₃	17.57	17.18	17.28	17.02	31.06	30.59
	<u>461</u>	<u>462</u>	<u>463</u>	<u>464</u>	<u>465</u>	<u>466</u>
SiO ₂	23.74	20.18	20.27	23.45	19.49	24.78
Li ₂ O	6.13	4.68	5.23	7.01	5.42	7.42
CaO	11.50	9.78	9.183	13.13	10.19	13.92
ZnO	16.71	13.09	14.31	13.07	14.77	20.20
MgO	8.28	6.49	6.53	9.44	7.31	10.00
B ₂ O ₃	14.29	11.22	11.26	16.30	13.53	14.38
TiO ₂	---	4.30	2.16	---	---	---
Y ₂ O ₃	19.43	30.32	30.50	17.62	29.28	9.33

Table III
Experimental Glass Composition in Mol Percent

<u>Actual Ingredient</u>	<u>14</u>	<u>25</u>	<u>40</u>	<u>56</u>	<u>62</u>	<u>63</u>
SiO ₂	52.3	49.5	58.4	67.8	54.6	54.6
Al ₂ O ₃	18.7	20.4	20.9	---	15.2	15.6
MgO	29.2	11.1	16.3	---	29.2	28.9
La ₂ O ₃	---	---	---	---	---	0.95
Ce ₂ O ₃	---	---	4.53	---	1.0	---
BeO	---	17.8	---	---	---	---
Li ₂ O	---	---	---	26.8	---	---
P ₂ O ₅	---	---	---	0.37	---	---
ZnO	---	---	---	4.91	---	---
	<u>64</u>	<u>65</u>	<u>66</u>	<u>67</u>	<u>68</u>	<u>69</u>
SiO ₂	54.6	54.6	53.7	54.7	53.4	57.3
Al ₂ O ₃	15.5	15.6	15.3	15.3	18.3	14.6
MgO	28.8	28.9	28.3	29.3	28.8	28.0
Y ₂ O ₃	1.39	---	---	---	---	---
Sm ₂ O ₃	---	0.89	---	---	---	---
Ta ₂ O ₅	---	---	---	0.76	---	---
ZrO ₂	---	---	2.56	---	---	---
	<u>70</u>	<u>71</u>	<u>72</u>	<u>73</u>	<u>74</u>	<u>75</u>
SiO ₂	55.3	49.4	56.9	59.1	56.1	61.2
Al ₂ O ₃	12.6	14.1	15.1	8.66	9.6	---
MgO	29.3	36.5	25.4	26.4	30.0	---
CaO	---	---	---	---	---	21.2
Y ₂ O ₃	2.83	---	---	3.13	4.3	---
Ce ₂ O ₃	---	---	2.60	2.70	---	---
Na ₂ O	---	---	---	---	---	17.6

Table III (Cont'd)

<u>Actual Ingredient</u>	<u>76</u>	<u>77</u>	<u>82</u>	<u>83</u>	<u>97</u>	<u>98</u>
SiO ₂	61.9	61.2	54.3	42.9	65	55
Al ₂ O ₃	---	---	24.5	---	7	9
MgO	---	---	18.1	11.3	---	---
CaO	26.2	31.8	---	11.8	7	9
Ce ₂ O ₃	---	---	---	0.86	---	---
ZrO ₂	---	---	1.6	0.81	---	---
BeO	---	---	---	22.2	---	---
Na ₂ O	11.9	7.0	0.05	---	---	---
Li ₂ O	---	---	---	5.06	---	---
TiO ₂	---	---	---	5.06	---	---
K ₂ O	---	---	---	---	7	9
SrO	---	---	---	---	7	9
BaO	---	---	---	---	7	9
	<u>99</u>	<u>100</u>	<u>101</u>	<u>102</u>	<u>103</u>	<u>104</u>
SiO ₂	45	35	35	45	45	45
Al ₂ O ₃	11	13	21	11	11	11
K ₂ O	11	13	11	---	---	11
Li ₂ O	---	---	---	11	11	---
CaO	11	13	11	11	11	11
SrO	11	13	11	---	11	11
ZnO	---	---	---	11	---	---
BaO	11	13	11	---	---	---
MgO	---	---	---	11	11	11
	<u>105</u>	<u>106</u>	<u>107</u>	<u>108</u>	<u>109</u>	<u>127</u>
SiO ₂	45	35	55	65	35	60
Al ₂ O ₃	---	---	---	---	---	10
Y ₂ O ₃	11	13	9	7	21	10
Li ₂ O	11	13	9	7	11	---
CaO	11	13	9	7	11	---
ZnO	11	13	9	7	11	---
MgO	11	13	9	7	11	20

Table III (Cont'd)

<u>Actual Ingredient</u>	<u>128</u>	<u>129</u>	<u>130</u>	<u>131</u>	<u>132</u>	<u>133</u>
SiO ₂	70	50	60	70	50	60
Al ₂ O ₃	6.66	13.33	10	6.66	13.33	10
MgO	13.33	26.67	---	---	---	10
CaO	---	---	20	13.33	26.67	10
Y ₂ O ₃	10	10	10	10	10	10
	<u>134</u>	<u>135</u>	<u>136</u>	<u>137</u>	<u>138</u>	<u>139</u>
SiO ₂	60	54.31	53.31	51.31	47.31	39.31
Al ₂ O ₃	10	15.56	15.56	15.56	15.56	15.56
MgO	---	28.89	28.89	28.89	28.89	28.89
Y ₂ O ₃	10	---	---	---	---	---
BeO	20	---	---	---	---	---
La ₂ O ₃	---	1.00	2.00	4.00	8.00	16.00
	<u>140</u>	<u>141</u>	<u>142</u>	<u>143</u>	<u>144</u>	<u>145</u>
SiO ₂	47.31	39.31	43.0	31.0	10	40.0
Al ₂ O ₃	15.56	15.56	14.4	18	29	---
MgO	27.89	26.89	7.6	10	---	19.0
CaO	---	---	24	30	50	19.0
Y ₂ O ₃	---	---	10	10	10	10.0
La ₂ O ₃	8.00	16.00	---	---	---	---
Ce ₂ O ₃	1.00	2.00	1.00	1.00	1.00	1.0
ZrO ₂	---	---	---	---	---	1.0
TiO ₂	---	---	---	---	---	5.0
Li ₂ O	---	---	---	---	---	5.0
	<u>146</u>	<u>147</u>	<u>148</u>	<u>149</u>	<u>150</u>	<u>151</u>
Y ₂ O ₃	10.0	---	---	---	---	8.0
La ₂ O ₃	---	10.0	10.0	---	---	---
Ce ₂ O ₃	1.0	1.0	1.0	1.0	1.0	---
Sm ₂ O ₃	---	---	---	10.0	10.0	---
SiO ₂	40.0	40.0	40.0	40.0	40.0	49.4
CaO	16.5	19.0	16.5	20.0	17.5	---
MgO	16.5	19.0	16.5	19.0	16.5	36.5
ZrO ₂	1.0	1.0	1.0	---	---	---
TiO ₂	5.0	5.0	5.0	5.0	5.0	---
Li ₂ O	5.0	5.0	5.0	5.0	5.0	---
Al ₂ O ₃	5.0	---	5.0	---	5.0	6.1

Table III (Cont'd)

<u>Actual Ingredient</u>	<u>152</u>	<u>153</u>	<u>154</u>	<u>155</u>	<u>156</u>	<u>157</u>
SiO ₂	49.4	49.4	49.4	49.4	49.4	49.4
Al ₂ O ₃	6.1	6.1	6.1	7.05	12.1	7.05
MgO	36.5	36.5	36.5	36.5	36.5	36.5
La ₂ O ₃	8.0	---	---	---	---	---
Ce ₂ O ₃	---	8.0	---	---	---	---
Sm ₂ O ₃	---	---	8.0	---	---	---
Ta ₂ O ₅	---	---	---	7.05	---	---
Cr ₂ O ₃	---	---	---	---	2.0	---
V ₂ O ₃	---	---	---	---	---	7.05
	<u>158</u>	<u>159</u>	<u>160</u>	<u>161</u>	<u>162</u>	<u>163</u>
SiO ₂	49.4	57.4	57.4	57.4	49.4	49.4
Al ₂ O ₃	4.1	6.6	6.6	6.6	6.1	10.1
MgO	36.5	28.0	28.0	28.0	36.5	36.5
Y ₂ O ₃	5.0	8.0	---	---	---	---
La ₂ O ₃	5.0	---	8.0	---	---	---
Rare Earth Oxides	---	---	---	8.0	8.0	4.0
	<u>164</u>	<u>165</u>	<u>166</u>	<u>167</u>	<u>168</u>	<u>169</u>
SiO ₂	49.4	47.5	51.67	51.67	51.67	41.67
Al ₂ O ₃	---	7.2	23.0	16.0	16.0	19.0
MgO	36.6	12.0	18.33	15.83	15.83	18.33
CaO	---	12.0	---	---	---	---
Y ₂ O ₃	---	10.0	---	---	10.0	15.0
Li ₂ O	---	5.66	---	---	---	---
TiO ₂	---	5.66	---	---	---	---
Ce ₂ O ₃	---	---	---	10.0	---	---
V ₂ O ₅	---	---	7.0	6.5	6.5	6.0
Rare Earth Oxides	14.0	---	---	---	---	---
	<u>170</u>	<u>171</u>	<u>172</u>	<u>173</u>	<u>174</u>	<u>175</u>
SiO ₂	51.67	51.67	41.67	41.67	49.67	60
Al ₂ O ₃	5.0	5.0	16.0	16.0	16.0	5
MgO	18.33	18.33	15.83	15.83	13.83	20
Y ₂ O ₃	---	20.0	---	---	14.0	10
Ce ₂ O ₃	20.0	---	20.0	---	---	---
V ₂ O ₅	5.0	5.0	6.5	6.5	6.5	5.0
Sm ₂ O ₃	---	---	---	20.0	---	---

Table III (Cont'd)

<u>Actual Ingredient</u>	<u>176</u>	<u>177</u>	<u>178</u>	<u>179</u>	<u>180</u>	<u>181</u>
SiO ₂	70	39.31	47.31	39.31	31.0	10.0
Al ₂ O ₃	3.66	10.0	10.0	10.0	10.0	20.0
MgO	13.33	28.89	27.89	26.89	10.0	---
CaO	---	---	---	---	30.0	50.0
Y ₂ O ₃	10	---	---	---	10.0	10.0
Ce ₂ O ₃	---	---	1.00	2.00	1.00	1.00
V ₂ O ₅	3.0	5.56	5.56	5.56	8.00	9.00
La ₂ O ₃	---	16.0	8.0	16.0	---	---
	<u>182</u>	<u>183</u>	<u>184</u>	<u>185</u>	<u>186</u>	<u>187</u>
SiO ₂	40.0	40.0	40.0	40.0	40.0	40.0
Al ₂ O ₃	---	5.0	---	5.0	---	5.0
MgO	19.0	16.5	19.0	16.5	19.0	16.5
CaO	14.0	9.0	14.0	9.0	15.0	12.5
Y ₂ O ₃	10.0	10.0	---	---	---	---
Ce ₂ O ₃	1.0	1.0	1.0	1.0	1.0	1.0
Sm ₂ O ₃	---	---	---	---	10.0	10.0
La ₂ O ₃	---	---	10.0	10.0	---	---
V ₂ O ₅	5.0	5.0	5.0	5.0	5.0	5.0
ZrO ₂	1.0	1.0	1.0	1.0	---	---
TiO ₂	5.0	5.0	5.0	5.0	5.0	5.0
Li ₂ O	5.0	5.0	5.0	5.0	5.0	5.0
	<u>188</u>	<u>189</u>	<u>190</u>	<u>191</u>	<u>192</u>	<u>193</u>
SiO ₂	49.4	49.4	49.4	49.4	49.4	49.4
Al ₂ O ₃	6.1	6.1	6.1	6.1	6.1	6.1
MgO	30.5	30.5	30.5	30.5	30.5	28.5
Y ₂ O ₃	8.0	---	---	---	---	5.0
Ce ₂ O ₃	---	8.0	---	---	---	---
Sm ₂ O ₃	---	---	8.0	---	---	---
La ₂ O ₃	---	---	---	8.0	---	5.0
V ₂ O ₅	6.0	6.0	6.0	6.0	6.0	6.0
Rare Earths	---	---	---	---	8.0	---

Table III (Cont'd)

<u>Actual Ingredient</u>	<u>194</u>	<u>195</u>	<u>196</u>	<u>197</u>	<u>198</u>	<u>199</u>
La ₂ O ₃	12.68	11	---	---	---	---
ThO ₂	6.68	6	6	6	6.32	7
BaO	11.52	11	11	11	10.86	11
B ₂ O ₃	63.25	60	60	60	59.8	60
Ta ₂ O ₅	5.98	5	5	---	5.68	---
V ₂ O ₅	---	7	7	7	---	---
Y ₂ O ₃	---	---	11	11	17.25	17
ZrO ₂	---	---	---	5	---	5
	<u>200</u>	<u>201</u>	<u>202</u>	<u>203</u>	<u>204</u>	<u>205</u>
SiO ₂	48	48	48	51.5	50.5	50.5
Al ₂ O ₃	13.33	13.33	13.33	---	---	---
MgO	26.67	26.67	26.67	36.5	36.5	36.5
Y ₂ O ₃	6	6	---	12	12	---
La ₂ O ₃	6	---	6	---	---	12
Ce ₂ O ₃	---	6	6	---	1.0	1.0
	<u>206</u>	<u>207</u>	<u>208</u>	<u>209</u>	<u>210</u>	<u>211</u>
SiO ₂	50	46	50	48	48	89
Al ₂ O ₃	13.33	13.33	13.33	13.33	13.33	---
MgO	---	26.67	26.67	26.67	26.67	---
Y ₂ O ₃	10	14	10	10	---	---
La ₂ O ₃	---	---	---	---	10	---
Ce ₂ O ₃	---	---	---	2.0	2.0	---
CaO	26.67	---	---	---	---	---
BaO	---	---	---	---	---	11
	<u>212</u>	<u>213</u>	<u>214</u>	<u>215</u>	<u>216</u>	<u>217</u>
SiO ₂	82	77	60	44.8	7.8	---
Al ₂ O ₃	---	3	6	---	34.6	35.7
MgO	---	---	34	4.52	---	---
CaO	---	---	---	32.1	57.8	59.3
BaO	18	---	---	2.35	---	5.0
La ₂ O ₃	---	20	---	---	---	---
TiO ₂	---	---	---	11.95	---	---
ZrO ₂	---	---	---	4.37	---	---

Table III (Cont'd)

<u>Actual Ingredient</u>	<u>218</u>	<u>219</u>	<u>220</u>	<u>221</u>	<u>222</u>	<u>223</u>
SiO ₂	12.65	6.48	3.35	---	---	---
Al ₂ O ₃	31.25	37.20	38.45	40.3	---	---
MgO	---	2.59	2.68	2.80	---	---
CaO	51.35	42.15	43.5	45.5	---	---
BaO	4.93	2.59	2.68	2.80	---	---
Na ₂ O	---	4.86	5.02	5.25	---	---
K ₂ O	---	1.62	1.67	1.75	---	---
La ₂ O ₃	---	1.30	1.34	1.40	10.0	---
Fe ₂ O ₃	---	1.30	1.34	0.35	---	---
Ta ₂ O ₅	---	---	---	---	7.37	7.37
B ₂ O ₃	---	---	---	---	70.4	70.4
ThO ₂	---	---	---	---	12.3 ⁴	12.3 ⁴
Y ₂ O ₃	---	---	---	---	---	10.0
	<u>224</u>	<u>225</u>	<u>226</u>	<u>227</u>	<u>228</u>	<u>229</u>
La ₂ O ₃	13.1	---	33.0	---	---	---
Ta ₂ O ₅	4.83	4.83	16.20	16.20	15.35	14.02
B ₂ O ₃	43.8	43.8	---	---	---	---
ThO ₂	16.18	16.18	---	---	---	---
ZrO ₂	---	---	12.43	12.43	---	16.78
TiO ₂	---	---	38.42	38.42	84.65	69.1
LiVO ₃	22.13	22.13	---	---	---	---
Y ₂ O ₃	---	13.1	---	33.0	---	---
	<u>230</u>	<u>231</u>	<u>232</u>	<u>233</u>	<u>234</u>	<u>235</u>
La ₂ O ₃	12.92	---	---	---	---	---
Ta ₂ O ₅	6.33	---	---	---	---	---
B ₂ O ₃	60.35	---	---	---	---	---
ZrO ₂	20.45	---	---	---	---	---
SiO ₂	---	40	48	50	46	50
Al ₂ O ₃	---	14	13.33	13.33	10	10
MgO	---	36	26.67	26.67	30	30
Y ₂ O ₃	---	10	10	5	10	10
Ce ₂ O ₃	---	---	2	---	4	---
V ₂ O ₃	---	---	---	5	---	---

Table III (Cont'd)

<u>Actual Ingredient</u>	<u>236</u>	<u>237</u>	<u>238</u>	<u>239</u>	<u>240</u>	<u>241</u>
SiO ₂	43	45	45	30	30	30
Al ₂ O ₃	15	15	15	20	20	20
MgO	30	30	30	43	43	43
Y ₂ O ₃	10	10	5	5	—	—
Ce ₂ O ₃	2	—	—	2	7	—
V ₂ O ₃	—	—	5	—	—	—
La ₂ O ₃	—	—	—	—	—	7
	<u>242</u>	<u>243</u>	<u>247</u>	<u>248</u>	<u>249</u>	<u>250</u>
SiO ₂	10	8	40	35	30	40
Al ₂ O ₃	27.75	24	12	13	14	12
MgO	—	4	12	13	14	16
Y ₂ O ₃	—	10	—	—	—	—
Ce ₂ O ₃	4	4	—	—	—	—
La ₂ O ₃	4	—	—	—	—	—
CoO	4	4	—	—	—	—
CaO	46.25	42	12	13	14	12
Li ₂ O	4	—	12	13	14	8
ZrO ₂	—	4	—	—	—	—
ZnO	—	—	12	13	14	12
	<u>251</u>	<u>252</u>	<u>253</u>	<u>254</u>	<u>255</u>	<u>256</u>
SiO ₂	40	40	20	40	40	40
Al ₂ O ₃	12	12	16	—	—	12
Li ₂ O	4	6	16	12	12	12
CaO	12	18	16	12	12	—
ZnO	12	12	16	12	12	12
MgO	20	12	16	12	12	12
Y ₂ O ₃	—	—	—	12	—	12
La ₂ O ₃	—	—	—	—	12	—
	<u>257</u>	<u>258</u>	<u>259</u>	<u>260</u>	<u>261</u>	<u>262</u>
SiO ₂	40	54.2	54.7	64.9	65.3	67.3
Al ₂ O ₃	12	22.4	12.93	9.2	11.5	12.1
Li ₂ O	12	—	—	—	—	—
CaO	—	9.1	—	25.9	8.34	—
ZnO	12	—	—	—	—	—
MgO	12	12.1	18.90	—	14.92	3.9
La ₂ O ₃	12	—	—	—	—	—
CaF ₂	—	4.0	12.93	—	—	—
BeO	—	—	—	—	—	16.8

Table III (Cont'd)

<u>Actual Ingredient</u>	<u>263</u>	<u>264</u>	<u>265</u>	<u>266</u>	<u>267</u>	<u>268</u>
B ₂ O ₃	---	3.32	---	---	---	---
BaO	---	23.83	---	---	---	---
TiO ₂	---	71.8	---	---	---	---
Na ₂ O	---	1.1	---	---	---	---
SiO ₂	67.3	---	40	25	30	25
Al ₂ O ₃	12.1	---	12	15	14	14
MgO	3.9	---	12	15	14	14
La ₂ O ₃	16.8	---	12	---	---	---
ZnO	---	---	12	15	---	14
Li ₂ O	---	---	12	15	14	14
CaO	---	---	---	15	14	14
BeO	---	---	---	---	14	---
ZrO ₂	---	---	---	---	---	5
	<u>269</u>	<u>270</u>	<u>271</u>	<u>272</u>	<u>273</u>	<u>274</u>
SiO ₂	20	25	25	25	30	25
Al ₂ O ₃	14	8	8	---	12	15
Li ₂ O	14	15	15	15	12	15
CaO	14	15	15	15	12	---
MgO	14	15	15	15	12	15
Y ₂ O ₃	---	7	---	---	---	---
La ₂ O ₃	---	---	7	15	---	---
BeO	---	---	---	15	22	15
ZnO	14	15	15	---	---	15
ZrO ₂	5	---	---	---	---	---
CeO ₂	5	---	---	---	---	---
	<u>275</u>	<u>276</u>	<u>277</u>	<u>283</u>	<u>284</u>	<u>285</u>
SiO ₂	50	50	41.67	25	25	25
Al ₂ O ₃	8.33	8.33	8.33	8	8	12
Li ₂ O	---	8.33	8.33	15	15	12
La ₂ O ₃	8.33	8.33	8.33	7	7	12
BeO	25	25	25	---	---	---
ZnO	8.33	---	---	15	8	12
CeO ₂	---	---	8.33	---	---	---
CaO	---	---	---	2	2	---
MgO	---	---	---	15	15	12
B ₂ O ₃	---	---	---	10.5	10.5	15
Ce ₂ O ₃	---	---	---	0.5	0.5	---
ZrO ₂	---	---	---	2	2	---
CuO	---	---	---	---	7	---

Table III (Cont'd)

<u>Actual Ingredient</u>	<u>286</u>	<u>287</u>	<u>288</u>	<u>289</u>	<u>290</u>	<u>291</u>
SiO ₂	30	20	25	25	25	25
Al ₂ O ₃	12	12	12	12	8	12
Li ₂ O	12	12	12	12	15	12
ZnO	12	12	6	12	15	12
MgO	12	12	12	12	15	12
B ₂ O ₃	10	20	15	9	15	15
La ₂ O ₃	12	12	12	12	---	---
CuO	---	---	6	6	---	---
Y ₂ O ₃	---	---	---	---	7	12
	<u>292</u>	<u>293</u>	<u>294</u>	<u>295</u>	<u>296</u>	<u>297</u>
SiO ₂	25	25	15	20	20	25
Al ₂ O ₃	12	8	8	8	8	8
Li ₂ O	12	12	15	15	15	15
CaO	---	15	15	15	10	15
ZnO	12	12	15	15	15	8
MgO	12	12	15	15	15	15
B ₂ O ₃	15	9	10	15	10	---
La ₂ O ₃	12	---	---	---	---	---
CuO	---	---	---	---	---	7
Y ₂ O ₃	---	7	7	7	7	7
	<u>298</u>	<u>299</u>	<u>300</u>	<u>301</u>	<u>302</u>	<u>303</u>
SiO ₂	25	25	25	25	25	25
Al ₂ O ₃	8	8	---	8	8	8
Li ₂ O	15	15	15	15	8	15
CaO	15	15	15	15	15	8
ZnO	8	---	15	15	15	15
MgO	15	15	15	15	15	15
B ₂ O ₃	---	15	15	---	---	---
La ₂ O ₃	7	7	---	---	---	---
CuO	7	---	---	---	7	7
Y ₂ O ₃	---	---	---	---	7	7
Rare Earth Oxide	---	---	---	7	---	---

Table III (Cont'd)

<u>Actual Ingredient</u>	<u>304</u>	<u>305</u>	<u>306</u>	<u>307</u>	<u>308</u>	<u>309</u>
SiO ₂	35	35	35	25	25	45
Al ₂ O ₃	15	15	15	8	8	10
Li ₂ O	---	---	---	13	15	10
CaO	---	---	---	15	15	---
ZnO	10	5	5	8	6	---
MgO	30	30	30	15	15	---
CuO	---	5	---	7	5	---
Y ₂ O ₃	10	10	10	7	7	---
CoO	---	---	5	2	4	---
BeO	---	---	---	---	---	25
La ₂ O ₃	---	---	---	---	---	10
	<u>310</u>	<u>311</u>	<u>312</u>	<u>313</u>	<u>314</u>	<u>315</u>
SiO ₂	40	35	30	25	40	40
Al ₂ O ₃	12	14	16	18	12	10
Li ₂ O	12	14	16	18	12	10
CaO	---	---	---	---	---	10
MgO	---	---	---	---	25	10
BeO	25	25	25	25	---	10
La ₂ O ₃	11	12	13	14	11	10
	<u>316</u>	<u>317</u>	<u>318</u>	<u>319</u>	<u>320</u>	<u>321</u>
SiO ₂	40	40	45	45	45	40
Al ₂ O ₃	10	10	15	15	15	15
Li ₂ O	10	10	---	---	---	---
ZnO	10	---	---	---	---	---
MgO	10	10	30	30	30	30
BeO	10	10	10	---	---	---
Y ₂ O ₃	---	---	---	---	---	15
La ₂ O ₃	10	10	---	10	---	---
ZrO ₂	---	---	---	---	10	---
CuO	---	10	---	---	---	---

Table III (Cont'd)

<u>Actual Ingredient</u>	<u>322</u>	<u>323</u>	<u>324</u>	<u>325</u>	<u>326</u>	<u>327</u>
SiO ₂	35	35	30	30	30	30
Al ₂ O ₃	15	15	12	10	10	10
Li ₂ O	---	10	12	10	10	10
ZnO	10	---	12	10	10	10
MgO	30	30	24	20	20	20
BeO	10	10	10	10	10	---
Y ₂ O ₃	---	---	---	10	---	10
ZrO ₂	---	---	---	---	10	10
	<u>328</u>	<u>329</u>	<u>330</u>	<u>331</u>	<u>332</u>	<u>333</u>
SiO ₂	30	30	39	39	39	39
Al ₂ O ₃	10	10	12	12	12	12
Li ₂ O	10	10	---	---	---	---
ZnO	10	10	12	12	12	12
MgO	20	20	---	---	25	25
Y ₂ O ₃	10	10	---	12	---	12
La ₂ O ₃	10	---	12	---	12	---
ZrO ₂	---	10	---	---	---	---
BeO	---	---	25	25	---	---
	<u>334</u>	<u>335</u>	<u>336</u>	<u>337</u>	<u>338</u>	<u>339</u>
SiO ₂	35	35	35	30	30	30
Al ₂ O ₃	15	15	15	15	15	15
MgO	30	---	---	30	30	---
Y ₂ O ₃	---	---	10	12.5	---	---
La ₂ O ₃	10	10	---	---	12.5	12.5
BeO	---	30	30	---	---	30
ZnO	10	10	10	12.5	12.5	12.5
	<u>340</u>	<u>341</u>	<u>342</u>	<u>343</u>	<u>344</u>	<u>345</u>
SiO ₂	25	30	30	30	45	45
Al ₂ O ₃	10	10	10	10	15	15
MgO	20	20	10	10	15	---
Y ₂ O ₃	10	---	10	---	10	10
La ₂ O ₃	---	10	---	10	---	---
BeO	15	10	20	20	15	30
ZnO	10	10	10	10	---	---
Li ₂ O	10	10	10	10	---	---

Table III (Cont'd)

<u>Actual Ingredient</u>	<u>346</u>	<u>347</u>	<u>348</u>	<u>349</u>	<u>350</u>	<u>351</u>
SiO ₂	20	50	50	50	24	36
Al ₂ O ₃	10	8.33	8.33	8.33	13	11
MgO	10	---	---	---	13	11
Y ₂ O ₃	10	---	---	---	---	---
La ₂ O ₃	---	8.33	8.33	---	---	---
ZrO ₂	10	---	8.33	---	---	---
BeO	20	25	25	25	24	20
ZnO	10	8.33	---	8.33	---	---
Li ₂ O	10	---	---	---	13	11
CaO	---	---	---	---	13	11
CeO ₂	---	---	---	8.33	---	---
	<u>352</u>	<u>353</u>	<u>354</u>	<u>355</u>	<u>356</u>	<u>357</u>
SiO ₂	25	30	35	39	39	39
Al ₂ O ₃	10	10	10	12	12	12
MgO	15	10	5	24	24	24
Y ₂ O ₃	10	10	10	10	---	3
ZrO ₂	10	10	10	---	10	---
BeO	10	10	10	---	---	---
ZnO	10	10	10	6	6	6
Li ₂ O	10	10	10	6	6	6
CeO ₂	---	---	---	3	3	---
Rare Earth Mix	---	---	---	---	---	10
	<u>358</u>	<u>359</u>	<u>360</u>	<u>361</u>	<u>362</u>	<u>363</u>
SiO ₂	39	39	39	39	39	39
Al ₂ O ₃	12	12	12	12	12	12
MgO	24	24	24	24	24	24
Y ₂ O ₃	10	10	10	10	10	10
ZnO	6	5	6	6	6	---
Li ₂ O	6	5	6	6	6	6
V ₂ O ₃	3	---	---	---	---	---
WO ₃	---	5	---	---	---	---
CoO	---	---	3	---	---	---
Fe ₂ O ₃	---	---	---	3	---	---
B ₂ O ₃	---	---	---	---	---	6
CuO	---	---	---	---	3	3

Table III (Cont'd)

<u>Actual Ingredient</u>	<u>364</u>	<u>365</u>	<u>366</u>	<u>367</u>	<u>368</u>	<u>369</u>
SiO ₂	39	39	39	39	39	39
Al ₂ O ₃	12	12	12	12	12	12
MgO	24	24	---	12	6	---
BeO	10	6	25	25	25	25
Y ₂ O ₃	---	10	---	10	10	10
ZrO ₂	---	---	12	---	---	---
Ce ₂ O ₃	3	3	3	2	2	2
ZnO	6	---	9	---	6	---
Li ₂ O	6	6	---	---	---	---
	<u>370</u>	<u>371</u>	<u>372</u>	<u>373</u>	<u>374</u>	<u>375</u>
SiO ₂	39	39	39	39	39	25
Al ₂ O ₃	12	12	12	12	12	6
MgO	---	4	---	---	---	16
BeO	25	25	25	25	25	---
Y ₂ O ₃	10	10	---	10	10	---
La ₂ O ₃	---	---	2	---	---	12
Ce ₂ O ₃	2	2	---	2	---	---
Rare Earth Mix	---	---	10	---	---	---
ZnO	6	4	12	---	6	8
Li ₂ O	---	---	---	6	6	12
B ₂ O ₃	---	---	---	---	---	9
CuO	---	---	---	---	2	---
CaO	6	4	---	6	---	12
	<u>376</u>	<u>377</u>	<u>378</u>	<u>379</u>	<u>380</u>	<u>381</u>
SiO ₂	20	17	24	24	24	24
Al ₂ O ₃	6	6	6	3	---	3
MgO	16	16	16	16	16	16
ZrO ₂	---	---	12	12	12	12
La ₂ O ₃	12	12	---	3	6	---
ZnO	8	8	8	8	8	8
Li ₂ O	12	12	12	12	12	12
B ₂ O ₃	14	17	10	10	10	10
CaO	12	12	12	12	12	12
CuO	---	---	---	---	---	3

Table III (Cont'd)

<u>Actual Ingredient</u>	<u>382</u>	<u>383</u>	<u>384</u>	<u>385</u>	<u>386</u>	<u>387</u>
SiO ₂	24	24	24	2.5	2.5	10
Al ₂ O ₃	3	3	3	52	47	---
Li ₂ O	12	12	12	8	8	8
CaO	12	12	12	29.5	26.5	30
ZnO	8	8	8	4	4	4
MgO	16	16	16	4	4	2
B ₂ O ₃	10	10	10	---	---	6
La ₂ O ₃	---	---	---	---	4	4
ZrO ₂	12	12	---	---	---	---
TiO ₂	---	3	---	---	---	2
BeO	---	---	3	---	---	34
Fe ₂ O ₃	3	---	---	---	4	---
Re ₂ O ₃	---	---	12	---	---	---
	<u>388</u>	<u>389</u>	<u>390</u>	<u>391</u>	<u>392</u>	<u>393</u>
SiO ₂	24	25	29	17	22	22
Al ₂ O ₃	---	6	6	6	6	10
Li ₂ O	12	12	12	12	10	10
CaO	12	12	12	12	10	---
ZnO	---	8	8	8	10	10
MgO	12	16	16	16	15	20
B ₂ O ₃	10	9	14	17	11	11
ZrO ₂	---	---	---	---	4	5
TiO ₂	4	---	---	---	---	---
BeO	14	---	---	---	---	---
Re ₂ O ₃	12	---	---	---	---	---
Y ₂ O ₃	---	12	12	12	12	12
	<u>394</u>	<u>395</u>	<u>396</u>	<u>397</u>	<u>398</u>	<u>399</u>
SiO ₂	22	20	45	40	25	25
Al ₂ O ₃	10	10	15	25	8	8
Li ₂ O	8	10	10	10	10	7
CaO	---	---	---	---	13	10
ZnO	7	10	---	---	---	6
MgO	30	20	15	25	16	16
B ₂ O ₃	11	10	---	---	14	14
ZrO ₂	---	10	15	---	---	---
CuO	2	---	---	---	---	---
Y ₂ O ₃	10	10	---	---	14	14

Table III (Cont'd)

<u>Actual Ingredient</u>	<u>400</u>	<u>401</u>	<u>402</u>	<u>403</u>	<u>404</u>	<u>405</u>
SiO ₂	25	25	25	25	25	49.3
Al ₂ O ₃	---	8	8	8	8	14.0
Li ₂ O	10	5	5	5	5	0.70
CaO	15	12	9	6	3	---
ZnO	6	---	---	---	---	---
MgO	16	20	20	20	20	---
B ₂ O ₃	14	14	14	14	14	---
CuO	---	2	2	2	2	---
TiO ₂	---	---	3	3	3	---
BeO	---	---	---	---	3	14.0
Fe ₂ O ₃	---	---	---	3	3	---
Y ₂ O ₃	14	14	14	14	14	22.0
	<u>406</u>	<u>407</u>	<u>408</u>	<u>409</u>	<u>410</u>	<u>411</u>
SiO ₂	49.3	50	45	39	45	45
Al ₂ O ₃	14.0	8.33	10	12	15	15
Li ₂ O	0.70	---	---	---	---	---
La ₂ O ₃	22.0	---	10	12	---	10
BeO	14.0	25	25	25	15	15
ZnO	---	8.33	10	12	---	---
MgO	---	---	---	---	15	15
Re ₂ O ₃	---	8.33	---	---	10	---
	<u>412</u>	<u>413</u>	<u>414</u>	<u>415</u>	<u>416</u>	<u>417</u>
SiO ₂	40	50	40	34	45	45
Al ₂ O ₃	15	8.33	10	---	12	15
Li ₂ O	---	---	---	11	3	3
CaO	---	---	---	11	---	---
ZnO	---	8.33	10	---	---	---
MgO	15	---	---	11	15	15
La ₂ O ₃	15	---	10	---	---	---
BeO	15	25	30	22	15	15
Y ₂ O ₃	---	8.33	---	11	10	7

Table III (Cont'd)

<u>Actual Ingredient</u>	<u>418</u>	<u>419</u>	<u>420</u>	<u>421</u>	<u>422</u>	<u>423</u>
SiO ₂	45	42	42	42	40	40
Al ₂ O ₃	15	15	12	10	9	9
Li ₂ O	3	3	3	3	5	2
ZnO	---	---	3	---	---	3
MgO	12	15	15	20	18	18
BeO	18	15	15	15	18	18
Y ₂ O ₃	7	10	10	10	10	10
	<u>424</u>	<u>425</u>	<u>426</u>	<u>427</u>	<u>428</u>	<u>429</u>
SiO ₂	28.8	42.9	16	20	14	14
Al ₂ O ₃	11.6	7.0	16	9	9	9
Li ₂ O	---	---	10	11	13	10
CaO	15.9	---	16	14	16	15
MgO	14.7	25.6	16	10	16	10
B ₂ O ₃	---	---	---	10	6	6
ZrO ₂	4.8	---	---	---	---	---
BeO	23.5	24.6	16	16	16	26
Y ₂ O ₃	---	---	10	10	10	10
	<u>430</u>	<u>431</u>	<u>432</u>	<u>433</u>	<u>434</u>	<u>435</u>
SiO ₂	41.66	41.66	41.66	41.66	41.66	39
Al ₂ O ₃	8.33	8.33	8.33	8.33	8.33	10
ZnO	8.33	---	---	---	---	6
MgO	---	8.33	15	15	15	10
La ₂ O ₃	8.33	8.33	8.33	8.33	8.33	---
BeO	25	25	25	25	25	15
Nd ₂ O ₃	8.33	8.33	1.66	.83	.42	---
Li ₂ O	---	---	---	---	---	6
CaO	---	---	---	---	---	2
CuO	---	---	---	---	---	2
Y ₂ O ₃	---	---	---	---	---	10

Table III (Cont'd)

<u>Actual Ingredient</u>	<u>436</u>	<u>437</u>	<u>438</u>	<u>439</u>	<u>440</u>	<u>441</u>
SiO ₂	39	39	29	39	39	39
Al ₂ O ₃	10	10	10	10	10	16
Li ₂ O	6	6	6	6	6	6
CaO	2	2	2	2	8	2
ZnO	6	6	6	---	---	---
MgO	10	10	10	16	10	10
B ₂ O ₃	---	---	10	---	---	---
CuO	---	---	2	2	2	2
TiO ₂	2	---	---	---	---	---
BeO	15	15	15	15	15	15
Fe ₂ O ₃	---	2	---	---	---	---
Y ₂ O ₃	10	10	10	10	10	10
	<u>442</u>	<u>443</u>	<u>444</u>	<u>445</u>	<u>446</u>	<u>447</u>
SiO ₂	39	39	39	39	39	25
Al ₂ O ₃	---	---	10	10	6	---
Li ₂ O	6	6	6	6	6	10
CaO	2	8	10	2	2	15
ZnO	10	10	8	6	6	10
MgO	16	10	---	20	14	15
B ₂ O ₃	---	---	---	---	---	13
CuO	2	2	2	2	2	---
BeO	15	15	15	5	15	---
Y ₂ O ₃	10	10	10	10	10	12
	<u>448</u>	<u>449</u>	<u>450</u>	<u>451</u>	<u>452</u>	<u>453</u>
SiO ₂	25	25	25	38	38	38
Al ₂ O ₃	---	---	6	---	---	---
Li ₂ O	7	6	6	10	7	6
CaO	15	15	9	15	15	15
ZnO	8	4	4	10	8	4
MgO	15	20	20	15	15	20
B ₂ O ₃	13	13	13	---	---	---
CuO	2	2	2	---	2	2
TiO ₂	3	3	3	---	3	3
Y ₂ O ₃	12	12	12	12	12	12

Table III (Cont'd)

<u>Actual Ingredient</u>	<u>454</u>	<u>455</u>	<u>456</u>	<u>457</u>	<u>458</u>	<u>459</u>
SiO ₂	38	25	25	25	25	25
Al ₂ O ₃	6	---	---	---	---	---
Li ₂ O	6	15	15	15	10	14
CaO	9	15	15	10	15	14
ZnO	4	15	15	15	15	14
MgO	20	15	10	15	15	115
CuO	2	---	---	---	---	---
TiO ₂	3	---	---	---	---	---
Y ₂ O ₃	12	5	5	5	5	10
B ₂ O ₃	---	10	15	15	15	8
	<u>460</u>	<u>461</u>	<u>462</u>	<u>463</u>	<u>464</u>	<u>465</u>
SiO ₂	25	25	25	25	25	25
MgO	13	13	12	12	15	14
Li ₂ O	13	13	12	13	15	14
CaO	13	13	13	13	15	14
ZnO	13	13	12	13	10	8
B ₂ O ₃	13	13	12	12	15	15
ZrO ₂	---	10	---	---	---	---
Y ₂ O ₃	10	---	10	10	5	10
TiO ₂	---	---	4	2	---	---
	<u>466</u>	<u>467</u>	<u>468</u>	<u>469</u>	<u>470</u>	
SiO ₂	25	25	25	25	25	
Al ₂ O ₃	---	8	8	8	8	
MgO	15	15	15	15	15	
Li ₂ O	15	10	7	5	15	
CaO	15	15	15	15	10	
ZnO	15	15	15	15	15	
B ₂ O ₃	12.5	5	8	10	5	
Y ₂ O ₃	2.5	7	7	7	7	

Cordierites in which calcia is substituted for magnesia. - Glasses resulting when calcia was substituted for magnesia in the cordierite-rare earth base are, in part, UARL numbers 130, 131, 132, 133, and 206. The chief effect of such a substitution was found to be a marked decrease in Young's modulus amounting in some cases to as much as a 25% reduction so these experiments were abandoned.

Cordierites in which calcia is substituted for alumina. - This series of glasses includes among others UARL numbers 215, 415, and 423. Such glasses could be rapidly chilled to form very nice water-white optical grade glass slugs approximately 1 1/4 in. in diameter and 1 3/8 in. thick but they were much too fluid to yield acceptable glass fibers. Since they did show both high modulus and high specific modulus, research in this area should be continued on a high priority basis.

Fluoborate optical glasses. - One of the types of glass not previously studied in connection with glass fiber formation is the fluoborate optical glass system (Refs. 46,47). These glasses contain little or no silica which as we have seen contributes to a low elastic modulus as well as very little alkali. UARL prepared two such glasses, 32 and 34, but neither appeared promising as a source of high modulus glass fibers so the research on these glasses was stopped.

Morey's glasses from acid-forming elements. - A distinctly different type of nonsilicate, nonalkali glass system not previously studied by glass fiber research investigators is built on acid forming elements having relatively high atomic weights. These glasses due to Morey (Ref. 48) and improved for manufacture by DePaoli (Ref. 49) may be made, for example, from a mixture of titania and tantalum oxide or from tantalum oxide, zirconia and lanthana. They typically include no alkali and little or no silica and are, therefore, too refractory to be melted in conventional glass fiber apparatus. Published data for those of these glasses produced by Eastman Kodak Company (Ref. 50) supports the idea that these glasses have elastic moduli considerably larger than conventional glasses and the lack of silica lends hope that such systems may not suffer atmospheric deterioration to the degree experienced by silicate glasses. UARL has attempted to melt a number of these glasses including, for example, UARL 2, 3, 5, 8, 9, 10, 20, 22, 23, 59, 60, 61, 222, 223, 224, 226, 227, 228, 229, and 230. In general, even though our furnaces attain temperatures of 1760°C (Super-kanthal elements) in air and platinum-40% rhodium crucibles were used, we could not obtain congruent melting despite rigid adherence to the prescriptions given in Refs. 48 and 49 and even for the few glasses of this type that we could successfully melt, the values obtained for Young's modulus were not outstanding. Our lack of success with these glasses is not fully understood at this time and would indicate the need for further research in this area.

Calcia-alumina glasses of National Bureau of Standards and Bausch and Lomb Optical Co. - The prior research efforts on the origination of new high modulus high strength glass fibers included a very significant effort by the National Bureau of Standards (Refs. 28-35) devoted to glasses whose primary constituents were calcia and alumina with very little silica. The stability of these glasses was subsequently improved by Hafner, et al (Ref. 51). UARL melted a number of these compositions centered around the binary eutectic composition in order to

check our modulus measurements against the published values of N.B.S. as well as to gain experience in melting high temperature glasses known to show rapid devitrification. We also tried a number of original compositional variants. Typical glasses in this series are UARL numbers 84, 85, 86, 93, 96, 215, 216, 217, 218, 242, 424, and 425. Many of these glasses were very difficult to chill in large discs, others have very high preparation temperatures, some were extremely fluid and could not be used for fiber formation. The two best compositions in this series are original N.B.S. compositions, our numbers 424 and 425, but we have not been able to draw fibers from these at high rates of speed as yet. Incidentally, the formation of glass from the binary calcia-alumina eutectic can be explained on the basis of Zachariasen's rules of glass formation according to Rawson (Ref. 52).

Calcia-yttria glasses. - Since yttria behaves in many ways as a chemical analogue of aluminum, a natural extension of research on calcia-alumina glasses is to form a similar series of calcia-yttria glass compositions again centered on the composition of the binary eutectic. UARL melts 88, 89, 90, 91, 92, 94, 95 and 243 were prepared on this basis but no unusual results were obtained and this approach has, therefore, been discontinued.

"Invert" analog glass systems. - Douglas (Ref. 93) summarizes the Zachariasen rules relating the probability of glass formation to the structure of the crystalline form of the material as

1. An oxygen atom is linked to not more than two atoms, A;
2. A must be small;
3. The oxygen polyhedra share corners with each other, not edges or faces and form three-dimensional networks;
4. At least three corners in each oxygen polyhedra must be shared. Exceptions to all of these rules are now known and attention must be turned to the kinetics of the problem. The quantitative relation of the kinetic behavior to structure is an immense task.

The very new UARL experimental glasses considered in this section of the report belong to a region of glass compositions analogous to Stevells "invert" glasses and in contrast, to almost all of the glasses considered earlier their formation cannot be explained by Zachariasen's three-dimensional network concept.

The concept developed by J. M. Stevells and his associates from 1954 on was that by a proper combination of oxides, stable metasilicate glasses could be obtained. A typical example cited by Stevells is 50 mol % SiO₂ and 12.5 mol % of the four materials Na₂O, K₂O, CaO, BaO. Dr. Stevells explained this "anomalous" case of glass formation by saying that "by choosing a batch with a great number of network modifiers the 'glue' between the chains is so irregular that crystallization is prevented." Obviously, by using a combination of alkali oxides and a combination of alkaline earth oxides as preferred by Stevells, the liquidus temperature can be lowered and the field of glass formation can be increased.

Stevels' "invert" glasses comprised silica, two or more monovalent oxides, usually Na_2O and K_2O , and two or more alkaline earth oxides. The UARL glasses, on the other hand, although analogous to Stevels' invert glasses, consist of silica, lithia, two or more divalent oxides or fluorides, one or more trivalent oxides, and may include a second tetravalent oxide or a pentavalent oxide. This combination of divalent and trivalent oxides has proven equally effective in blocking crystallization while yielding higher moduli.

Weyl (Ref. 53) states further that Trap and Stevels characterized the coherence of their silicate glasses by a structural parameter Y denoting the average number of bridging ions per SiO_4^{4-} tetrahedron. This parameter may be calculated from the expression

$$Y = 6 - \frac{200}{P} \quad \text{where } P = \text{mol \% SiO}_2$$

so that when $P = 33 \frac{1}{3}$, $Y = 0$ and SiO_4^{4-} groups are isolated; when $P = 40\%$, $Y = 1$ and on the average SiO_4^{4-} groups appear in pairs. Commercial silicate glasses, on the other hand, have Y values between 3.0 and 3.5 in agreement with the Zachariasen rules for stable glass formation which state that a stable silicate glass should consist of SiO_4^{4-} tetrahedra sharing at least three of their corners with other SiO_4^{4-} tetrahedra. On the other hand, the "invert" glasses developed by Trap and Stevels have Y values lower than 2.0 in direct contradiction of the accepted rules for stable glass formation.

When the glass composition was changed to lower and lower SiO_2 concentrations, Trap and Stevels (Ref. 53) found that some properties such as thermal expansivity, electrical deformation losses, and viscosity go through maxima or minima reaching extreme values as the parameter Y passes through the value 2.0. It is the feeling at this laboratory, UARL, that the modulus of elasticity may likewise achieve a decided maximum. However, extensive research with the "invert" glasses in the first eight quarters of this contract failed to yield any marked change in modulus. The ninth and tenth quarters, however, yielded a sixty percent increase in modulus while research in the eleventh quarter resulted in an invert glass with an elastic modulus in excess of twenty million psi as will be shown in a later section and recent quarters have produced another dozen "invert" glasses with equally high or higher moduli.

In Tables I, II, and III there are many UARL invert analogue glasses. For example, UARL compositions 266 through 277, 283 through 302, 309 through 318, 322 through 343, and 346 through 349 may be considered typical UARL invert analogue glasses. Table XXXV shows that UARL 329, a nontoxic "invert" analogue glass, has a measured Young's modulus of 20.7 million psi and a specific modulus of 189 million inches, while 337, also a nontoxic composition, yields corresponding numbers of 20.7 million psi and 147 million inches. When beryllia is added to the "invert" analogue glasses these numbers are UARL 325 with a Young's

modulus of 20.2 million psi and 158 million inches; for 331, 20.9 and 158, for 336, 21.0 and 166; for 340, 20.9 and 163; for 343, 19.4 and 140; for 347, 21.6 and 164; for 350, 19.8 and 197; and for 352, 20.0 and 146. In short, at this time the UARL invert analogue glass compositions seem to be the most promising of the glasses studied for the purposes of obtaining high modulus and high specific modulus.

Role of microstructure in two-phase systems. - Up to the year 1952, it was customary to think of glass as a homogeneous material but the application of electron microscopy to glass research has greatly altered our concept concerning the homogeneity of glass (Refs. 53-73). For example, in a number of cases the melting of glasses is accompanied by the appearance of opalescence due to the formation of small drop-shaped regions of a separate phase. This phenomenon depends on the composition since any phase separation of this type has two aspects, namely, the equilibrium or decreasing compatibility of a substance and the rate of nucleation. According to Weyl (Ref. 53), the higher the temperature of a molten glass, the greater is its solvent power for noble metals such as Ag and Au, for sulfides and selenides like CdS and CdSe, and for oxides containing either cations with a higher charge than silicon (P^{5+} , W^{6+}) or cations too large to fit into the tetrahedral structure of the glass (Sn^{4+} , Ti^{4+}). The quantity of a compound that becomes compatible in the melting range of silicate glasses varies widely. It amounts to only a fraction of one percent for gold and copper; it is of the order of one to five percent for sulfides, selenides, phosphates and titanates, and yet in some alkali-boric oxide-silica glasses the incompatibility utilized for making a Vycor glass amounts to nearly half the volume of the total glass. These glasses, with phase-separated droplets large enough to cause noticeable light scattering, are similar to colloidal solutions whose particles are detected and characterized by Faraday-Tyndall effect of light-scattering measurements.

A second group of glasses appears completely clear to the naked eye but, when examined by the electron microscope, they may be seen to have micelles or heterogeneities of the order of 200 to 600 angstroms. In this respect, Weyl (Ref. 53) states that there is a strong resemblance between this description of the structure of a glass developing shrinkage voids on cooling and a liquid structure changing in the direction toward a Frenkel-type liquid on heating. Both structures are characterized by fissures and by clusters or subcolloidal micelles. The permanency of the shrinkage voids causes the glass structure to approach that of a molecular liquid and one might compare the subcolloidal micelles and the walls of the matrix with molecules having strong intramolecular and weak intermolecular forces. Weyl (Ref. 53) feels that this picture explains why a fiber of a glass with a multitude of subcolloidal micelles such as the ternary eutectic in the system Li_2O - BaO - SiO_2 exhibits a flexibility or ductility resembling a molecular organic polymer. Vitreous silica with a much smaller number of flaws exhibits no ductility. This concept is also associated with the sonic spectra of glasses where goblets of vitreous silica cannot be made to give a pleasant ringing sound but goblets of glasses incorporating large amounts of lead oxide do and the electron microscope readily reveals the two-phase nature of the lead silicate glasses.

Glasses also exist which are completely transparent in the quenched state but which readily develop crystal nuclei under suitable heat treatment. Such glasses have been termed neo-ceramic by Janakiramarao (Ref. 73). The resulting opaque or translucent "neo-ceramic" product acquires properties different from those of the parent glass, but still retains some of the properties of its vitreous state such as conchoidal fracture and freedom from porosity. The fact that a "neo-ceramic" glass in its quenched state is thoroughly transparent and homogeneous even when examined under an ultramicroscope and displays no Tyndall effect but develops myriads of uniformly distributed nuclei of considerable size when heat treated, indicates that crystallites existed in the parent glass. On heat treatment, the incompatibility of the structural groups and the relative freedom of ions favor the growth of the crystallites or heterogeneous regions to form nuclei of micelles of definite chemical composition at the expense of the surrounding parent glass. The nucleation and growth of finely dispersed crystals from the glass matrix, particularly if these crystals are not cubic but have one dimension appreciably larger than other dimensions, allows the possibility of noteworthy amounts of crystal orientation or whisker growth in a glass fiber while being drawn from the melt.

To summarize then, UARL feels that the three types of microstructure demonstrated as existing in glass (Refs. 53-73) have not been considered in connection with the mechanical properties of such glasses even though studied in connection with other properties such as thermal expansion and electrical characteristics. It is proposed, therefore, that a basic investigation be carried out of the effect on mechanical properties such as elastic modulus and strength of the three basic types of structure found in two-phase glasses, that is, colloidal or light-scattering structures which may be isolated droplets of a second phase or continuous interpenetrating two-phase structures, micellar or subcolloidal structures which may be isolated droplets or crystals, and two-phase glasses containing one component in the crystalline and the other in the vitreous state. It is clear that such structures must definitely affect the mechanical properties of such glasses even though no prior systematic investigation of this nature has been carried out. It is not obvious, however, whether such structures strengthen glasses and enhance their moduli or act conversely although preliminary investigations at UARL reported below indicate a favorable trend. Such an investigation cannot be dismissed as academic in connection with the enhancement of the properties of glass fibers since R. J. Charles (Ref. 59) has shown that borosilicate glasses such as Vycor and Pyrex are fully phase-separated when rapidly cooled from the melt. Since this is believed to be a typical spinodal decomposition, like results would be anticipated for all spinodal decompositions and, indeed, preliminary experiments with fibers drawn from UARL experimental glass 278, whose composition is given below, confirm that two-phase separation as the fiber is drawn is indeed possible.

To examine the possibilities of this type of approach, UARL has carried out a brief preliminary study in which five experimental two-phase glasses selected on the basis of a preliminary examination of the literature (Refs. 53-73) were melted, heat treated, examined by electron microscopic procedures, and in

two cases Young's modulus was determined before and after heat treatment on circular rods formed by aspiration directly from the molten glass. The compositions of the five glasses are given in Table I in terms of the actual ingredients used in the batch.

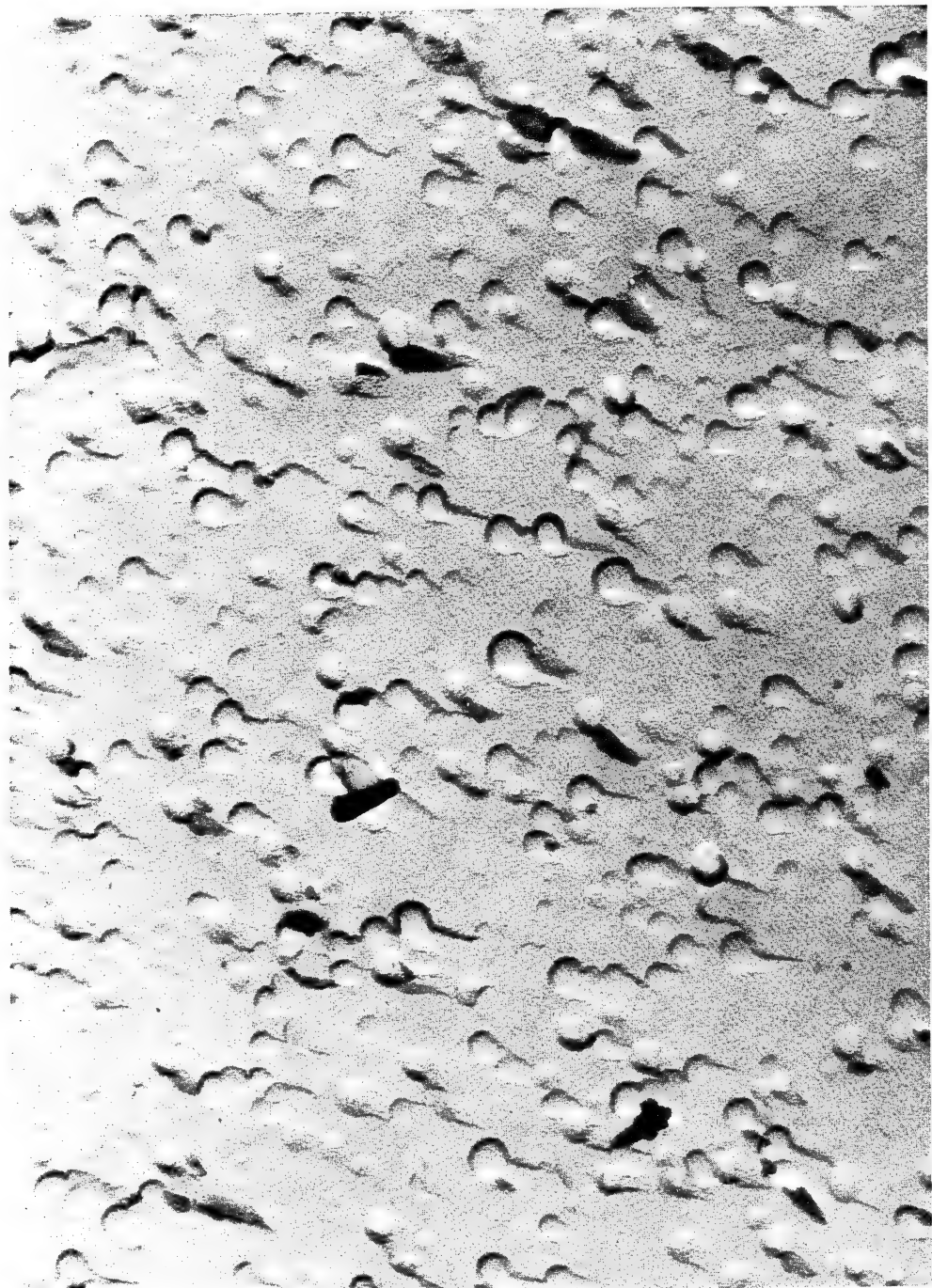
The modulus contained for these glasses is shown in Table I and summarized directly below

	<u>278</u>	<u>279</u>	<u>280</u>	<u>281</u>	<u>282</u>
Modulus (millions psi) as formed	13.29	11.96	5.56	6.42	5.14
Modulus (millions psi) after heat treatment	15.23	-----	6.23	-----	-----
Reference for Composition	61	61	72	63	63

The results of the electron microscopic investigations of these glasses are shown in Figs. 3-16. For the most part, except where specifically noted otherwise, the electron micrographs are taken at 20,000 diameters and comprise platinum preshadowed carbon replicas of fresh fracture surfaces except for Fig. 8, which is a replica of an "as cast" surface. Parlodion was flowed over the surface immediately upon fracture so that atmospheric exposure was held to a minimum.

Figures 3 through 5 are of fracture samples of UARL glass 278. This glass and its companion glass, UARL 279, studied below were selected from an investigation originally carried out by Hummel, Tien, and Kim (Ref. 61) of the opaque white glasses that can be obtained in the systems $\text{Li}_2\text{O}-\text{TiO}_2-\text{SiO}_2$ and $\text{CaO}-\text{TiO}_2-\text{SiO}_2$ from the separation of immiscible liquids. Their work represents one of the early attempts to exploit liquid opacification in place of the more usual practices of opacifying glasses, glazes, and enamels by the inclusion of gaseous or crystalline particles in the vitreous matrix. Figure 3 is an electron micrograph of a very dense opal glass successfully produced by liquid opacification incorporating droplets of a second immiscible glass in the first glass viewed as a vitreous matrix. This figure might well pass for the "classical" since 1956 phase separation photograph since it shows essentially only an abundance of droplets (spherical elevations) on an otherwise featureless background. Figure 4 is a fracture surface of the same glass after heat treatment at 800°C for ten hours. The glass is again a dense opal glass and the electron micrograph shows droplets of glass 2 now greatly increased in size again a background of glass 1 which has now undergone further decomposition as represented by the multitude of much smaller droplets present. In Fig. 5 the heat treatment has become sufficiently extended to produce lath-like crystals in a glassy matrix. The contrast of Fig. 3 with Fig. 4 would seem to confirm that phase separation of a second glass can enhance the modulus of the glass since, as noted in the table, glass 278 after heat treatment has a Young's modulus of 15.23 million psi in comparison to its original value of 13.29 million psi.

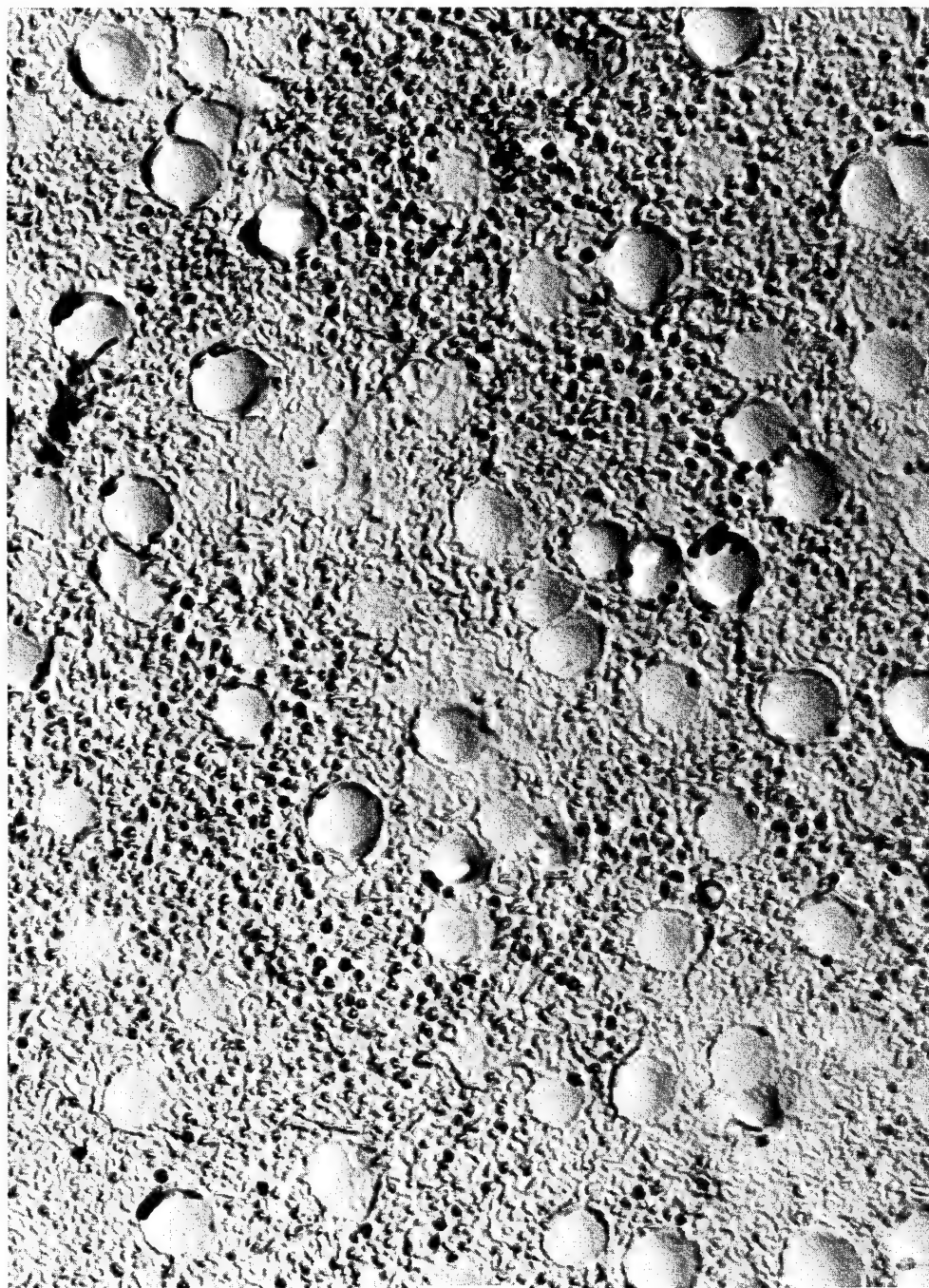
Figures 6-9 are concerned with UARL experimental glass 279. This glass, also taken from Hummel, et al (Ref. 61), is very different from 278. The substitution of zirconia for titania in the composition results in a glass which is transparent after melting and cooling to room temperature in place of the



278

20,000X

FIGURE 3. STRUCTURE IN GLASS



278a @ 800°C

20,000X

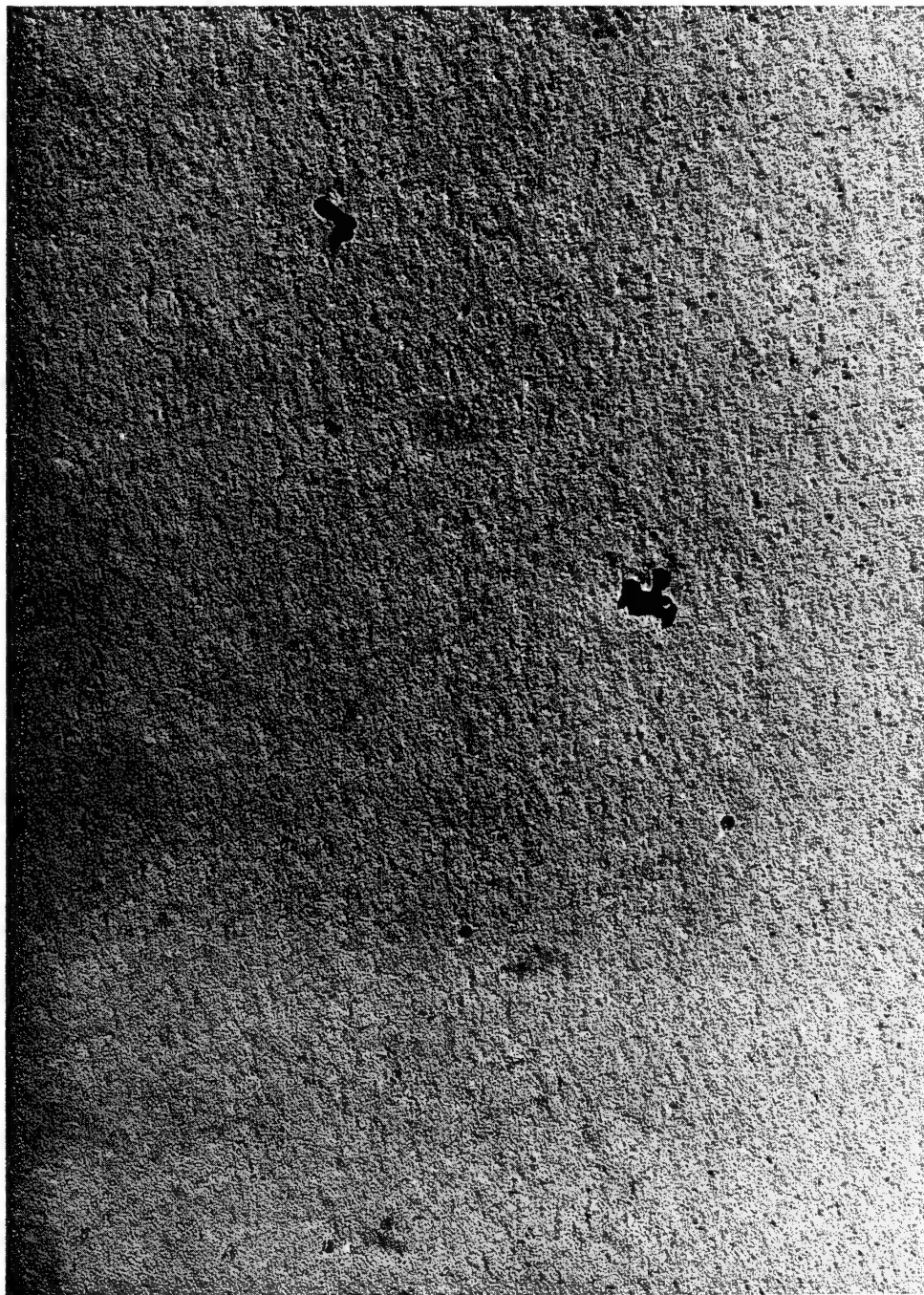
FIGURE 4. STRUCTURE IN GLASS



278b @ 800°C

20,000X

FIGURE 5. STRUCTURE IN GLASS



279a

30,000X

FIGURE 6. STRUCTURE IN GLASS



FIGURE 7. STRUCTURE IN GLASS

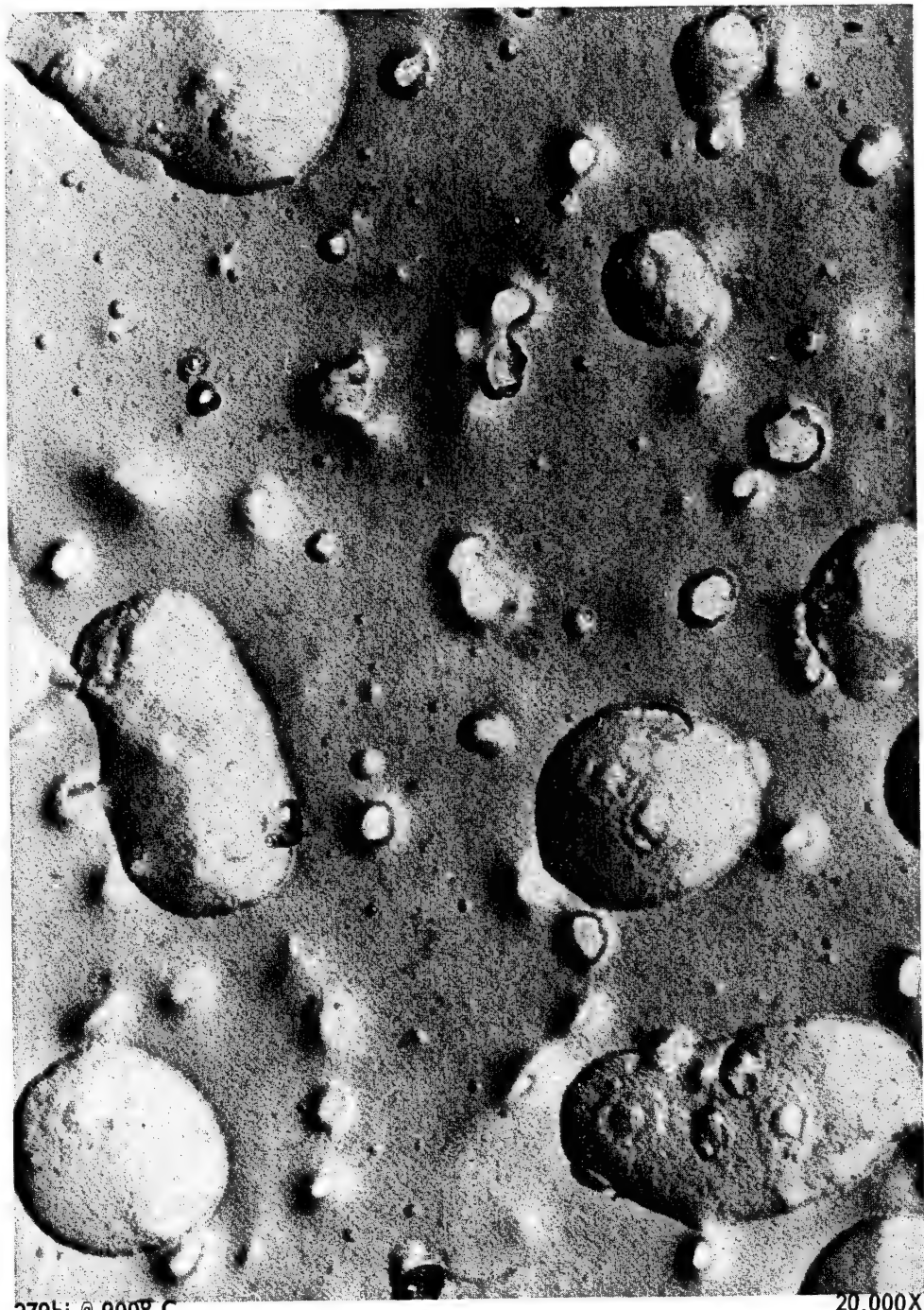


FIGURE 8. STRUCTURE IN GLASS



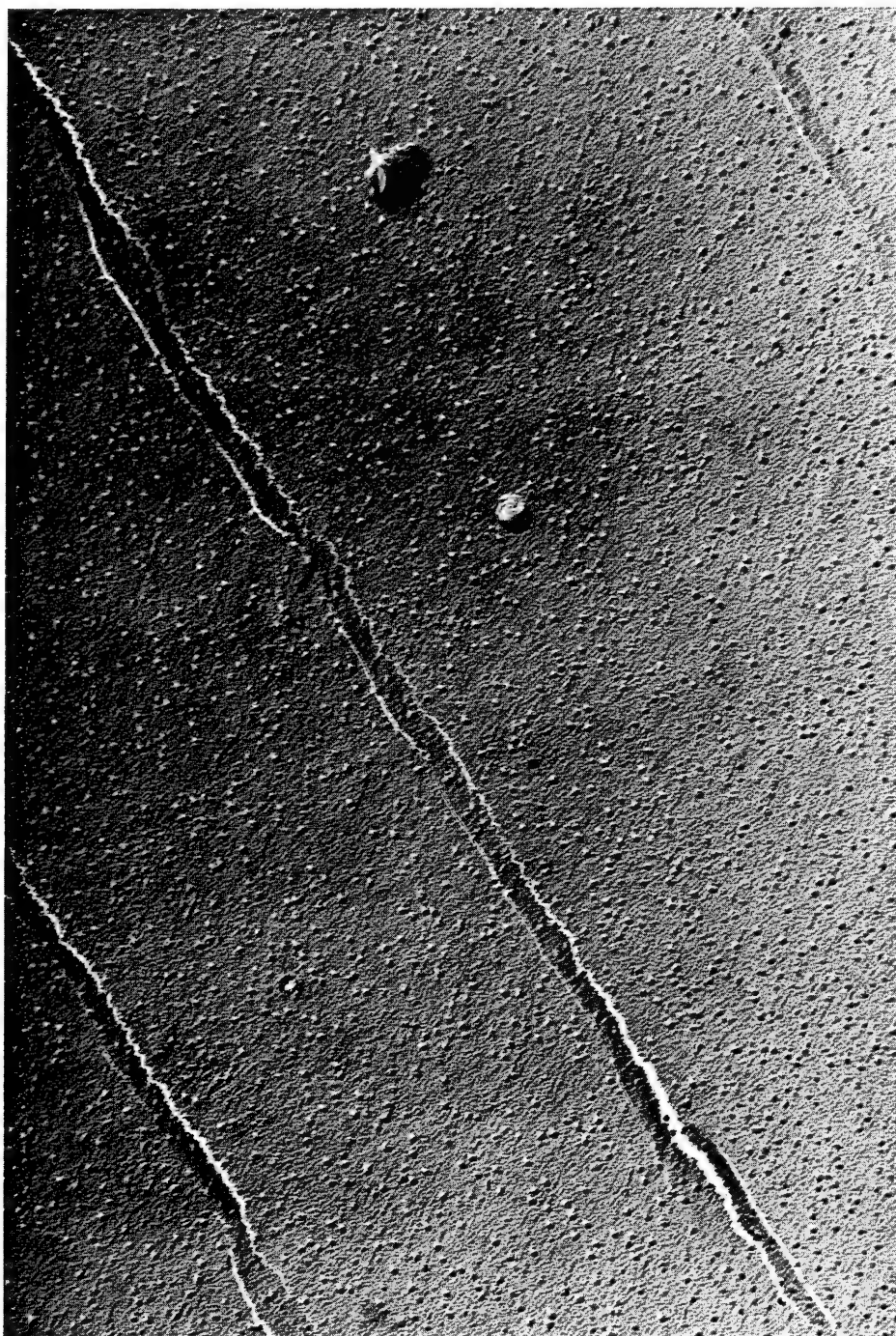
FIGURE 9. STRUCTURE IN GLASS



280a

30,000X

FIGURE 10 STRUCTURE IN GLASS



280 @ 650°C

20,000X

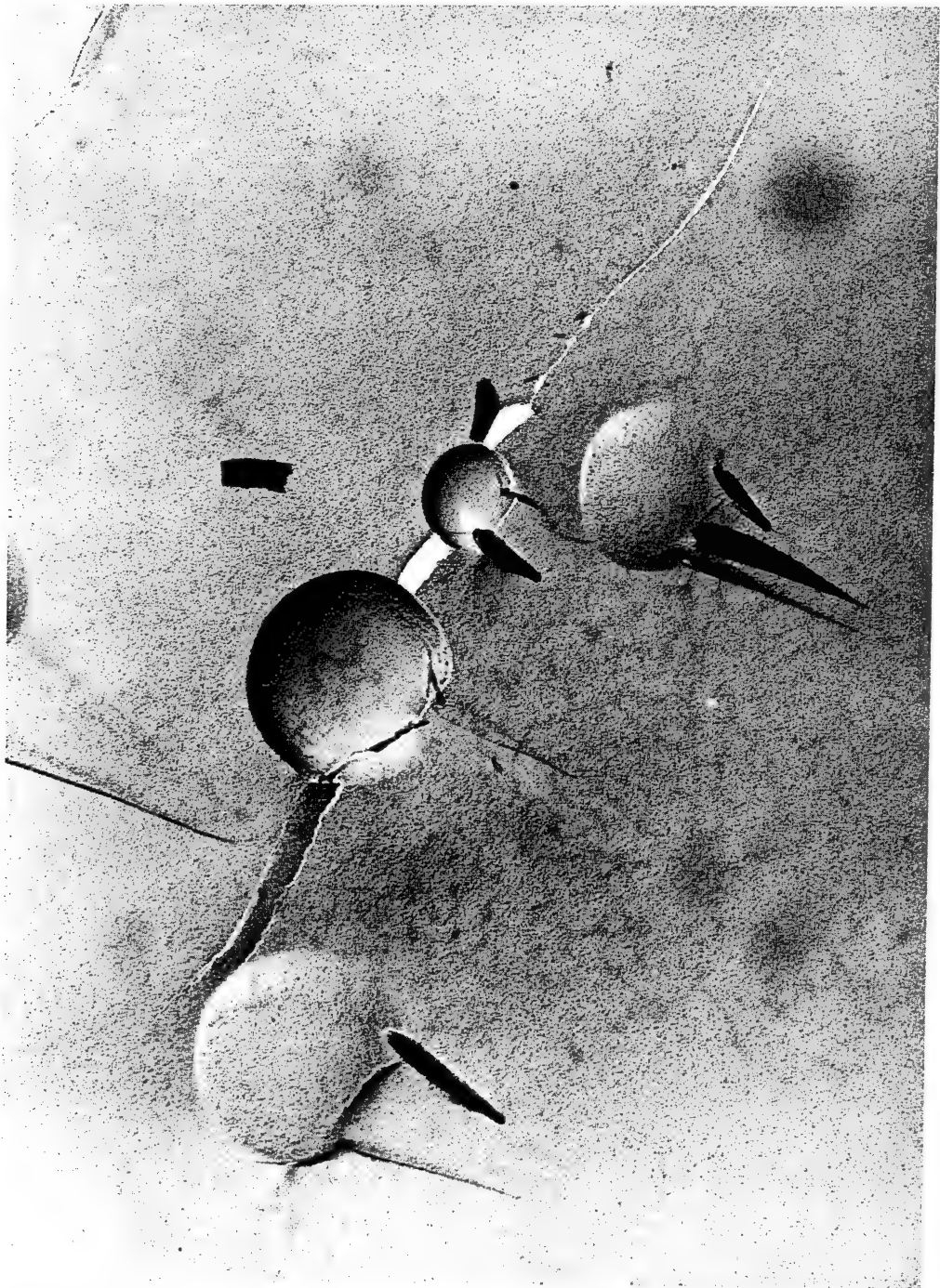
FIGURE 11. STRUCTURE IN GLASS



20,000X

281

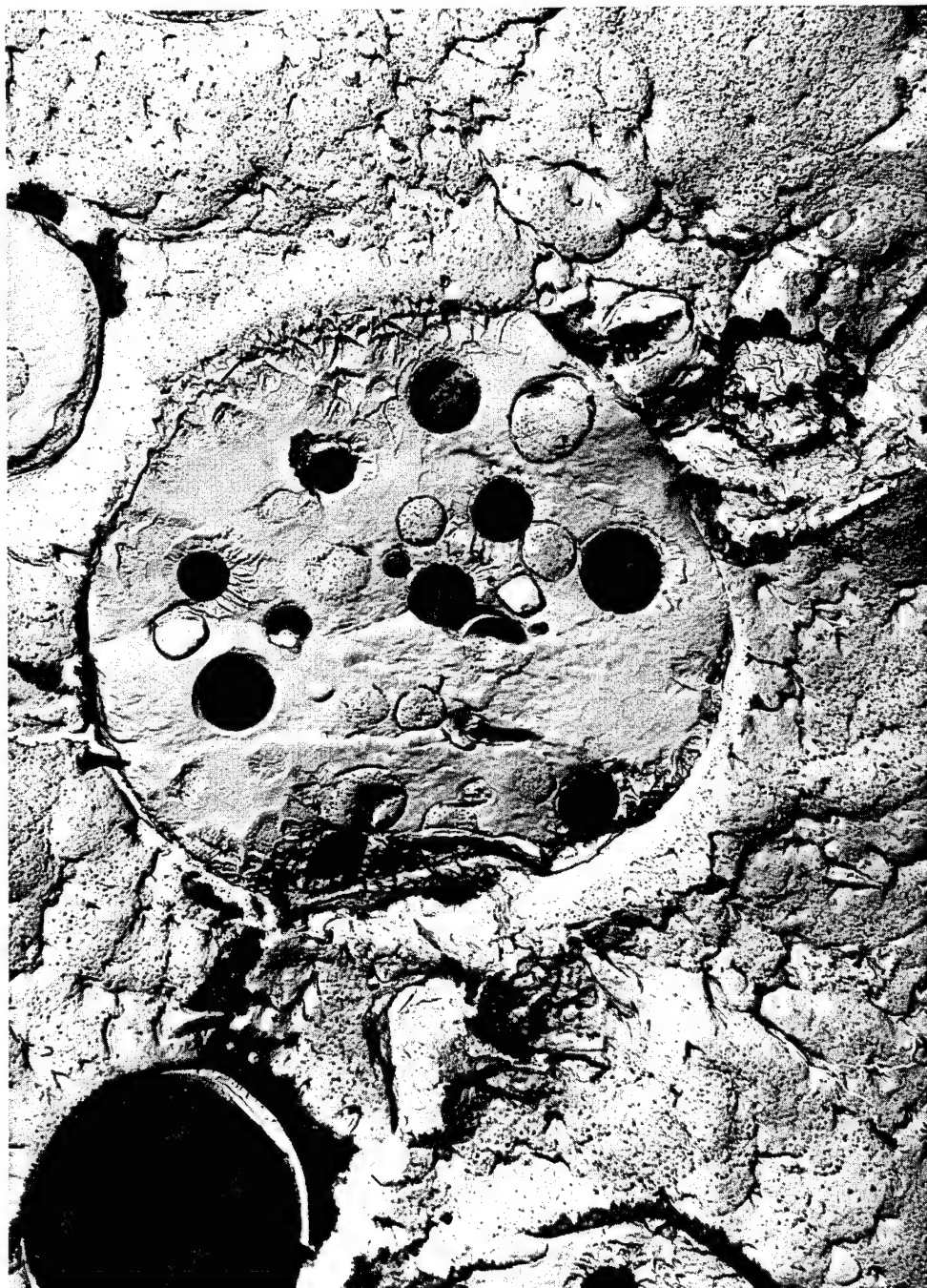
FIGURE 12. STRUCTURE IN GLASS



281b @ 900°C

20,000X

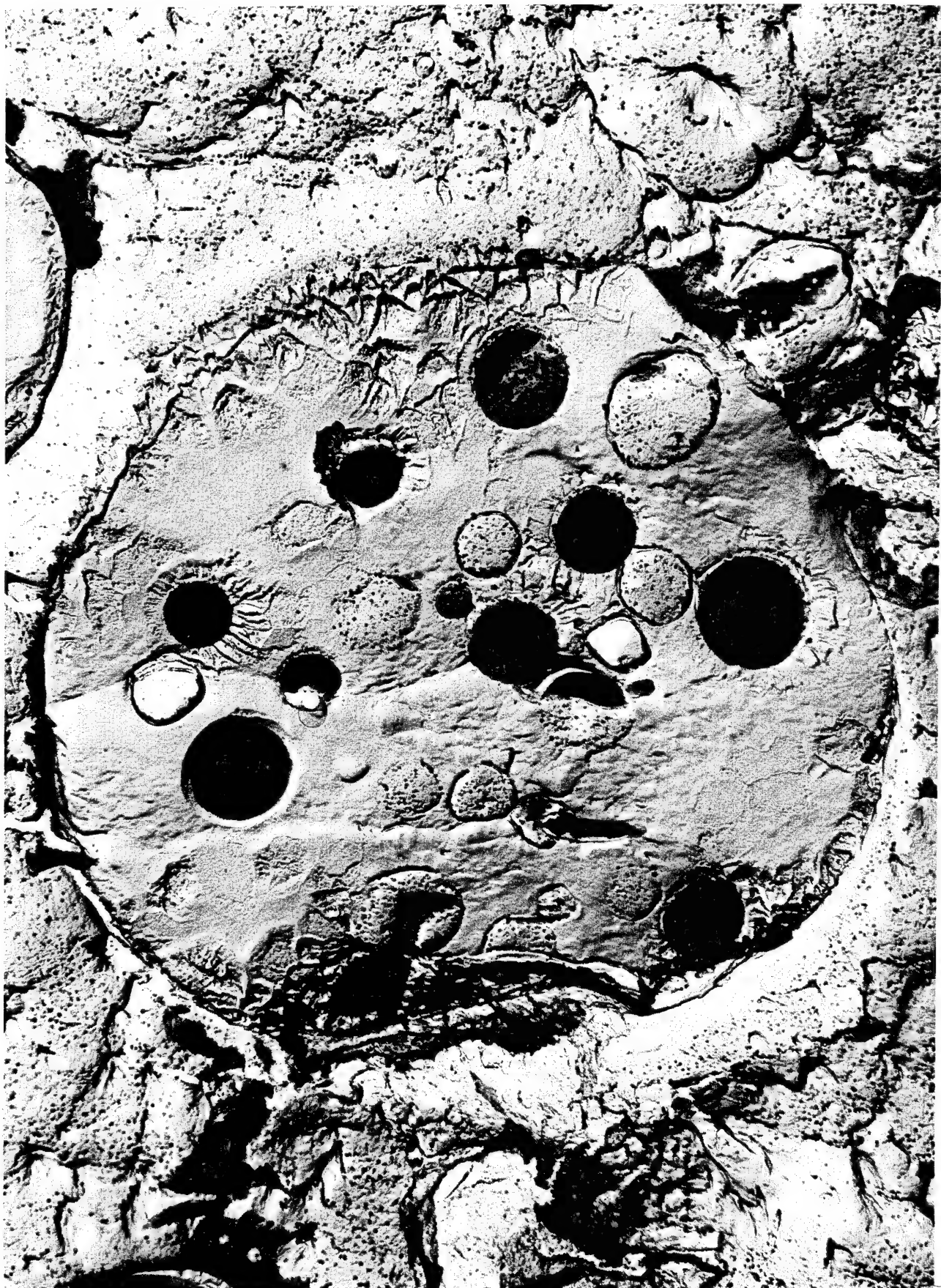
FIGURE 13. STRUCTURE IN GLASS



282

7,200X

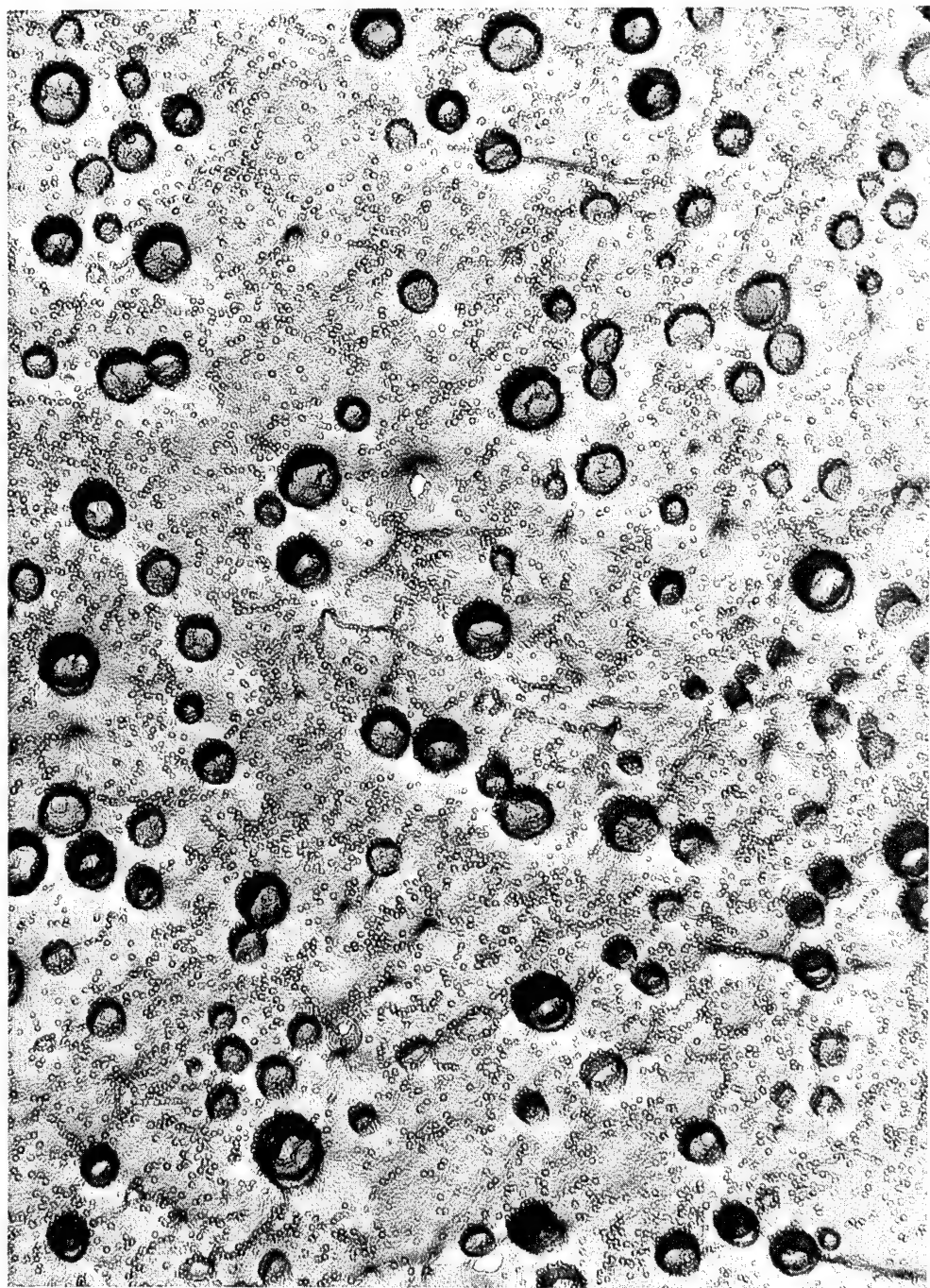
FIGURE 14. STRUCTURE IN GLASS



282

FIGURE 15. STRUCTURE IN GLASS

12,000X



282a @ 650°C

20,000X

FIGURE 16. STRUCTURE IN GLASS

very dense opal of UARL 278. Figure 6 confirms the true transparency of this glass since even at the increased magnification of 30,000 the micrograph is essentially featureless, representing only a homogeneous glass. In Fig. 7, taken of a freshly fractured surface of this glass after heat treatment at 900°C for 3 hrs, it will be noted that again true glass immiscibility has developed, as evidenced by the isolated droplets of glass 2 in the vitreous matrix of glass 1 and, indeed, the glass is again a dense opal. Figure 8, the micrograph not based on a fractured surface, shows the as-cast surface of glass 279 after heat treatment for 3 hrs at 900°C. In Fig. 9, the complete crystallization present in the outside surface of the heat treated specimen has resulted in an oriented array of massive lath-form crystals.

Figures 10 and 11 are based on UARL glass 280, a Vycor-like composition selected by Watanabe, Noake, and Aiba (Ref. 72) for investigation. This glass has the usual composition of the Corning Vycor-glass before the second phase is reached. As melted, the glass forms a completely homogeneous glass, as evidenced by the featureless micrograph of Fig. 10. After heat treatment for 3 hrs at 650°C, the glass has lost its pristine brilliance and now appears slightly opalescent. This opalescence is completely explained by Fig. 11, which shows that a second glass phase is not present in the form of very tiny droplets in contrast to the droplets of glasses 278 and 279. This phase is believed to be due to a spinodal-type decomposition. While the modulus of this glass, a high borosilicate, is very low, the phase-separable second glass again raises the value of Young's modulus from 5.56 million psi to 6.23 million psi.

Figures 12 and 13 are from UARL glass 281, which, together with UARL glass 282, is selected from a study by Levin and Cleek (Ref. 63) of the "Shape of Liquid Immiscibility Volume in the System Barium Oxide-Boric Oxide-Silica." The composition for UARL glass 281 is selected from those in the center of the spinodal decomposition region while that for 282 is on the edge of the dome. Glass 281, as melted and after cooling to room temperature, is a dense opal similar to 278. As can be seen from Fig. 12, a slight phase separation is apparent. After heat treatment at 900°C for 3 hrs, it will be noticed from Fig. 13 that a marked growth of the isolated droplets of phase 2 has resulted.

Figures 14, 15, and 16 are based on glass 282. As already mentioned, this glass is chosen from the edge of Levin and Cleek's (Ref. 63) dome of spinodal immiscibility. As prepared, it is again a dense opal. The monstrous size of the separated liquid phase 2 is apparent in both Fig. 14 (7200X) and Fig. 15 (12,000X), as is the fact that we now have droplets in droplets in droplets. Figure 16 represents this glass after heat treatment for 3 hrs at 650°C. Apparently the very large droplets have now gone into solution while the smaller droplets have continued to grow.

Elements present in Figs. 7, 12, and 13 resulting from the fractography process itself may best be understood from the work of Ohlberg, Golob and Hollabaugh (Ref. 64) who showed that the tail-like structures emanating from the dispersed phase are related to the crack front propagation and are affected by the relative values of the cohesive strength of the dispersed phase and the

adhesive strength between the dispersed phase and the matrix. The appearance of a single tail emanating from the dispersed phase indicates that the cohesive strength of this phase is weaker than the adhesive strength at the droplet-matrix interface. A double tail emanating from a dispersed phase indicates its cohesive strength is greater than the adhesive strength between the matrix and the dispersed phase. Finally, if the dispersed phase is water soluble and special precautions are not taken, a fracture surface will evidence only depressions rather than the expected elevations and depressions characteristic of adhering droplets and complementary holes.

Systematic Modifications of Glass Systems Investigated

Compositional changes to improve workability of "invert" glasses. - The invert glasses of Tables I, II, and III while yielding high moduli, proved difficult to fiberize. The available glass literature was scrutinized in an attempt to find those additions most likely to lower the liquidus, increasing the working range, and yield viscosity temperature relationships suitable for fiberization. Examination of books and patents by Weyl and Marboe (Ref. 63), Rawson (Ref. 52), Stanworth (Ref. 74), Tiede et al (Ref. 75), Armistead (Ref. 76), Bastian (Ref. 77), and Labino (Ref. 78) yielded the following suggestions for additives to improve the fiberizability of the UARL "invert" analogues.

1. B_2O_3 - Add B_2O_3 , possibly as much as the amount of silica present but keep total of two at 40 mol % or less but probably more than 25 mol %. Effect on modulus in invert glasses is not easy to predict. At best, it will contribute slightly more than SiO_2 but at worst since it is known that in silica base glasses, the B_2O_3 contribution depends on $(R_2O-Al_2O_3)/B_2O_3$, it may contribute nothing.

B_2O_3 in silica base glasses decreases the liquidus and viscosity to a marked degree. In "inverts" it should still lower liquidus but should raise viscosity especially when substituted for CaO or MgO or ZnO .

B_2O_3 content should be greater than 8 wt % to increase stability of glass and decrease devitrification tendencies but below 13 wt % to preserve chemical durability.

B_2O_3 should markedly decrease density thus increasing specific modulus.

2. Bivalent Oxides MgO , ZnO , CaO , BeO , CuO

MgO - Add MgO since it increases modulus and the greater the percentage of MgO the longer the working range of the composition and the lower the melting temperature and softening point of the fiber (8 to 15 wt % MgO).

ZnO - Behaves like MgO as judged by refractive index, resistivity, fluorescence intensity, spectral band intensity. Does not enter holes like CaO but MgO and ZnO both enter network instead.

Use at least 2 to 8 wt % bivalent oxides such as ZnO, CdO to reduce tendency of glass to devitrify.

ZnO will improve durability but will generally increase liquidus.

Do not use MgO in amount greater than 30% by weight to avoid devitrification and, for same reason, ZnO must be less than 60% by weight.

CaO - CaO and MgO are added to keep viscosity at a minimum and normally cannot be tolerated in low liquidus glasses. Do not let sum of CaO, BeO, and MgO exceed 55 wt %. CaO must be in range of 16 to 25% by weight to prevent devitrification but the lower the silica content, the lower this range. CaO enters holes and increases density.

BeO - Use BeO in range of 10 to 12% by weight to increase modulus without attendant devitrification problems.

CuO - Add CuO in amount of 9 to 10.5 wt % while maintaining the ratio of the sum of MgO and CaO to CuO + Al₂O₃ + Fe₂O₃ + TiO₂ at approximately 1 to 1 to secure low softening and yield a process capable of forming ultrafine fibers in range of 10 to 20 millionths of an inch. It is expected to yield molten glass having very high interfacial tension (viscosity) and low surface tension and softening point.

3. Al₂O₃ - Use Al₂O₃ to reduce tendency of glass to devitrify. Use Al₂O₃ in place of SiO₂ to increase modulus.

4. Other Trivalent Oxides - Fe₂O₃, Mn₂O₃. Up to 3 wt % Fe₂O₃ is deemed beneficial to formation of continuous fibers but no one can state why. Use 3 to 10 wt % to reduce tendency of glass to devitrify.

5. Rare Earth Trivalent Oxides such as La₂O₃ and Y₂O₃ - Our own prior experience indicates that these ingredients markedly increase the modulus but that additions must be held to reasonable amounts so that the density of the glass does not become too high. Lanthana adds to glass forming characteristics markedly. Yttria is too costly to allow large additions if the glass is to be competitive commercially.

6. Co₂O₃ - Add small amounts of cobalt oxide to reduce devitrification and to improve drawing properties. Preferred range of use seems to be 2 to 7% by weight.

7. SiO₂ - If anything, increase the SiO₂ slightly to increase viscosity (hold in range 25 to 40 wt %).

8. Other Tetravalent Oxides

CeO₂ - Add to each of the compositions to increase modulus, lower liquidus, promote continuous formation of fibers. But do not add really large amounts since it markedly increases density. Fe₂O₃ is not the full equivalent of ceria since it does not have identical effects on the liquidus.

ZrO_2 - Add to increase modulus, improve durability, decrease rate of crystal formation, increase resistance to devitrification. Up to 11 wt % ZrO_2 may be used. ZrO_2 will raise acceptable working temperature. Presumably the ZrO_2 may be partially substituted for Al_2O_3 .

TiO_2 - Add to allegedly enhance fiber formation but do not let $ZrO_2 + TiO_2$ exceed 25% by weight and ZrO_2 and TiO_2 must each alone be below 16 wt %.

TiO_2 and ZrO_2 improve durability, liquidus, viscosity and decrease rate of crystal formation.

9. R_2O 's - Use Li_2O only. Possesses a much higher molal modulus contribution. Use in presence of BeO to increase modulus.

The first few altered UARL invert analogue glass compositions prepared in accordance with these suggestions are those of Tables I, II, and III glass compositions 283 through 303, 309 through 318, 322 through 329, and 330 through 349. While it is obvious that this type of research can never be regarded as complete or finished, it is already abundantly apparent that rules, such as those above predicated on experience with glasses comprised of silica networks, do not hold for the non-network "invert" glasses. In particular, substitution of B_2O_3 for SiO_2 fails to decrease the density while the substitution of CuO for ZnO markedly lowers the density. In this respect the behavior of the CuO leads to further evidence that the CuO may actually enter the silica network as suggested by Ram, et al (Ref. 54) based on viscosity measurements of copper ruby glasses. This suggestion that the CuO may be present in the actual silica network in the form of $\equiv Si-O-Cu$ just as water in glass is now believed to be present as $\equiv Si-O-H$ thus forming smaller flow units than the bigger parent unit $\equiv Si-O-Si\equiv$ so that the viscosity of glasses containing $\equiv Si-O-H$ or $\equiv Si-O-Cu$ should be lower than that of the respective parent glasses.

Attempts to produce higher specific moduli glasses through B_2O_3 additions. - A systematic attempt has been made to produce higher specific moduli glasses in the UARL cordierite-rare earth oxide and UARL invert analogue glass families by substituting B_2O_3 for silica. These two systems were selected because most of the promising high moduli glasses developed by UARL belong to one or the other of these fields. The secondary aims of this work have been to lower or raise the viscosity of a given composition in order to increase its working range, to raise or lower its surface tension, and, in general, to increase the ease with which glass fibers can be mechanically drawn at high speed from a given glass. In all cases, the primary aim is to improve the modulus to density ratio. The addition of the fused boric oxide is also expected to increase the stability of the glass, i.e. cause a decrease in devitrification tendency.

The glasses of Tables I, II, and III having a significant amount of boric oxide content are separated to form Table IV and the compositions expressed in mol % in place of actual grams of ingredients. Table IV also lists the density if measured at this time, Young's modulus, specific modulus and molal sum. It

Table IV
Composition in Mol % of Borate-Series Glasses

<u>Actual Ingredient</u>	<u>290</u>	<u>291</u>	<u>299</u>	<u>300</u>	<u>375</u>
SiO ₂	25	25	25	25	25
Al ₂ O ₃	8	12	8	--	6
Li ₂ O	15	12	15	15	12
CaO	--	--	15	15	12
ZnO	15	12	--	15	8
MgO	15	12	15	15	16
B ₂ O ₃	15	15	15	15	9
Y ₂ O ₃	7	12	--	--	--
La ₂ O ₃	--	--	7	--	12
Young's Modulus (10 ⁶ psi)	14.5	15.67	14.57	14.45	16.58
Density (gms/cm ³)	3.24	3.32	3.19	2.89	3.68
Specific Modulus (10 ⁷ in.)	12.3	13.1	12.7	13.9	12.4
Molal Sum	72.16	82.98	75.36	56.6	89.8
	<u>376</u>	<u>377</u>	<u>378</u>	<u>379</u>	<u>380</u>
SiO ₂	20	17	24	24	24
Al ₂ O ₃	6	6	6	3	--
Li ₂ O	12	12	12	12	12
CaO	12	12	12	12	12
ZnO	8	8	8	8	8
MgO	16	16	16	16	16
B ₂ O ₃	14	17	10	10	10
La ₂ O ₃	12	12	--	3	6
ZrO ₂	--	--	12	12	12
Young's Modulus (10 ⁶ psi)	15.80	15.02	14.4	17.3	15.7
Density (gms/cm ³)	3.68	3.61	3.17	3.14	--
Specific Modulus (10 ⁷ in.)	11.8	11.5	12.5	15.2	--
Molal Sum	90.3	90.5	65.6	72.3	79.0

Table IV (Cont'd)

<u>Actual Ingredient</u>	<u>381</u>	<u>382</u>	<u>383</u>	<u>384</u>	<u>387</u>
SiO ₂	24	24	24	24	10
Al ₂ O ₃	3	3	3	3	--
Li ₂ O	12	12	12	12	8
CaO	12	12	12	12	30
ZnO	8	8	8	8	4
MgO	16	16	16	16	2
B ₂ O ₃	10	10	10	10	6
La ₂ O ₃	--	--	--	--	4
ZrO ₂	12	12	12	--	-
CuO	3	--	--	--	--
TiO ₂	--	--	3	--	2
BeO	--	--	--	3	34
Re ₂ O ₃ (rare earth oxide)	--	--	--	12	--
Fe ₂ O ₃	--	3	--	--	--
Young's Modulus (10 ⁶ psi)	15.87	17.7	22.75	18.62	17.85
Density (gms/cm ³)	2.96	3.01	3.14	3.89	3.28
Specific Modulus (10 ⁷ in.)	14.9	16.3	20.0	13.2	15.0
Molal Sum	64.9	67.3	64.9	87.9	56.6

	<u>388</u>	<u>389</u>	<u>390</u>	<u>391</u>	<u>392</u>
SiO ₂	24	25	20	17	22
Al ₂ O ₃	--	6	6	6	6
Li ₂ O	12	12	12	12	10
CaO	12	12	12	12	10
ZnO	--	8	8	8	10
MgO	12	16	16	16	15
B ₂ O ₃	10	9	14	17	11
Y ₂ O ₃	--	12	12	12	12
ZrO ₂	--	--	--	--	4
TiO ₂	4	--	--	--	--
BeO	14	--	--	--	--
Re ₂ O ₃ (rare earth oxide)	12	--	--	--	--
Young's Modulus (10 ⁶ psi)	17.28	17.2	16.80	17.38	16.24
Density (gms/cm ³)	3.58	3.45	3.35	3.31	--
Specific Modulus (10 ⁷ in.)	13.4	13.8	13.9	14.6	--
Molal Sum	82.6	77.8	78.2	78.5	81.8

Table IV (Cont'd)

<u>Actual Ingredient</u>	<u>393</u>	<u>394</u>	<u>395</u>	<u>398</u>	<u>399</u>	<u>400</u>
SiO ₂	22	22	20	25	25	25
Al ₂ O ₃	10	10	10	8	8	--
Li ₂ O	10	8	10	10	7	10
CaO	--	--	--	13	10	15
ZnO	10	7	10	--	6	6
MgO	20	30	20	16	16	16
B ₂ O ₃	11	11	10	14	14	14
Y ₂ O ₃	12	10	10	14	14	14
ZrO ₂	5	--	10	--	--	--
CuO	--	2	--	--	--	--
Young's Modulus (10 ⁶ psi)	16.46	16.59	16.00	16.30	16.89	--
Molal Sum	83.5	75.4	83.3	81.3	83.6	79.1

is immediately apparent that, in general, the values for Young's modulus for these glasses are inferior to many other glasses developed at UARL while the specific modulus is not markedly increased. In addition, these glasses do not fiberize readily. Two exceptions to these general remarks are UARL 382 and 383. UARL 383, in particular, is the highest modulus glass yet developed and has the highest specific modulus but attempts to fiberize this glass have been unsuccessful to date. Work toward a more complete understanding of the results found for UARL 383 is in progress. Another factor encountered in the study of the glasses with appreciable borate content is that the addition of beryllia to such glasses (for example, UARL 387 and 388) does not raise Young's modulus as much as does the addition of beryllia to a silica-alumina-magnesia glass.

Compositional guideposts for further research on beryllia containing glasses. - At the risk of stealing interest from the later sections of this report we would like at this point to conclude our remarks about compositional research by the inclusion of the summary Table V which shows those compositions that seem to us to indicate the directions we should move in further research on beryllia containing glasses.

Compositional guideposts for further research on non-BeO containing glasses. - Table VI is made up of selected data for nonberyllia containing glasses to serve as a counterpart of Table V. It, like Table V, represents the result of examination of all our test data to date. It is evident that of the several hundred nontoxic glass compositions thus far prepared, only a relatively few point a direction in which to move to obtain high-modulus high-strength nontoxic glass fibers. Far fewer dependable leads are available for the nontoxic glass compositions than is the case for the beryllia containing compositions. For example, examination of Table V shows that twelve of the beryllia glasses based on our much studied composition UARL 344 have moduli over nineteen million psi whereas the best recent nonberyllia glass, UARL 454 (Table VI) has a modulus of 18.93 million psi. However, this new UARL 454 is much more workable than the antecedent glass, UARL 270, and is a step toward catching up with the very favorable working characteristics of the beryllia glass, UARL 344 (Table V).

Just as in the case of our earlier experimental compositions, once a composition has been selected, 500-gram batches of the specified raw materials are melted in high purity (99.9%) alumina crucibles in air using kilns heated by Super-kanthal hairpin electrical resistance elements, Fig. 17. Starting materials used are 5 micron particle-size high purity silica, high purity alumina of 325 mesh, laboratory reagent grade magnesium oxide, 99.9% lanthanum oxalate, and other comparable materials such as reagent grade zinc carbonate or calcium carbonate. These materials customarily yield a water-white optical grade glass free of seed, stone and bubbles when properly compounded and held at temperatures of 1000-1650°C for at least two hours. Less commonly, glasses may be prepared in beryllia crucibles in air and in the same kilns, or in platinum crucibles in air in the platform kiln which is heated by the high temperature variety of Super-kanthal heating elements and can reach temperatures of 1700°C, or in tungsten crucibles in purified argon or vacuum atmospheres. Alumina crucibles of even very slightly lower purity, i.e., 99.3 to 99.7% have not proven useful for this type of glass research. In some cases where marked departure occurs from the more usual optical clarity, the melt may be ground and remelted in platinum before forming the rods used for Young's modulus measurement and before drawing any fibers. Since the results with "invert analog" compositions have been outstanding to date, this proposal would continue efforts in this field of glass research.

Table V

New Compositional Guide for Beryllia Containing Glasses

Glass	<u>SiO₂</u>	<u>Al₂O₃</u>	<u>MgO</u>	<u>Li₂O</u>	<u>CaO</u>	<u>ZnO</u>	<u>La₂O₃</u>	<u>Ce₂O₃</u>	<u>B₂O₃</u>	<u>ZrO₂</u>	<u>BeO</u>	<u>Y₂O₃</u>	^a <u>CuO</u>	^b <u>Re₂O₃</u>	^c <u>TiO₂</u>	Young's Mod. 10 ⁶ psi	Spec. Mod. 10 ⁶ in.	Fiber Mod. 10 ⁶ psi
2731,2	30	12	12	12	12	8.33	8.33	8.33	22	25	10	10	18.4	186	---	---	---	
2751,2,3	50	8.33	8.33	8.33	8.33	8.33	8.33	8.33	25	25	10	10	16.8	127	15.94	17.0	17.0	
2761,2,3	50	8.33	8.33	8.33	8.33	8.33	8.33	8.33	25	10	10	10	15.8	129	184	184	184	
3232	35	15	30	10	12	12	12	12	10	10	10	10	18.4	184	184	184	184	
3242	30	12	24	12	12	12	12	12	10	10	10	10	17.78	166	166	166	166	
3253	30	10	20	10	10	10	10	10	10	10	10	10	20.2	158	158	158	158	
329	20	10	20	10	10	10	10	10	10	10	10	10	20.2	189	189	189	189	
3311,2	39	12	12	12	12	12	12	12	10	25	12	12	20.9	158	19.8	19.8	19.8	
336	35	15	15	10	20	10	10	10	30	30	10	10	21.0	166	166	166	166	
340	25	10	20	10	10	10	10	10	15	10	10	10	20.9	163	163	163	163	
3441,2,3	45	15	15	15	15	15	15	15	15	15	10	10	20.3	170	18.6	18.6	18.6	
3452	45	15	8.33	8.33	8.33	8.33	8.33	8.33	30	30	10	10	21.1	175	175	175	175	
3471,2	50	8.33	8.33	8.33	8.33	8.33	8.33	8.33	25	25	10	10	21.6	164	17.4	17.4	17.4	
3481,2	50	8.33	8.33	8.33	8.33	8.33	8.33	8.33	8.33	25	10	10	17.7	134	17.5	17.5	17.5	
3502,3	24	13	13	13	13	13	13	13	24	24	10	10	19.75	197	197	197	197	
352	25	10	10	10	10	10	10	10	10	10	10	10	20.0	146	146	146	146	
3671	39	12	12	12	12	6	6	6	2	2	25	25	19.03	149	17.5	17.5	17.5	
3681	39	12	12	12	12	4	4	4	2	2	25	25	19.08	144	18.8	18.8	18.8	
3701	39	12	12	12	12	4	4	4	2	2	25	25	18.5	142	17.7	17.7	17.7	
3711	39	12	12	12	12	4	4	4	2	2	25	25	18.5	144	18.4	18.4	18.4	
373	39	12	12	12	12	6	6	6	2	2	10	10	19.0	150	150	150	150	
3881	24	12	12	12	12	12	12	12	14	14	10	10	17.3	134	16.8	16.8	16.8	
4051,2	49.3	14	0.7	0.7	0.7	0.7	0.7	0.7	14	22	25	25	19.7	146	18.7	18.7	18.7	
4081,2,3	45	10	3	3	3	3	3	3	15	15	15	15	18.3	131	19.8	19.8	19.8	
4101,2,3	45	15	15	15	15	15	15	15	15	15	15	15	18.23	139	17.8	17.8	17.8	

Table V (Cont'd)

Glass	<u>SiO₂</u>	<u>Al₂O₃</u>	<u>MgO</u>	<u>Li₂O</u>	<u>CaO</u>	<u>ZnO</u>	<u>La₂O₃</u>	<u>Ce₂O₃</u>	<u>B₂O₃</u>	<u>ZrO₂</u>	<u>BeO</u>	<u>Y₂O₃</u>	<u>aCuO</u>	<u>bRe₂O₃</u>	<u>cTiO₂</u>	Young's Mod. 10 ⁶ psi	Spec. Mod. 10 ⁶ in.	Fiber Mod. 10 ⁶ psi
4111,2,3	45	15	15	3		10							15	10	15	18.0	135	15.6
4161,2	45	12	15										15	10	19.61	164	19.8	
4171,2	45	15	15	3									15	7	19.4	173	18.8	
4181,2	45	15	12	3									18	7	19.4	172	18.5	
4191,2	42	15	15	3									15	10	20.2	170	19.0	
4201,2	42	12	15	3	3								15	10	19.5	161	19.6	
421 ¹ ,2	42	10	20	3									15	10	20.4	169	---	
422	40	9	18	5									18	10	20.6	171	---	
423	40	9	18	5									18	10	20.7	165		
425 ²	42.9	7.0	25.6		2	18	3						24.6		19.5	197		
426		16	16	16	10	16							16	10	20.6	165		
4331,2	41.66	8.33	15										8.33		25	19.12	146.5	
4341,2	41.66	8.33	15										8.33		25	19.43	153.5	
4381,2	29	10	10	6	2	6							10	2	15	18.25	157	

¹Fiberizable²Forms clear glass slug³Has favorable liquidus

Table VI

Compositional Guideposts for the Development of Nontoxic (no BeO) Improved High Modulus Glasses

Table VI (Cont'd)

Glass	Compositions in Mol Percent										Bulk Properties								
	SiO ₂	Al ₂ O ₃	MgO	Li ₂ O	CaO	ZnO	La ₂ O ₃	Ce ₂ O ₃	B ₂ O ₃	ZrO ₂	Y ₂ O ₃	aCuO	bTiO ₂	Young's Mod.	Spec. Mod.	Fiber Mod.	10 ⁶ psi	10 ⁶ in.	Molar Sum
453	38	20	6	15	4							12	a ₂ b ₃	18.93	145			77.7	
454 ^y	38	6	20	6	9	4						12	a ₂ b ₃	15.96	135			80.5	
455 ^y	25	15	15	15	15	15	10					5		15.02	130			64.4	
456 ^y	25	10	15	15	15	15	15	15				5		15.93	139			65.9	
457 ^y	25	15	15	10	15							5						65.1	
458 ^y	25	15	10	15	15							5		15.23	132			66.4	
459 ^y	25	15	14	14	14							8		17.34	140			72.6	
460	25	13	13	13	13							13		16.83	138			73.6	
461	25	13	13	13	13							13		14.80	135			63.4	
462	25	12	12	13	12							12		16.46	137			74.5	
101																			
463 ^y	25	12	13	13	13							12		10	b ₂	17.50	142		74.1
464 ^y	25	15	15	15	10							15		5		16.07	146		64.1
465	25	14	14	14	8							15		10		16.67	140		77.1
466	25	15	15	15	15							12.5	2.5			15.85	143		60.5
467	25	8	15	10	15							5		7					
468	25	8	15	7	15							8		7					
469	25	8	15	5	15							10		7					
470	25	8	15	15	10							5		7					

^xFiberizable^yGood Quality Glass^zFavorable Liquidus

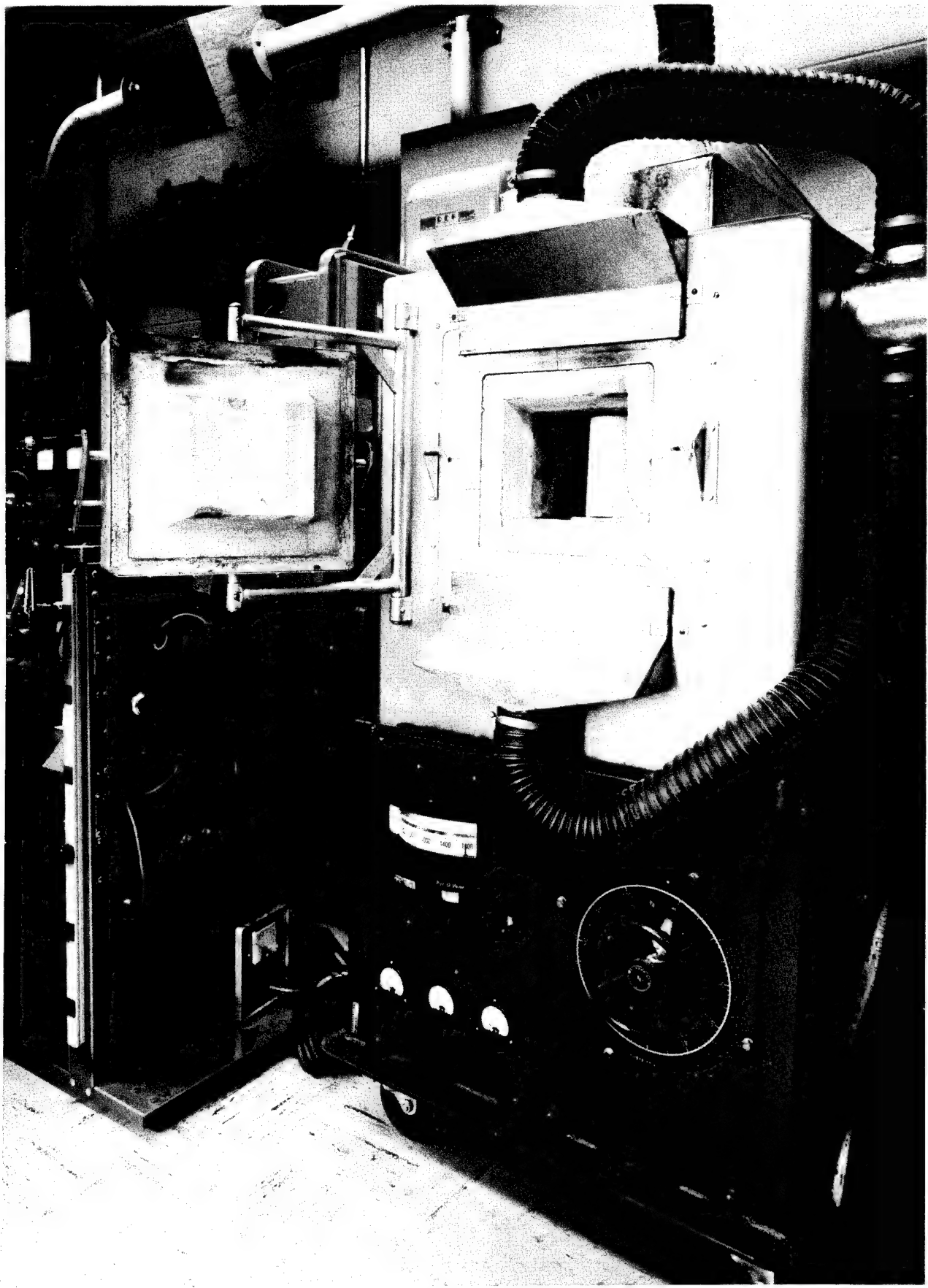


FIGURE 17. SUPER-KANTHAL HAIR-PIN KILN USED FOR MELTING OXIDE MIXTURES

CHARACTERIZATION OF THE NEW EXPERIMENTAL GLASSES I.

Many of the experimental glasses prepared in this program are characterized by density measurements, their conductivity and viscosity in the molten state, direct optical observations of their kinetics of crystallization, estimated liquidus and working range, their glass forming characteristics and fiberizability. This work is summarized in this section. Further characterization of the experimental glasses was concerned with modulus strength and impact studies and these results are placed in a subsequent section.

Density Measurements

Density of the experimental glasses was determined for UARL by the Glass Testing Division of the Hartford Division of the Emhart Corporation. For samples with densities less than 3.00 gms/cm³ the heavy-liquid-of-known-density comparison procedure is used while for samples with densities greater than 3.00 gms/cm³ the Archimedean method is employed. The results of all density measurements are shown in Table VII in metric units. The observed densities range from 2.20 to 5.22 gms/cm³. Possibly the only noteworthy deviation from predicted density is provided by UARL 284 where a partial substitution of copper for zinc lowers the density from 3.52 to 3.23 gms/cm³ but numerous small deviations in density are apparent when the density is plotted against molal sum and straight line relationships are only approximately obeyed by these experimental glasses.

Electrical Conductivity Measurements

To study the electrical conductivity of the molten oxides as a function of time and temperature, the glasses were melted as described above and broken up and packed into the tungsten crucible shown in Fig. 18. This crucible, which is pictured at the conclusion of the measurement, is made to serve as a conductivity cell by introducing a tungsten ball, one-quarter inch in diameter, on the end of a tungsten rod into the exact center of the crucible and by tying a tungsten rod to the outside of the crucible with 25 mil tantalum wire. The whole assembly is then placed in the tungsten resistance furnace shown in Fig. 19 and heated until the glass is completely remelted. Power to the furnace is then turned off and the electrical conductivity of the molten oxide system is measured continuously through the solidification process as the furnace cools. The temperature of the crucible is measured at thirty-second intervals to obtain the required data connecting electrical conductivity with crystallization or lack of crystallization rates.

The actual measurement of the electrical conductivity is carried out by connecting externally the UARL "log ohmmeter" described schematically in Fig. 20 to the two leads from the tungsten crucible conductivity cell. These leads are brought out of the furnace using vacuum-type electrical lead-ins. The log

Table VII

Summary of all Density Determinations for Bulk Specimens
of UARL Experimental Glasses

<u>Number</u>	Density <u>gms/cm³</u>	<u>Number</u>	Density <u>gms/cm³</u>	<u>Number</u>	Density <u>gms/cm³</u>	<u>Number</u>	Density <u>gms/cm³</u>
25	2.5672	125	2.7818	194	4.479	258	2.7232
38	2.6415	126	3.4634	195-2	4.167	259	2.8988
40-3	2.9574	127	3.2557	200	3.584	260	2.6191
56	2.4368	131	3.1386	201	3.550	261	2.5783
62-3	2.7404	134	3.0671	202	3.769	262	2.3180
63-1	2.6847	135	2.6303	203	3.490	263	4.0091
64-1	2.6818	136	2.8035	205	4.0576	265	3.9818
65-1	2.7197	137	3.0834	210	3.8972	266	3.1872
66	2.6112	138	3.5498	212	3.0360	267	2.7162
66-1	2.6784	140	3.678	214	2.5854	268	3.1986
67-3	2.6499	151	3.2541	215	3.1277	269	3.4357
68-2	2.6295	155	3.5452	219	2.9689	270	3.5259
69	2.5910	157	2.6962	222	4.4871	271	3.7692
69-3	2.5952	159	3.2216	223	5.2235	273	2.7472
70-1	2.7526	160	3.2211	224	5.1584	274	2.9926
71	2.6627	161	3.4523	225	4.6850	275	3.6460
72-2	2.8877	162	3.6150	231	3.4337	276	3.3983
73-2	3.0152	163	3.1876	232	3.5892	277	3.9086
74	2.9983	164	4.0593	233	3.0314	278	2.6073
75	2.6342	165	3.3088	234	3.7081	279	2.6941
82-3	2.5875	166	2.6295	235	3.3261	280	2.0556
83	2.8376	167	3.4085	237	3.3335	281	2.4152
93	3.1167	168	3.2047	238	3.0462	282	2.2126
96	2.9676	169	3.6355	244	3.63	283	3.6391
97	2.8426	170	4.202	247	2.9870	284	3.3233
98	2.9168	171	3.810	248	3.0906	285	3.6569
99	3.186	172	3.934	249	3.0114	286	3.7951
102	2.9188	173	4.525	250	4.3226	287	3.6206
103	2.9089	174	3.472	251	3.0660	288	3.6110
106	3.6859	175	3.189	252	3.0680	289	3.9026
107	3.3799	176	3.151	253	3.2534	290	3.2423
108	3.1140	177	4.196	254	3.6307	291	3.3225
110	2.6128	178	3.613	255	4.1231	292	3.6614
113	3.5298	179	4.331	256	3.5838	293	3.2873
114	3.2237	188	3.2548	257	3.7271	294	3.3745

Table VII (Cont'd)

<u>Number</u>	Density gms/cm ³						
295	3.1942	337	3.9452	375	3.6819	412	4.0954
296	3.2892	338	4.1815	375A	3.6819	413	3.4375
297	3.5426	339	4.1550	376	3.6820	414	3.8764
298	3.9706	340	3.5589	376R	3.6820	415	3.2899
299	3.1904	341	3.9190	377	3.6108	416	3.2877
300	2.8883	342	3.5616	377R	3.6108	417	3.0915
301	3.8131	343	3.8365	378	3.2971	418	3.0884
302	3.7684	344	3.2901	378A	3.1701	419	3.2665
303	3.7256	345	3.3434	379	3.1448	420	3.3605
304	3.6248	346	3.5527	380	3.7107	421-Spe	3.3370
305	3.6629	347	3.6345	381	2.9591	421	3.3356
306	3.6654	348	3.6505	382	3.0054	422	3.3222
307	3.6950	349	3.5261	383	3.1418	423	3.4505
308	3.5651	350	2.7817	384	3.8927	424	3.0401
309	3.5951	351	2.7814	385	2.8006	425	2.7355
310	3.6864	352	3.7924	386	3.3705	426	3.4378
311	3.7008	353	3.9158	387	3.2777	427	3.1550
312	3.2789	354	3.5718	388	3.5767	428	3.2284
314	3.7178	355	3.7860	389	3.4540	429	3.2496
315	3.5831	356	3.3507	390B	3.3462	430	4.3482
316	3.8017	357	3.9424	391A	3.3062	431	4.2720
317	3.8051	358	3.4014	392	3.5920	432	3.7345
318	2.7173	359	3.7040	393	3.6019	433	3.6325
319	3.6270	360	3.5183	394	3.3024	434	3.5304
320	2.9286	361	3.4989	395	3.7273	435	3.4605
321	3.6319	362	3.4997	396	3.2443	436	3.4461
322	2.9967	363	3.5680	398	3.2622	437	3.5067
323A	2.7711	364	3.0985	399	3.3742	438	3.2348
324A	2.9708	365	3.5453	400	3.3266	439	3.3510
325A	3.5446	366	3.4697	401	3.3031	440	3.3426
326	3.0939	367	3.5310	402	3.3063	441	3.2739
327	3.6914	368	3.6229	403	3.3728	442	3.5959
328	4.3740	369	3.5272	404	3.5661	443	3.6695
329	3.0380	370	3.6285	405	3.7262	444	3.5011
330		371	3.5664	406	4.3956	445	3.4488
331	3.6638	372	4.0747	407	3.6398	446	3.5049
332	4.2390	373	3.4937	408	3.8661	447	3.2975
333	3.7066	373A	3.4937	409	4.0420	448	3.5173
334	3.9453	374	3.4216	410	3.6381	449	3.3944
335	3.8562	374A	3.4276	411	3.7073	450	3.3598

Table VII (Cont'd)

<u>Number</u>	Density <u>gms/cm³</u>
451	3.5527
452	3.6114
453	3.6837
454	3.6142
455	3.2860
456	3.2099
457	3.1765
458	3.2094
459	3.4538
460	3.3785
461	3.0354
462	3.3294
463	3.4296
464	3.0700
465	3.3184
466	3.0731
461 _{xtal}	3.3823
96-2	2.9298
236	3.4629
267A	2.7322

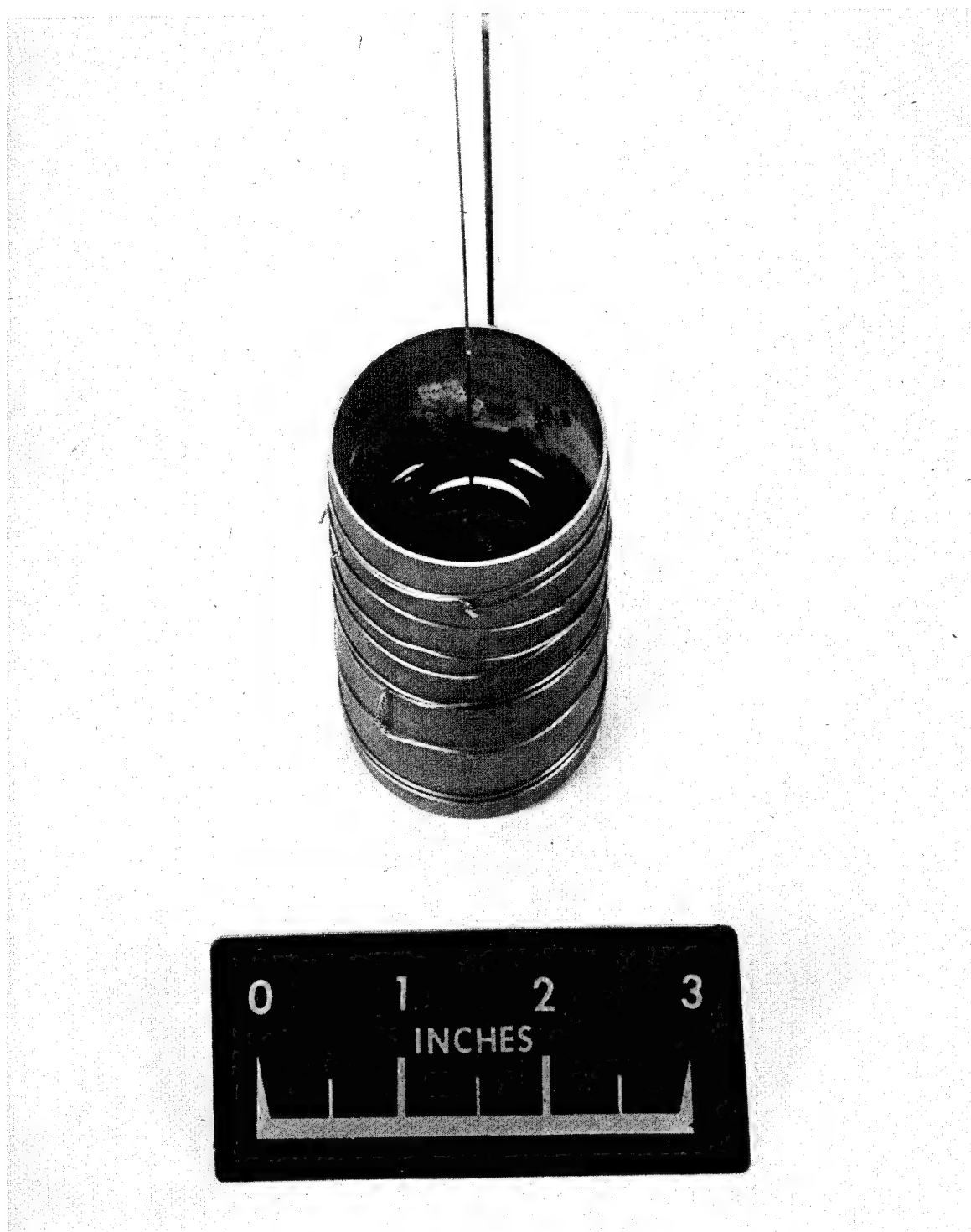
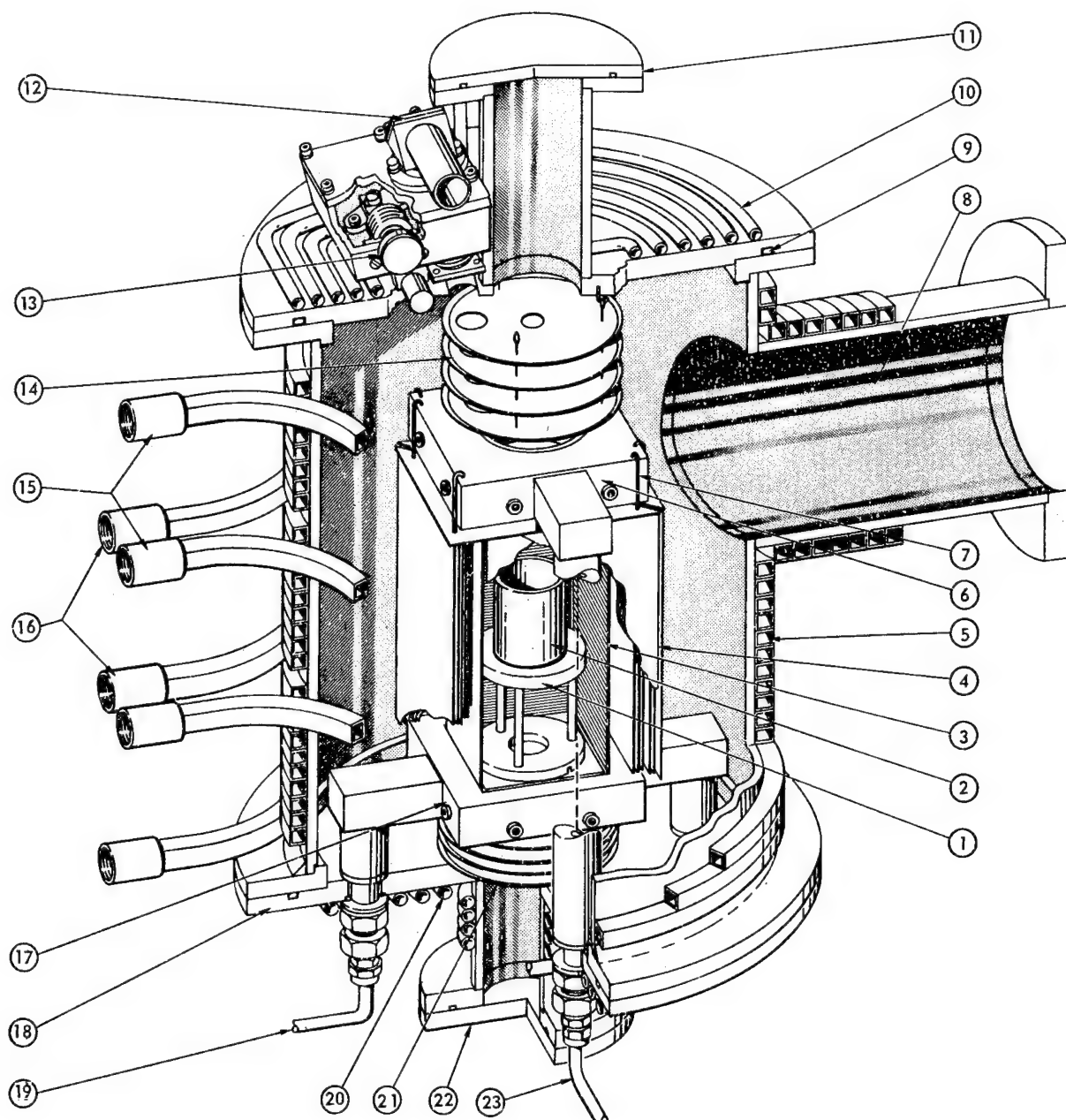


FIGURE 18. TUNGSTEN CRUCIBLE CONDUCTIVITY CELL



1 TUNGSTEN PEDESTAL FOR CRUCIBLE	13 PROTECTOR MECHANISM FOR SIGHT GLASS
2 TUNGSTEN CRUCIBLE	14 TOP TANTALUM RADIATION SHIELDS
3 FLAT TUNGSTEN HEATING ELEMENT (4)	15 COOLING WATER IN
4 TANTALUM RADIATION SHIELDS	16 COOLING WATER OUT
5 SIDE COPPER COOLING COILS	17 BOTTOM WATER COOLED ELECTRODE SUPPORT CONDUCTOR
6 TOP WATER COOLED ELECTRODE SUPPORT CONDUCTOR	18 BOTTOM PLATE FOR MOUNTING
7 SUPPORT PIN FOR TANTALUM SHIELDS	19 WATER IN BOTTOM ELECTRODE
8 TO VACUUM SYSTEM	20 BOTTOM COPPER COOLING COILS
9 "O" RING GASKET SEALS	21 BOTTOM TANTALUM RADIATION SHIELDS
10 TOP COPPER COOLING COILS	22 BOTTOM INTERCHANGABLE COVER FOR MEASURING APPARATUS
11 TOP INTERCHANGABLE COVER FOR MEASURING APPARATUS	23 WATER IN TOP ELECTRODE
12 SIGHT GLASS	

FIGURE 19. TEMPERATURE TUNGSTEN RESISTANCE FURNACE

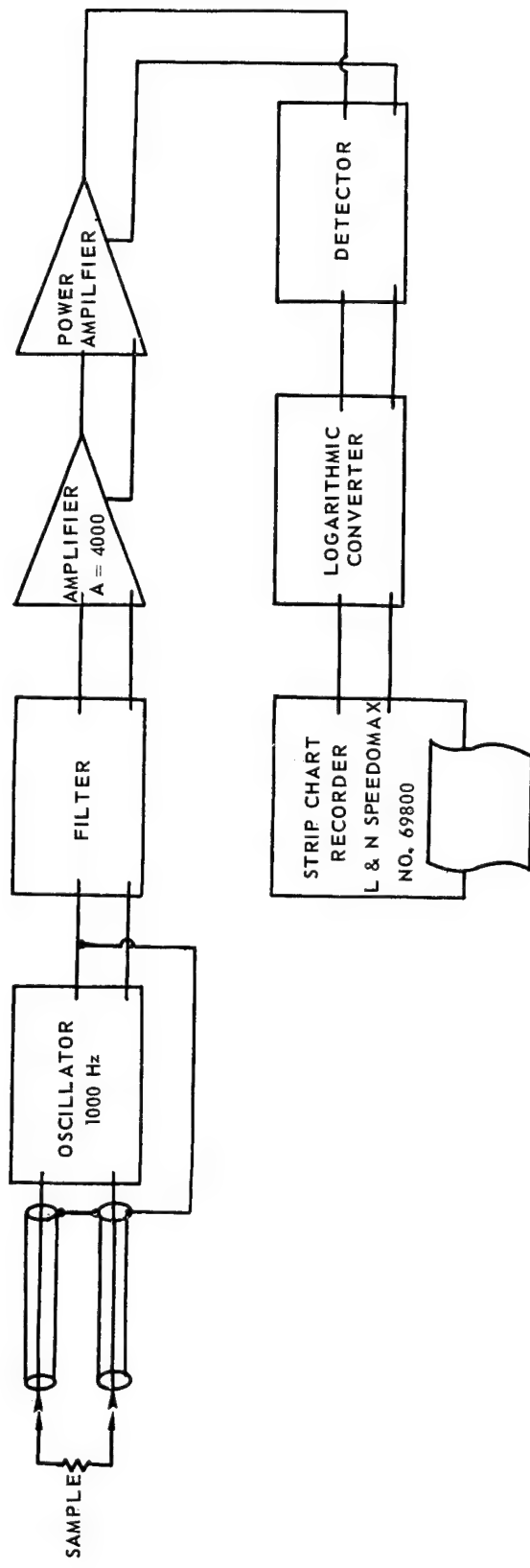


FIGURE 20. LOG OHMMETER

ohmmeter of Fig. 20 is designed to measure resistance from 10^{-1} ohms to 10^{+6} ohms and generates a d-c signal voltage proportional to the logarithm of the resistance. The scale for this instrument is divided into six ranges: 10^{+6} ohms to 10^{+5} ohms, 10^{+5} to 10^{+3} ohms, 10^{+3} to 10^{+2} ohms, 10^{+2} to 10 ohms, 10 to 1 ohm, and 1 to 10^{-1} ohm. Over each range, the amplitude of the signal applied to the unknown resistor and the sampling resistor are adjusted so that the power dissipated in the sample is less than 500 microwatts, and the sample resistor is less than 6.5% of the resistance being measured.

In each range position, a constant amplitude, 1000 cycle/sec, sinusoidal voltage is applied to the unknown and the current through it measured by a sampling resistor. This signal is passed through a series of filters consisting of a band-pass filter from 800 to 2000 cycles/sec, a twin-tee notch filter at 60 cycles/sec and a twin-tee notch filter at 180 cycles/sec in cascade. These filters effectively remove the large amount of noise generated in the sample by the massive (1000's of amperes) 60 cycle heater current present in the tungsten furnace. The signal is then linearly amplified by a guarded amplifier to a level of 0.5 volts p-p to 50 volts p-p and used to drive a power amplifier. The power amplifier isolates the guarded amplifier from the detector. The d-c voltage from the detector is then applied to the logarithmic converter which puts out a d-c voltage proportional to the logarithm of the input voltage. A unity gain operational amplifier following the logarithmic converter provides the low output impedance necessary to drive the strip chart recorder.

The electrical conductivity device has been used successfully for several of the molten oxide systems. However, this type of measurement did not seem as useful in selecting those molten oxide systems for further study as did direct measurements of viscosity, kinetics of crystallization by optical methods and moduli measurements. The program has consequently been discontinued.

Viscosity Measurements

The device initially used to measure the viscosity of the molten oxide systems at high temperature is the Brookfield Synchro-Electric Viscometer. The principle of operation of the device is simple. A cylinder or disc or spindle is rotated in the fluid under test through a beryllium-copper spring. The deflection of the spring is read on a dial. The dial reading with the usual disc is multiplied by a simple constant to obtain the resulting viscosity at the particular rotational speed or when special design spindles are used, the device is calibrated through the use of oils of known viscosity. Measurements made at different speeds are used to describe the complete flow properties of the material at hand.

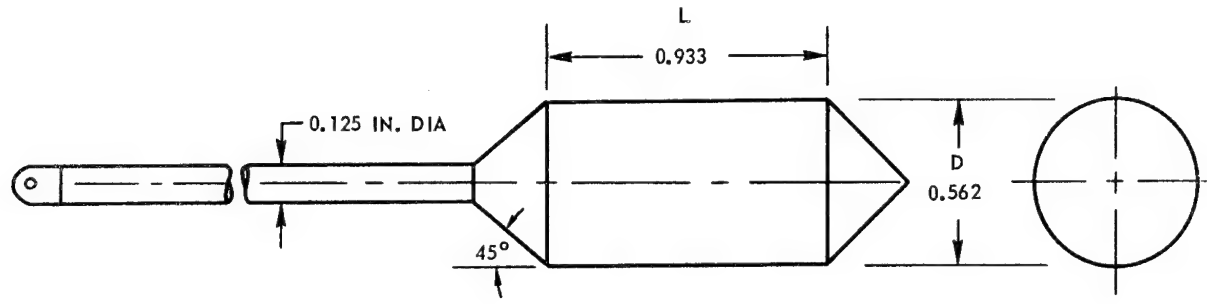
The Brookfield viscometer had never been used before at temperatures as high as those likely to occur in this contract. However, this merely meant that the device must be equipped with a long shaft entering the furnace and with a spindle of suitable high temperature material. Tungsten was selected as the

material for both the spindle and shaft because of its known compatibility with all the molten oxide systems investigated to date, and Brookfield Engineering Laboratories then designed the tungsten spindle shown in Fig. 21. This tungsten spindle and the Brookfield viscometer were calibrated using the National Bureau of Standards standard viscosity oil "P" by placing an exact silica replica of the tungsten crucible normally used in the constant temperature bath shown in Fig. 22, filling the silica crucible with oil "P" and running the tungsten spindle in the crucible in such a way as to exactly simulate high temperature operations as shown in Fig. 22. With this constant temperature bath, oil temperatures could be held constant to within $\pm 0.005^{\circ}\text{C}$ in the range from -5°C to $+107^{\circ}\text{C}$. With this bath, the calibration data obtained for the tungsten spindle is shown in Table VIII and graphically in Fig. 23.

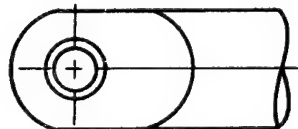
The viscosity data for N.B.S. standard oil "P" shown as the fourth column of Table VIII was obtained both by taking the data furnished on the certificate accompanying our shipment of oil "P", plotting it as shown by the solid line of Fig. 24, taking the data furnished in the article published by Shartsis and Spinner (Ref. 79) and plotting it as the dotted line of Fig. 24, and extrapolating the solid line of Fig. 24 to give a suitably displaced similarly shaped curve. Experience gained in measuring the viscosity of fused silica (Ref. 80) had shown this procedure to be trustworthy. The completed plot of Fig. 24 is then used to furnish the data tabulated in Table IX.

The Brookfield viscometer and tungsten spindle with its elongated shaft were installed on the tungsten resistance furnace as shown in Fig. 25. The spindle is brought out of the tungsten furnace through a high vacuum fitting. Originally the spindle is at rest, the ground glass previously melted in other furnaces is placed in the crucible, the whole system is evacuated, flushed with purified argon by loosening the vacuum fitting and allowing the argon (at a positive pressure of 5 in. of water) to stream out, reevacuated and refilled with purified argon. The system is heated until the glass is molten as judged by visual examination and the tungsten spindle inserted into the melt and positioned at the proper depth. The temperature of the furnace is adjusted to the desired values and the viscosity of the selected experimental glass is measured at the various temperatures.

Viscosity-temperature curves were measured for a number of experimental glass compositions with the results shown in Figs. 26-34 and as tabulated in Table X and summarized in Table XI. It is immediately apparent that many of these experimental glasses have much steeper temperature viscosity curves than a typical "hard" glass. Successful formation of fibers from such glasses requires accurate temperature control, care in sizing the orifice through which the glass is drawn, and variable speed drawing equipment. However, with considerable attention to such details it has proven possible to successfully fiberize all of these glasses in our laboratory using the equipment described in a later section. In Table XI where all of the viscosity data obtained to date is summarized by listing those temperatures at which a given glass has a viscosity of approximately 300 poises, it will be noted that the glasses melted to date have a wide range of refractoriness. In general, as will be shown later, only the more refractory of these glasses have proven interesting in the search for glasses that can be fiberized and which have an unusually high modulus.



BROOKFIELD VISCOMETER MODEL: RVT
 CONTAINER DIAMETER: 2 IN.
 MINIMUM CONTAINER DEPTH: 2 IN.



<u>SPEED (R.P.M.)</u>	<u>RANGE (CPS)</u>
100	0 - 3000
50	60,000
20	15,000
10	30,000
5	60,000
2.5	120,000
1	150,000
0.5	600,000

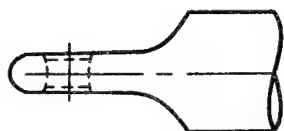


FIGURE 21. LARGE TUNGSTEN SPINDLE USED FOR HIGH TEMPERATURE VISCOSITY MEASUREMENT

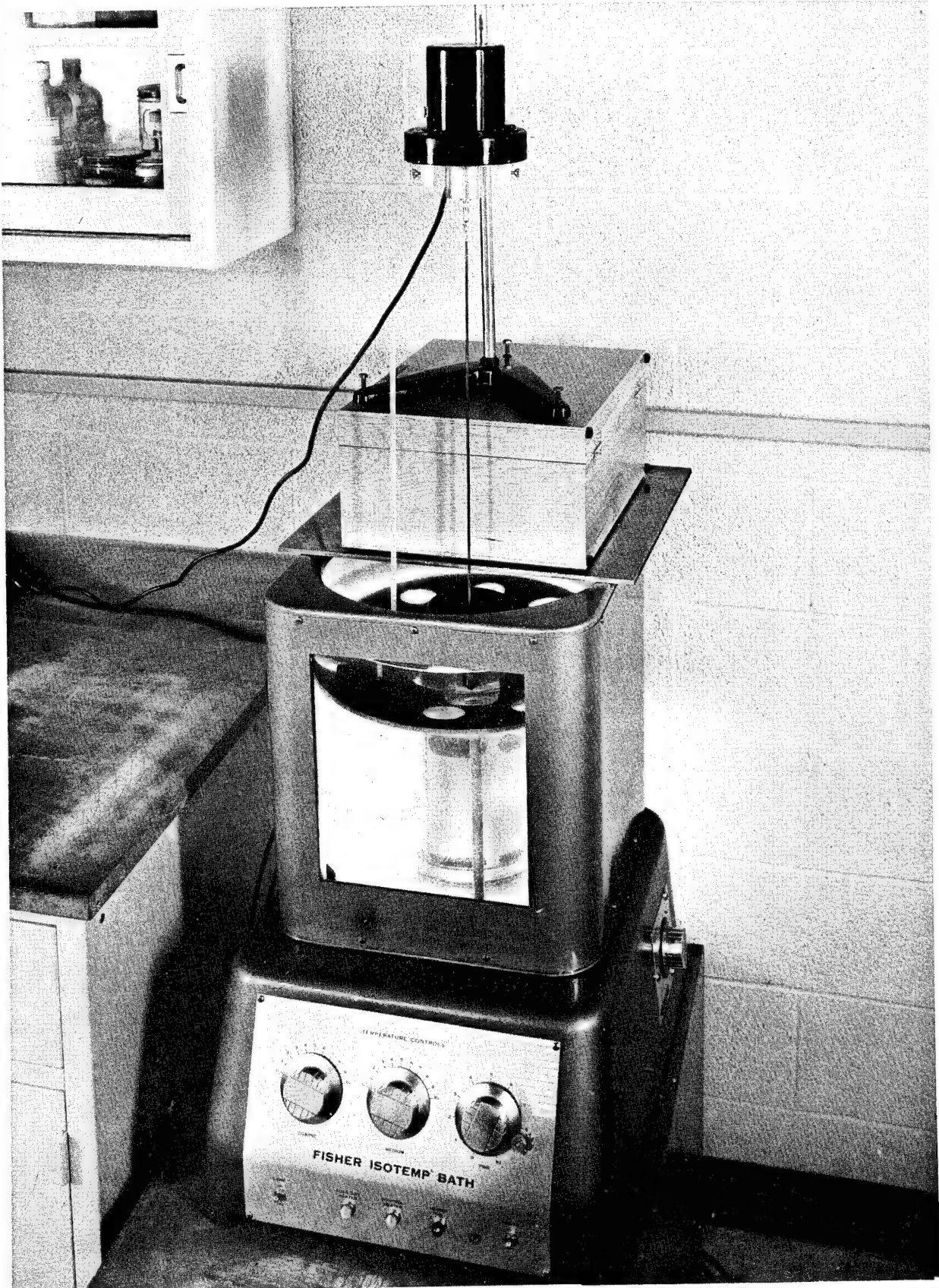


FIGURE 22. BROOKFIELD VISCOMETER AND CONSTANT TEMPERATURE BATH USED
FOR CALIBRATION

Table VIII

Calibration of Large Tungsten Spindle in N.B.S. Standard Oil "P"

<u>Viscometer Speed(rpm)</u>	<u>Reading (arb. div.)</u>	<u>Temp. (°C)</u>	<u>Viscosity Oil P (poises)</u>
20.0	74.0	51.0	80
20.0	79.5	47.5	111
20.0	95.7	44.0	145
10.0	37.2	51.0	80
10.0	39.8	47.5	111
10.0	48.1	44.0	145
10.0	73.0	41.0	175
5.0	18.3	51.0	80
5.0	19.6	47.5	111
5.0	24.0	44.0	145
5.0	36.5	41.0	175
5.0	52.0	37.9	214
5.0	60.5	35.0	275
5.0	66.0	32.0	362
5.0	81.1	29.0	450
5.0	82.7	28.0	510
2.5	9.4	51.0	80
2.5	9.75	47.5	111
2.5	12.1	44.1	145
2.5	18.4	41.0	175
2.5	25.5	38.0	214
2.5	30.4	35.0	275
2.5	36.5	32.0	362
2.5	41.4	29.0	450
2.5	41.0	28.0	510
2.5	48.7	27.0	555
2.5	65.2	24.0	780
2.5	81.8	21.0	970
2.5	83.6	18.0	1290

Table VIII (Cont'd)

<u>Viscometer Speed(rpm)</u>	<u>Reading (arb. div.)</u>	<u>Temp. (°C)</u>	<u>Viscosity Oil P (poises)</u>
1.0	4.05	51.0	80
1.0	4.45	47.5	111
1.0	4.9	44.0	145
1.0	7.5	41.0	175
1.0	10.1	37.9	214
1.0	12.4	35.0	275
1.0	14.2	32.0	362
1.0	16.4	29.0	450
1.0	16.5	28.0	510
1.0	19.5	27.0	555
1.0	26.1	24.0	780
1.0	32.5	21.0	970
1.0	31.6	18.0	1290
1.0	66.3	14.8	1790
1.0	88.3	12.0	2380
0.5	2.85	44.1	145
0.5	4.2	41.0	175
0.5	5.6	37.9	214
0.5	6.6	35.0	275
0.5	7.7	32.0	362
0.5	8.8	29.0	450
0.5	8.8	28.0	510
0.5	10.0	27.0	555
0.5	13.5	24.0	780
0.5	16.8	21.0	970
0.5	16.8	18.0	1290
0.5	35.5	14.9	1790
0.5	46.75	12.0	2380
0.5	51.2	9.0	off graph used
0.5	57.5	5.85	off graph used

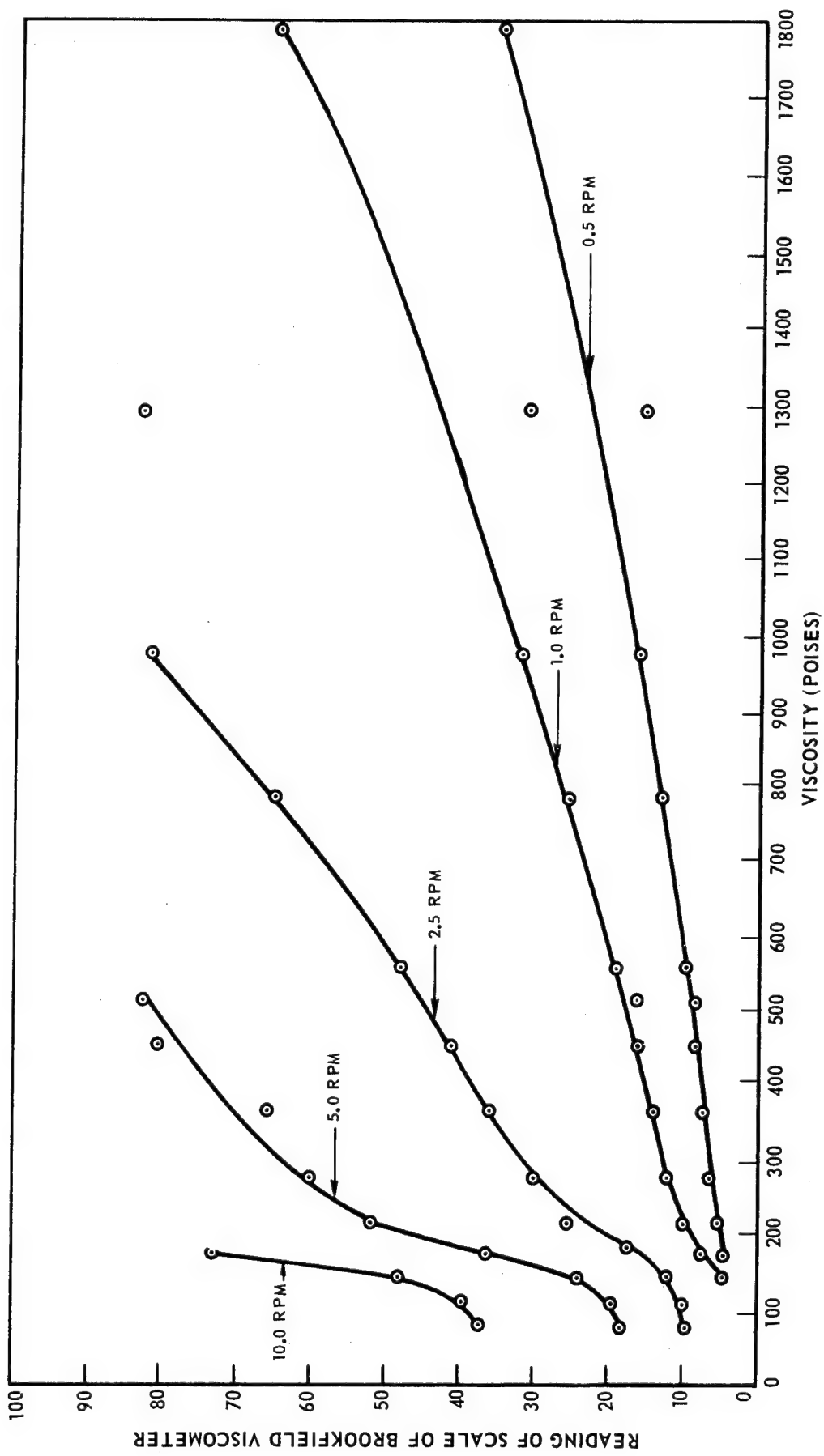


FIGURE 23. CALIBRATION DATA FOR LARGE TUNGSTEN SPINDLE, BROOKFIELD VISCOMETER,
AND STANDARD OIL "P" FROM N. B. S.

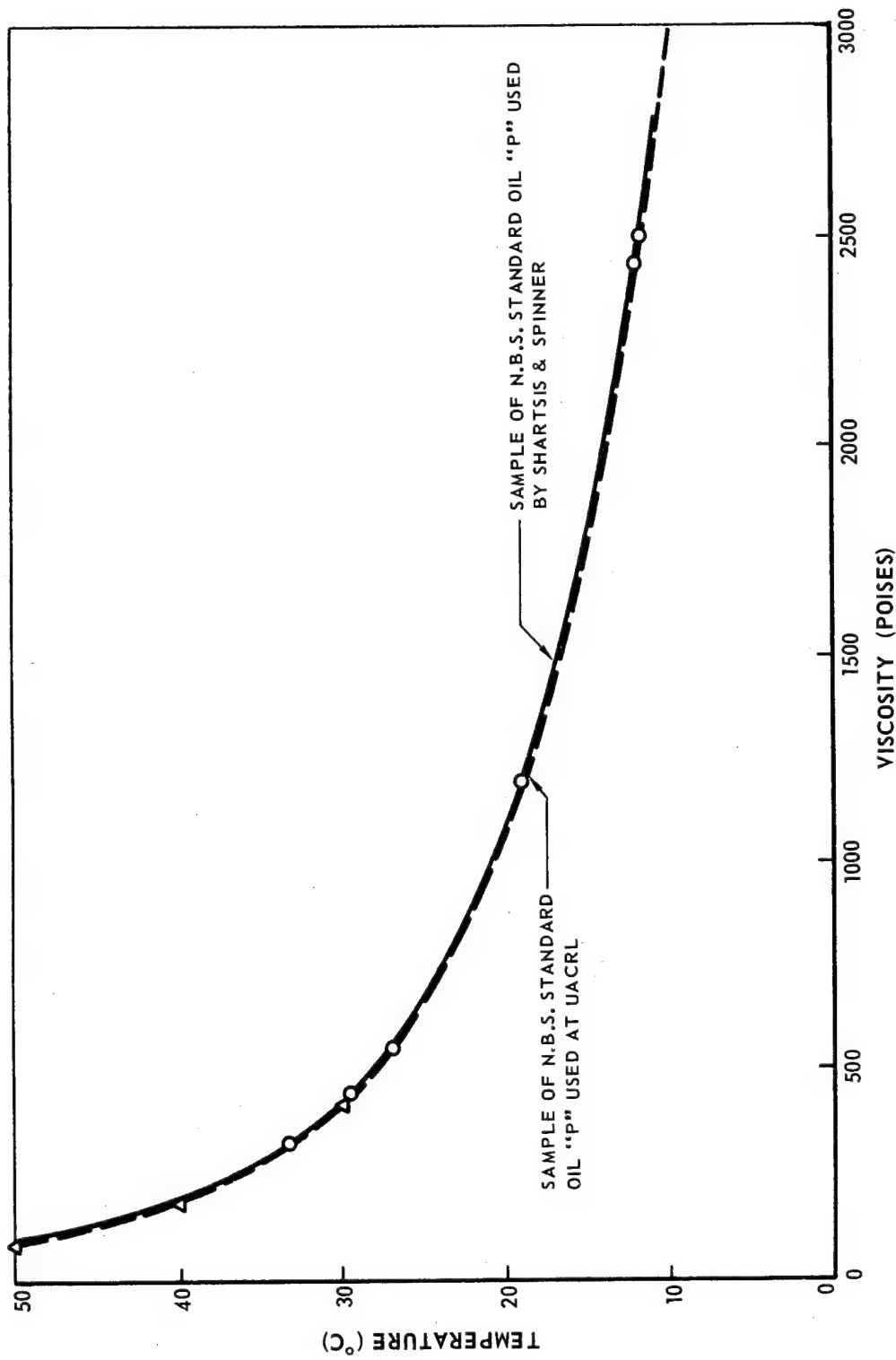


FIGURE 24. EXTRAPOLATED CALIBRATION CURVE FOR N. B. S. VISCOSITY STANDARD "P"

Table IX

Extrapolated and Certificate Values of Viscosity for
N.B.S. Viscosity Standard Oil "P"

<u>Temperature</u> °C	<u>Viscosity (poises)</u>	<u>Temperature</u> °C	<u>Viscosity (poises)</u>
30.0	417.8 certif.	33.36	329 (Ref. 8)
40.0	183.3 certif.	29.50	448 (Ref. 8)
50.0	86.6 certif.	26.98	569 (Ref. 8)
		11.98	2,439 (Ref. 8)
		19.10	1,193 (Ref. 8)
		11.81	2,499 (Ref. 8)

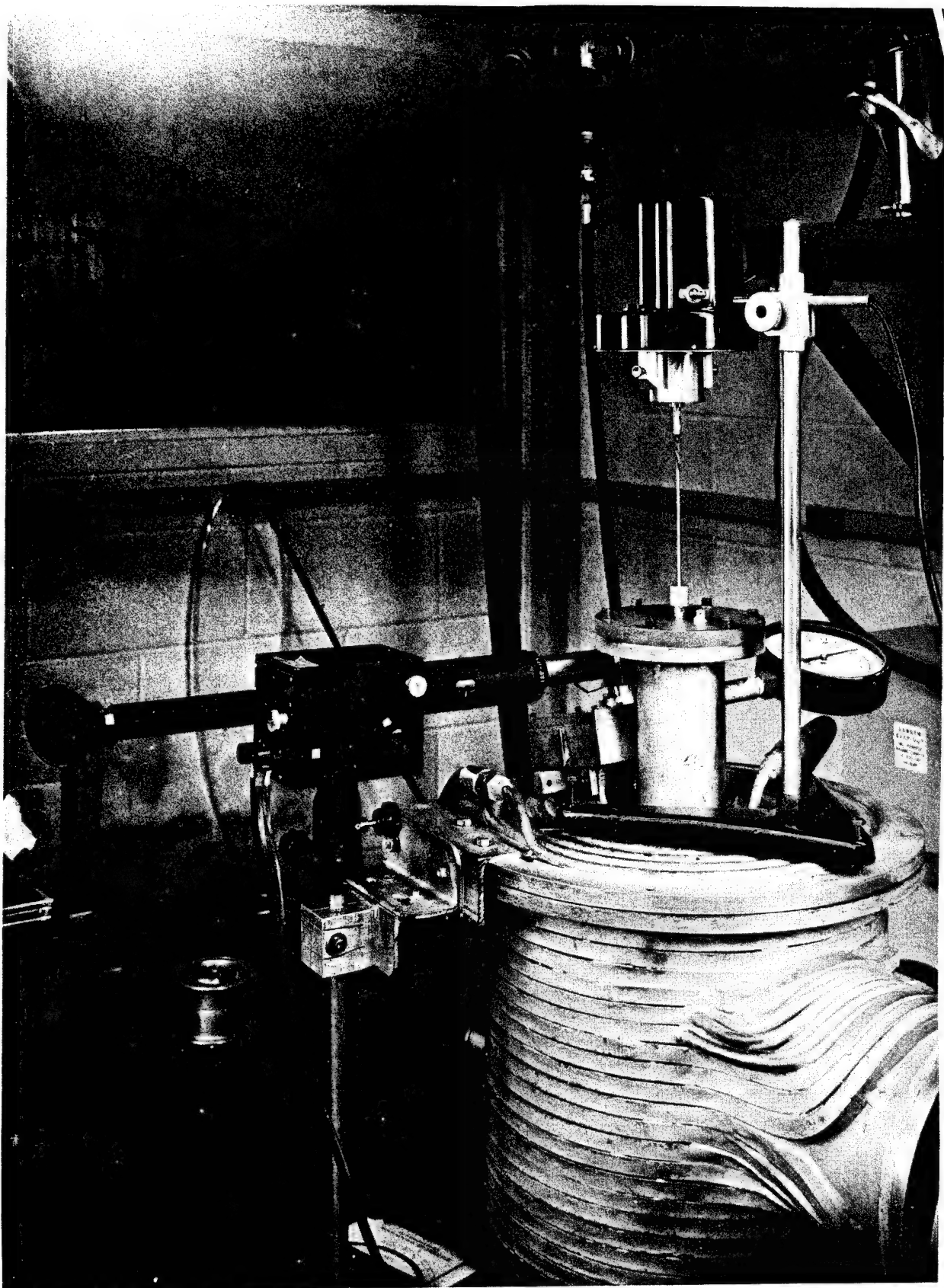


FIGURE 25. BROOKFIELD VISCOMETER INSTALLED ON TUNGSTEN FURNACE
FOR HIGH TEMPERATURE VISCOSITY MEASUREMENTS

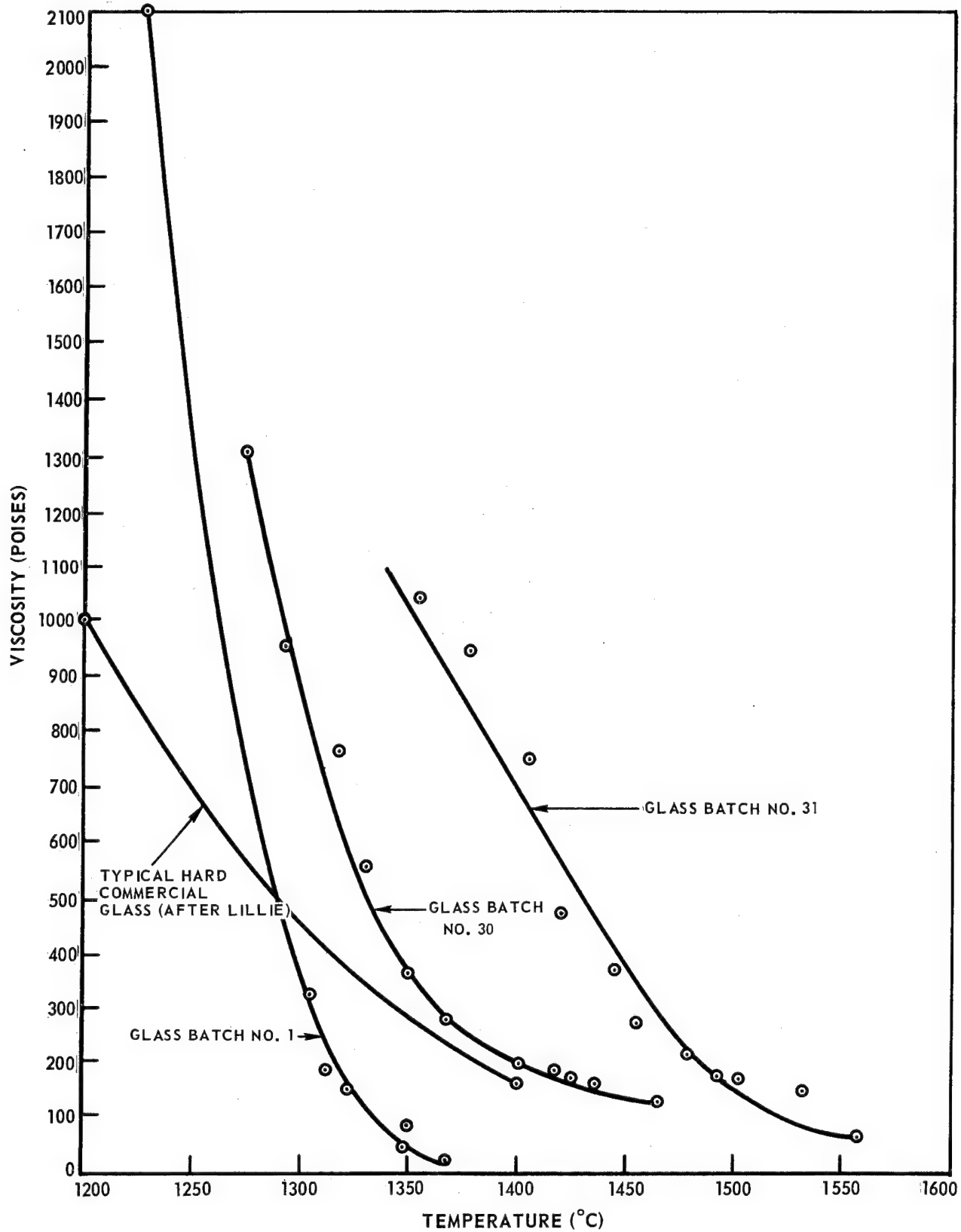


FIGURE 26. EXPERIMENTALLY DETERMINED VISCOSITY-TEMPERATURE RELATIONS

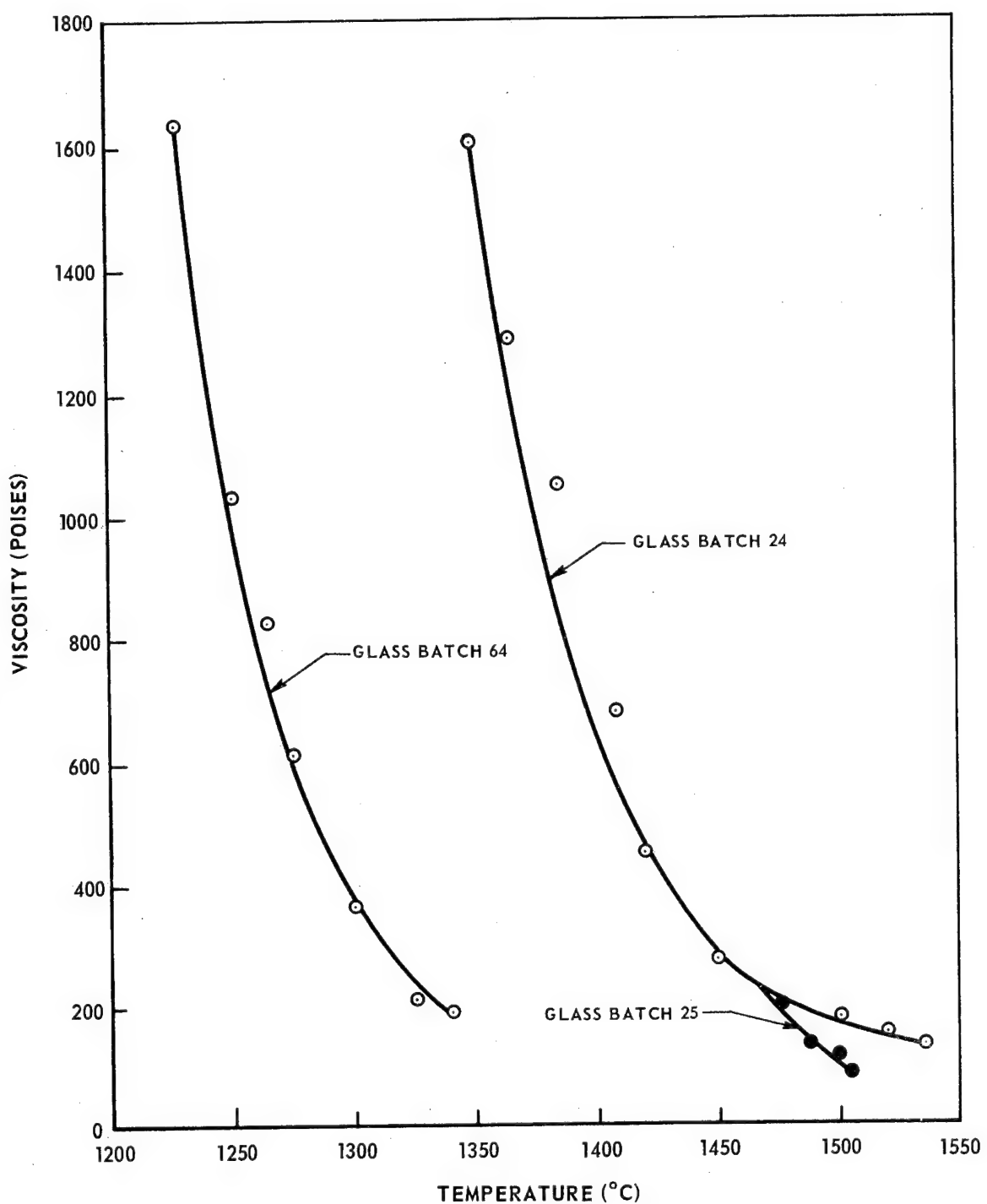


FIGURE 27. EXPERIMENTALLY DETERMINED VISCOSITY-TEMPERATURE RELATIONS

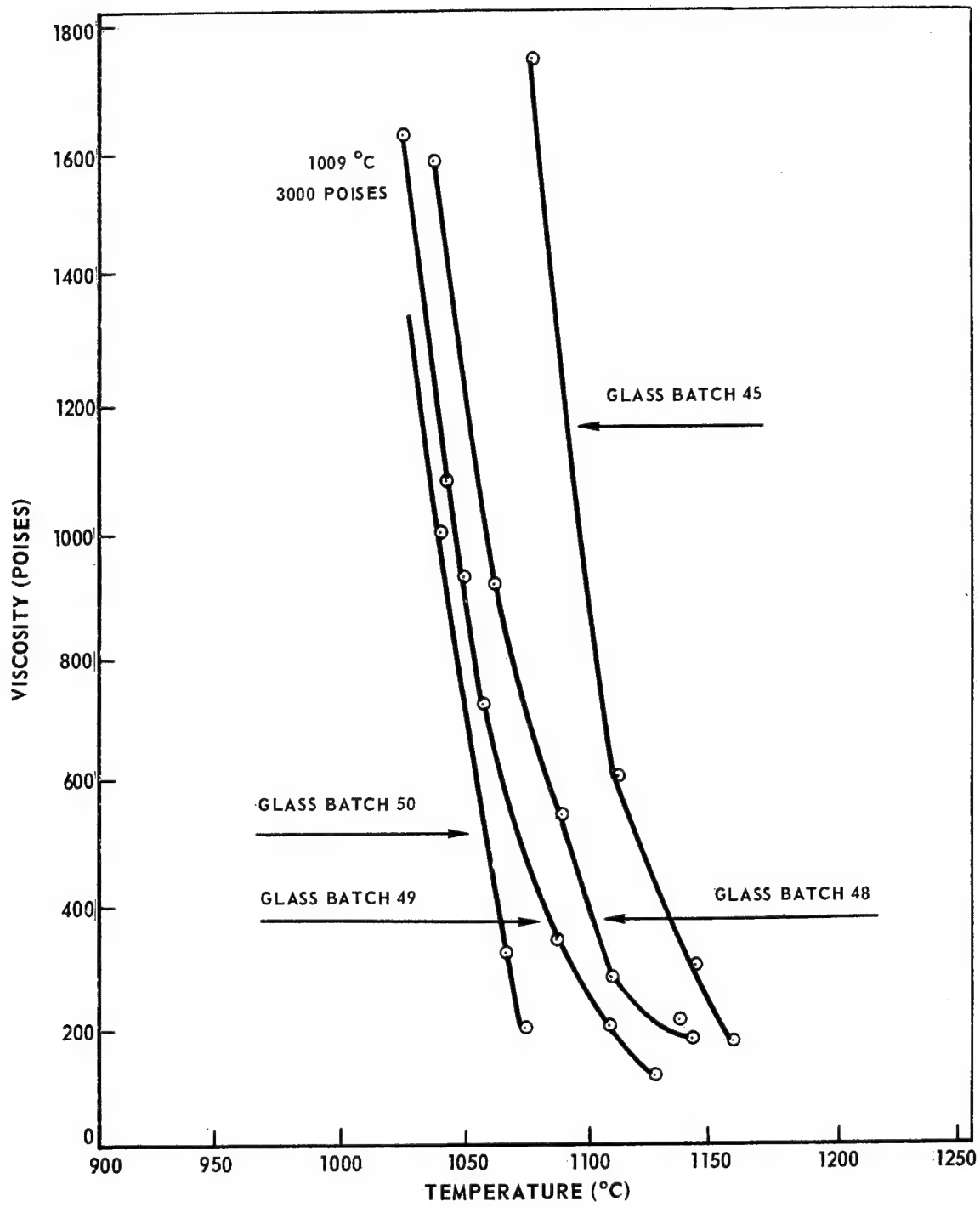


FIGURE 28. EXPERIMENTALLY DETERMINED VISCOSITY-TEMPERATURE RELATIONS

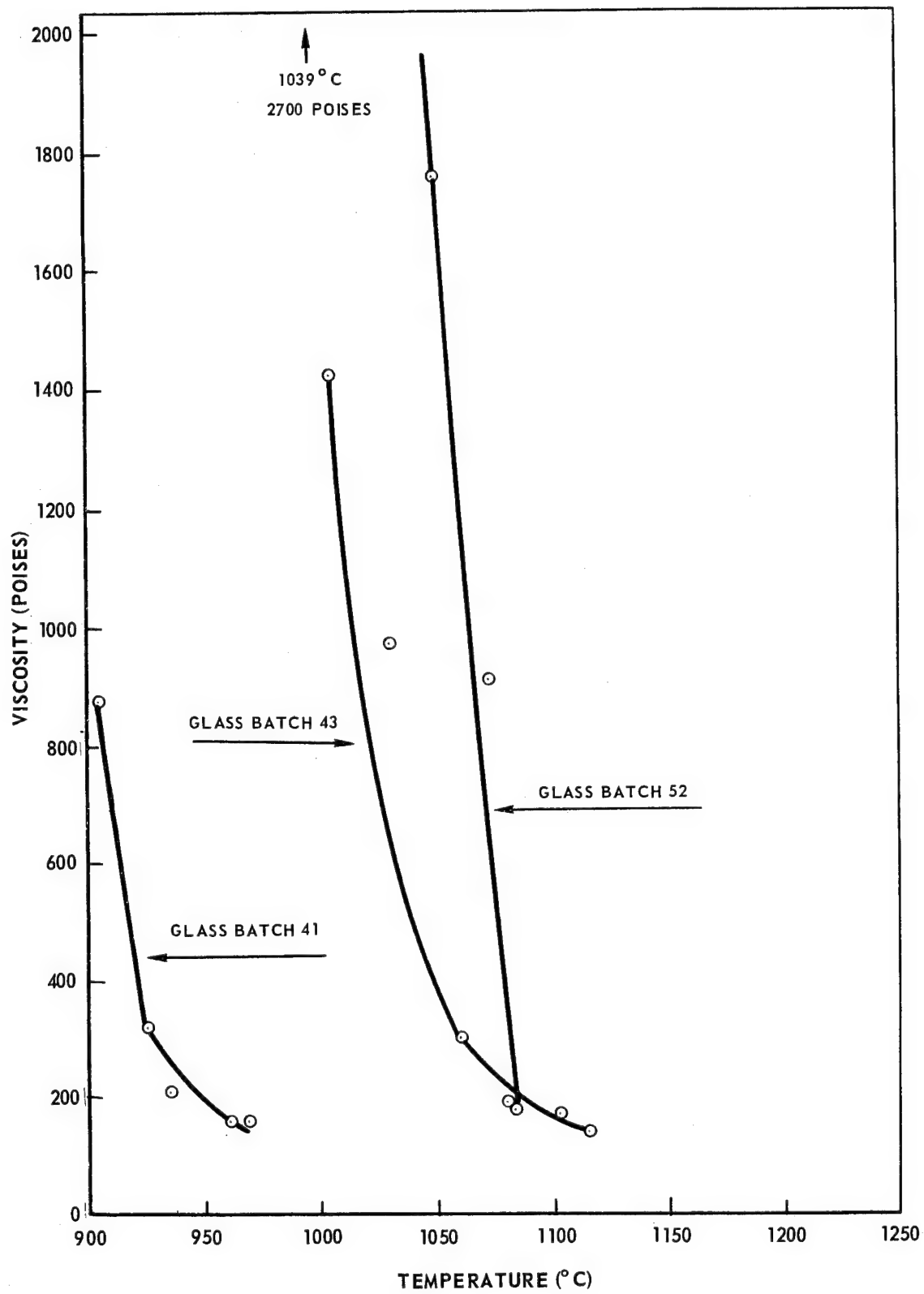


FIGURE 29. EXPERIMENTALLY DETERMINED VISCOSITY-TEMPERATURE RELATIONS

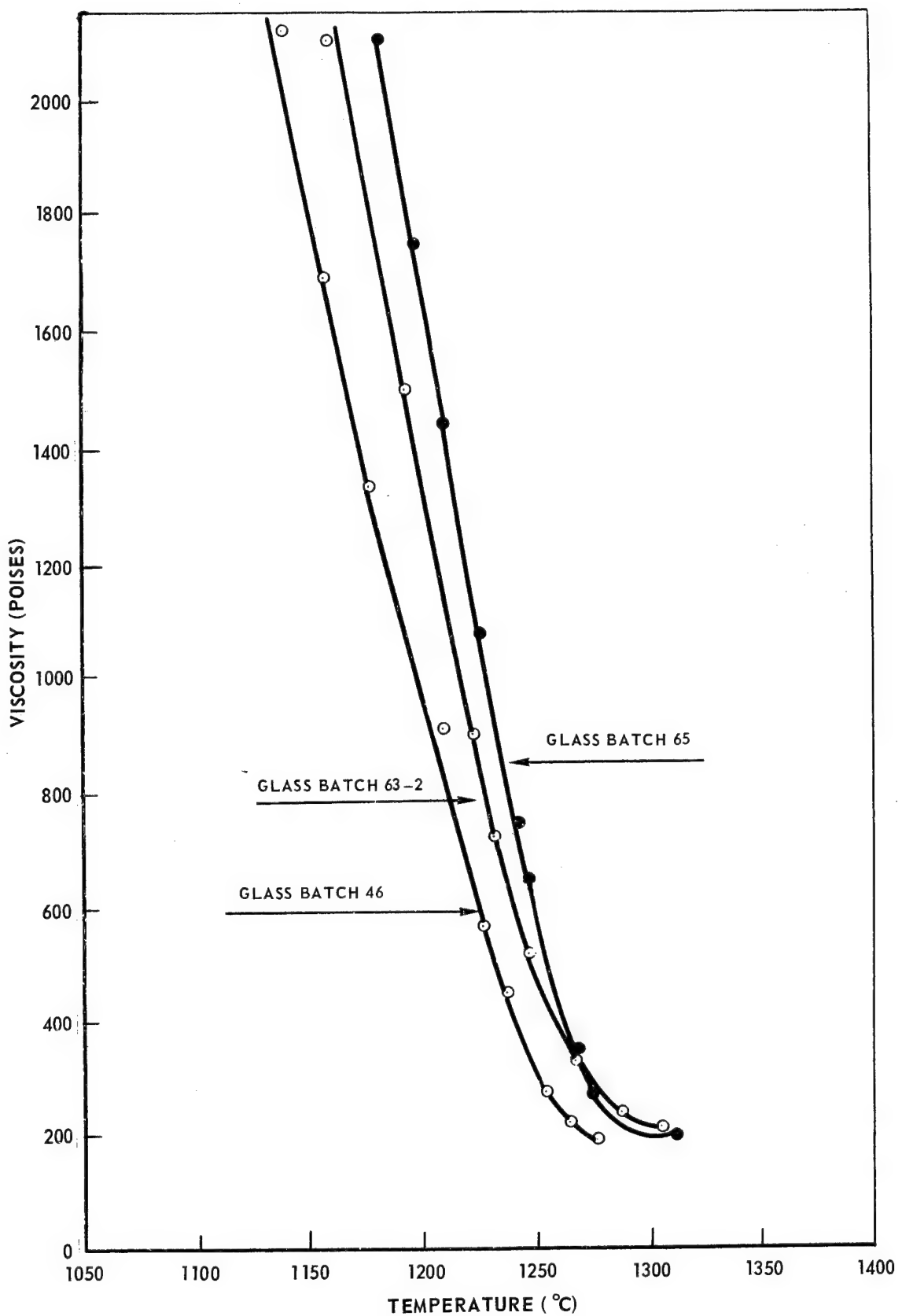


FIGURE 30. EXPERIMENTALLY DETERMINED VISCOSITY-TEMPERATURE RELATIONS

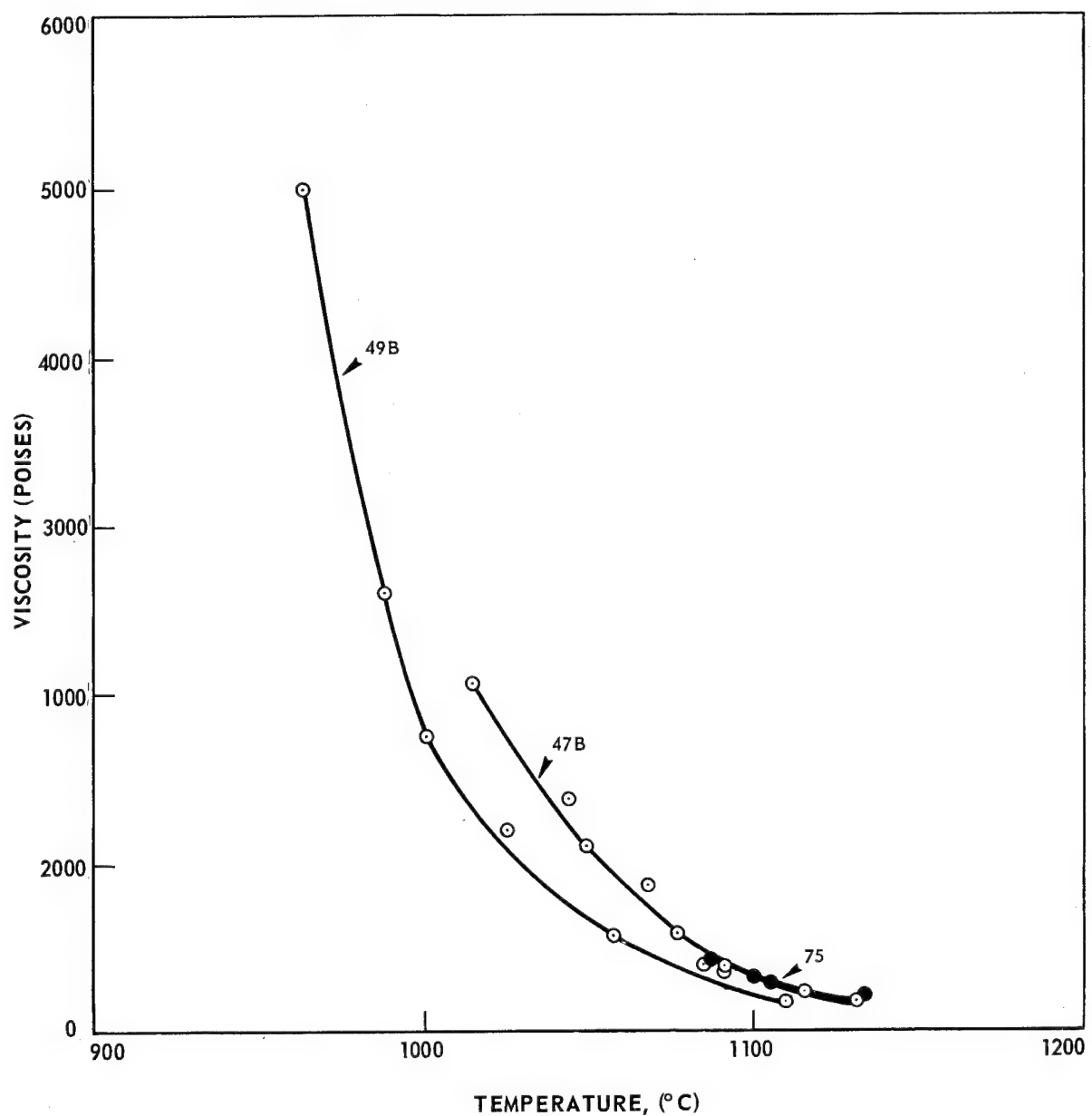


FIGURE 31. EXPERIMENTALLY DETERMINED VISCOSITY-TEMPERATURE RELATIONS

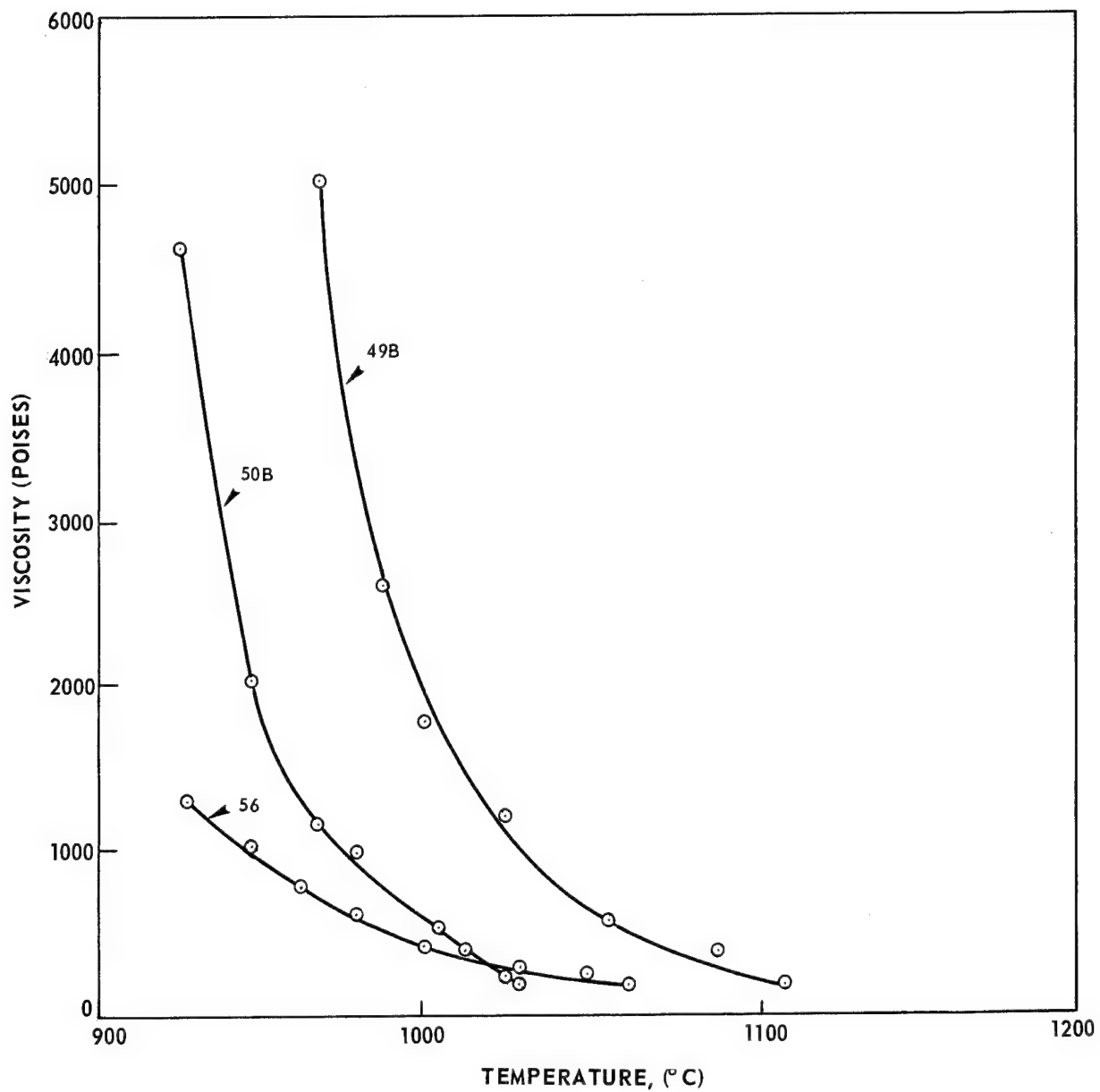


FIGURE 32. EXPERIMENTALLY DETERMINED VISCOSITY-TEMPERATURE RELATIONS

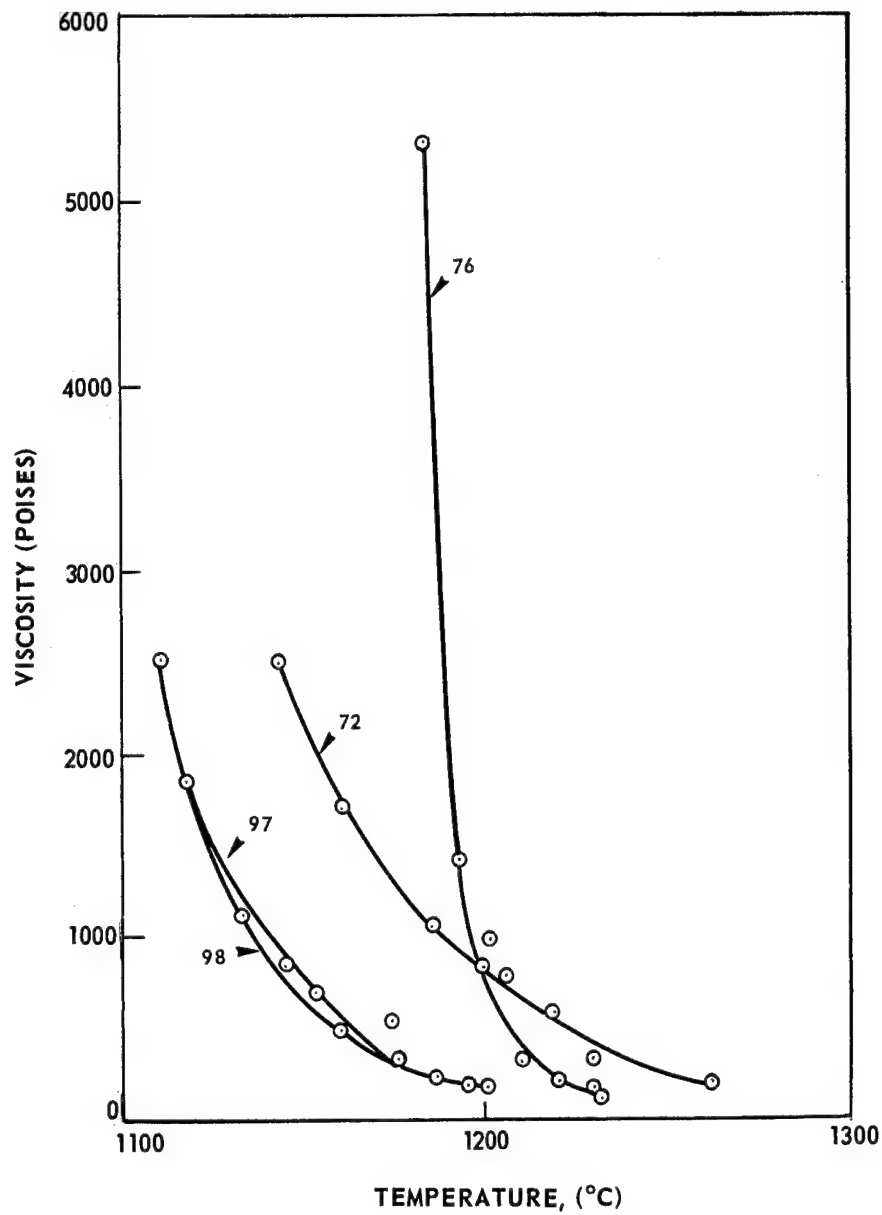


FIGURE 33. EXPERIMENTALLY DETERMINED VISCOSITY-TEMPERATURE RELATIONS

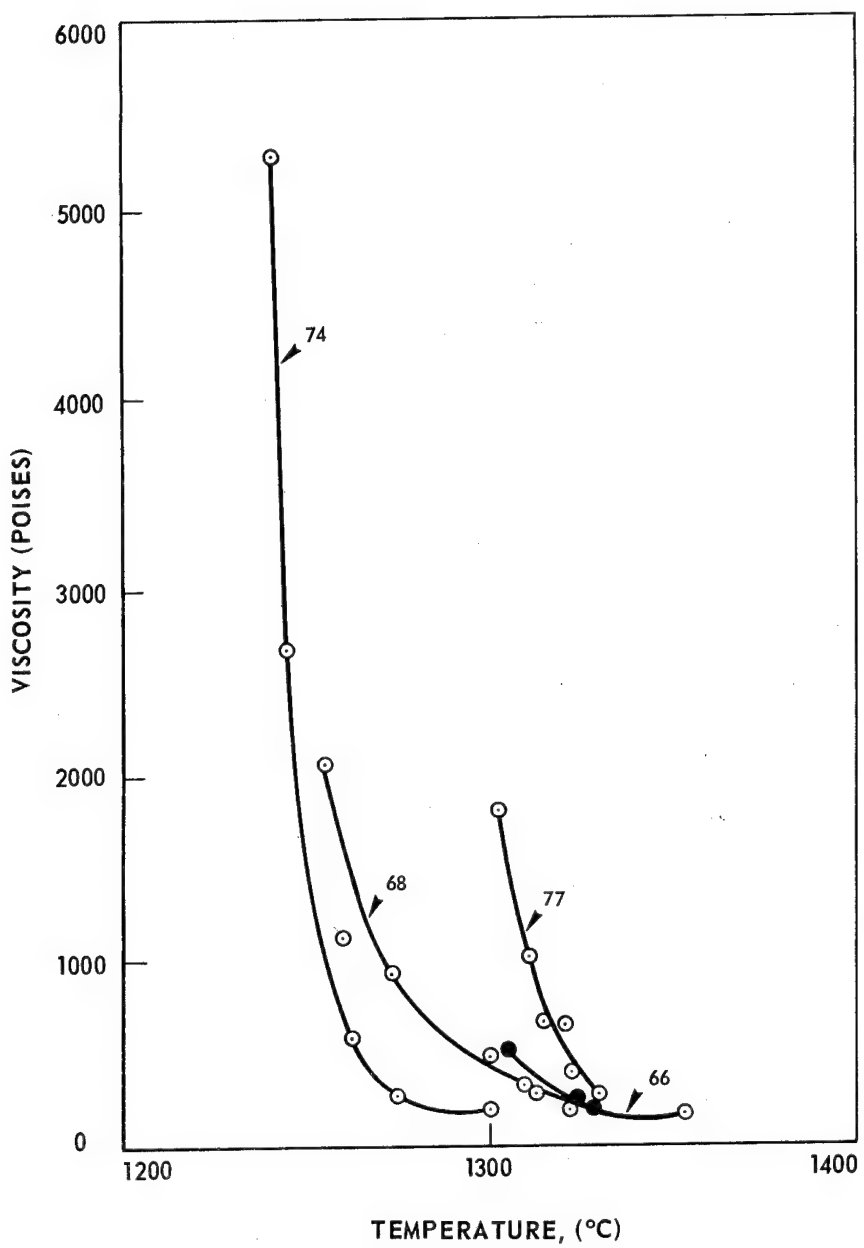


FIGURE 34. EXPERIMENTALLY DETERMINED VISCOSITY-TEMPERATURE RELATIONS

Table X
Experimental Determination of Viscosity Individual Runs

Glass Batch No. 1

<u>Temp.</u>	<u>Viscosity</u>
<u>°C</u>	<u>(poises)</u>

1281	2150	1350	1600	1478	200
1305	335	1365	1285	1488	140
1313	184	1385	1050	1498	115
1333	160	1407	685	1509	80
1348	87	1420	450		
		1450	275		
		1485	200		
		1500	175		
		1520	150		
		1540	130		
		1570	95		
		1590	80		

Glass Batch No. 24

<u>Temp.</u>	<u>Viscosity</u>
<u>°C</u>	<u>(poises)</u>

Glass Batch No. 25

<u>Temp.</u>	<u>Viscosity</u>
<u>°C</u>	<u>(poises)</u>

Glass Batch No. 30

<u>Temp.</u>	<u>Viscosity</u>
<u>°C</u>	<u>(poises)</u>

Glass Batch No. 31

<u>Temp.</u>	<u>Viscosity</u>
<u>°C</u>	<u>(poises)</u>

Glass Batch No. 41

<u>Temp.</u>	<u>Viscosity</u>
<u>°C</u>	<u>(poises)</u>

1247	1310	1358	1043	905	880
1267	954	1378	947	925	320
1292	765	1405	748	935	210
1305	557	1420	475	959	160
1327	365	1445	373	969	160
1342	281	1455	270		
1377	193	1483	213		
1392	186	1492	175		
		1508	170		
		1532	147		
		1558	57		

Table X (Cont'd)

Glass Batch No. 43		Glass Batch No. 45		Glass Batch No. 46	
Temp. °C	Viscosity (poises)	Temp. °C	Viscosity (poises)	Temp. °C	Viscosity (poises)
983	2500	1077	1750	1143	2100
1005	1425	1112	600	1157	1690
1030	965	1145	300	1177	1335
1060	300	1160	175	1209	905
1080	190			1227	570
1103	165			1237	450
1115	135			1254	275
				1266	235
				1278	190

Glass Batch No. 47B		Glass Batch No. 48		Glass Batch No. 49	
Temp. °C	Viscosity (poises)	Temp. °C	Viscosity (poises)	Temp. °C	Viscosity (poises)
1015	2060	1038	1590	1011	2500
1043	1390	1062	920	1025	1630
1048	1100	1090	535	1042	1080
1067	855	1110	280	1050	930
1086	397	1137	210	1057	725
1091	360	1140	180	1087	345
1115	230			1110	200
1132	170			1128	170

Glass Batch No. 49B		Glass Batch No. 50		Glass Batch No. 50B	
Temp. °C	Viscosity (poises)	Temp. °C	Viscosity (poises)	Temp. °C	Viscosity (poises)
967	5000	1009	3000	924	4600
988	2600	1040	1000	947	2000
1000	1755	1067	320	968	1150
1025	1192	1078	205	980	970
1056	555			1004	273
1090	278			1025	210
1110	180			1030	177

Table X (Cont'd)

Glass Batch No. 52		Glass Batch No. 56		Glass Batch No. 63-2	
Temp. °C	Viscosity (poises)	Temp. °C	Viscosity (poises)	Temp. °C	Viscosity (poises)
1034	4500	928	1265	1157	2600
1039	2700	948	1007	1170	2060
1050	1760	963	780	1193	1500
1072	910	979	600	1223	900
1083	180	1000	402	1231	725
		1029	263	1248	520
		1012	385	1268	330
		1050	230	1287	235
		1068	175	1310	200

Glass Batch No. 64		Glass Batch No. 65		Glass Batch No. 66	
Temp. °C	Viscosity (poises)	Temp. °C	Viscosity (poises)	Temp. °C	Viscosity (poises)
1207	2300	1173	2900	1304	510
1228	1630	1185	2100	1324	215
1250	1030	1197	1745	1326	205
1265	825	1211	1420		
1276	615	1226	1075		
1299	365	1242	745		
1326	210	1248	650		
1340	190	1268	365		
		1277	275		
		1289	235		
		1315	205		

Glass Batch No. 68		Glass Batch No. 72		Glass Batch No. 74	
Temp. °C	Viscosity (poises)	Temp. °C	Viscosity (poises)	Temp. °C	Viscosity (poises)
1255	2090	1142	2500	1240	5300
1272	940	1160	1727	1246	1695
1300	475	1184	1055	1259	1053
1213	292	1200	860	1262	594
1320	205	1218	583	1275	279
1330	207	1228	325	1300	207
1335	180	1260	200		
1352	165				
1310	315				

Table X (Cont'd)

Glass Batch No. 75		Glass Batch No. 76		Glass Batch No. 77	
Temp. °C	Viscosity (poises)	Temp. °C	Viscosity (poises)	Temp. °C	Viscosity (poises)
1078	577	1182	5300	1302	1805
1088	433	1192	14000	1310	1018
1100	327	1201	972	1315	683
1105	275	1206	757	1320	650
1133	193	1210	300	1322	396
		1221	210	1329	229
		1230	155		
		1231	150		
Glass Batch No. 97		Glass Batch No. 98			
Temp. °C	Viscosity (poises)	Temp. °C	Viscosity (poises)		
1118	1850	1111	2500		
1145	860	1132	1135		
1153	697	1145	833		
1173	540	1160	487		
1185	225	1176	272		
1195	197	1200	177		

Table XI

Summary of Experimental Viscosity Determinations

Batch	Temperature at Which Viscosity is Approximately 300 Poises (°C)	Batch	Temperature at Which Viscosity is Approximately 300 Poises (°C)
1	1305	52	1088
24	1450	56	1026
25	1470	63-2	1269
31	1342	64	1326
32	1455	65	1267
41	925	66	1317
43	1060	68	1312
45	1170	72	1230
46	1254	74	1275
47B	1103	75	1102
48	1110	76	1210
49	1087	77	1327
49B	1087	97	1182
50	1067	98	117 ¹
50B	1003		

This equipment has also been used to obtain the results for UARL 344, a composition which has been produced in amounts of 100 million feet of monofilament and incorporated in composites with the results shown in our later sections. The viscosity temperature curve for UARL 344 is sketched in Fig. 35 and compared with Owens-Corning "E" glass shown in the same figure, although with a different temperature scale. While the working range of the UARL 344 glass is not as great as that of the "E" glass, it appears to be more than sufficient since it is approximately 100°C. And, indeed, it has proven possible by a variation of operating parameters to draw large amounts of good quality fibers from the UARL 344 composition at high rates of speed over a very considerable temperature range.

The effect of a progressive change in composition is readily apparent in Fig. 28 where data is plotted for four "invert" glasses. Additional amounts of titania and of the potassium-calcium-strontium-barium fraction progressively lower the working temperature of the glass as can be seen from Table I.

In the previous section the procedure for measuring the electrical conductivity of the molten oxides as a continuous function of temperature using a conductivity cell and central "ball" electrode has been described in detail. In this section the method of using the viscometer together with tungsten shaft and spindle to measure viscosity at various temperatures has likewise been described in detail. Since both systems use the same tungsten crucibles with either a rotating tungsten spindle or tungsten ball in the exact center of the crucible, it strongly suggests the possibility that the two measurements can be made simultaneously so as to obtain precise correlation. Numerous methods of making "low" friction electrical contact to the rotating viscometer spindle and shaft were investigated including ball bearings, brushes, and similar methods but all methods investigated were found to be unsatisfactory because of non-reproducible effects on the viscometer readings caused by drag. It does not appear possible, therefore, to make the two measurements simultaneously and we shall continue to carry them out separately.

Direct Optical Measurement of Kinetics of Crystallization

The direct microscopic observation of the kinetics of crystallization of two crystal species, cordierite and sapphirine originating in molten $MgO-Al_2O_3-SiO_2$ systems was made possible by the construction of a microfurnace.

This UARL microfurnace design owes much to the earlier furnace constructed by Morley (Ref. 81) for exactly the same type research, namely, the study of crystallization kinetics in molten glass. The microfurnace consists essentially of a platinum-10% rhodium tube, 0.250 in. O.D. and with a wall thickness of 3 mils, which is damped between the two copper bars (0.125 in. x 0.500 in.). A circular shelf of platinum is welded to the inside of the tube, and the crucible is placed in a 0.128 in. hole in this shelf. Crucibles are fabricated by cutting platinum tubing (0.125 in. dia with 5 mil wall thickness) into pieces 0.065 in. long and then pressing them in a die so that they form a 40 degree included angle.

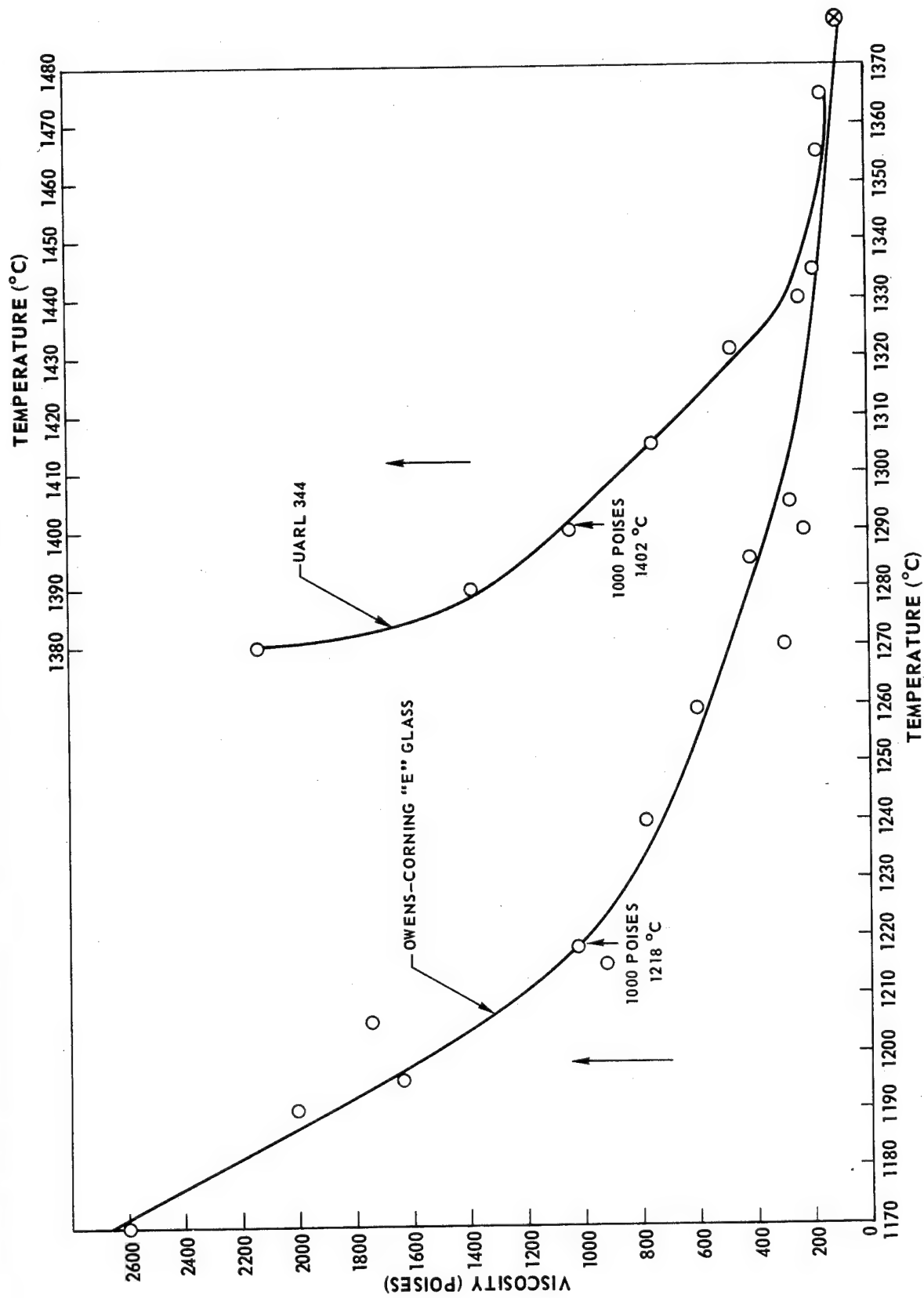


FIGURE 35. VISCOSITY-TEMPERATURE CURVES FOR OWENS-CORNING "E" GLASS COMPARED TO UARL 344 GLASS

Figure 36 shows the microfurnace without radiation shielding. Subsequently radiation shielding was found necessary and was added by welding two rings of 0.057 in. Kanthal wire to the nichrome plates at the two ends of the heater tube. An inner shield of 4 mil platinum-rhodium sheet and an outer shield of 5 mil nichrome sheet were welded to the inner nichrome wire ring that is on the lower nichrome plate. Two 5 mil nichrome shields were welded to the outer nichrome wire ring on the upper circular nichrome plate.

Figure 36 also shows the 1/8 in. dia copper tubing which is used to supply water-cooling to the copper electrical connectors. The power supplied the furnace comes from a filament transformer of 0.975 KVA capacity and a 20 ampere Variac. To attain a temperature of 1400°C a current of 140 amperes at 1.1 volts (60 cycle a-c) has proven adequate.

The entire experimental arrangement with the exception of the power supply is shown in Fig. 37. It comprises the microfurnace, microscope and camera, micromanipulator used to weld and position the thermocouple, the x-y recorder used for plotting time-temperature response of the furnace, and the 3 mil platinum-platinum 10% rhodium thermocouple carefully positioned in the center of the furnace. Experience has shown that the furnace temperature can be maintained to within $\pm 4^{\circ}\text{C}$ at 1250°C.

In actual use, the crucible is inserted into the furnace, a large fragment of glass is placed in the crucible and the crucible then heated. Smaller glass fragments are later added to completely fill the crucible. The glass is then heated until all of the bubbles disappear and then cooled to the temperature selected for crystal growth observation. The thermocouple is then lowered into the melt and photographs are taken of the crystals growing on the thermocouple at selected time intervals. Seed crystals can be grown on the thermocouple by placing it in the melt and then withdrawing it to a cooler part of the furnace, a step that may or may not be necessary depending on the composition of the glass under investigation. High-speed film is used (Polaroid-ASA 3000) and good quality pictures are readily obtainable. The actual sizes of the crystals in the photographs can readily be obtained by calibrating the optical system employed.

With this equipment measurements of the rate of growth of cordierite in Batch 1 were made and sufficient data (Table XII) were taken to completely delineate a plot of the rate of growth versus temperature (Fig. 38). The features of this curve which are similar to the curve expressing the rate of growth of cordierite in Batch 1-B (Fig. 38) are: measurable growth rates begin at about 950°, the maximum occurs at 1200-1250°, very low growth rates at 1375° to 1410°, periods of no measurable growth for periods of 5 and 9 min, and at higher temperatures there are rates of solution of 20 μ/min . The main difference from the growth-rate curve for Batch 1-B is that the growth rate is much higher, approximately 500 μ/min as compared to about 300 μ/min for Batch 1-B. The composition of Batch 1 is 50.3 wt % SiO_2 , 30.5 wt % Al_2O_3 , 19.45 wt % MgO , and

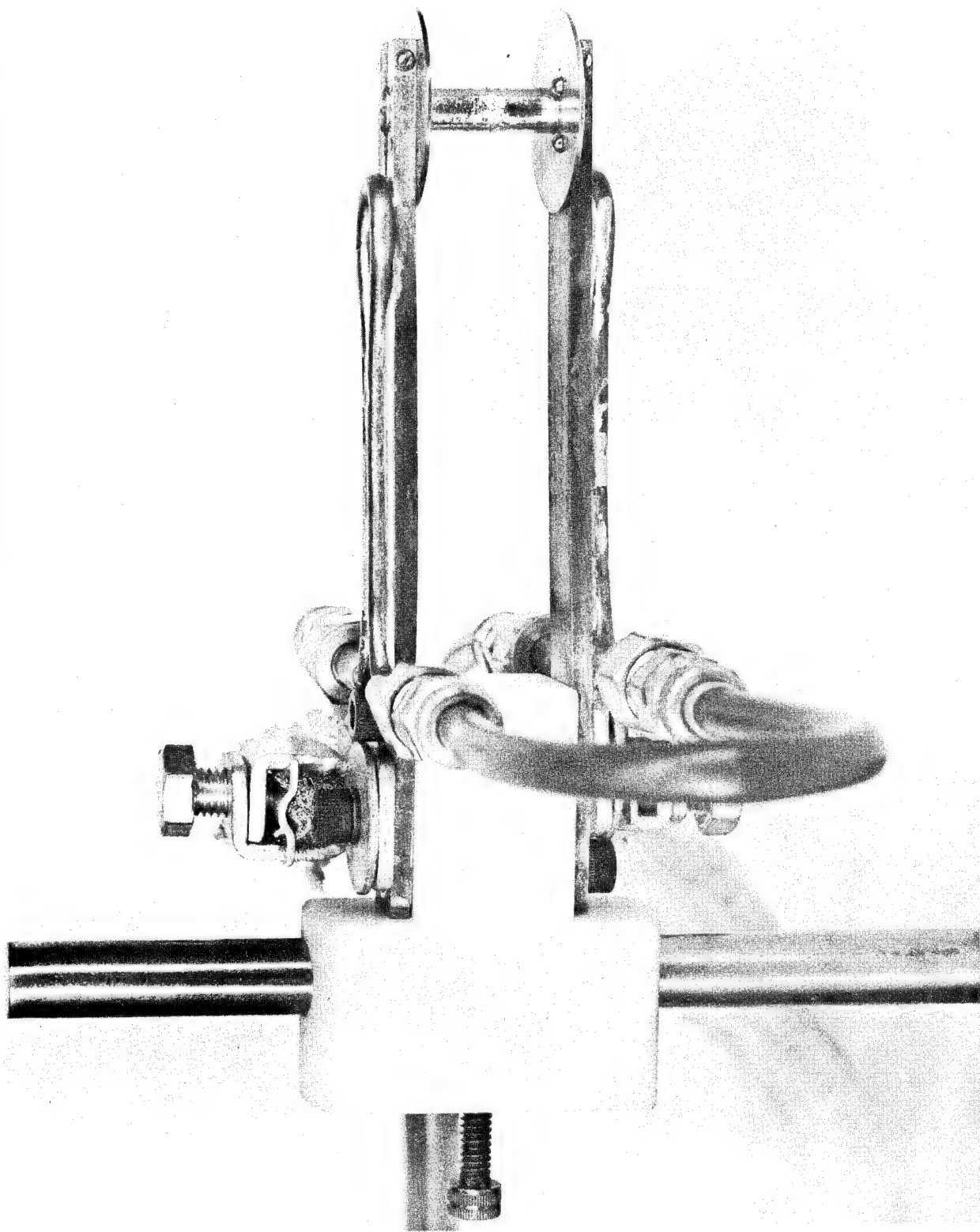


FIGURE 36. CLOSE-UP OF MICRO-FURNACE WITH HEAT SHIELDS REMOVED

FIGURE 37. MICRO-FURNACE AND ASSOCIATED EQUIPMENT IN POSITION FOR USE

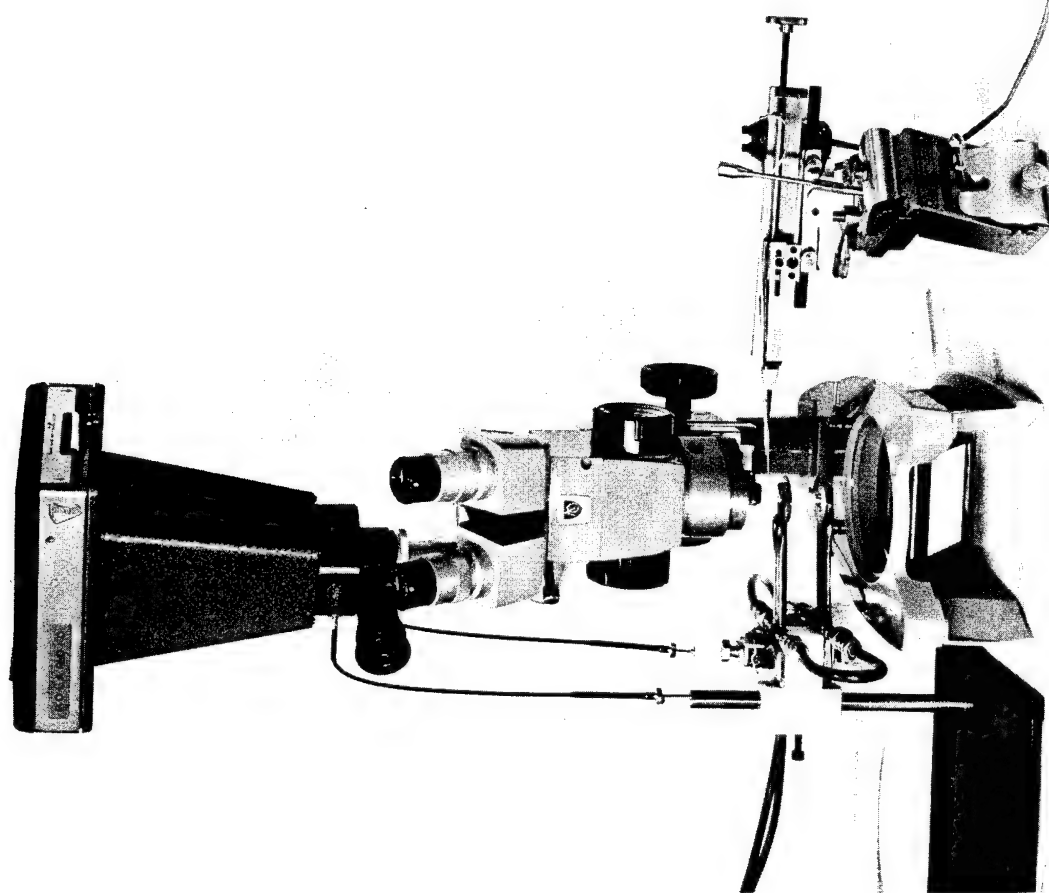


Table XII
Rate of Growth of Cordierite in Batch 1

<u>No.</u>	<u>Temp.</u>	<u>Rate, /min</u>	<u>No.</u>	<u>Temp.</u>	<u>Rate, /min</u>
1	1376 \pm 4	0 in. 30 min	23	1032 \pm 2	58
2	1189 \pm 4	475	24	1400 \pm 2	.2
3	1415 \pm 3	-20	25	1334 \pm 1	100
4	1343 \pm 4	11	26	1285 \pm 3	275
5	1278 \pm 4	250	27	1253 \pm 2	485
6	1139 \pm 4	360	28	1342 \pm 3	80
7	1154 \pm 6	320	29	1194 \pm 2	450
8	1025 \pm 5	42	30	1412 \pm 2	-380
9	962 \pm 5	5	31	1392 \pm 3	0 in. 12 min
10	1278 \pm 6	250	32	1316 \pm 3	92
11	1297 \pm 4	183	33	1407 \pm 3	-2
12	1411 \pm 5	0 in. 5 min	34	1258 \pm 3	475
13	1395 \pm 6	0 in. 9 min	35	1086 \pm 6	200
14	1355 \pm 5	5	36	1128 \pm 4	340
15	1220 \pm 2	485	37	1101 \pm 4	200
16	1155 \pm 2	370	38	1322 \pm 2	103
17	1428 \pm 2	-15	39	1316 \pm 3	100
18	1289 \pm 2	275	40	1363 \pm 3	2.4
19	1282 \pm 2	330	41	1296 \pm 3	135
20	1011 \pm 4	25	42	1305 \pm 4	120
21	1061 \pm 2	88	43	1328 \pm 3	50
22	1249 \pm 2	425			

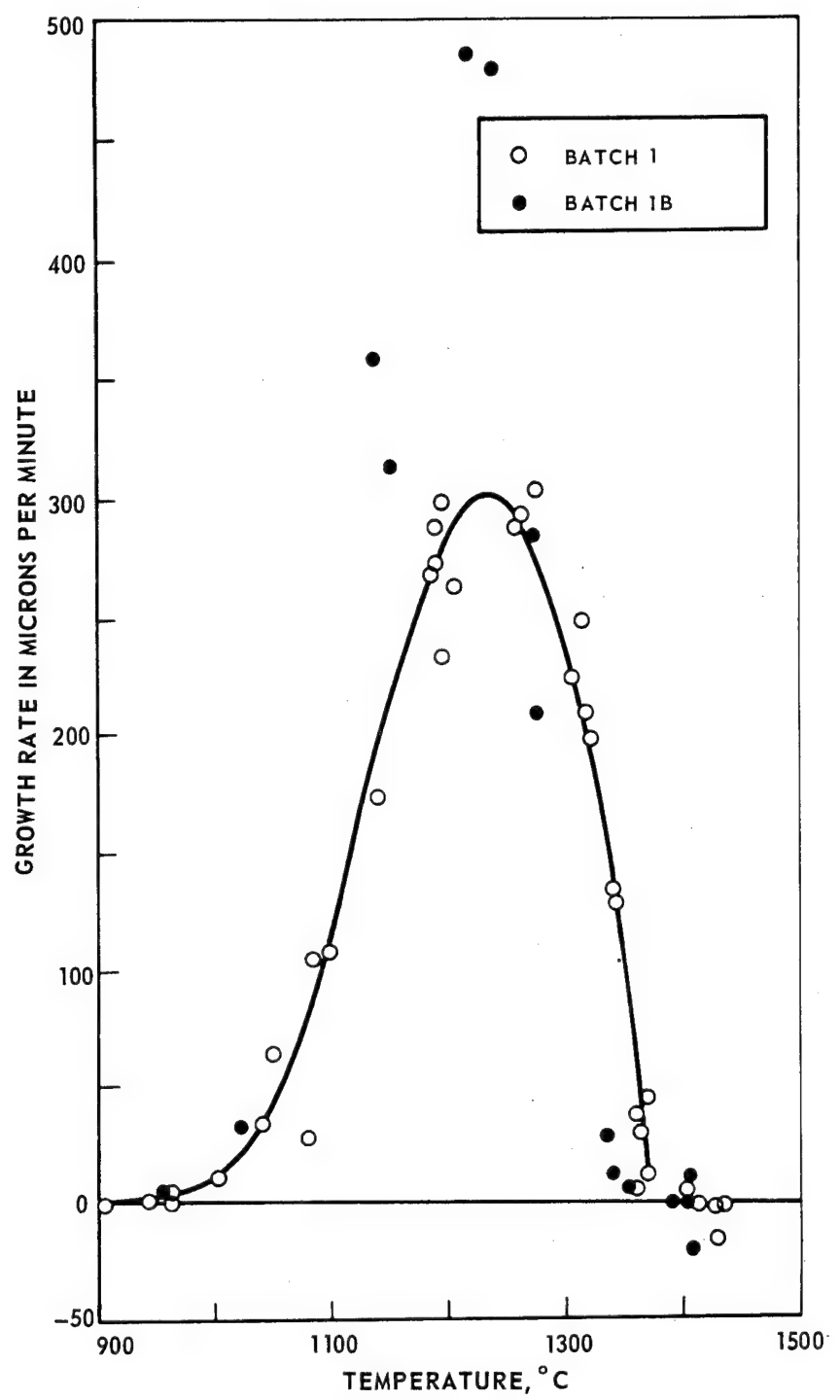
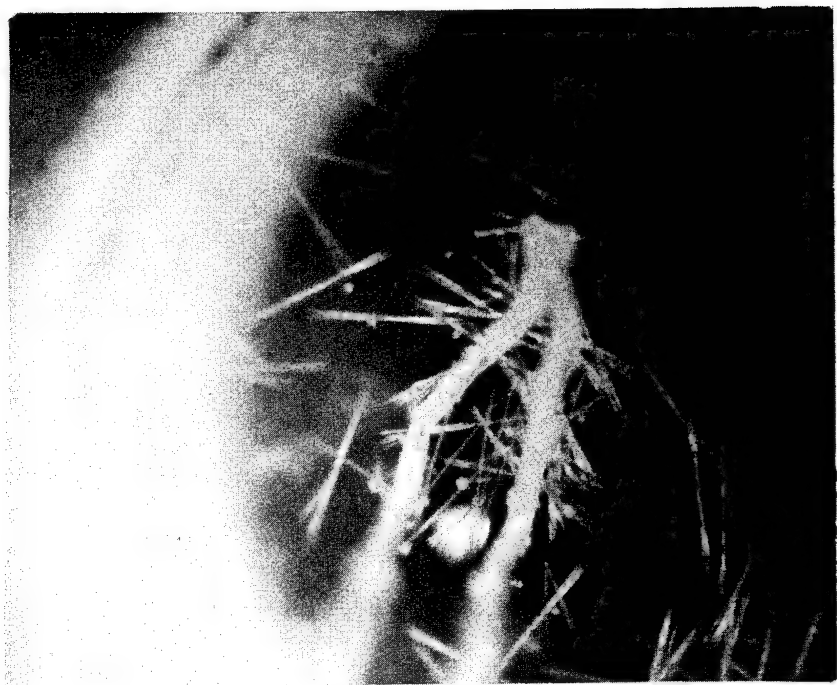


FIGURE 38. EFFECT OF TEMPERATURE ON THE RATE OF GROWTH OF CORDIERITE CRYSTALS

the composition of Batch 1-B is 55 wt % SiO_2 , 30 wt % Al_2O_3 , and 15 wt % MgO . The difference in these compositions is that Batch 1 has about 5 wt % less silica and 5 wt % more magnesia, and might be expected to have a lower viscosity than would Batch 1-B at the same temperature. The maximum growth rate of 485 microns per minute is the fastest we have measured. At this rate of growth measurements can be made only for very short times, usually 30 to 90 seconds.

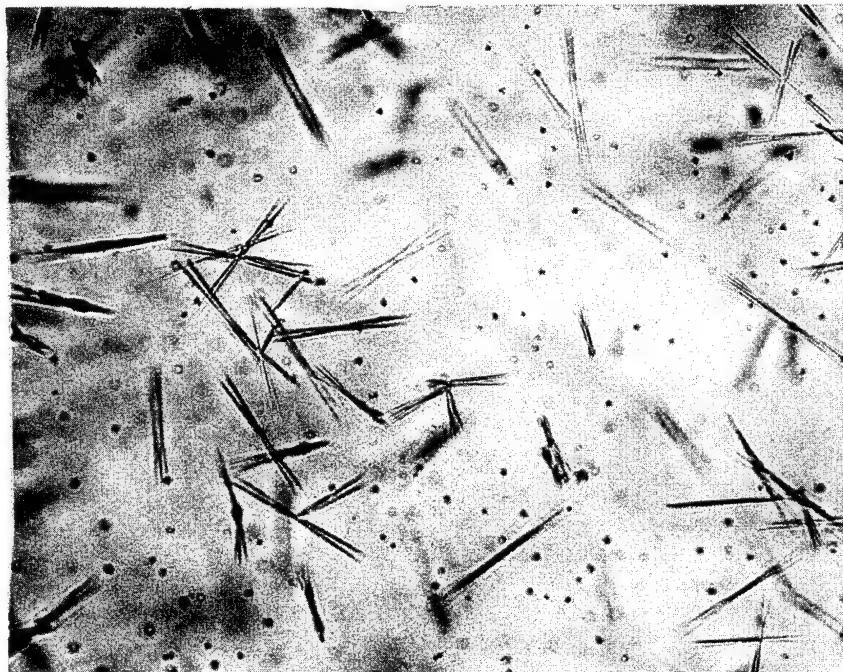
Figure 38 also shows that the rate of growth at the high temperature end of the curve approaches the liquidus temperature tangentially and that the curve is not symmetrical as the liquidus temperature is exceeded, that is, as the rate of growth changes to the rate of solution. The growth curve for Batch 1-B has this same feature. Our few data concerning the asymmetry in these curves are supported by a paper presented at the annual meeting of the American Ceramic Society, by Drs. G. S. Meiling and D. R. Uhlmann (Ref. 82). These authors, in a paper entitled "Crystallization and Melting Kinetics of Sodium Disilicate", describe a pronounced asymmetry in the growth-rate and melting rate curves in the vicinity of the melting point. The scatter in this curve at approximately 1325°C is associated with a change in the morphology of the crystalline aggregate. When the melt is seeded at this temperature, only a few single crystals grow on the thermocouple instead of the rounded masses of crystals which grow at lower temperatures. The measurements of the size of the rounded crystalline aggregates are made by tracing the outlines of the aggregates onto tracing paper and then circumscribing these outlines with a series of concentric circles. It is then easy to measure the change in radius, which represents the change in length of the crystals, as a function of time. Alternately, a circle can be drawn on the polaroid prints and then transferred to a separate piece of paper. This method of measurement cannot be used for the clusters of single crystals, which do not grow with equal velocities. The measurements on these crystals are made along the length of the prism, and the maximum values are reported. All of our measurements are of the change in crystal length as a function of time and do not reflect the amount of glass which has crystallized. This is because of the occurrence of hollow crystals which seem to occur at all temperatures except the higher and lower temperatures; that is, at the faster rates of growth. In Batch 1, the three measurements of the rate of solution were made upon aggregates of crystals and are not as accurate as the measurements of the rate of growth. This is because the crystals melt along grain boundaries and drift away from the thermocouple. However, measurement No. 3, at a temperature of $1412 \pm 2^\circ\text{C}$, with a value of -380 microns per minute is sufficiently accurate so that it can be stated that the rate of solution has a very steep negative slope. Solution measurements should be made upon single, solid crystals, which can be grown at temperatures of about 1395° in Batch 1.

Several interesting crystal habits have been observed during the devitrification studies. The first of these is the habit that has been observed for sapphirine in Batch 1-B. Figure 39 shows sapphirine photographed at a temperature of 1222°C with a magnification of 40 times, while Fig. 40 shows sapphirine crystals which were photographed at room temperature at a magnification of 200 times. This unusual crystal habit appears to consist of two or three crystals



MAGNIFICATION: 40X

FIGURE 39. SAPPHIRINE CRYSTALS IN MOLTEN GLASS AT 1222 °C



MAGNIFICATION: 200X

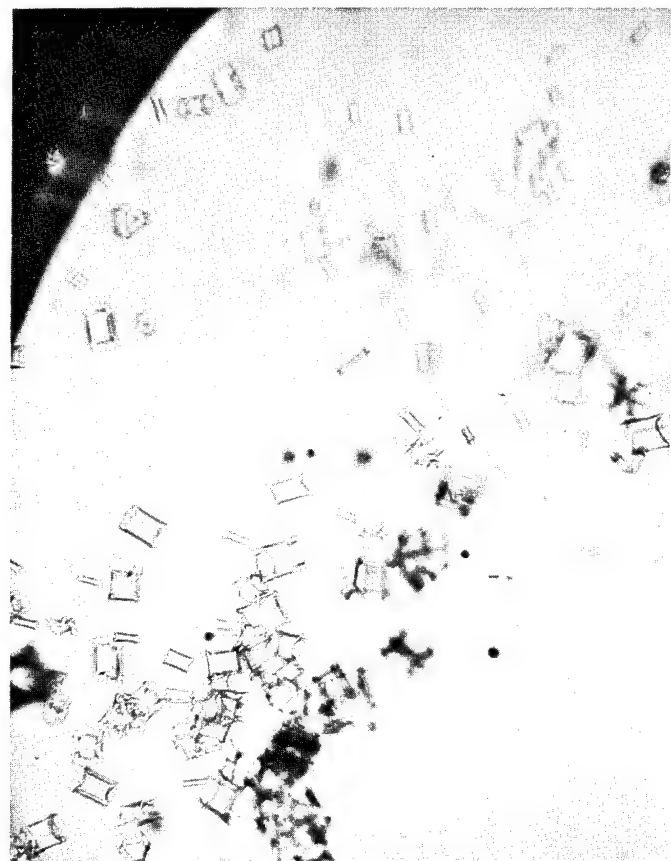
FIGURE 40. SAPPHIRINE CRYSTALS IN GLASS

joined at their mid sections. The work of Keith and Schairer (Ref. 83) describes sapphirine as occurring as elongated and usually faceted monoclinic crystals and reports one twinned crystal but made no observation of the twinning. Our work has revealed many dendritic habits of sapphirine which are dependent upon the growth rate, but our observations are made at temperatures considerably below the liquidus. Long hollow prisms of cordierite have also been observed, similar to those reported by Schreyer and Schairer (Ref. 84). These are shown in Figs. 41 and 42. These photographs were made at room temperature of cordierite which was grown in Batch 1. The crystals in Fig. 42 were originally completely solid, and became hollow on the ends when the growth rate was increased. It has also been possible to start with hollow crystals, and grow them at a slower growth rate until they become solid.

The rate of growth of cordierite in Batch 64 was measured, the data are listed in Table XIII and plotted in Fig. 43. The composition of this batch, as determined by chemical analysis, is 51.66 wt % SiO₂, 27.92% Al₂O₃, 17.2% MgO, and 3.12% Y₂O₃. The maximum rate of growth of cordierite in this glass is 190 microns per minute, and the liquidus temperature is 1394 + 2°. Crystals held at a temperature of 1393 ± 2° for 20 min showed no measurable change in size, and crystals at a temperature of 1395 ± 2° had a rate of solution of 8 microns per minute. The cordierite which was grown in this glass was nucleated with seed crystals which were suspended in distilled water and then applied to the thermocouple, which was then lowered into the glass in the crucible, just as in the earlier measurements. The cordierite which was grown in this glass had the same crystal habit as that which was observed in Batches 1 and 1-B. The X-ray diffraction pattern was also the same as for the cordierite grown in Batches 1 and 1-B. Sapphirine was also grown in Batch 64 and was apparently nucleated by platinum just as in Batch 1. The sapphirine was allowed to crystallize for a longer period of time (3 hrs at 1165°) than was that grown in Batch 1 and the X-ray diffraction pattern was of better quality, with even better agreement with the data obtained from the ASTM cards.

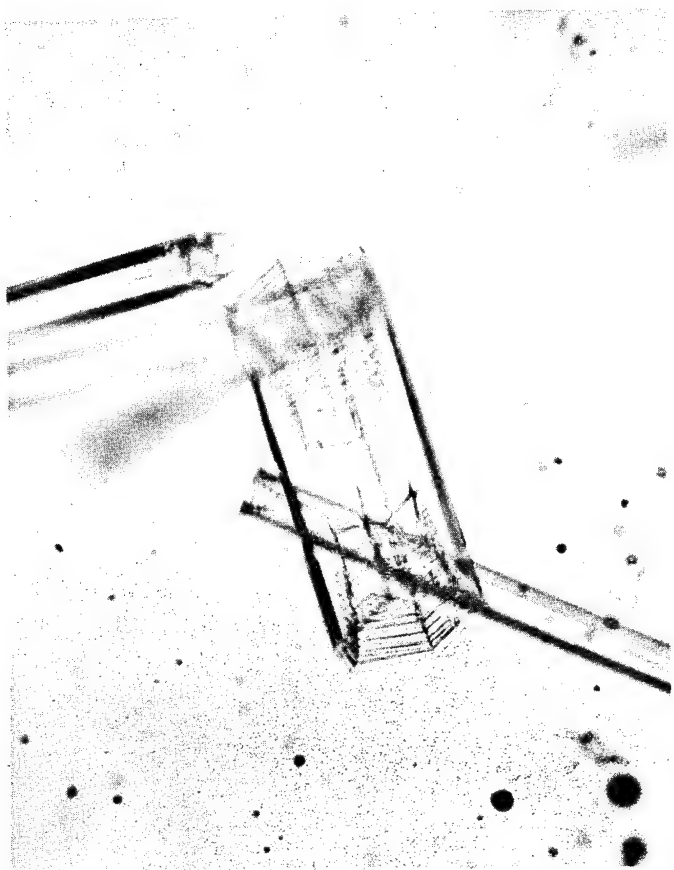
The rate of growth of cordierite in Batch 63 is shown in Fig. 44 and the data are listed in Table XIV. The composition of this glass, as determined by chemical analysis, is 53.5 wt % SiO₂, 23.08% Al₂O₃, 17.24% MgO, and 5.64% La₂O₃. The maximum rate of growth of cordierite in this glass was 66 microns per minute, which is about 1/3 of the maximum rate observed in batch 64 and about 1/8 of that observed in batch 1. The liquidus temperature of this glass is 1350 ± 5°. The smaller amount of scatter in this data is due to the slower growth rates, which allow the measurements to be made over longer periods of time, while the measurements of crystal size can be made with the same precision. It is probable that sapphirine will nucleate and grow in this glass as in the others, but this has not yet been determined.

The rate of devitrification of a glass-forming system is usually considered to be proportional to the amount of undercooling below the liquidus temperature and inversely proportional to the viscosity of the system. This suggests that the slower rate of growth in batch 1-B, as compared to that observed in batch 1, is due to increased viscosity because of the higher silica content. In batch 64 (see Table XV) for glass compositions, liquidus temperatures, maximum rates of



MAGNIFICATION: 100X

FIGURE 41. CORDIERITE CRYSTALS IN GLASS



MAGNIFICATION: 100X

FIGURE 42. CORDIERITE CRYSTALS IN GLASS

Table XIII

Rate of Growth of Cordierite in Batch 64

<u>No.</u>	<u>Temp.</u>	<u>Rate</u>	<u>No.</u>	<u>Temp.</u>	<u>Rate</u>
1	1281 \pm 2	56	22	1366 \pm 4	3
2	1233 \pm 2	150	23	1393 \pm 2	0 in. 20 min
3	1271 \pm 3	75	24	1268 \pm 3	120
4	1088 \pm 4	88	25	1293 \pm 7	58
5	1084 \pm 2	80	26	1279 \pm 3	100
6	974 \pm 6	15	27	1259 \pm 6	175
7	1028 \pm 4	37	28	1212 \pm 2	180
8	1134 \pm 2	135	29	1261 \pm 4	175
9	1030 \pm 6	35	30	1203 \pm 2	190
10	1158 \pm 4	120	31	1216 \pm 6	175
11	1168 \pm 4	155	32	1048 \pm 2	41
12	1186 \pm 4	175	33	1187 \pm 2	153
13	1118 \pm 4	105	34	1260 \pm 4	160
14	1206 \pm 2	188	35	1252 \pm 3	150
15	1096 \pm 3	100	36	1247 \pm 2	165
16	1359 \pm 8	0 in. 5 min	37	1333 \pm 3	8
17	1366 \pm 2	2	38	1318 \pm 4	18
18	1378 \pm 3	0 in. 10 min	39	1143 \pm 4	125
19	1395 \pm 2	-8	40	1156 \pm 2	140
20	1260 \pm 4	120	41	1315 \pm 2	20
21	1334 \pm 4	30	42	1340 \pm 2	10

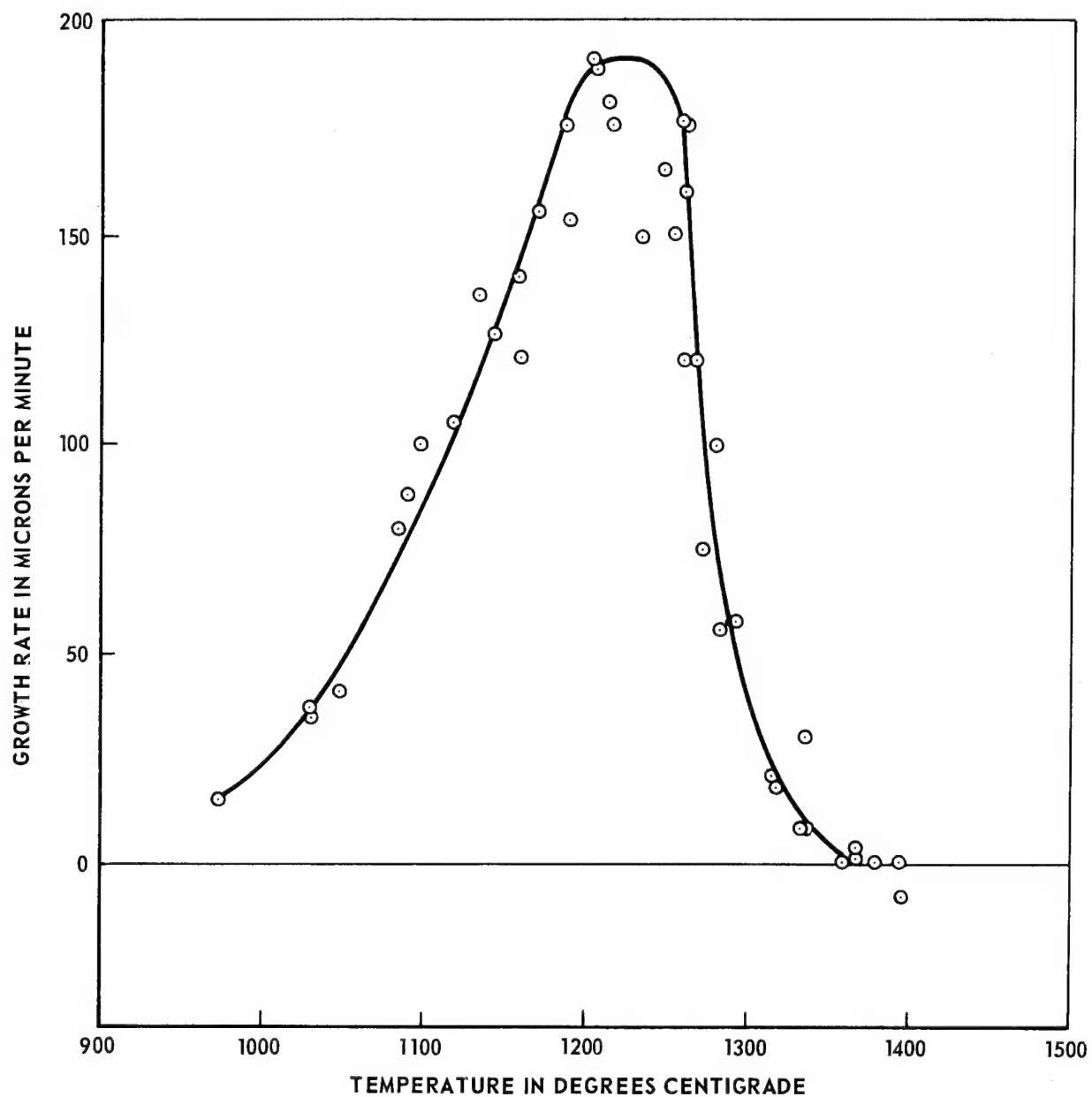


FIGURE 43. EFFECT OF TEMPERATURE UPON THE RATE OF GROWTH
OF CORDIERITE IN BATCH 64

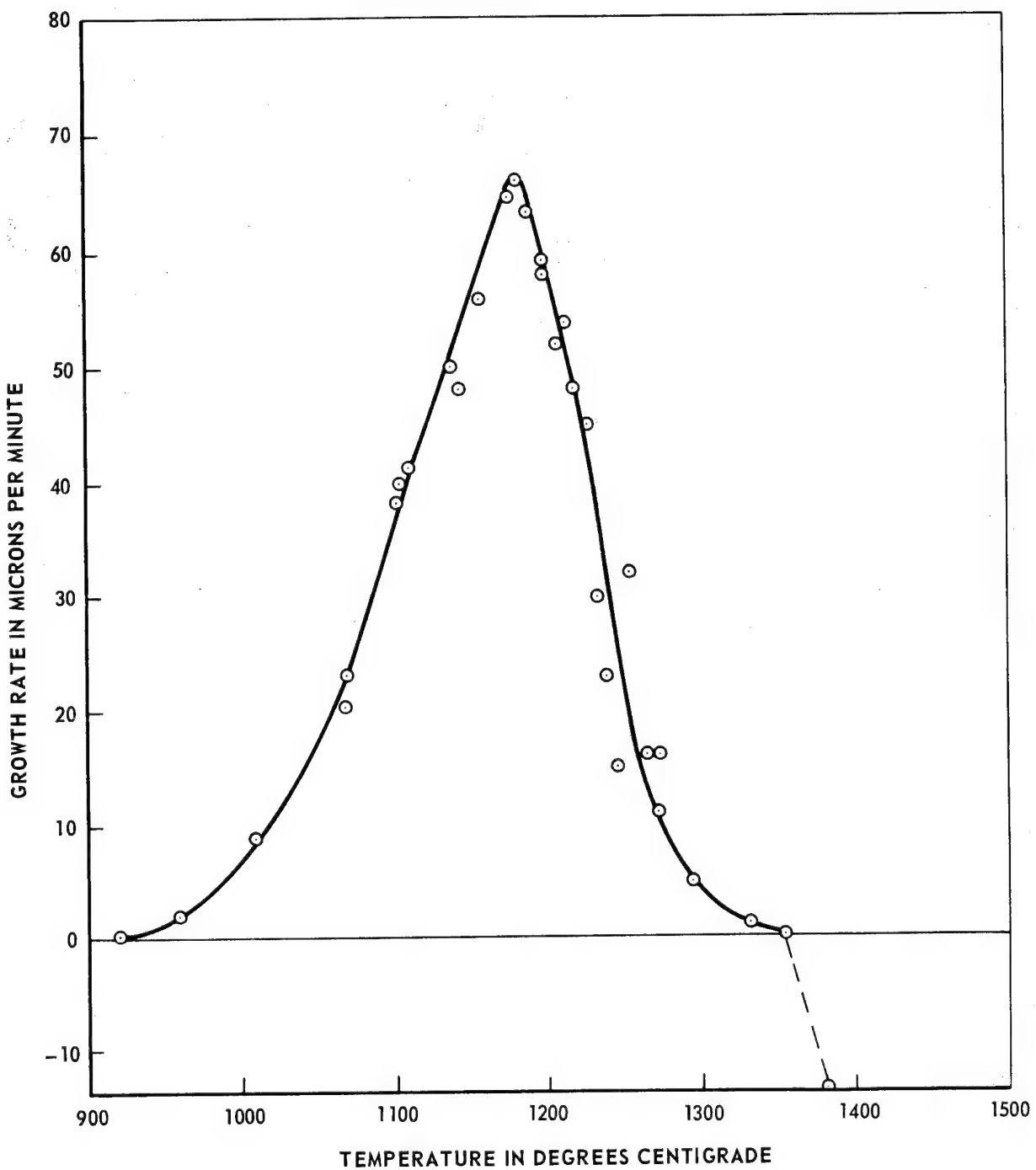


FIGURE 44. EFFECT OF TEMPERATURE UPON THE RATE OF GROWTH
OF CORDIERITE IN BATCH 63

Table XIV

Rate of Growth of Cordierite in Batch 63

<u>No.</u>	<u>Temp.</u>	<u>Rate</u>	<u>No.</u>	<u>Temp.</u>	<u>Rate</u>
1	1189 \pm 2	63	14	959 \pm 4	2
2	1182 \pm 2	66	15	1069 \pm 2	23
3	900 \pm 5	0 in. 10 min	16	1010 \pm 3	9
4	1213 \pm 2	54	17	1272 \pm 2	11
5	1198 \pm 2	59	18	1383 \pm 2	-15
6	1156 \pm 3	56	19	1353 \pm 4	0 in. 30 min
7	1138 \pm 2	50	20	1294 \pm 2	5
8	1178 \pm 3	65	21	1331 \pm 4	1
9	1103 \pm 2	40	22	1266 \pm 2	16
10	1067 \pm 4	20	23	1226 \pm 2	45
11	1219 \pm 3	48	24	1253 \pm 2	32
12	1144 \pm 4	48	25	1347 \pm 2	slow solution
13	1272 \pm 2	16	26	836 \pm 2	0 in. 120 min

Table XV
Comparative Rates of Cordierite Growth
in Several Glasses

<u>Batch No.</u>	<u>Comp. (wt%)</u>	<u>Liquidus</u>	<u>Max. Growth Rate,</u>	<u>Temp. of</u>
		<u>Temperature</u>	<u>μ/min</u>	<u>Max. Growth</u>
1	51.1 SiO ₂ 29.7 Al ₂ O ₃ 18.9 MgO	1410 \pm 3°	485	1225°
1-B	55.0 SiO ₂ 30.0 Al ₂ O ₃ 15.0 MgO	1435 \pm 5°	300	1225°
64	51.66 SiO ₂ 27.92 Al ₂ O ₃ 17.20 MgO 3.12 Y ₂ O ₃	1394 \pm 2	190	1225
63	53.50 SiO ₂ 23.08 Al ₂ O ₃ 17.24 MgO 5.64 La ₂ O ₃	1350 \pm 5	66	1180

Ionic Radii in Angstroms*

Al ⁺⁺⁺	=	0.51
Mg ⁺⁺	=	0.66
Si ⁺⁺⁺⁺	=	0.42
Y ⁺⁺⁺	=	0.92
La ⁺⁺⁺	=	1.14

*Ahrens, L. H., Geochim et Cosmochim. Acta, 2, (1952) p. 155-169

growth and temperatures at which the maximum growth rate occurs), which contains 3.1% yttria in addition to the base glass of magnesia, alumina, and silica, the viscosity versus temperature curve (Fig. 45) is not greatly different from that of batch 1, and yet the maximum rate of growth in No. 64 is less than one-half of that measured in batch 1. In batch 63, which contains 5.6% lanthana, the viscosity is much lower than in Batches 64 and 1 at the same temperature, but the maximum rate of growth is about one-eighth of that observed in Batch 1.

These observations suggest that the maximum rate of crystal growth can be affected by changing the viscosity of the system or by adding larger cations (ionic radii are listed in Table XV) which cannot be easily incorporated into the crystal which is growing in the glass. These large cations could become concentrated in the glass surrounding the growing crystal as the other cations (Mg^{++} , Al^{+++} , Si^{++++}) are being incorporated into the crystal. The factors limiting the maximum rate of crystal growth could be the diffusion of Mg^{++} , Al^{+++} , and Si^{++++} to the growing crystal and/or the diffusion of the foreign ions away from the crystal-glass interface. If this were the case, one would expect that the rate of change in size of the crystal as a function of time at a constant temperature would decrease as the concentration of foreign ions in the glass increased. Two representative growth curves for cordierite in batches 1 and 63 are shown in Fig. 46. It can be seen that, for these relatively short times, the rate of change of crystal length is linear as a function of time. It is probable that measurements with the electron microprobe could be useful in elucidating the mechanism by which the rate of crystal growth can be so significantly altered. These measurements could show concentration gradients within the glass which surrounds the crystal and also whether the yttria and the lanthana are incorporated into the cordierite crystal. It is well established that cordierite has channels extending through the crystal structure which are parallel to the "c" axis, which also is the direction of fastest growth. These channels which can contain alkali ions and water molecules should also be able to contain the yttrium and lanthanum ions. It may be possible that if these ions are incorporated into the crystal, they may cause a perturbation in a growth step, such as in a screw dislocation mechanism. Microprobe measurements could ascertain if these larger cations are contained in the crystal.

The rate of growth of cordierite was measured in glass batch No. 62. The composition of this glass, as determined by chemical analysis, is 53.41 wt % SiO_2 , 25.06 wt % Al_2O_3 , 15.36 wt % MgO , and 5.63 wt % Ce_2O_3 . The oxidation state of the cerium ion in this glass was not determined, but is reported here as Ce_2O_3 . The crystal growth-rate data obtained for this glass are listed in Table XVI and are plotted in Fig. 46. It can be seen from Fig. 46 that the maximum rate of growth of cordierite in this glass is about 115 microns per minute; that appreciable rates of crystal growth begin at about $1000^\circ C$, and that the liquidus temperature is $1370 \pm 5^\circ C$. The maximum growth rate of 115 microns per minute is about one-fourth that measured for batch 1 (485 microns per minute), but is approximately twice that of batch 63 (66 microns per minute) which contains 5.6 wt % La_2O_3 . This glass becomes less transparent at higher temperatures, which may be due to a change in the oxidation state of the cerium ion. Upon

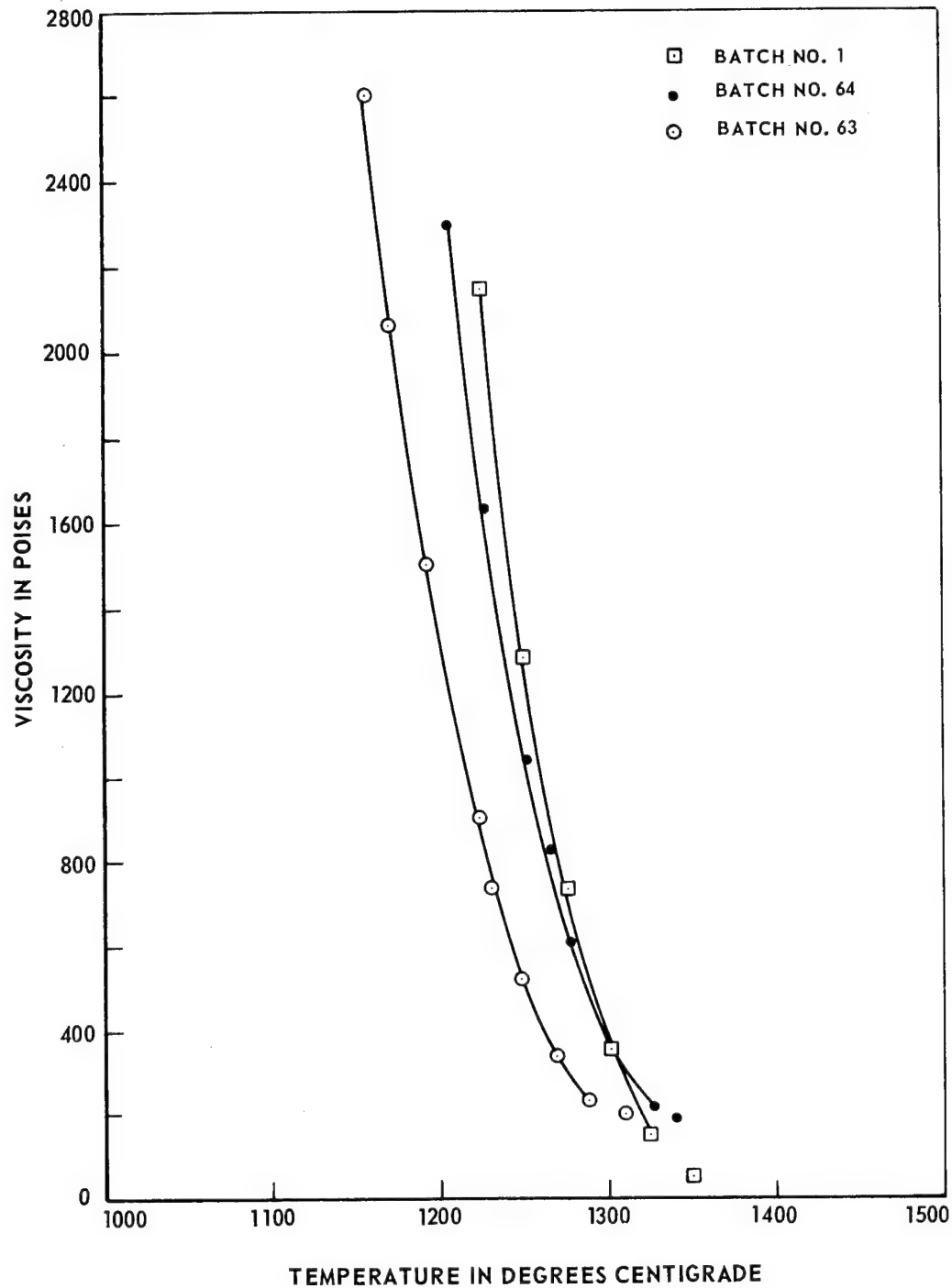


FIGURE 45. VISCOSITY-TEMPERATURE CURVES FOR THREE GLASSES

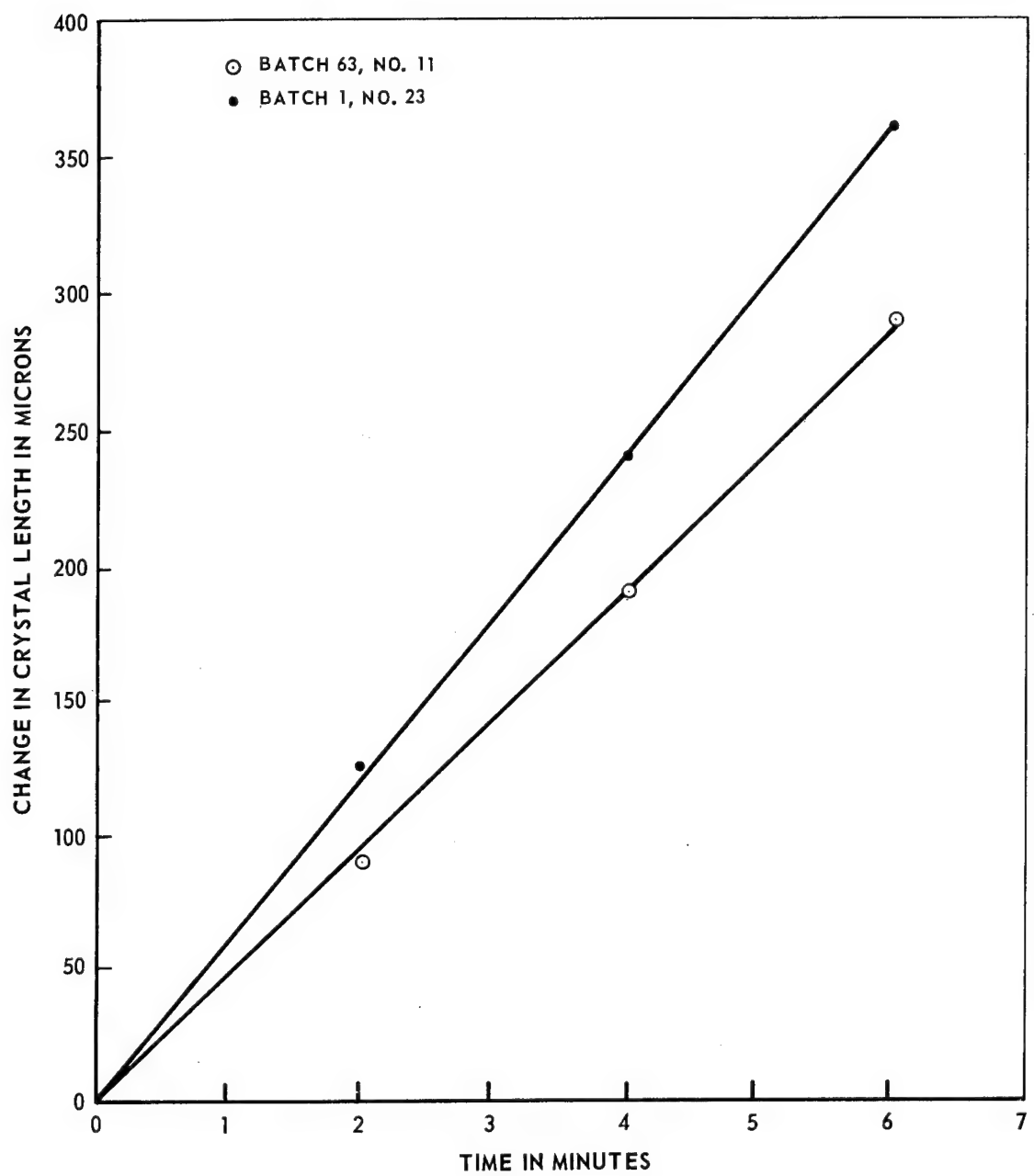


FIGURE 46a. REPRESENTATIVE GROWTH CURVES FOR CORDIERITE, THE INCREASE OF CRYSTAL LENGTH WITH TIME

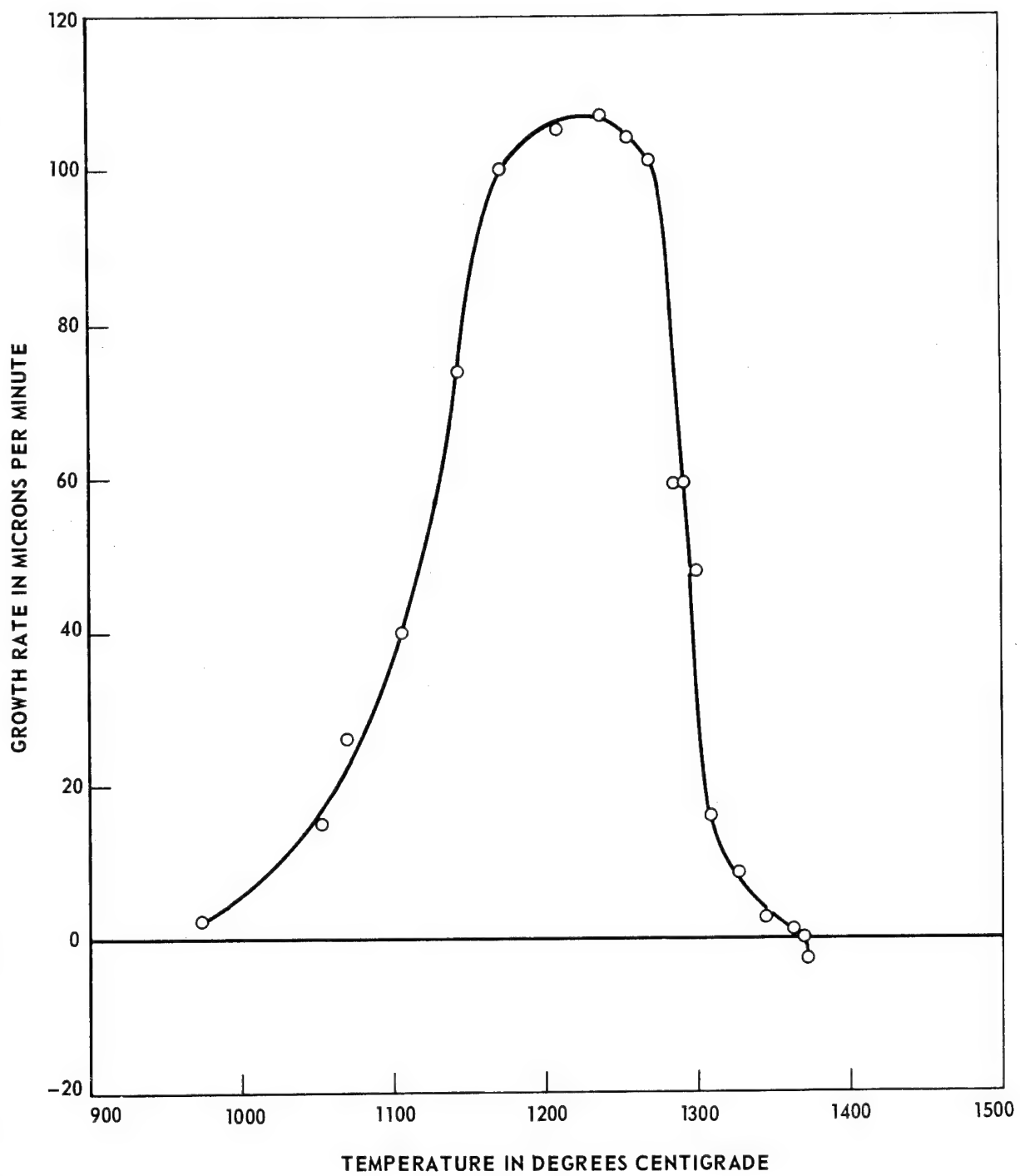


FIGURE 46b. EFFECT OF TEMPERATURE UPON THE RATE OF GROWTH
OF CORDIERITE IN BATCH 62

Table XVI

Growth Data for Cordierite in Batch 62

<u>No.</u>	<u>Temp.</u>	<u>Rate</u>	<u>No.</u>	<u>Temp.</u>	<u>Rate</u>
1	1309 \pm 2	16.1	11	1256 \pm 3	114
2	1369 \pm 5	0 in 60 min	12	1300 \pm 4	48
3	1372 \pm 3	-2.5	13	1210 \pm 4	115
4	1172 \pm 4	100	14	1107 \pm 3	40
5	1285 \pm 3	59	15	1143 \pm 2	74
6	1344 \pm 2	2.5	16	1053 \pm 2	15
7	1363 \pm 3	1	17	1291 \pm 3	59.7
8	1328 \pm 3	8.5	18	1238 \pm 3	117
9	1270 \pm 2	101	19	1069 \pm 4	26
10	974 \pm 4	2			

cooling to lower temperatures, the glass becomes more transparent again. This change in transparency is not so great as to impede the crystal growth measurements. The cordierite which was grown in this glass was nucleated with seed crystals of cordierite, just as in our preceding work. The devitrification product in this glass was determined to be cordierite by means of powder X-ray diffraction.

Another feature of interest which can be observed in Fig. 46 is that the high temperature end of the curve approaches the liquidus temperature asymptotically just as in our other growth-rate curves for cordierite. This means, of course, that the rate of growth is not continuous with the rate of solution as the curve passes through the liquidus temperature, but that instead there is a more or less pronounced change in slope. This conflicts with the data of Swift (Ref. 85), which were obtained on soda-lime-aluminosilicate glasses. His measurements were made by two different methods, but essentially consisted of heating the glass for certain periods of time, then removing it from the furnace and measuring the changes in crystal length microscopically by using a micrometer ocular. Because of the discrepancy between our results and those of Swift, it was decided to attempt to reproduce the data of Swift by using the same glass composition as used in his work, but by using our microfurnace, with our methods of measurement. Accordingly, a soda-lime-aluminosilicate glass was prepared in a 60 gram batch. This glass was melted in a platinum crucible at approximately 1300°C for 30 min, then removed from the furnace and stirred with a platinum-20% rhodium stirring rod until the glass became too viscous for further stirring. The glass was reheated and stirred in this manner four more times. The stirring rod remained in the crucible during the reheating and stirring operations, so that no glass was removed from the crucible during the mixing procedure. The composition of Swift's glass was 69 wt % SiO₂, 17 wt % Na₂O, 12 wt % CaO and 2 wt % Al₂O₃. A chemical analysis of a portion of our glass gave a composition of 69.46 wt % SiO₂, 16.78 wt % Na₂O, 11.48 wt % CaO, and 2.14 wt % Al₂O₃. The measurements of the rate of crystal growth were measured in our usual manner, the crystals being nucleated with seed crystals of devitrite. The devitrification product was identified as devitrite by powder X-ray diffraction. The sample for the X-ray diffraction analysis was obtained by allowing glass contained in a micro-crucible to crystallize for 14 hrs at 925°C, a temperature near which the highest crystal growth rate occurs. A rather weak diffraction pattern was obtained for this sample, but the pattern contained all of the diffraction lines for devitrite (Na₂Ca₃Si₆O₁₈) except for a few of the less intense lines. Some of the intensities on our pattern do not match those from the ASTM card; this may be due in part to the difficulty in estimating the intensities of our rather weak pattern. Because of this discrepancy in intensities, the X-ray diffraction data are presented in Table XVII.

The crystal growth-rate data for our soda-lime-aluminosilica glass are presented in Fig. 47 and are listed in Table XVIII. Also shown in Fig. 47 is the growth-rate data of Swift for a glass of the same composition and the data of Milne (Ref. 86) for a glass of nearly the same composition, the main difference being that silica is substituted for the alumina, so that Milne's glass contains 72 wt % SiO₂, 16 wt % Na₂O, and 12 wt % CaO. Our data and that of Swift and Milne

Table XVII

X-Ray Diffraction Data for Devitrites

$\text{Na}_2\text{Ca}_3\text{Si}_6\text{O}_{16}$ (ASTM)		Devitrification Product		$\text{Na}_2\text{Ca}_3\text{Si}_6\text{O}_{16}$ (ASTM)		Devitrification Product			
d	/	I		d	/	I	d	/	I
9.88		14					2.390		6
4.76		25	4.75	M			2.316		14
4.16		20	4.15	M+			2.251		8
3.82		25	3.83	W			2.225		8
3.30		60	3.30	S			2.159		8
3.23		30	3.23	W+			2.138		6
3.09		55	3.08	W			2.063		12
2.983		45	2.97	S			2.030		14
2.915		25	2.91	W-			2.004		6
2.836		8	2.84	W-			1.968		4
2.773		100	2.76	M-			1.951		4
2.664		12	2.65	W-			1.930		4
2.554		10	2.55	W-			1.881		18
2.509		6					1.842		14
2.473		6	2.48	W-			1.809		18
									S-

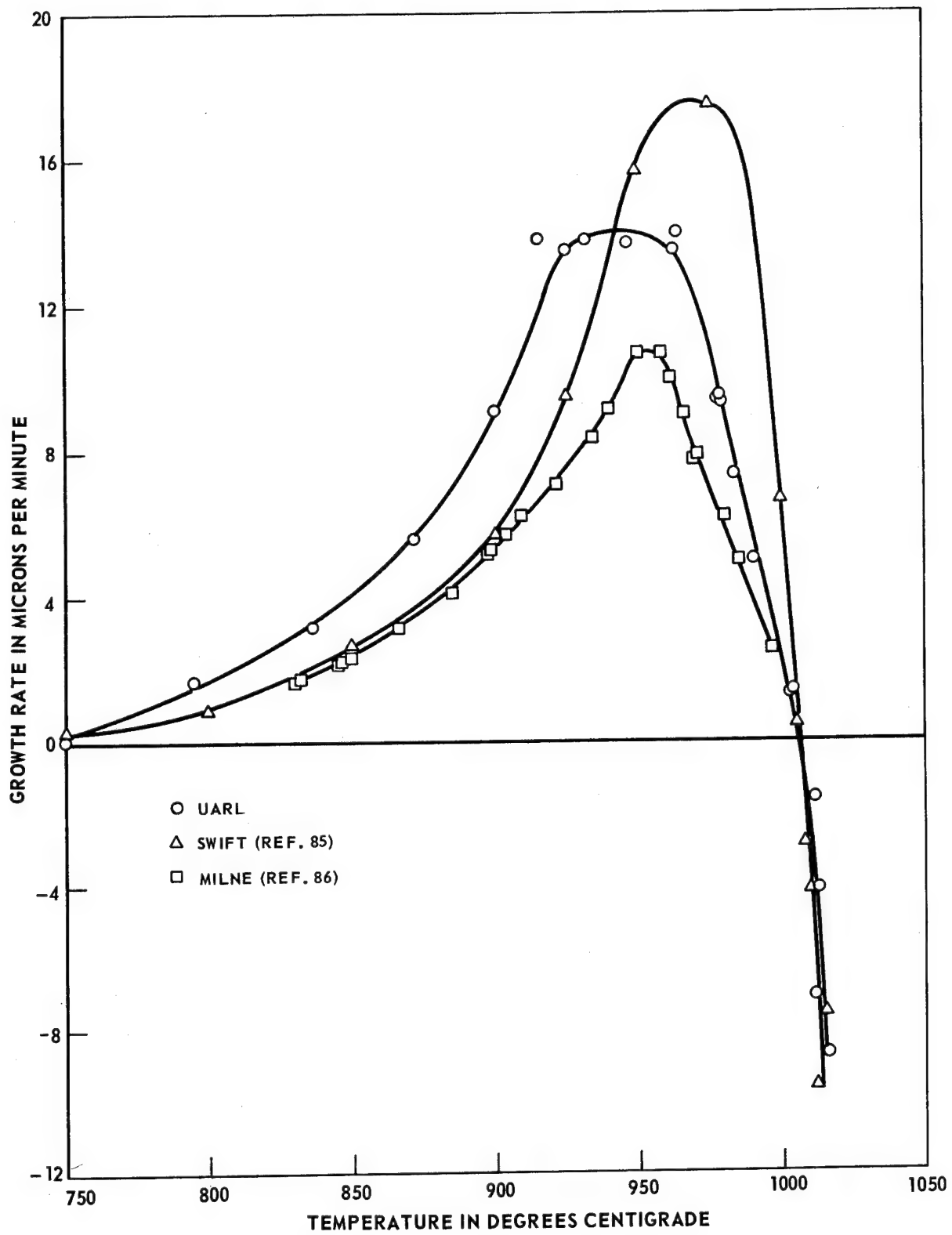


FIGURE 47. EFFECT OF TEMPERATURE UPON THE RATE OF GROWTH OF DEVITRITE

Table XVIII

Growth Rate Data for Devitrite in Soda-Lime-Aluminosilicate glass

<u>No.</u>	<u>Temp.</u>	<u>Rate</u>	<u>No.</u>	<u>Temp.</u>	<u>Rate</u>
1	964 \pm 5	14.0	13	748 \pm 4	0 in 41 min
2	900 \pm 5	9.1	14	963 \pm 2	13.5
3	872 \pm 4	5.6	15	916 \pm 3	13.8
4	794 \pm 3	1.66	16	978 \pm 2	9.4
5	1004 \pm 4	1.41	17	978 \pm 3	9.5
6	990 \pm 3	5.0	18	932 \pm 4	13.8
7	947 \pm 4	13.7	19	925 \pm 2	13.5
8	836 \pm 3	3.1	20	1014 \pm 2	-20.0
9	1003 \pm 3	1.3	21	983 \pm 4	7.36
10	979 \pm 3	9.3	22	1011 \pm 3	-1.6
11	1026 \pm 2	-29	23	1012 \pm 2	-4.1
12	1016 \pm 2	-8.7	24	1011 \pm 2	-7.1

(when extrapolated) give very nearly the same liquidus temperature, and it appears that the data would also agree if extrapolated to the temperature (about 750°C) where measurable crystal growth begins. Our rate of solution measurements are also in very close agreement with those of Swift. The most important differences are that different maximum rates of growth are obtained, and that our rate of growth curve is not continuous with the rate of solution curve through the liquidus temperature but instead exhibits a change in slope in this region. The high temperature end of our growth-rate curve and that of Milne (which is presumably for the rate of growth of devitrite) can be fitted to a straight line in this temperature region, but since no rate of solution measurements were plotted by Milne, no further comparison is possible regarding the shape of the rate of devitrification curve. A further examination of devitrification curves as obtained by Swift and replotted here is possible by reference to Fig. 48, which includes data for 3 glasses with 0, 2, and 4 wt % Al_2O_3 substituted for silica. The glass with 2 wt % Al_2O_3 is the same as that shown in Fig. 47. It can be observed in Fig. 48 that the data used to draw the curves are fewer in number than those obtained in our work and by Milne. It should also be noticed that the low temperature end of the curve for the 2 wt % Al_2O_3 glass is concave upward, while any such curvature for the 0 and 4 wt % Al_2O_3 glasses is much less pronounced. All of our observations indicate that there may be at least two types of devitrification curves, one exemplified by our results on the soda-lime-aluminosilica glass, and the other by the data obtained on the cordierite-composition based glasses. In the former, the high temperature end of the curve can be fitted to a straight line, which may have a more or less pronounced change in slope as the curve passes through the liquidus temperature. In the other type of curve, the high temperature end of the curve is not linear with temperature, and there is an asymptotic approach to the liquidus temperature. The data obtained for these cordierite composition based glasses contain much more scatter than do the data obtained on the soda-lime-aluminosilica glasses, which were taken at much lower temperatures. The difference in the liquidus temperatures is 350 to 400°C.

These soda-lime-aluminosilicate glasses have maximum growth rates for devitrite of 11 to about 18 microns per minute. This is about one-fourth of the growth rate observed for cordierite in batch 63 (66 microns per minute) and much smaller than that measured in batch 62 (115 microns per minute). This rather large difference is probably due to the much higher silica content in the soda-lime-aluminosilica glasses. A comparison of more importance can be made between the growth rates for batches 63 and 62, which have the same content of SiO_2 . The difference in the growth rates in these glasses appears to be inversely proportional to the difference in the ionic size of the rare-earth ion which is added to the other components in the glass. Thus, lanthanum (in batch 63) gives a much slower devitrification rate than does cerium (in batch 62) when present in these glasses in equal amounts. Comparative temperature-growth curves which effectively summarize all of our remarks are shown in Fig. 49.

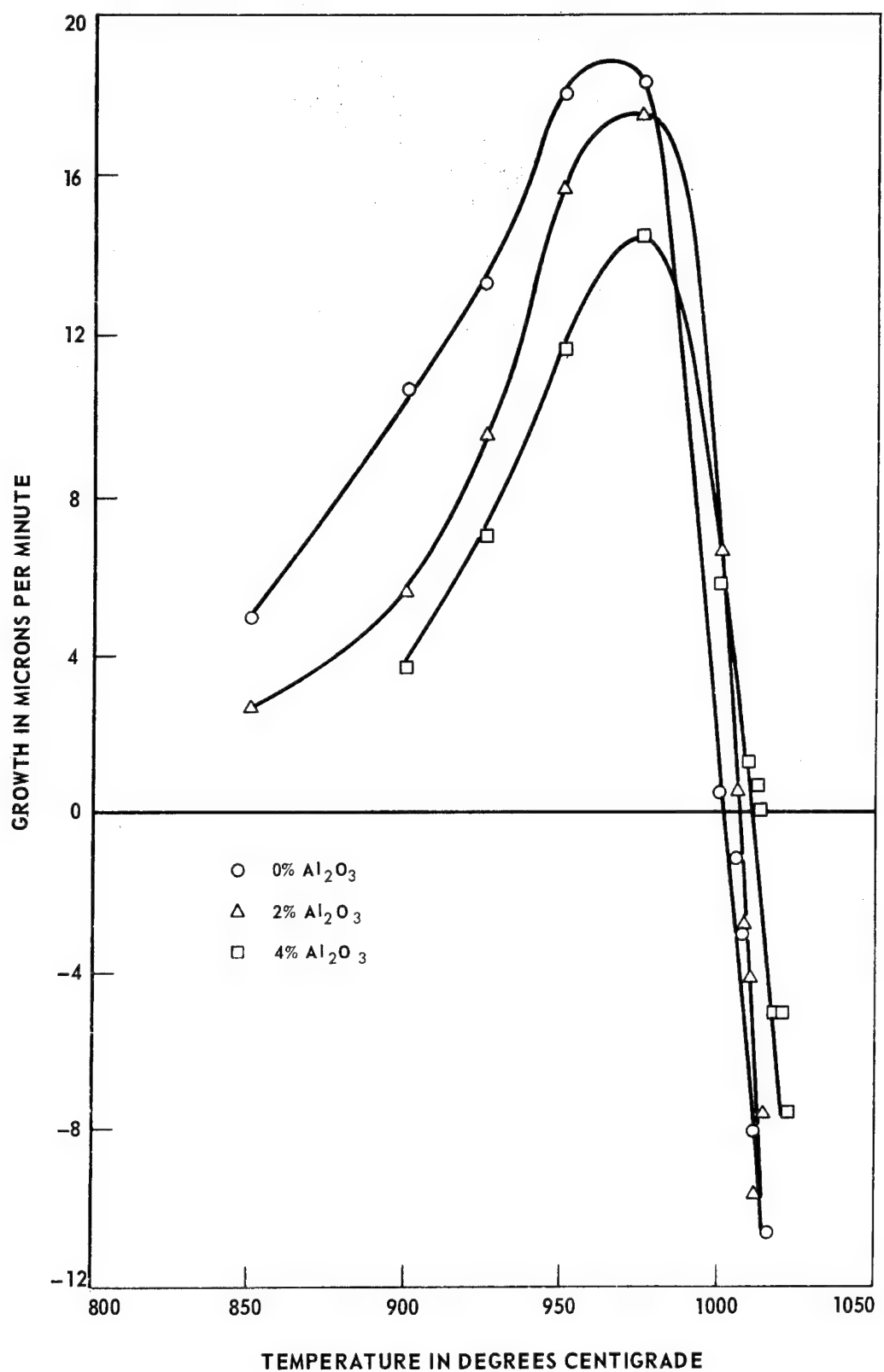


FIGURE 48. EFFECT OF TEMPERATURE UPON THE RATE OF GROWTH OF DEVITRITE AFTER SWIFT (REF. 85)

	BATCH N.C.	% RARE EARTH OXIDE
—	1	—
— —	64	3.1% Y_2O_3
— - -	62	5.6% Ce_2O_3
- - - -	63	5.6% La_2O_3

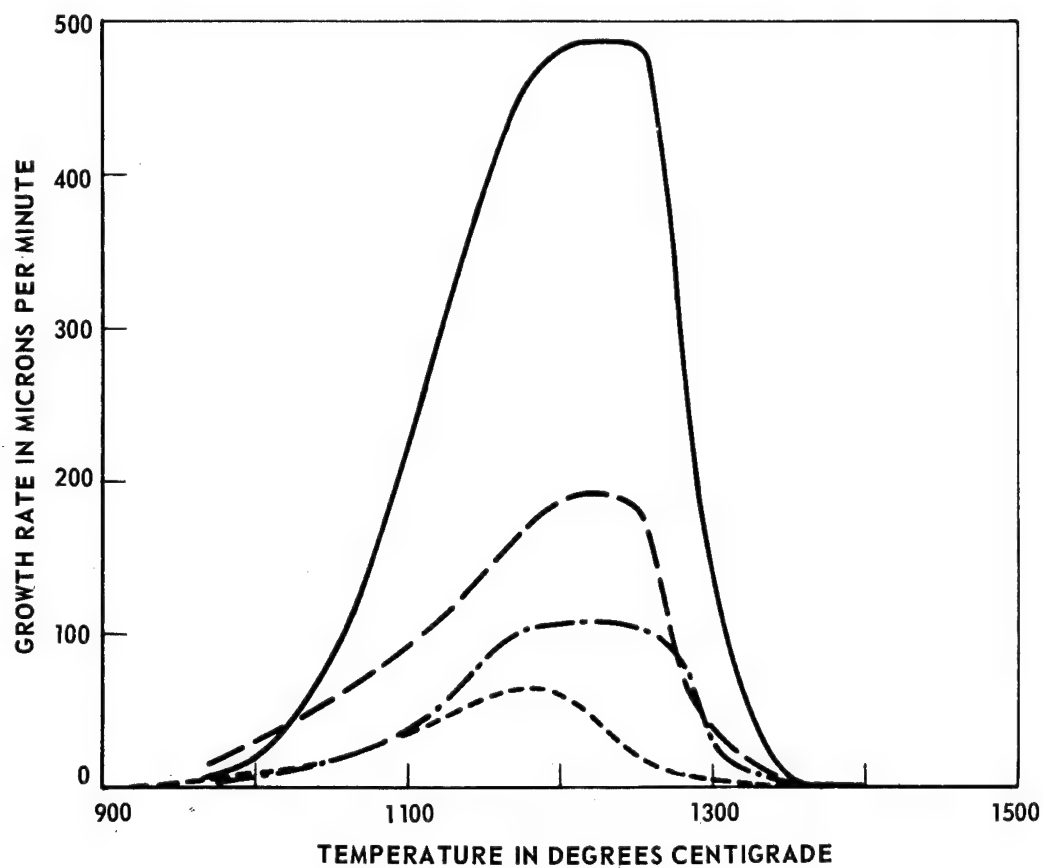


FIGURE 49. EFFECT OF RARE-EARTH ADDITIVES ON TEMPERATURE-GROWTH RATE CURVE OF CORDIERITE

Role of Lanthana in Kinetics of Crystallization of
UARL Cordierite Based Glasses

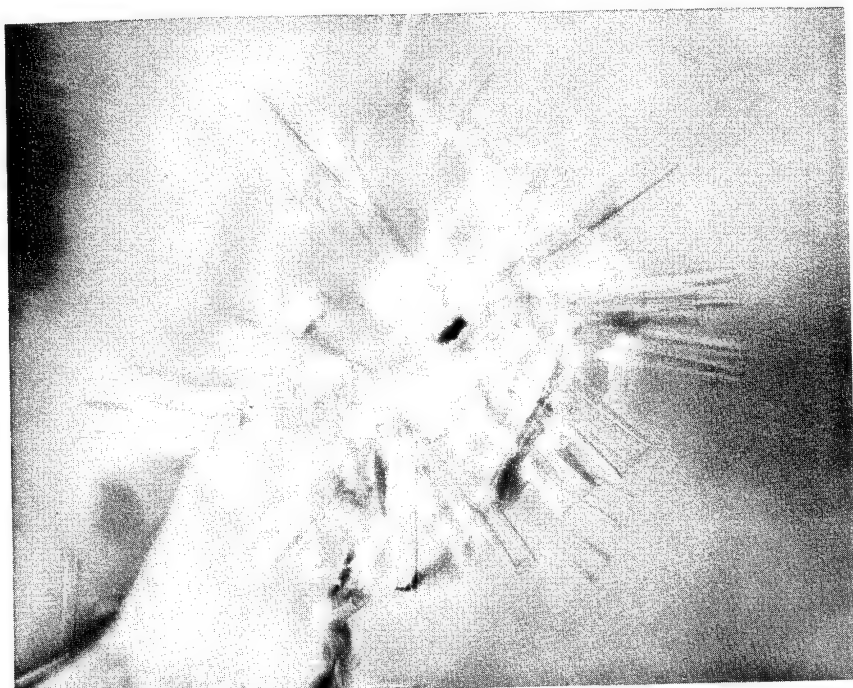
In the quarterly status reports, rates of crystal growth of cordierite have been presented as functions of temperatures for various glasses. The compositions of some of these glasses consist of MgO, Al₂O₃, and SiO₂, and in other glasses about 5 wt % of a rare earth-oxide. These glass compositions and the maximum rates of growth of cordierite are listed below:

<u>Batch</u>	<u>1</u>	<u>1-B</u>	<u>62</u>	<u>63</u>	<u>64</u>
wt % MgO	18.9	15.0	15.36	17.24	17.20
wt % Al ₂ O ₃	29.7	30.0	25.06	23.08	27.92
wt % SiO ₂	51.1	55.0	53.41	53.50	51.66
wt % R ₂ O ₃	0	0	5.6 Ce ₂ O ₃	5.6 La ₂ O ₃	3.12 Y ₂ O ₃
growth rate, max.	485	300	117	66	190

If these compositions are recalculated so as to consider only the MgO-Al₂O₃-SiO₂ ratios, the results are as listed below:

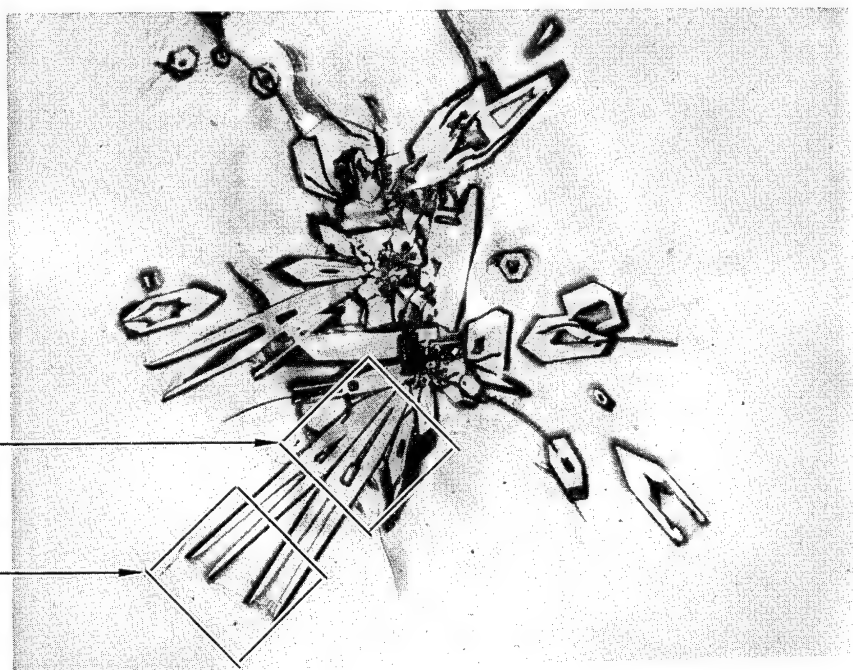
<u>Batch</u>	<u>1</u>	<u>1-B</u>	<u>62</u>	<u>63</u>	<u>64</u>
wt % MgO	18.9	15.0	16.3	18.3	17.8
wt % Al ₂ O ₃	29.7	30.0	26.7	24.6	28.8
wt % SiO ₂	51.0	55.0	57.2	57.1	53.3

It can be seen from these tabulations that the much lower rate of devitrification in batch 63 is not due to the high silica content, because batch 62 has nearly the same silica content, less magnesia and more alumina. Further, batch 1-B has similar MgO-Al₂O₃-SiO₂ ratios as does batch 63, but has a maximum rate of crystal growth of 300 microns per minute as compared to 66 microns per minute in batch 63. As a consequence of these observations it was decided to use the electron microprobe to determine if the mechanism by which the devitrification rate is so altered could be found. Specifically, it was desired to determine if the large lanthanum ions in batch 63 could be incorporated into the cordierite crystals in any manner and, if not, to determine if the lanthanum would be concentrated in an area surrounding that part of the crystal which is growing the fastest. Accordingly, a sample of glass from batch 63 was placed in a crucible in the microfurnace, and a cluster of hollow cordierite crystals (Fig. 50a) were grown at a temperature of 1290 + 5°C, which corresponds to a rate of growth of about 5 microns per minute. The crucible was then removed from the microfurnace, embedded in bakelite, and then sectioned and polished so that the crystals were exposed on the polished surface. In order to be certain that the crystals were exposed on the polished surface, it was necessary to etch the sample (as shown in Fig. 50b), and then repolish it for the electron microprobe analysis.



50A TRANSMITTED LIGHT

100X



AREA 1

AREA 2

50B REFLECTED LIGHT

ETCHED CONDITION

100X

FIGURE 50. LIGHT PHOTOMICROGRAPHS SHOWING THE APPROXIMATE LOCATIONS OF BEAM SCAN ANALYSES

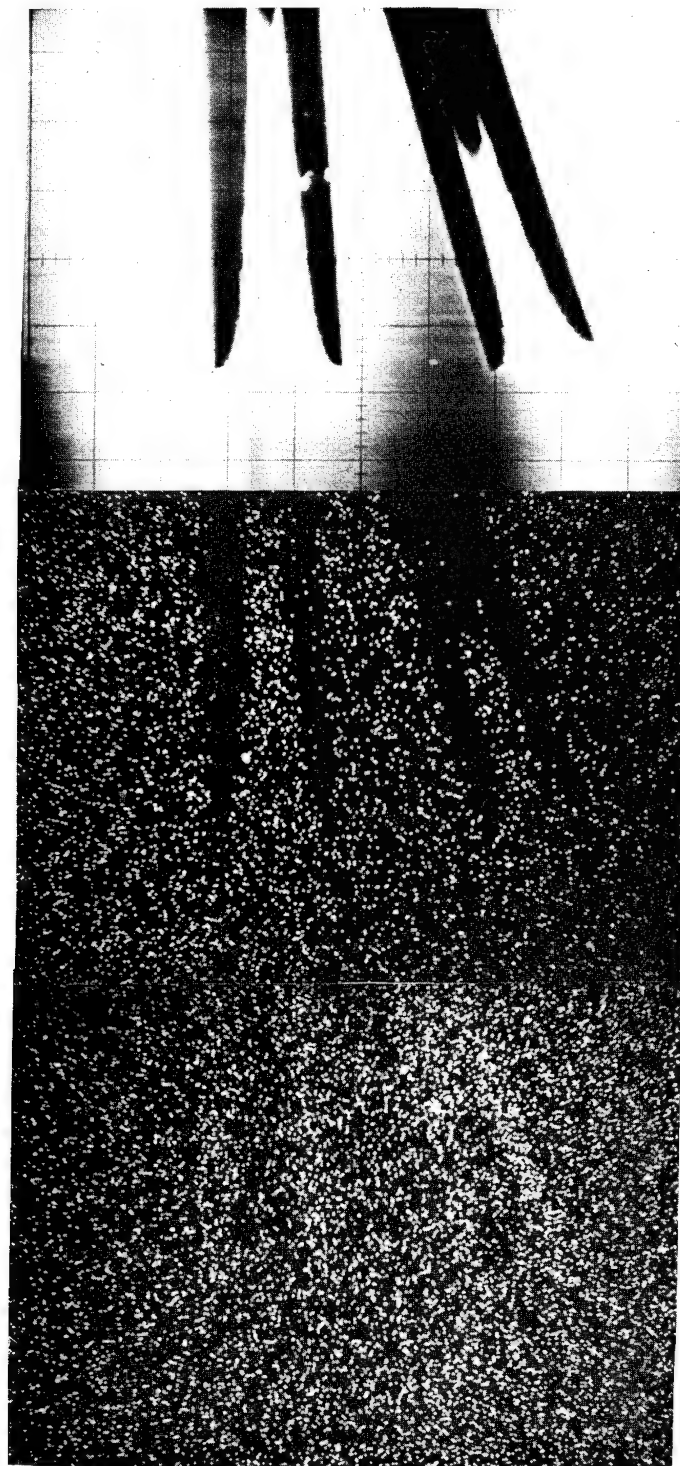
This specimen preparation is necessary because the electron microprobe analyzer can sample the specimen only to a depth of about two microns. The microprobe utilizes a high energy (20 kv) electron beam which can be focused to a spot one micron in diameter on the surface of the specimen. This spot can be viewed with an optical microscope so that the specimen can be analyzed in the desired area. The high energy electrons impinging upon the specimen cause the constituent elements to emit characteristic X-rays. These X-rays may be analyzed with respect to wavelength and intensity to yield spectra from which qualitative and quantitative analyses may be made. This is accomplished by diffracting the X-rays with a crystal and measuring them with an appropriate detector. The output of the detector is channeled through electronic signal processing equipment to a strip chart recorder. The record from the strip chart recorder thus contains peaks whose location and amplitude are proportional to the elements present in the sample. By tuning the spectrometer to a specific spectral line, sweeping the beam across the sample and displaying the detector output on an oscilloscope, a picture of the elemental distribution can be shown. This can then be photographed to provide a permanent record, as shown in Figs. 51a and 51b for lanthanum and aluminum. Specimen current images may also be photographed from the oscilloscope. In this measurement, that portion of the electron beam which penetrates into the sample gives rise to a current flow which is proportional to the atomic number of the elements upon which the beam is impinging. In this measurement, the darker areas are composed of elements having a lower atomic number than are the lighter areas, as shown in Figs. 51a and 51b. The electron microprobe analyses of the cordierite crystals grown in batch 63 consisted of specimen current, lanthanum X-ray, and aluminum X-ray images which were recorded on polaroid film, and lanthanum distribution scans across selected areas which provided a more accurate measurement of the lanthanum distribution than could be obtained from the pictorial representation. The paths which were scanned are shown in Fig. 52 and the scans are shown in Figs. 53a, b, c, d, e, and f.

The specimen current images show that the elements comprising the crystals are of lower atomic numbers than the elements constituting the matrix. This is because the crystals contain more alumina and silica and less magnesia than does the glass matrix, and also because, as shown in Fig. 51a, the crystals contain very little, if any, lanthanum. Figures 51a and 51b also show the enrichment in aluminum in the crystals as compared to the glass matrix. The area shown in Fig. 51b is the area in which scans were made in order to determine the lanthanum distribution, and Fig. 52 is a schematic representation of the paths scanned by the electron beam so as to get the distribution of lanthanum in and surrounding the crystals. Figure 52 is drawn accurately with respect to scale so that the separation between scans is 12.7 microns. The scans were concentrated near the end of the hollow crystal, which was, of course, the area where the fastest rate of growth was occurring. The results of the scans are shown in Figs. 53a, b, c, d, e, and f. Scans 1 and 2 in Fig. 53a show that the crystal contains very little, if any, lanthanum while the center portion is enriched in lanthanum up to about 7 or 8 wt %. Scan 3 contains only one side of the crystal, and shows about 7 or 8 wt % La_2O_3 immediately adjacent to the crystal and a linearly decreasing amount as the beam scanned out into the matrix. The distance



MAG: 330X

FIGURE 51A. ELECTRON BEAM SCAN ANALYSIS OF AREA 1 AS INDICATED IN FIG. 50.
THE CRYSTALS APPEAR DARKER INDICATING THEM TO BE OF LOWER ATOMIC NUMBER
THAN THE MATRIX.



MAG: 330X

FIGURE 51B. ELECTRON BEAM SCAN ANALYSIS OF AREA 2 AS INDICATED IN FIG. 50
THE LANTHANUM DISTRIBUTION SCANS WERE ALSO OBTAINED IN THIS AREA
(REF. FIG. 52)

THE LANTHANUM DISTRIBUTIONS ACROSS THESE PATHS ARE GIVEN IN FIGS. 4a-4f

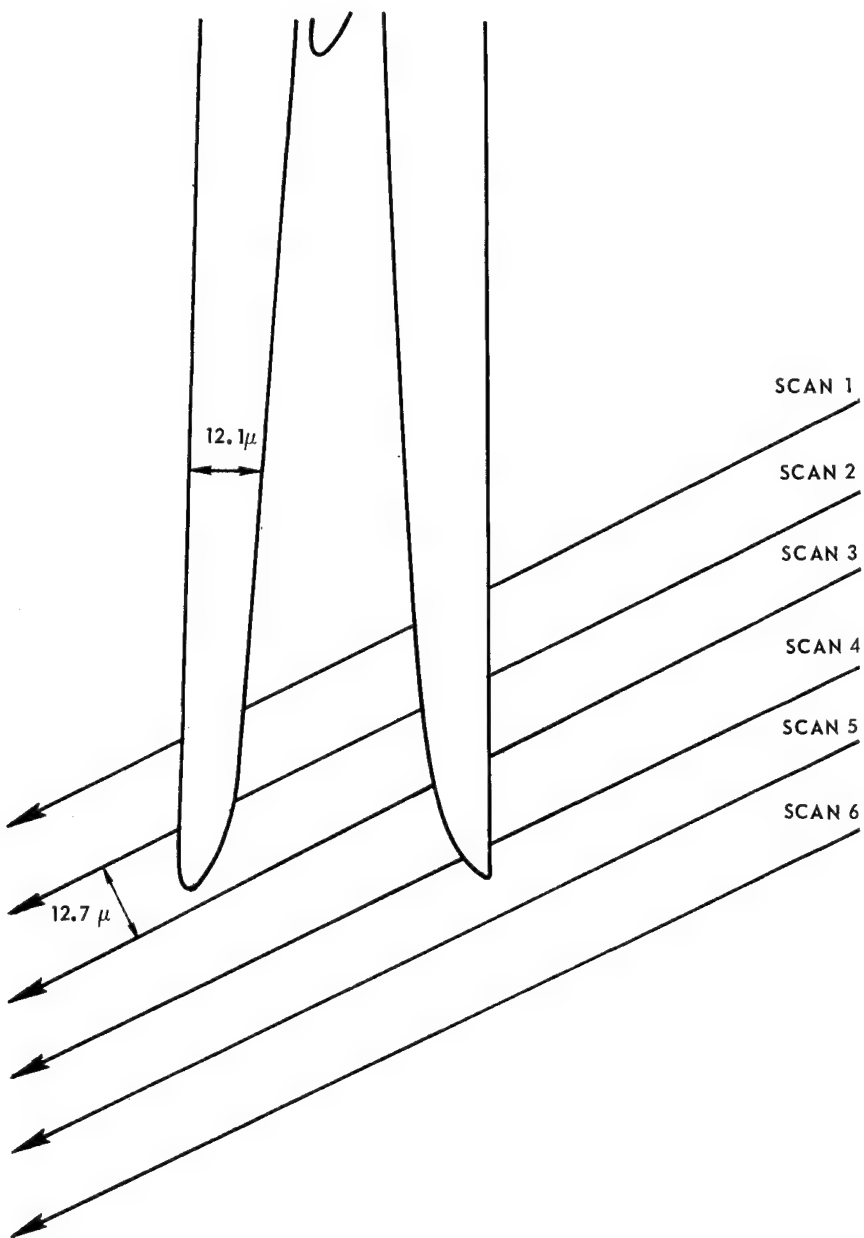


FIGURE 52. SCHEMATIC REPRESENTATION OF THE PATHS SCANNED BY THE ELECTRON BEAM

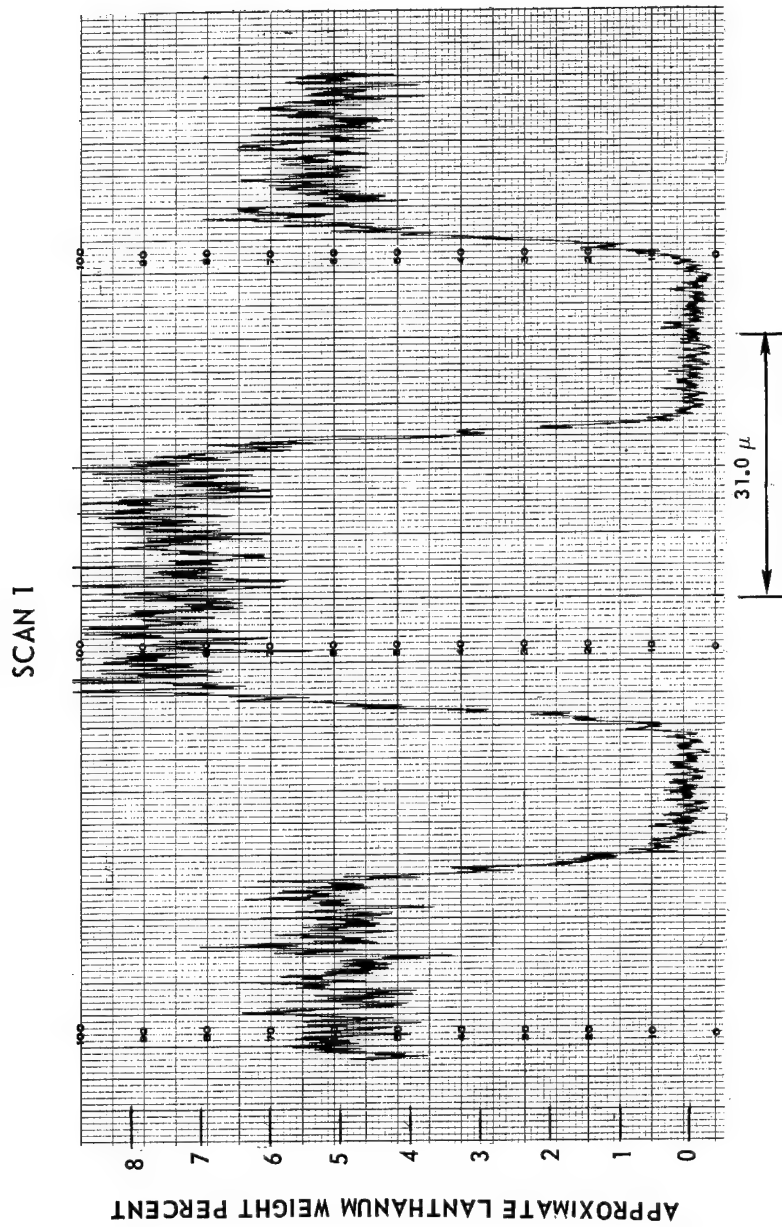


FIGURE 53a. LANTHANUM DISTRIBUTION SCANS ACROSS PATH SHOWN SCHEMATICALLY IN FIG. 52

SCAN 2

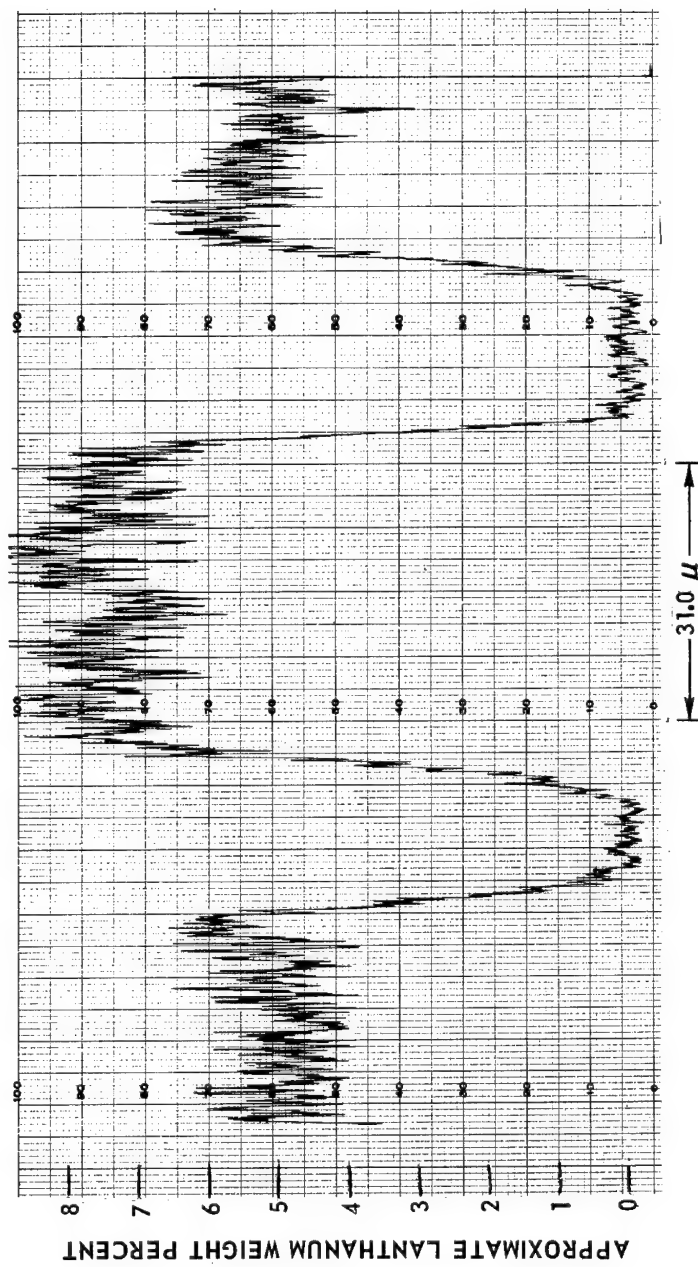


FIGURE 53b. LANTHANUM DISTRIBUTION SCANS ACROSS PATH SHOWN SCHEMATICALLY IN FIG. 52

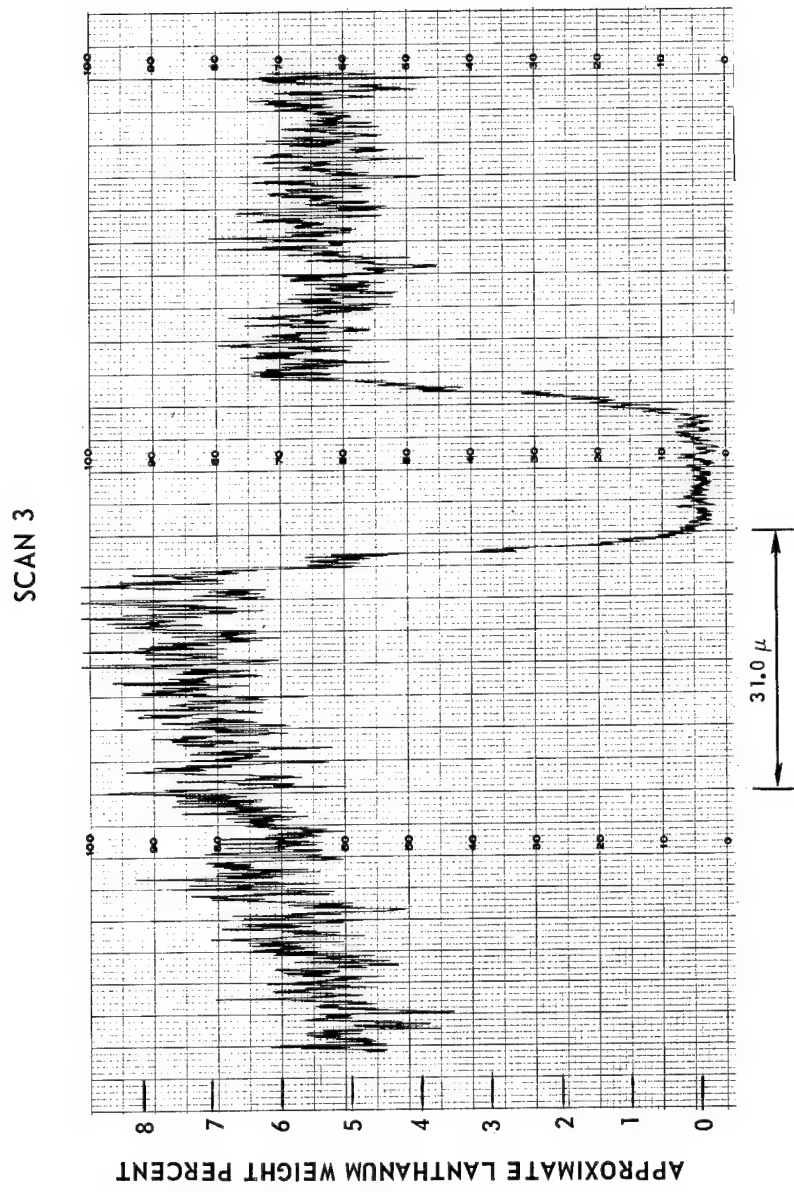


FIGURE 53c. LANTHANUM DISTRIBUTION SCANS ACROSS PATH SHOWN SCHEMATICALLY IN FIG. 52

SCAN 4

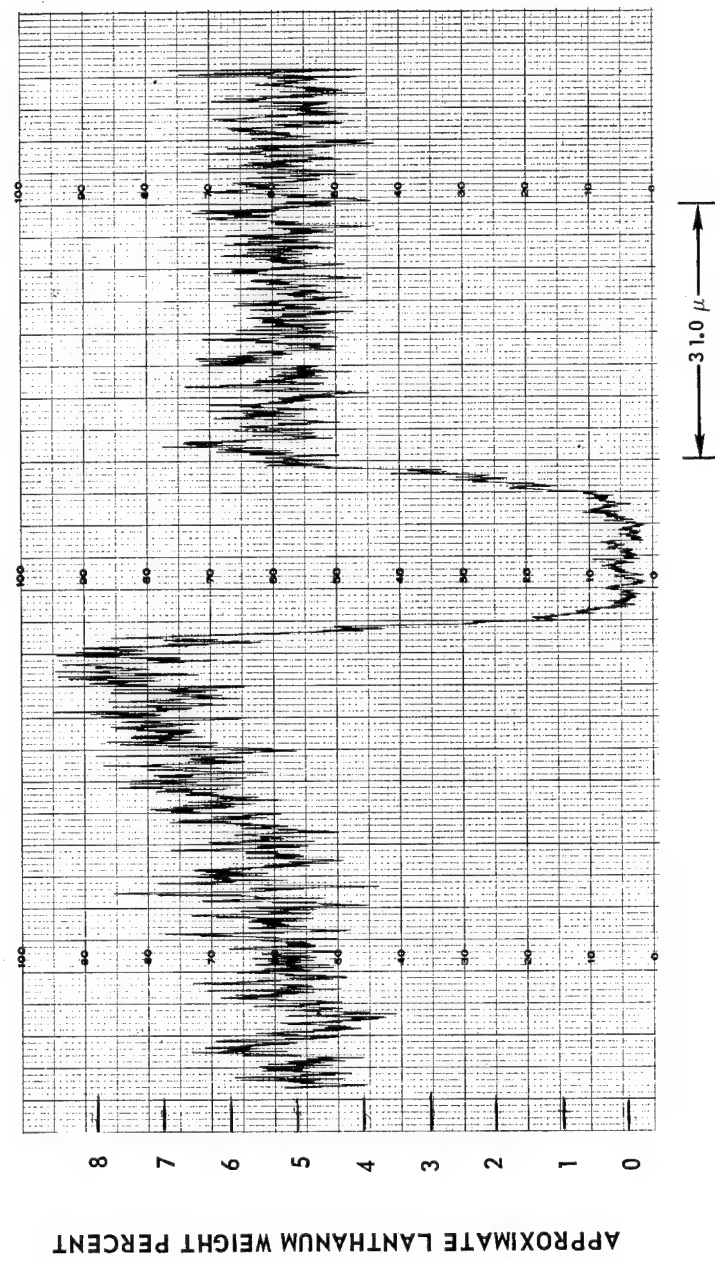


FIGURE 53d. LANTHANUM DISTRIBUTION SCANS ACROSS PATH SHOWN SCHEMATICALLY IN FIG. 52

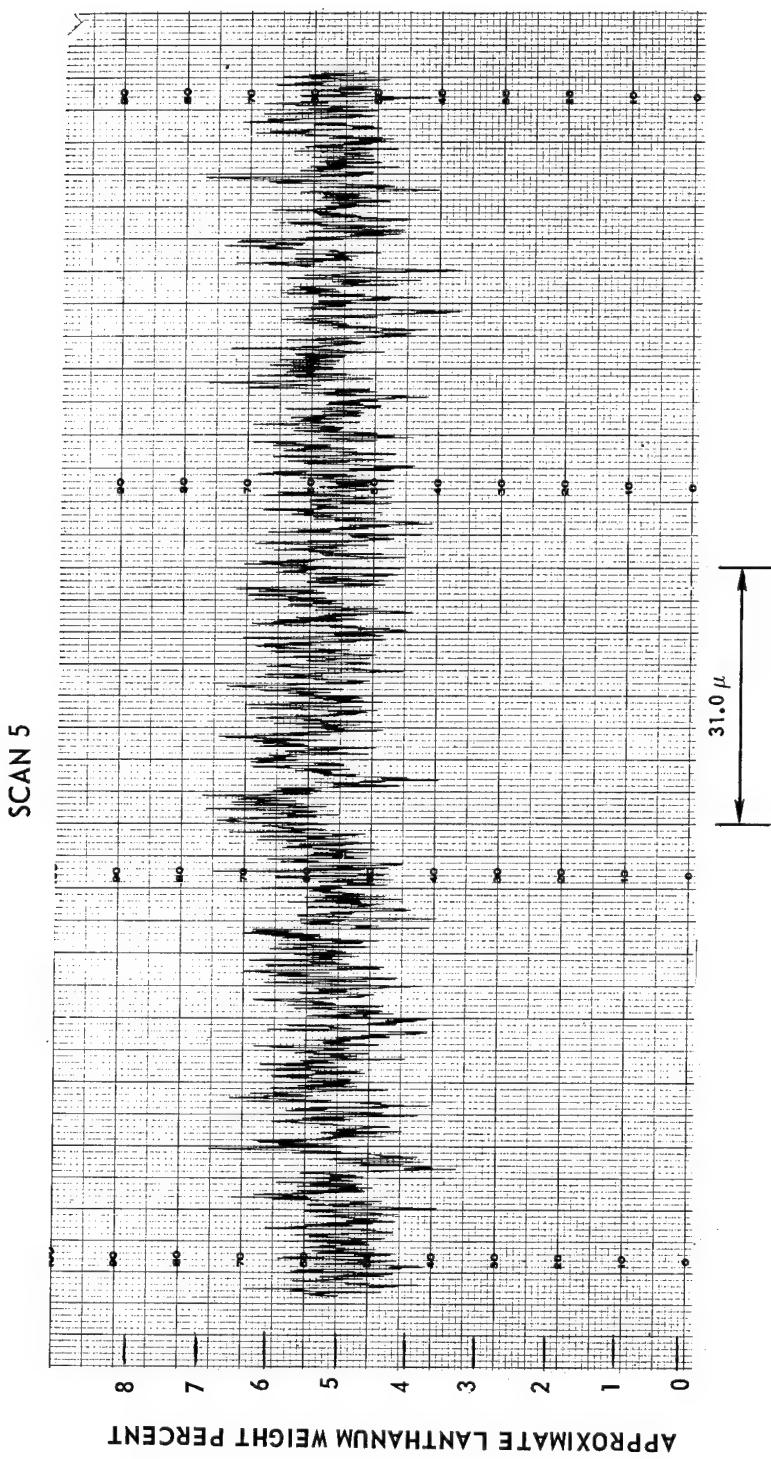


FIGURE 53e. LANTHANUM DISTRIBUTION SCANS ACROSS PATH SHOWN SCHEMATICALLY IN FIG. 52

SCAN 6

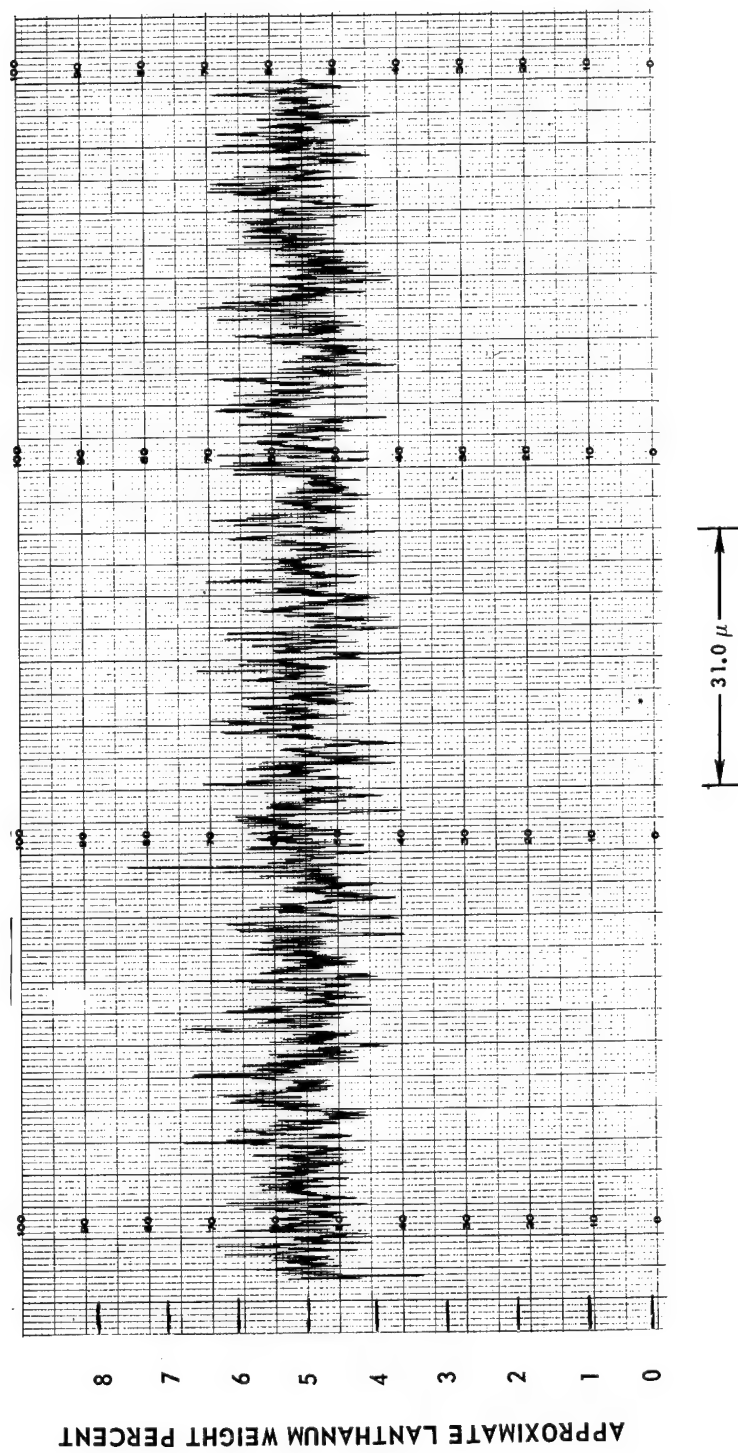


FIGURE 53f. LANTHANUM DISTRIBUTION SCANS ACROSS PATH SHOWN SCHEMATICALLY IN FIG. 52

scanned by the beam from the edge of the crystal to the end of the scan is about 60 microns, which means that the beam passed by the end of the other side of the crystal about 3 microns away from the end, without showing any increase in the concentration of lanthanum. Scan 4 is nearly the same as scan 3, and shows about 7-8 wt % La_2O_3 very near the tip of the crystal which decreases linearly away from the crystal edge. Scans 5 and 6 show no variation in the La_2O_3 content throughout the scan.

The results show that the lanthanum is diffusing away from the crystal-glass interface at the ends of the growing crystal and that if a lanthanum enriched zone is present, it is less than one micron in thickness. The analyses do show that there is a lanthanum enriched zone within the hollow portion of the crystal, in which the only diffusion path is toward the open end of the crystal. The mechanism by which the lanthanum ion alters the rate of crystal growth may be an adsorption of lanthanum ions on the growing crystal face, and apparently is not due to a thicker lanthanum enriched zone within the glass.

Estimation of Liquidus and Working Range

The direct microscopic observation of the kinetics of crystallization of molten oxides as well as the direct measurement of their liquidus and the estimation of their working range is readily possible by means of a microfurnace and is invaluable in deciding which experimental glass compositions are likely to fiberize readily.

During this report period, many of the new experimental glasses were characterized by optical examination in UARL's microfurnace. These characterizations essentially consisted of evaluating those properties of the glasses which are of importance in forming fibers. The properties consisted of the liquidus temperature, and the temperature at which the viscosities of the glasses were equal to 1000 and 100 poises. The rate of crystallization was also noted at a temperature of 50° below the liquidus temperature. This temperature was selected on the basis of our earlier examinations, which revealed that at such a temperature a fairly high rate of crystal growth would occur.

The liquidus temperature was determined by filling the crucible with the glass in the same manner as used in the determinations of the rate of crystal growth. The glass was heated until homogenized by convection currents, and then cooled to allow crystals to nucleate and grow to a few tens of microns in diameter. The crucible is then reheated until the crystals disappear, the temperature is noted and the process is then repeated until a satisfactory liquidus temperature is obtained. The viscosities of the experimental glasses were estimated by comparing their behavior when stirred with the thermocouple with that of a standard glass. "E" glass was used as the standard, and the viscosity versus temperature data of Tiede (Ref. 87) were used to obtain the temperatures at which the viscosity of E glass was 1000 and 100 poises. The viscosities which are estimated in this manner are not exact measurements, of course, but should be of value in drawing

fibers of these glasses, and these were obtained by heating the glass above the liquidus temperature until all of the crystals were melted, and then lowering the temperature to 50° below the liquidus temperature and noting the rate of crystal growth which occurred in a 10 min interval. This rate is reported in semiquantitative terms, such as slow, moderate, and rapid. A rapid growth rate would be measured in hundreds of microns per minute and a slow rate would be measured in a few tens of microns per minute, or less. Even with the precautions outlined above, the results of liquidus estimation may be very greatly in error as pointed out by Hafner (Ref. 51).

The data collected from many of the experimental glasses is shown in Table XIX. For some of the missing glass numbers in the range of the current tests, UARL 333 through UARL 377, only partial data could be obtained or the liquidus was too high for range of operation of the microfurnace or the glass too strongly absorbing to permit such visual observations. The significance of the data obtained can be seen from the fact that UARL 370, 371, and 372 proved very suitable for mechanically drawn fibers.

Evaluation of Glass Forming Characteristics and Fiberizability on UARL Experimental Glasses

The oxide materials previously melted in the kiln using the procedures described earlier in this report furnish the starting materials used in this phase of our research. From the previous firing in the kiln they have emerged either as fully melted and fined glasses, glass and interpenetrating crystalline masses, or materials that appear similar to clinkers or cinders. One chooses a sufficient amount of this material to fill a 15 milliliter platinum crucible and this material is then crushed or ground to approximately 10 mesh size and placed in the platinum crucible. The platinum crucible then is placed on the motor-driven platform of the Super-kanthal hairpin furnace and this furnace platform is raised until the crucible is in the center of this furnace, whose temperature is already at the desired value. The crucible is held at this temperature for a time varying from one-half hour to two hours dependent on the original condition of the charge and is then lowered as rapidly as possible. As soon as the crucible emerges from the furnace, one man grasps it in his tongs and a second man dips a twenty mil platinum wire into the molten glass and runs away from the crucible as rapidly as possible. Usually in this manner it is possible to hand draw a glass fiber, 2 to 5 mils in diameter and thirty to forty feet long, if the glass is to be termed readily fiberizable. The Super-kanthal hairpin kiln used in this experiment readily obtains a temperature of 1800°C in air.

In the simple fashion described above or by attempting to form buttons by pouring glass out of the crucible it is usually possible to obtain some crude idea concerning the working characteristics of the experimental glass. Indeed, tables of such working characteristics for various glasses were included in our two previous summary reports. As our experience in mechanically drawing fibers

Table XIX

Liquidus Temperature and Working Characteristics of
Several UARL Invert Analog Glasses

<u>Sample No.</u>	<u>Liquidus Temperature</u>	<u>100 Poises</u>	<u>1000 Poises</u>	<u>Rate of Growth 50° below Liquidus Temperature</u>
102	1301	1474	1296	very slow
247	1292	1447	1153	slow
249	1256	1279	1176	slow
250	1447	>1500	1297	very slow
251	1330	1439	1314	slow
252	1405	>1500	1259	very slow
253	1510	>1500	1376	rapid
256	1447	>1500	1338	rapid
257	1464	>1500	1407	rapid
265	1435	>1500	1372	rapid
267	1390	>1500	1281	very slow
273	1435	1470	1340	moderate (2 types)
275	1322	>1500	1281	slow
276	1346	1498	1272	no crystals
285	1276	1443	1243	moderate
286	1343	1422	1297	no crystals
287	1158	1473	1276	no crystals
290	1220	1440	1280	no crystals
291	1231	1414	1247	no crystals
292	1260	1385	1156	slow
293	1290	>1500	1372	rapid
294	1414	1473	1291	no crystals
295	1185	1426	1206	no crystals
296	1310	1431	1227	no crystals
299	1206	1406	1174	no crystals
300	----	1268	1055	no crystals
311	1475	>1500	1410	few crystals
316	1435	1477	1310	few isolated crystals
318	1490	>1500	1443	no crystals
319	1515	1495	1290	moderate to slow
322	1500	1435	1290	no crystals
325	1444	1322	1481	few large crystals
331	1483	1456	1381	rapid
335	1490	1510	1380	moderate

Table XIX (Cont'd)

<u>Sample No.</u>	<u>Liquidus Temperature</u>	<u>100 Poises</u>	<u>1000 Poises</u>	<u>Rate of Growth 50° below Liquidus Temperature</u>
333	1510	1490	1440	few isolated crystals
339	1520	1540	1430	none
340	1507	1520	1400	none
341	1438	1390	1515	none
342	1470	1350	1485	few isolated crystals
343	1410	1200	1420	none
347	1510	1406	1506	not apparent
348	1450	1310	1448	none
349	1480	1320	1450	none
350	1510	1422	1490	very rapid
351	1450	1331	1435	very slow
352	1435	1340	1422	moderate
353	1510	1315	1406	extremely rapid
354	1464	1290	1414	moderate
359	1490	1380	1500	few isolated crystals
367	1460	too opaque	too opaque	a very few isolated
368	1440	too opaque	too opaque	none
370	1500	1290	1460	none
371	1498	1290	1372	a very few isolated
372	1440	1300	1420	few isolated crystals
373	1510	1368(many crystals)	1435	none
374	1456	1300	1481	only micro-crystals
375	1347	1256	1332	many micro-crystals
376	1122	951	1150	none
377	1156	933	1222	none

continues to accumulate we find, however, that crude tests of this type are insufficiently selective to assure the production of high quality fiber by our simple mechanical drawing procedures. Much more informative are direct microfurnace observations of liquidus temperature and rates of devitrification. Also equally helpful are studies involving the pouring and controlled annealing of large glass patties, 3 to 4 in. in dia and 3/8 to 5/8 in. thick. The results of a typical study of this kind conducted for us by the Glass Testing Laboratory of the Hartford Division of the Emhart Corporation are shown in Table XX. The superior working characteristics of glasses containing either ceria or lanthana are evident.

Table XX

Glass Forming Characteristics of Selected Rare-Earth and Cordierite Based Glasses and Two Calcium-Silica Glasses

<u>Glass Number</u>	<u>Components</u>	<u>Remarks</u>
200	La ₂ O ₃ , Y ₂ O ₃ , MgO, Al ₂ O ₃ , SiO ₂	Melted at 1500°C. Annealed at 850°C.
203	Y ₂ O ₃ , MgO, SiO ₂	Melted above 1500°C. Devitrified in pouring, liquidus probably 1500°C, annealed at 900°C.
205	CeO ₂ , La ₂ O ₃ , MgO, SiO ₂	Same as 203 but a little less prone to devitrify & possibly a little lower viscosity at 1500°C. Devitrified at 850°C to form a yellow opal.
206	Y ₂ O ₃ , CaO, Al ₂ O ₃ , SiO ₂	Did not melt at 1500°C, only sintered. Top portion of melt at higher temperatures was a clear glass but bottom half opaque.
207	Y ₂ O ₃ , MgO, Al ₂ O ₃ , SiO ₂	Devitrified on pouring. Very fluid at 1500°C. Annealing satisfactory at 850°C.
208	Y ₂ O ₃ , MgO, Al ₂ O ₃ , SiO ₂	Melted easily at 1500°C to form a stable glass, quite fluid at 1500°C, annealed at 780°C.
209	CeO ₂ , Y ₂ O ₃ , MgO, Al ₂ O ₃ , SiO ₂	Same as 208 but more fluid at 1500°C.
210	CeO ₂ , Ca ₂ O ₃ , MgO, Al ₂ O ₃ , SiO ₂	Same as 208 & 209 but even more fluid at 1500°C. Much less prone to devitrify. Annealed at 750°C.
214	MgO, Al ₂ O ₃ , SiO ₂	Melted at 1500°C. Fairly stiff at melting. Turns to opal on cooling. Annealed at 800°C.
215	ZrO ₂ , TiO ₂ , BaO, CaO, MgO, SiO ₂	Glass almost watery at 1500°C. Most stable glass in series with respect to devitrification. Has longer working range. Annealed at 700°C.
219	Fe ₂ O ₃ , La ₂ O ₃ , BaO, CaO, MgO, Al ₂ O ₃ , SiO ₂	Melted at 1500°C. Quite fluid but devitrified rapidly on slight cooling. Annealed at 800°C. Pots are semi-crystalline.

CHARACTERIZATION OF THE EXPERIMENTAL GLASSES II.
YOUNG'S MODULUS FOR BULK SPECIMENS

Many characteristics of the newly derived UARL experimental glasses had to be evaluated to act as guidelines for the directions which our research should follow. The easiest and most convenient of these glass properties is the Young's modulus of bulk samples of the new glass. This section relates the several methods used to measure Young's modulus on bulk glass samples, the method that can be used to successfully predict by calculation what Young's modulus will be obtained for one specialized glass family only, and the progress UARL has achieved in originating high modulus glasses.

Young's Modulus Measured on Bulk Samples of Glass

In accordance with the work of Pickett (Ref. 88), a rectangular or cylindrical beam in flexure vibrates at a resonant frequency determined by the dimensions, density and Young's modulus of the specimen. If shear and inertia effects are considered, the formula for rectangular specimens is:

$$E = \frac{(9.65)(10^{-7})ML^3f^2}{a^3b} [1 + 7.4 (a/L)^2] \longrightarrow \text{kilograms/cm}^2$$

where M = mass of sample in grams

a = thickness of sample in inches or centimeters

L = length of sample in inches or centimeters but units must be same as for a

b = width of sample in centimeters

f = resonant frequency of sample in cycles/sec

E = Young's modulus for sample in kilograms per square centimeter.

Original and improved sonic measurement equipments. - The equipment originally assembled to carry out the dynamic measurement of Young's modulus for bulk samples of glass is shown in Fig. 54. The specimen is placed on two narrow supports fashioned from sponge rubber, a highly absorbing material. A microphone driven by a variable frequency oscillator is placed below the center of the specimen. This microphone excites the short column of air between itself and the specimen and this column of air, in turn, drives the specimen. At a given critical frequency the specimen resonates and this motion is detected by a phonographic pick-up cartridge which touches the specimen directly over one of the supports. This signal from the phonographic pickup is then fed through an amplifier to one set of plates of an oscilloscope. The other set of plates of the oscilloscope is supplied from the oscillator output, so that at the resonant frequency a Lissajous figure of maximum dimension is seen on the oscilloscope because of the 90° phase shift occurring during detection. At any frequency other than the resonant frequency only a simple

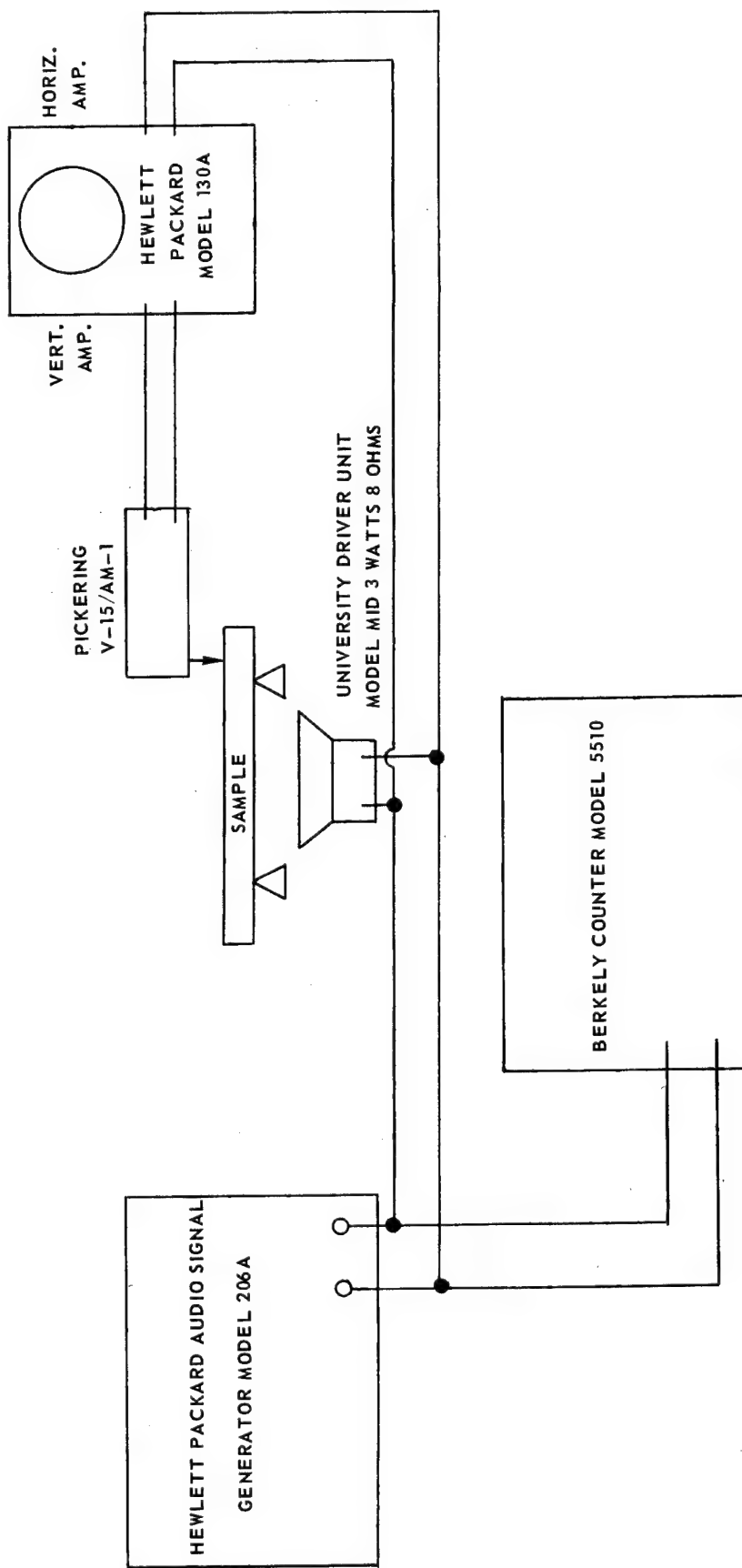


FIGURE 54. SONIC EQUIPMENT ASSEMBLED FOR MEASUREMENT OF YOUNG'S MODULUS

horizontal trace forms on the oscilloscope screen so that resonance is readily detectable. The circuitry shown in Fig. 54 when applied to six different specimens of the cordierite based glass yield the data given below.

Dynamic Modulus for Cordierite Based Glasses

Specimen	Mass (gms)	Dimensions			Young's Modulus $\text{Kg/cm}^2 \times 10^5$	Young's Modulus $\text{lbs/in}^2 \times 10^6$
Batch 4-#1	1.2242	0.125	0.320	1.796	10.35	14.8
Batch 4-#2	1.3698	0.1255	0.319	2.023	10.59	15.1
Batch 4-#3	1.2508	0.126	0.320	1.850	10.55	15.0
Batch 14-#1	1.70083	0.1273	0.324	2.406	10.52	15.0
Batch 14-#2	1.5334	0.1275	0.324	2.173	10.55	15.0
Batch 14-#3	1.4098	0.1277	0.324	2.025	10.74	15.0

The results obtained are valid as far as we can tell since using the same equipment values for Corning Glass Works Code 7940 (fused silica) of 10.5×10^6 psi, Code 7740 (Pyrex*) of 9.3×10^6 psi, and Code 7052 (high alumina-silica) of 8.2×10^6 psi were obtained and these results are concordant with those found in Corning's publication, B-83, Properties of Selected Commercial Glasses.

The equipment just described and as pictured in Fig. 54 was entirely satisfactory if glass samples two inches or greater in length were available. But for many glasses without spending undue amounts of time working out the proper annealing cycle for the method of sampling first employed, the longest lengths available were only 1 1/8 inches. To carry out significant measurements on such short samples it was necessary to assemble apparatus capable of operating at much higher frequencies and this, in turn, meant purchasing much higher fidelity components.

Equipment selected for improved measurements is shown in Fig. 55. This system sketched as a block diagram measures the resonant frequency of glass rods in the region between 1000 and 40,000 Hz. The sample is supported at the nodal points for the fundamental resonance by thin flexible supports that have a resonant frequency below 1000 Hz. A 30 watt driver below the center of the sample drives a column of air which in turn excites the sample. The vertical displacement of the end of the bar is detected by the transducer, a high quality semiconductor phonograph cartridge and tone arm adjusted for a tracking force of approximately 0.1 gram. The differential output from the transducer is amplified by a preamplifier which also supplies excitation to the transducer. The output of the preamplifier is passed through a high pass R-C filter to remove low frequency noise due to building and support vibrations and is amplified in a guarded differential amplifier. This amplified signal is displayed on a CRO and the peak detected is used to drive the vertical axis of an x-y recorder.

*Registered trademark, Corning Glass Works, Corning, N.Y.

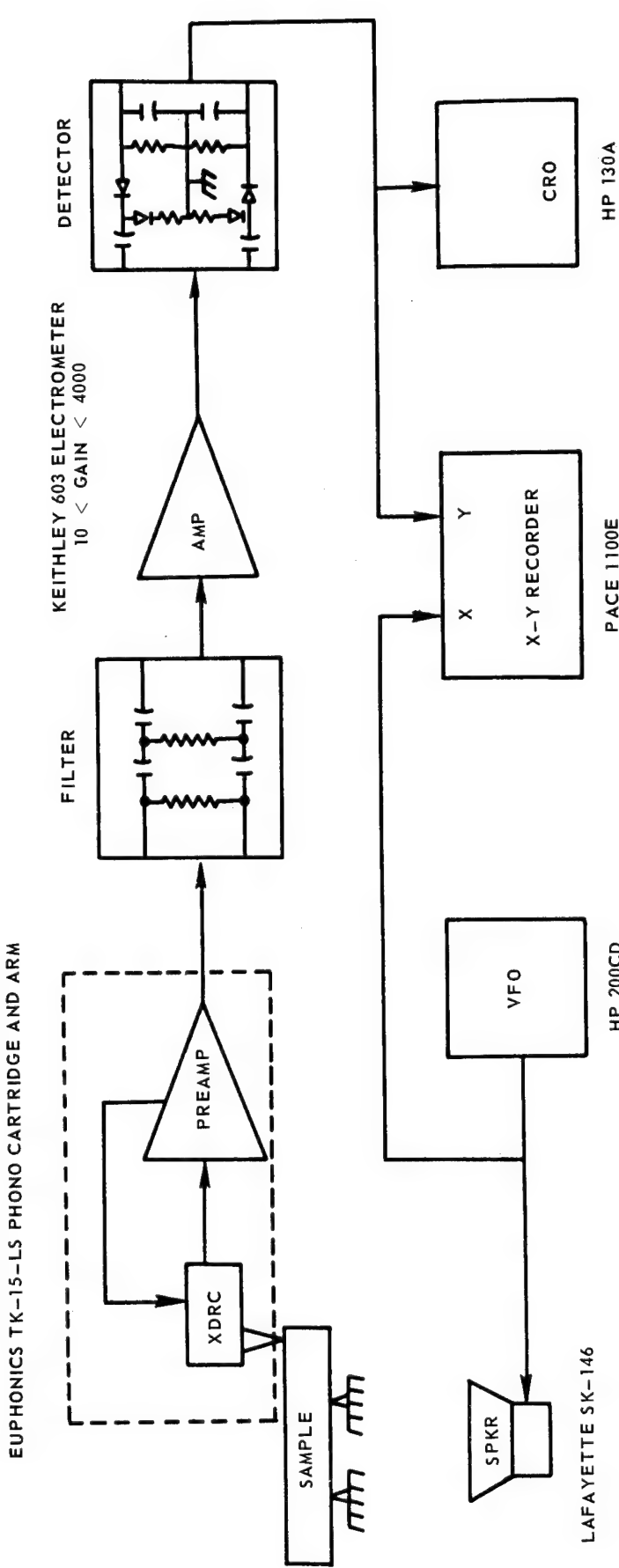


FIGURE 55. IMPROVED APPARATUS FOR MEASUREMENT OF YOUNG'S MODULUS

Primary excitation is supplied to the driver unit by a variable frequency audio oscillator through an audio amplifier. A potentiometer mechanically coupled to the frequency control on the oscillator supplies a d-c voltage to the horizontal axis of the x-y recorder proportional to the logarithm of the driving frequency. With this system, any spurious resonances due to the driver unit, transducer or supporting structures will appear the same for different samples and can thus be eliminated from the data by the operator. Resonances with amplitudes smaller than those from extraneous sources can be easily resolved by comparative recordings for several sample lengths. The overall system has a frequency response from 3000 to 40,000 Hz with an amplitude variation of only three decibels. Needless to say, the improved equipment has proven much simpler for a technician to operate than its predecessor described in the earlier paragraphs of this section.

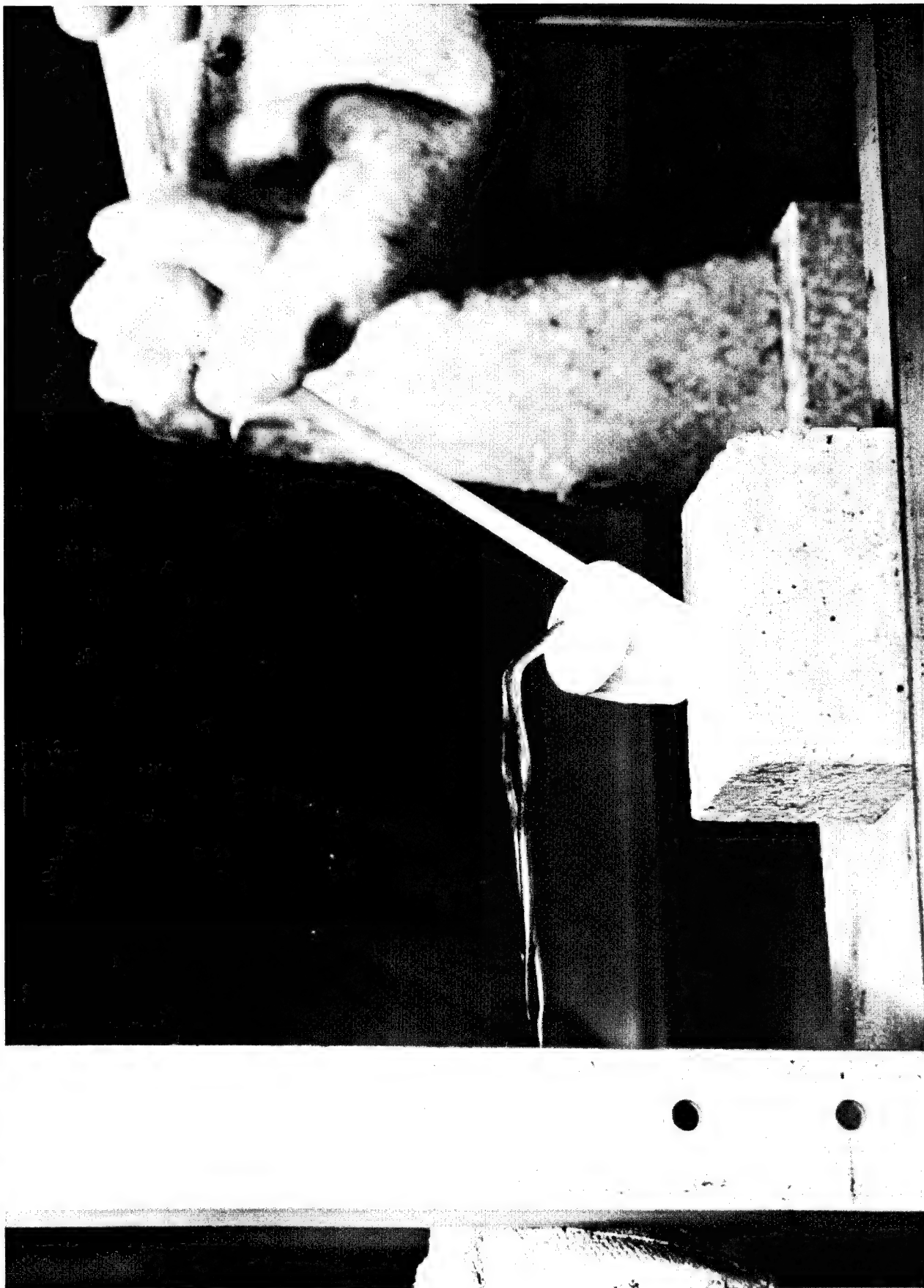
Original and improved methods of sample preparation. - The original method of sample preparation consisted of casting a slab of the glass to be tested. This slab was immediately placed in a program controlled annealing kiln and cooled to room temperature in a thirty-six hour period, the rate of cooling in the estimated annealing range being about 8°C per hour. Once cooled, the sample was taken to the nearest optical lens shop where it was mounted on laps, cut to approximately the desired rod size and finished by optical grinding techniques. These samples were typically 1.800 inches long, 0.1240 inches wide, and 0.1240 inches high. The commercial lens maker who cut and ground these samples for us had difficulty in holding these dimensions to tolerances better than ± 0.003 inches and this was particularly true because these glasses were harder than the usual optical glasses. Needless to say, these samples were very expensive averaging thirty to forty dollars each and the complete cycle of sample preparation extended over times greater than a week. The reproducibility obtainable with these precision machined samples is shown below.

Reproducibility of Dynamic Modulus for
Precision Machined Square Rods

Specimen Glass & Spec No.	Young's Modulus 10^6 psi	Specimen Glass & Spec No.	Young's Modulus 10^6 psi	Specimen Glass & Spec No.	Young's Modulus 10^6 psi
30-1	10.15	30-7	9.94	31-1	11.55
30-2	10.18	30-8	10.23	31-2	11.45
30-3	10.17	30-9	10.05	31-3	11.87
30-4	10.0	30-10	10.38	31-4	11.25
30-5	10.38				
30-6	10.35				

In the second year of the contract a new, more rapid, more convenient, much less expensive, and very much faster method of preparing the bulk glass samples necessary for sonic modulus measurement was originated. This technique consisted of forming the modulus specimen by drawing the molten glass up into fused silica tubes using a syringe to apply suction to the tubes as shown in Figs. 56 and 57.

FIGURE 56. PREPARATION OF SAMPLES FOR MODULUS MEASUREMENT



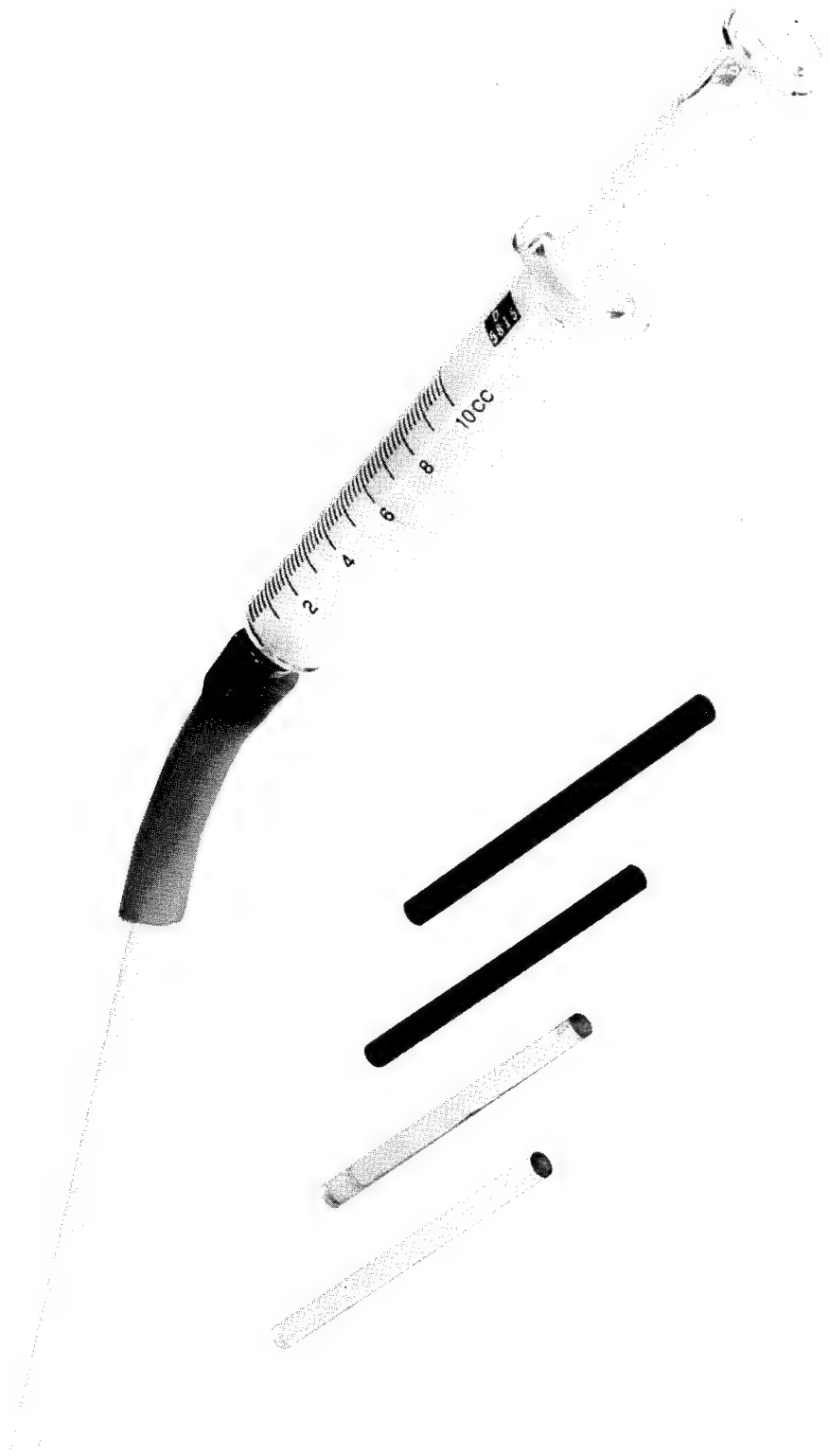


FIGURE 57. ROD CASTING SYRINGE AND EXAMPLES OF GLASS RODS

In most cases a light dusting of magnesia powder inside the silica tube is used to prevent the glass from adhering to the walls of the tube, but in the cases of the higher thermal expansion glasses which immediately start shrinking away from the walls of the very low expansion silica such a coating is unnecessary. After the rods are removed from the silica tube, the ends are trimmed off square with a cut-off wheel and the sample is ready for measurement. Since this type of sample has a very different fictive temperature from the type of sample originally prepared, it is not expected that the results need to be precisely the same for the two types of samples, a point which is discussed in greater detail in the next section. This is not important, however, in day to day glass research where all that is needed are accurate relative modulus values for the various experimental batches so as to form a guide for ways in which to modify the composition to achieve a desired property.

Results obtained - Young's modulus of bulk glass samples. - Comparative results for as-aspirated and precision machined bulk glass rods are shown in Table XXI. The as-cast or aspirated rods give a value about 2% lower on the average than the annealed sample, a result completely in agreement with expectations since it corresponds in direction but not to the extent of difference in modulus between a glass fiber and an annealed glass sample found in other laboratories.

The agreement found between dynamically determined moduli and those found by the static or transverse rupture method is tabulated in Table XXII. In this case all dynamic values listed are for precision ground-annealed glass bars and are, therefore, two percent higher than the usual dynamic values found in this report. The static measurements reported are for measured deflections versus measured loads in three-point loading apparatus equipped with an unusually sensitive load cell. The values obtained by the dynamic method are believed to be more nearly correct since this method gives the slope of the initial part of the stress-strain curve and thus corresponds to a value based on microstresses, while the transverse rupture method essentially yields a value for only very large strains and so corresponds to an average value for a stress-strain curve which is not really a straight line when examined closely. In addition, it should again be mentioned that the dynamic method applied to commercial glasses gave results in agreement with published data.

The amount of variation commonly encountered in this laboratory using the dynamic or sonic modulus determination applied to bulk glass rods formed by aspiration are shown in Table XXIII. The adequacy of the method for laboratory screening of original glass compositions is clearly indicated.

In Table XXIV, the results are shown of dynamic measurements carried out on aspirated rods using the improved sonic apparatus for a number of cordierite-rare earth glasses. It will be noted that these values of Young's modulus range from 14.96 million psi to 21.1 million psi and that in general the values of approximately 15 million psi for glasses originated in the first year of the contract have been steadily improved to values of nineteen million psi or better for recent glasses.

Table XXI
Comparison of Young's Modulus of As-Cast and
Annealed Glass Bars

<u>Glass</u>	<u>$E \times 10^{-6}$ psi</u> <u>As-Cast</u>	<u>$E \times 10^{-6}$ psi</u> <u>Annealed</u>	<u>Percent Increased</u>
68	14.4	14.7	2.1
	13.7	14.0	2.2
	13.8	14.1	2.2
	14.5	14.5	0
114	16.3	16.5	1.2
	16.6	17.0	2.4
	16.6	17.0	2.3
126	16.7	17.0	1.2
	16.9	17.3	2.4
129	16.9	17.0	0.6
	16.3	16.6	1.8
	16.5	16.2	1.8
135	14.3	14.6	2.1
	14.4	14.7	2.1
	14.3	14.5	0.7
	14.4	14.7	2.1
136	14.6	14.8	1.4
	14.3	14.5	1.4
	14.3	14.6	2.1
138	15.2	15.4	1.3
	15.4	14.8	2.5
	15.2	15.6	1.9

Table XXII

Comparative Results of Sonic and Transverse
Rupture Tests on Bulk Glass Rods

<u>Specimen</u>	Sonic Modulus (lbs/in ² x10 ⁶)	Transverse Rupture Value (lbs/in ² x10 ⁶)
1	14.5	13.79
2	14.8	14.50
3	15.1	14.06
4	15.2	14.33
5	14.55	13.92
6	15.38	13.55
7	14.58	13.81
9	15.0	13.76
10	14.4	13.20
11	15.36	14.50
Average	14.89	13.94
Average Deviation	<u>+0.32</u>	<u>+0.32</u>

Table XXIII

Reproducibility of Values of Young's Modulus Measured
on Rods Aspirated Directly from Melt

<u>Glass No.</u>	<u>Individual Determinations (10^6 psi)</u>					<u>Average Modulus (10^6 psi)</u>
40-3	15.6	15.1	15.6	15.5		15.5
62-3	13.59	14.77				14.18
67-3	14.5	14.6	14.24			14.43
68-3	14.4	13.8	13.7	14.6		14.1
69-3	14.11	14.37	14.00			14.16
72-2	14.4	13.9	13.8			14.0
76	15.7					15.7
83	16.0	16.0	16.0	16.0		16.0
93	16.06	15.80	15.70	15.64	15.66	15.90
	15.80	15.82	15.69	15.67	15.79	15.45
	15.50					
96	16.51	16.31	15.76	15.73	16.00	15.92
	16.17	15.90	16.38	15.93	18.76	16.18
	15.70	15.67	16.94	16.38		
96-2	15.59	15.28				15.4
97	15.52					15.5
99	10.7	10.5	10.4	10.5		10.5
102	15.00	14.97	14.61	15.13	15.50	15.04
108	14.79	14.67	14.84	14.68	14.69	14.81
110	14.69	14.07	14.73	14.99		14.62
114	16.4	16.7	16.8	16.7		16.7
125	16.2	15.8	16.2	16.2	16.3	16.14
126	16.5	17.1	16.7			16.8
127	15.49	16.10	16.51	16.06	15.81	16.13
129	16.9	16.1	16.3	16.6		16.5
131	13.99	13.66	13.93	13.80	14.61	14.00
134	15.3	15.4				15.4
135	14.6	14.5	14.6	14.0	14.6	14.3
	14.2					
136	14.6	14.2	14.4			14.4
137	13.3	13.6	13.3	13.0		13.3
138	15.3	15.2	15.4	15.3		15.3
140	15.1	15.7	15.5	16.2		15.6
155	15.6	15.7	15.7	15.7		15.7
157	13.3	13.6	13.3	13.0		13.3

Table XXIII (Cont'd)

<u>Glass No.</u>	<u>Individual Determinations (10^6 psi)</u>					<u>Average Modulus (10^6 psi)</u>
159	16.5	15.9	16.0	16.4		16.2
166	12.9	12.1	12.6			12.53
174	16.9	16.4	16.4	16.1		16.5
175	15.9	16.3	16.2	15.3		16.1
176	14.9	16.2	14.6	15.0		15.2
179	14.6	14.8	14.6	14.9		14.7
194	14.0	14.9	14.6	15.2		14.7
219	14.87	14.65	14.87			14.80
222	15.3	15.0	14.2			14.8
231	20.37	20.26	18.63	21.43	19.08	20.95
232	20.11	17.10	17.46	17.87	18.09	18.13
233	21.68	25.61	26.59	20.34	17.58	22.36
233A	17.64	15.15	15.38	15.27		15.86
234	17.95	17.87	18.14	18.22	17.95	18.16
235	17.5	17.2	17.4	17.4	17.4	17.4
236	18.0	17.8	17.4	18.1		17.8
237	18.00	17.99	18.43	18.47	18.61	18.36
	16.93					
238	16.8	16.8	16.8	16.4		16.6
247	15.0	15.2	15.0			15.07
248	20.5	16.0	15.42	14.03		16.48
249	15.9	15.6	16.0	16.0	15.8	15.86
250	14.35	14.86	15.27	14.82		14.83
251	16.08	15.48	16.05	15.82		15.86
252	14.65	15.32	14.63			14.87
253	12.28					12.28
256	17.35	17.40	18.05	17.10	17.68	15.95
	17.70	18.30	17.92	17.78		
257	17.85	18.65	18.28	17.43	17.95	18.28
	16.82	17.88	18.97	18.47		
258	13.5					13.5
259	13.08	12.31	14.0	12.67		13.24
263	14.85	14.22	15.08	14.30	14.00	14.49
265	16.58	16.68	16.17	15.67		16.28
266	16.62	16.97	17.12	16.22		16.73
267	14.62	15.70	15.40	15.6		15.34
268	17.00	17.03	16.75			16.93
269	17.8	17.1	16.95	16.85		17.18

Table XXIII (Cont'd)

<u>Glass No.</u>	<u>Individual Determinations (10^6 psi)</u>						<u>Average Modulus (10^6 psi)</u>
270-2	20.2	20.8	19.9	20.1			20.25
273-2	16.57	17.73	17.88	17.80	17.35	17.4	
273-1	17.90	18.28	18.97				18.39
273-D	17.25	17.13	17.38	17.90	16.23		17.18
274	21.2	17.3	18.42	18.32	17.75	17.57	17.23
	16.48	17.47	16.70	18.25			
275-0	16.48	16.64	16.52	16.65	17.21	16.54	16.67
275	16.65	17.21	16.54				16.80
276	15.47	15.0	15.82	16.48	16.32	15.82	
277-2	17.43	17.43	17.55	18.32	18.66	17.93	17.91
	17.57	17.80	17.43				
283	15.58	15.36	15.20	15.62	15.62	15.39	15.47
	15.67						
284	14.08	14.87	15.33	15.07	14.87		14.85
285	15.13	15.31	15.0	15.17	14.91	14.89	15.07
286	16.86	15.48	14.81	15.64	15.49	15.28	15.60
	16.46						
287	14.53	15.50	14.79	14.65	15.26	15.63	15.14
288	14.27	14.48	14.14	13.99	14.49	14.42	14.30
289	14.74	14.75	15.19	15.21	14.86		14.95
290	14.47	14.27	14.72	14.26	14.50	14.89	14.52
291	16.12	15.32	15.96	15.67	15.59	15.37	15.67
292	15.46	15.08	15.73	15.17	14.78	15.77	15.36
293	16.28	16.15	17.18	14.93	15.30	15.86	15.96
294							17.62
295							15.22
296	16.71	15.12	18.51	15.49	16.47	16.87	16.53
297	17.17	18.00	18.08	17.00	16.75	16.48	17.08
299	14.74	14.35	14.60	14.63	14.84	14.28	14.57
300	14.36	14.40	14.58	14.58	14.47	14.22	14.45
	14.68						
302	17.23	16.73	17.58	17.24	17.04		17.16
304	24.06	18.53	18.45	18.30	19.12	18.21	19.23
	17.91						
305	17.1	18.1	17.7	17.8	17.9	16.8	17.72
306	18.8	18.9	18.6	18.7	19.4	18.7	18.85

Table XXIII (Cont'd)

<u>Glass No.</u>	<u>Individual Determinations (10^6 psi)</u>						<u>Average Modulus (10^6 psi)</u>
309	16.92	16.43	16.91	18.12	16.59	16.21	16.86
310	16.04	19.58	16.59	15.88	16.20	15.65	16.66
311	16.31	14.71	14.98	15.98	16.49	16.91	15.90
312	17.26	15.81	16.77	16.25			16.52
314	16.39	17.23	16.68	17.07	17.19	17.47	16.99
	16.89						
315	16.89	17.04	16.17	16.97	16.14		16.63
316	16.55	16.57	16.18	16.37	16.52	16.26	16.46
	16.39						
317	15.84	16.32	16.87	16.78	16.64	15.53	16.33
318	15.26	15.68	18.08	15.91	15.57	15.44	15.97
319A	17.9	18.02	17.83				
319	15.96	15.03	15.86	15.26	15.01		15.42
320A	16.05	15.98	15.90	16.12	15.72	16.00	15.96
320B	17.23	19.33	16.32	16.31	16.23	16.79	17.03
321A	18.20	17.92	19.83	18.09	18.97	19.07	18.7
322	17.56	16.85	17.18	17.11	16.71		17.08
322A	18.52	18.11	18.63	17.82	19.76	18.87	18.60
323A	18.57	18.14	17.92	20.05	18.05	17.79	18.42
324A	18.04	17.99	17.41	17.25	18.35	17.62	17.78
325A	18.92	19.75	20.16	21.17	20.59	20.55	20.19
325	19.82	19.09	19.05	18.97	19.87	20.12	19.49
326A	16.53	17.28	17.05	17.23	16.79		16.98
326	16.89	16.68	17.83	15.62			16.76
327	18.69	17.99	17.88	18.34	18.88		18.36
329	20.68						20.68
331	20.79	20.99	21.02	20.97	21.21		20.85
331A	19.7	19.9	19.60	20.53	20.33	20.35	20.07
339	19.4	19.2	19.1	19.7			19.4
340	20.24	20.50	21.72				20.83
341	20.13	19.83	17.92	18.31	19.35	19.4	18.80
	17.91	18.32	18.28	18.84	18.53		
343	19.55	19.45	19.11	19.4			19.38
344	20.27	20.29	20.06				20.3
345	21.6	20.1	21.1	20.87	20.79	21.56	21.00
346	17.9	17.6	17.8	17.5	17.5		17.66
347	21.28	22.14					21.62
348	18.80	17.50	17.25	18.29			17.71

Table XXIII (Cont'd)

<u>Glass No.</u>	<u>Individual Determinations (10⁶ psi)</u>					<u>Average Modulus (10⁶ psi)</u>
349	16.73	16.80				16.8
350	20.04	19.32	19.94	19.71		19.75
351	16.59	17.08	17.24	17.26	17.17	16.96
352	20.40	19.60	19.11	20.90		20.0
353	19.86	19.26	19.52	18.89		19.4
354	18.47	18.36	18.13	18.44		18.4
355	18.11	17.81	18.50			18.1
356	13.01	14.81				13.9
357	17.11	17.11	18.51			17.6
358	12.54	12.07	14.66			13.1
359	18.76	17.40	17.55	16.72		17.6
360	18.36	17.99	19.18			18.5
361	18.15	18.38	17.72	20.23		18.6
362	17.92	18.06	17.85	18.23		18.0
363	19.74	19.45	18.78			19.26
364	16.97	16.36	16.77			16.70
365	19.04	19.03				19.04
366A	16.77	15.61				16.19
367	18.88	19.03	19.18			19.03
368	19.30	19.00	18.93			19.08
369	18.07	17.74	17.52			17.78
370	18.42	18.56	18.80			18.59
371	18.82	18.09	18.70			18.59
372	17.38	17.28	20.68			18.54
E	12.42	12.64	12.14	12.06	11.98	11.93
LaSF6	17.28	17.23	17.63	17.55		17.42
LaSF3	13.08	13.55	13.72	13.01		13.34
SFS1	7.18	6.74	7.06	6.92		6.98
SF6	7.34	6.90	6.58	6.82		6.91

Table XXIV
Values of Young's Modulus for Several
Cordierite-Rare Earth Glasses

<u>Glass No.</u>	<u>Young's Modulus (millions psi)</u>	<u>Glass No.</u>	<u>Young's Modulus (millions psi)</u>
14	14.96	304	19.2
64	15.14	305	17.7
66	15.14	306	18.9
70	15.23	323	18.4
114	16.5	337	20.9
117	16.54	344	20.3
125	16.1	345	21.1
138	16.5	363	19.3

Typical Compositions in Mole Percent

30₄-35SiO₂, 15Al₂O₃, 30MgO, 10ZnO, 10Y₂O₃

34₄-45SiO₂, 15Al₂O₃, 15MgO, 15BeO, 10Y₂O₃

The use and extension of the C. J. Phillips method for calculating Young's modulus of certain glasses. - In an outstanding paper entitled "Calculation of Young's Modulus of Elasticity from Composition of Simple and Complex Silicate Glasses" (Ref. 1), C. J. Phillips describes a method for calculating Young's modulus of elasticity for some 44 glasses by expressing the content of each oxide in mol percent and multiplying it by a modulus factor peculiar to that oxide. Coefficients are derived, however, for only certain oxides likely to be present in the usual glasses; namely, SiO_2 , Na_2O , K_2O , Li_2O , B_2O_3 , Al_2O_3 , CaO , MgO , PbO , BaO , ZnO , and BeO . The numerical value of the elastic constant is then the sum of the terms

$$C_1 P_1 + C_2 P_2 + \dots C_n P_n$$

where $C_1 \dots C_n$ are molal coefficients and $P_1 \dots P_n$ are the molar percentages of the corresponding oxides. Agreement between calculated and observed values is better than $\pm 0.3\%$ for thirty-five well-defined glasses.

In this report we extend the Phillips values to include those for less well-known but relatively common oxides such as yttria, lanthana, ceria, zirconia and correct his values for beryllia and magnesia. The latter correction is necessary only for alkali-free glasses. In general, those glasses developed at United Aircraft Research Laboratories which are included in these calculations are characterized as cordierite and/or beryl base glasses with rare-earth additions. The extended calculations cannot be assumed to apply to other types of glasses such as UARL's invert analog glasses, two-phase glasses, or as shown in this section to calcium aluminate base glasses.

The experimental UARL glasses included in this calculation like Loewenstein's glass Z_1^1 (Ref. 89) are alkali-free and it appears that in such alkali-free glasses the molar coefficient of magnesia is 14.8 kilobars per mol percent. The calculations of Table XXV are offered in evidence for this number. According to Weyl (Ref. 90) in alkali-free glasses, MgO_6 groups form in place of the MgO_4 groups of alkali-alkaline earth silicates and this formation of MgO_6 groups resulting from the lower polarizability of O^{2-} ions in alkali-free glasses causes the average coordination of the O^{2-} ions to increase, the structure to become more compact, and the value of the E modulus to increase. Using this value for magnesia, the value of the zirconia coefficient is recalculated from Loewenstein's glass Z_1^1 and a very much more reasonable result of 18.9 kilobars per mol % is obtained for ZrO_2 .

In one of our early summary reports, E910373-4, (Ref. 91) we showed that Phillips through a juxtaposition of the composition of his glass 73 had inadvertently obtained an incorrect value for the beryllia molar coefficient and in this same report we recalculated the BeO coefficient from published data on two Owens-Corning glass fiber compositions (Table XXVI) and found it to be 19.0 kilobars/mol %. Using these corrected values for magnesia and beryllia and experimental data obtained on the new UARL glasses, the Phillips type calculations are extended to glasses containing yttria and the very high values of 22.2, 25.5,

Table XXV

Calculation of Molar Modulus Coefficients by Method of
C. J. Phillips-Magnesia Contribution

Using known silica, alumina, zirconia, values to derive new magnesia value

1. The Basic Glass (1,4,14)

Actual batch for this glass 198 gms SiO_2 , 120 gms Al_2O_3 , 180 gms Basic magnesium carbonate $\text{MgCO}_3 \cdot \text{Mg(OH)}_2 \cdot 2\text{H}_2\text{O}$ with a conversion factor to MgO of 2.44.

<u>Actual Batch</u>	<u>Batch on Oxide Basis</u>	<u>Weight %</u>	<u>Atomic Weight</u>	<u>Mols</u>	<u>Mole %</u>
SiO_2	198	198	50.7	60.09	0.845 52.4
Al_2O_3	120	120	30.5	101.94	0.299 18.6
MgO	180	73.7	18.85	40.31	0.468 29.0
<u>Constituent Mole % Kilobars/mol Contribution</u>					
SiO_2	52.4	7.3		383	
Al_2O_3	18.6	12.1		225	
MgO	29.0	X		29X	
				<u>608+29X</u>	

But average exp. value for 1,4,14 = $14.96 \times 10^6 \text{ lbs/in}^2 = 10.52 \times 10^5 \text{ kg/cm}^2 = 1031 \text{ kilobars}$

$$\therefore \text{MgO contribution} = 1031 - 608/29 \approx 14.7 \text{ kilobars/mole \%}$$

2. Using Glass 66

<u>Constituent</u>	<u>Mole %</u>	<u>Kilobars/mol %</u>	<u>Contribution</u>
SiO_2	53.7	7.3	392
Al_2O_3	15.3	12.1	185
MgO	28.3	X	28.3X
ZrO_2	2.56	18.9	47.4
			<u>624+28.3X</u>

But average exp. value for 66 = $15.14 \times 10^6 \text{ lbs/in}^2 = 10.64 \times 10^5 \text{ kg/cm}^2 = 1043 \text{ kilobars}$

$$\text{MgO contribution} = 1043 - 624/28.3 = 14.8 \text{ kilobars/mole \%}$$

Table XXXI

The Use of Known Molar Modulus Coefficients to Obtain a
Corrected Phillips Coefficient for Beryllia

1. Owens-Corning Glass OCX-2124

<u>Constituent</u>	<u>Weight %</u>	<u>Molecular Weight</u>	<u>Mol Fraction</u>	<u>Mole %</u>	<u>Kilobars/mole %</u>	<u>Contribution (kilobars)</u>
SiO ₂	71.1	60.06	1.185	70.0	7.3	511
Al ₂ O ₃	21.5	101.94	0.211	12.5	12.1	151
BeO	7.4	25.02	0.296	17.4	X	17.4X
			<u>1.692</u>			

But Owens-Corning actually achieved 14.4×10^6 psi or 992 kilobars for Young's modulus of this glass

$$\therefore \text{BeO factor} = \frac{992-662}{17.4} = 19.0 \text{ kilobars/mole \%}$$

2. In Owens-Corning Patent U.S. 3,127,277-Example 4

<u>Constituent</u>	<u>Weight %</u>	<u>Molecular Weight</u>	<u>Mol Fraction</u>	<u>Mole %</u>	<u>Kilobars/mole %</u>	<u>Contribution (kilobars)</u>
SiO ₂	51	60.06	0.850	42.5	7.3	310
CaO	13	56.08	0.232	11.6	12.6	146
MgO	9	40.32	0.223	11.1	12.0	133
BeO	11	25.02	0.440	22.0	X	22X
ZnO ₂	2	123.22	0.016	0.8	18.9	15.1
TiO ₂	8	79.90	0.100	5.0	13.3	66.5
Li ₂ O	3	29.88	0.100	5.0	7.0	35
CeO ₂	3	172.13	0.018	0.9	18.6	16.7
			<u>1.979</u>			

But Owens-Corning actually achieved 16.6×10^6 psi or 1144 kilobars for Young's modulus of this glass

$$\therefore \text{BeO factor} = \frac{1144-722.3}{22} = 19.2 \text{ kilobars/mole \%}$$

722.3 kilobars

and 25.2 kilobars per mol % yttria result (Table XXVII). This high modulus factor for yttria is particularly significant in the development of the new UARL glasses for as has been shown in the first major section of this report, direct microscopic observations of the rate of crystallization of yttria containing glass has shown that this material successfully slows down the formation of cordierite crystals.

Table XXVIII extends the calculation of Young's modulus to glasses containing lanthana and ceria with results of 22.4 kilobars per mol % lanthana and 18.6 kilobars per mol % ceria (calculated as Ce_2O_3). Again these values like the yttria value are an unexpected gain from our primary concept of adding such rare-earth materials to slow the rate of crystallization. Finally, the corrected values of the molar contributions of magnesia and beryllia are used in Table XXIX to derive the molar contributions to Young's modulus for zinc and zirconia and together with all the previously determined experimental molal factors and those of Phillips, these are listed in Table XXX.

The reliability of this method of calculating Young's modulus is considered briefly in Table XXXI and is found satisfactory, although the errors are not as low as found in Phillip's paper. Attempts to extend these Phillips type of calculations based on simple and complex silicate glasses to the totally unallied calcium aluminate glass system. As is to be expected the calculations fail to yield a correct result and instead give a result 20% too high (Table XXXII). However, the calculations for both glasses give the same amount of discrepancy indicating that this type of calculation could probably be extended to calcium aluminate glasses if one is willing to carry out sufficient experimentation to find the new molal coefficients appropriate for this very different structure.

The Phillips type of calculation (Ref. 1) can be put to an unusual, most interesting use as shown in Table XXXIII to check the validity of claims found in the literature for high modulus glasses. It will be noted that the work of Refs. 94 and 95 cannot be correct if the Phillips calculation is valid.

Alternate calculation of Young's modulus from composition by method of S. D. Brown. - S. D. Brown, et al (Ref. 92) have suggested an alternate method of calculating Young's modulus from composition factors peculiar to each oxide present. In contrast to Phillips method as presented above, he bases his calculation of Young's modulus on "packing efficiency" of the discrete ions present. This packing efficiency was measured by a parameter called "the true ionic volume fraction" (f). The parameter is then defined as follows. It is assumed that every ion in the material has a definite spherical volume as determined by radii values given by Pauling (Ref. 96). The summation of these spherical volumes for all ions divided by the total macroscopic volume of the aggregate is the true ionic volume fraction and is calculated by

$$f = \frac{N\rho}{M} \sum_i n_i v_i$$

Table XXVII

Calculation of Young's Modulus from the Composition
by C. J. Phillips Method

Using known alumina, silica values plus new magnesia value to derive factor for yttria

1. Using Glass 70	<u>Constituent</u>	<u>Mol %</u>	<u>Kilobars/mol %</u>	<u>Contribution</u>
	SiO ₂	55.3	7.3	404
	Al ₂ O ₃	12.6	12.1	152
	MgO	29.3	14.7	431
	Y ₂ O ₃	2.83	X	<u>2.83X</u>
				<u>987+2.83X</u>

But #70 experimentally = 15.23×10^6 lbs/in² = 1050 kilobars

$$\therefore Y_2O_3 \text{ contribution} = 1050 - 987/2.83 = 22.2 \text{ kilobars/mol \%}$$

2. Using Glass 114	<u>Constituent</u>	<u>Mol %</u>	<u>Kilobars/mol %</u>	<u>Contribution</u>
	SiO ₂	51.7	7.3	377
	Al ₂ O ₃	22.5	12.1	272
	MgO	15.8	14.7	232
	Y ₂ O ₃	10.0	X	<u>10X</u>
				<u>881+10X</u>

But #114 experimentally = 16.5×10^6 lbs/in² = 1136 kilobars

$$\therefore Y_2O_3 \text{ contribution} = 1136 - 881/10 = 25.5 \text{ kilobars/mol \%}$$

3. Using Glass 64	<u>Constituent</u>	<u>Mol %</u>	<u>Kilobars/mol %</u>	<u>Contribution</u>
	SiO ₂	54.6	7.3	399
	Al ₂ O ₃	15.5	12.1	188
	MgO	28.8	14.7	422
	Y ₂ O ₃	1.39	X	<u>1.39X</u>
				<u>1009+1.39X</u>

But #64 experimentally = 15.14×10^6 lbs/in² = 1044 kilobars (on average)

$$\therefore Y_2O_3 \text{ contribution} = 1044 - 1009/1.39 = 25.2 \text{ kilobars/mol \%}$$

Table XXVIII

Calculation of Young's Modulus from the Composition
by C. J. Phillips Method

Using known silica, alumina factors and new magnesia factor to derive lanthana and ceria factors

1. Based on Glass 138	<u>Constituent</u>	<u>Mol %</u>	<u>Kilobars/mol %</u>	<u>Contribution</u>
	SiO ₂	47.3	7.3	345
	Al ₂ O ₃	15.6	12.1	189
	MgO	28.9	14.7	425
	La ₂ O ₃	8.0	X	8.0X
				959+8.0X

Experimentally 138 = 16.5×10^6 lbs/in² = 1138 kilobars

$$\text{La}_2\text{O}_3 \text{ contribution} = 1138 - 959/8 = 22.4 \text{ kilobars/mol \%}$$

2. Based on Glass 117	<u>Constituent</u>	<u>Mol %</u>	<u>Kilobars/mol %</u>	<u>Contribution</u>
	SiO ₂	51.67	7.3	377
	Al ₂ O ₃	10.0	12.1	121
	MgO	18.33	14.7	269
	Ce ₂ O ₃	20.0	Y	20.0Y
				767+20Y

Experimentally 117 = 16.54×10^6 lbs/in² = 11.64 kg/cm² = 1138 kilobars

$$\therefore \text{contribution of ceria} = 1138 - 767/20 = 371/20 = 18.6 \text{ kilobars/mol \%}$$

Table XXIX

Using Known Molar Modulus Coefficients to Obtain Similar
Coefficients for Zinc and Zirconia

1. Based on UARL Glass 368	<u>Constituent</u>	<u>Mol %</u>	<u>Kilobars/mol %</u>	<u>Contribution</u>
	SiO ₂	39	7.3	284.7
	Al ₂ O ₃	12	12.1	145.2
	MgO	6	14.7	88.2
	ZnO	6	X	6X
	Ce ₂ O ₃	2	18.6	37.2
	BeO	25	19.0	475.0
	Y ₂ O ₃	10	24.3	243.0
				1273.3 kilobars

Experimentally Young's modulus for UARL Glass 368 is 19.08×10^6 lbs/in² = 1312 kilobars

$$\therefore \text{zinc oxide contribution} = \frac{1312 - 1273.3}{6} = 6.45 \text{ kilobars/mol \%}$$

2. Based on UARL Glass 27	<u>Constituent</u>	<u>Mol %</u>	<u>Kilobars/mol %</u>	<u>Contribution</u>
	SiO ₂	70.2	7.3	512.5
	Al ₂ O ₃	0.6	12.1	7.3
	CaO	0.6	12.6	7.6
	Na ₂ O	15.4	3.4	52.4
	K ₂ O	1.6	1.8	2.9
	ZnO ₂	11.6	X	1.6X
				582.7 kilobars

Experimentally Young's modulus for UARL Glass 27 is 11.52×10^6 lbs/in² = 794.3 kilobars

$$\therefore \text{zirconia contribution} = \frac{794.3 - 582.7}{11.6} = 18.2 \text{ kilobars/mol \%}$$

Table XXX
 Summary of All Experimentally Determined
 Molar Modulus Coefficients

<u>Oxide</u>	Contribution per mol % (kilobars)	<u>Oxide</u>	Contribution per mol % (kilobars)
SiO ₂	7.3	ZnO	1.75 & rises with R ₂ O increase
Al ₂ O ₃	12.1	ZrO ₂	18.9
CaO	12.6	MgO	12.0 & rises with R ₂ O decrease
Li ₂ O	7.0		& SiO ₂ decrease to 14.8
B ₂ O	7.2	Ce ₂ O ₃	18.6
TiO ₂	13.3	Y ₂ O ₃	24.3
BeO	19.0	La ₂ O ₃	22.4

Table XXXI
Comparison of Calculated and Experimentally
Determined Moduli

1. For UARL Glass 367	<u>Constituent</u>	<u>Mol %</u>	<u>Kilobars/mol %</u>	<u>Contribution</u>
	<chem>SiO2</chem>	39	7.3	284.7
	<chem>Al2O3</chem>	12	12.1	145.2
	<chem>MgO</chem>	12	14.7	166.4
	<chem>Ce2O3</chem>	2	18.6	37.2
	<chem>BeO</chem>	25	19.0	475.0
	<chem>Y2O3</chem>	10	24.3	243.0
				<u>1351.5 kilobars</u>

Converting the 1351.5 kilobars calculated to $\text{lbs/in}^2 = (1351.5) (14.54) = 19.66 \times 10^6 \text{ lbs/in}^2$. Experimentally the Young's modulus for this glass is $19.03 \times 10^6 \text{ lbs/in}^2$ or $0.63 \times 10^6 \text{ lbs/in}^2$ lower

2. For UARL Glass 370	<u>Constituent</u>	<u>Mol %</u>	<u>Kilobars/mol %</u>	<u>Contribution</u>
	<chem>SiO2</chem>	39	7.3	284.7
	<chem>Al2O3</chem>	12	12.1	145.2
	<chem>CaO</chem>	6	12.6	75.0
	<chem>ZnO</chem>	6	6.45	38.7
	<chem>Ce2O3</chem>	2	18.6	37.2
	<chem>BeO</chem>	25	19.0	475.0
	<chem>Y2O3</chem>	10	24.3	243.0
				<u>1298.8 kilobars</u>

Converting this result of 1298.8 kilobars calculated to $\text{lbs/in}^2 = (1298.8) (14.54) = 18.87 \times 10^6 \text{ lbs/in}^2$ experimentally, the Young's modulus for this glass is $18.5 \times 10^6 \text{ lbs/in}^2$ or $0.37 \times 10^6 \text{ lbs/in}^2$ lower

Table XXXII

Discrepancies Resulting When Young's Modulus for Calcium Aluminate Glasses are Calculated by C. J. Phillips Factors Derived from Silica Glass Systems

<u>Glass 96</u>	<u>Constituent</u>	<u>Gms</u>	<u>Weight %</u>	<u>Molecular Weight</u>	<u>Mols</u>	<u>Mol %</u>	<u>Kilobars</u>	<u>Mol %</u>	<u>Contribution</u>
	CaO	165.3	36.7	56.08	0.654	45.9	12.6	462	
	Al ₂ O ₃	185.0	41.2	101.94	0.463	28.3	12.1	498	
	MgO	25.0	5.6	40.31	0.139	9.8	14.7	144	
	ZrO ₂	24.9	5.5	123.22	0.045	3.2	18.9	61	
	SiO ₂	50.0	11.1	60.09	0.185	12.9	7.3	94	
									1259

But actual exp. value = 16.30×10^6 psi = 1148 kg/cm² = 1125 kilobars

∴ Have a large discrepancy indicating that factors for calcium aluminate glasses are appreciably lower

<u>Glass 93</u>	<u>Constituent</u>	<u>Gms</u>	<u>Weight %</u>	<u>Molecular Weight</u>	<u>Mols</u>	<u>Mol %</u>	<u>Kilobars</u>	<u>Mol %</u>	<u>Contribution</u>
	CaO	140.0	28.0	56.08	0.498	38.0	12.6	478	
	Al ₂ O ₃	210.0	42.0	101.94	0.412	31.4	12.1	380	
	MgO	25.0	5.0	40.31	0.124	9.5	14.7	140	
	ZrO ₂	24.9	5.0	123.22	0.046	3.5	18.9	66	
	SiO ₂	50.0	10.0	60.09	0.166	12.6	7.3	92	
	BaO	50.7	10.0	153.3	0.065	5.0	11.35	57	
					1.311				1213

But actual experimental value = 15.72×10^6 psi = 11.05×10^5 kg/cm² = 1083 kilobars

∴ Again have a large discrepancy indicating that factors for calcium aluminate glasses are appreciably lower. Discrepancy for 93 = 130 kilobars; for 96 = 134 kilobars

Since these values are consistent, this mode of calculation is probably just as valid for calcium-aluminate glasses as for silica glasses once the proper molar values are known.

Table XXXIII

Use of Phillips Type Calculations to Evaluate Literature
Claims on High Modulus Glasses

1. An interesting glass composition appearing in the report literature (Ref. 94) on high modulus glasses is

<u>Constituent</u>	<u>Weight %</u>	<u>Molecular Weight</u>	<u>Mol Fraction</u>	<u>Mol %</u>	<u>Kilobars/mol %</u>	<u>Contribution (kilobars)</u>
SiO ₂	50	60.06	0.833	50	7.3	365
Al ₂ O ₃	35	101.94	0.343	21	12.1	254
MgO	7.5	40.32	0.160	10	12.0	120
BeO	7.5	25.02	0.300	19	19.0	361

$$1090 \text{ kilobars} = 15.83 \times 10^6 \text{ psi}$$

But the literature claim for this glass is a Young's modulus of $20.0 \times 10^6 \text{ lbs/in}^2$ or 1378 kilobars. The above calculated value indicates that the value given in the literature must be reduced to 15.83 $\times 10^6$ psi for the bulk glass.

2. Similarly, an interesting high modulus glass composition appearing in the U.S. patent literature (Ref. 95) is

<u>Constituent</u>	<u>Weight %</u>	<u>Molecular Weight</u>	<u>Mol Fraction</u>	<u>Mol %</u>	<u>Kilobars/mol %</u>	<u>Contribution (kilobars)</u>
SiO ₂	47.3	60.06	0.788	53.9	7.3	393
Al ₂ O ₃	35.8	101.94	0.351	24.1	12.1	290
Fe ₂ O ₃	0.9	159.70	0.006	0.41	13.3	5.5
Na ₂ O(K ₂ O)	1.2	61.98	0.019	0.13	3.4	0.4
TiO ₂	0.1	79.90	0.001	0.07	13.3	0.9
ZnO ₂	4.2	123.22	0.034	2.43	18.9	45.9
MgO	10.5	40.32	0.261	17.9	12.0	214

$$949.7 \text{ kilobars}$$

But the literature claim for this glass is a Young's modulus of $28.0 \times 10^6 \text{ lbs/in}^2$ or 1915 kilobars. The above calculated value indicates that this literature must be reduced to about $13.8 \times 10^6 \text{ lbs/in}^2$ or approximately half. When this glass is melted in the UARL laboratory and measured, values obtained agree with the calculation and not the literature claim.

where i designates a given ionic species, M is the molar formula weight of the material, ρ is its density, v_i is the volume of ionic species i , n_i is the number of ions of species i per molar formula of material and N is Avogadro's number.

For convenience, instead of considering individual ions, it can be assumed that the material is composed of j component oxides (e.g. Al_2O_3 , SiO_2 , etc.). Then in terms of weight fractions, x_j , of component j in the material, the f factor is given by

$$f = \rho \sum_i x_j \frac{Nv_j}{M_j} = \rho \sum x_j g_j$$

Typical g_j factors for various oxide components computed in this manner are 0.298 for B_2O_3 , 0.280 for BeO , 0.267 for Li_2O , 0.233 for SiO_2 , 0.189 for MgO , 0.183 for TiO_2 , 0.166 for CaO , and 0.123 for ZrO_2 . It will be noted immediately that these factors place even greater emphasis on low atomic number materials than do those of C. J. Phillips. It is also immediately apparent that in some cases these factors directly contradict those of Phillips; for example, the g_j factors for BeO and B_2O_3 are virtually identical while Phillips finds a molal contribution of only 7.3 kilobars/mol % contrasted to 19.8 kilobars/mol % for BeO .

The tabulation below shows the computation for two calcium aluminate glasses using S. D. Brown's coefficients. Unfortunately, the calculated results are not in concordance with the experimental results also taken from S. D. Brown's report. Because the experimental modular data of Brown are based on hand-drawn fibers, one cannot say with any degree of assurance whether the method of calculation has failed. However, the method of Phillips seems to be the better choice for calculating Young's modulus from compositional factors at this time.

Discrepancies resulting when calcium aluminate glasses are calculated by packing efficiency considerations of S. D. Brown. -

Calcium Aluminate Glass with Measured $\rho = 3.19$ gms/cm³
and $E = 16.7 \times 10^6$ psi

Oxide	Weight %	g_j	$x_j g_j$	
CaO	19.4	0.166	0.03224	$\rho \sum x_j g_j = 0.5606$
MgO	2.3	0.189	0.00435	= ionic volume fraction
BaO	8.8	0.086	0.00755	
Na ₂ O	2.4	0.181	0.00328	Calculated E
Al ₂ O ₃	48.8	0.209	0.10180	= (59.5)(0.561)-20.4
TiO ₂	4.6	0.183	0.00842	= 33.38 - 20.4
ZrO ₂	11.8	0.123	0.01453	= 13.0 x 10 ⁶ psi
K ₂ O	1.8	0.199	0.00358	
			0.17575	

S. D. Brown's R-105 Glass Has A Measured $\rho = 2.90 \text{ gms/cm}^3$
and $E = 16.0 \times 10^6 \text{ psi}$ Measured On Hand-Drawn Fibers

Oxide	Weight %	g_j	$x_j g_j$	
Al_2O_3	44.0	0.209	0.0920	$\rho \sum x_j g_j = 0.545$
SiO_2	3.5	0.233	0.0082	Calculated E
CaO	48.8	0.166	0.0810	$= (59.5) (0.545) - 20.4$
MgO	3.5	0.189	<u>0.0066</u>	$= 32.43 - 20.4$
			0.1878	$= 12.4 \times 10^6 \text{ psi}$

In comparison with Table XXXII where similar calculations are made by method of C. J. Phillips, the discrepancies calculated by the packing efficiency method are much larger as well as too low in place of too high. The consistency of the differences again indicates hope that the method can be made to work for calcium aluminate glasses when the correct factors have been determined.

Summary of progress in developing high modulus glasses at UARL. - The culmination of the kinetics of crystallization research and of the extension of the C. J. Phillips mode of calculations detailed in this report has been the origination of a number of cordierite and/or beryl base rare-earth glasses with unusually high moduli. The more outstanding results of this research are summarized in Table XXXIV. All the data for such glasses as well as all other UARL glasses is summarized in Tables XXXV and XXXVI.

An equally novel series of glass systems are those due to Stevles (Ref. 93) and called by him "invert" glasses. These glasses are glasses that do not conform with the Zachariasen three-dimensional network concept which states that at least three corners of each silica tetrahedron is shared so that not more than one corner is shared by a nonbridging oxygen ion, a concept obeyed in general by most commercial silicate glasses used for windows, plate glass, containers, and glass fibers. Stevles introduces a parameter Y_c to express the average number of bridging ions per SiO_4 tetrahedron where

$$Y_c = 6 - 200/P \quad P = \text{mol \% SiO}_2$$

so that when $P = 33 \frac{1}{3}$, $Y = 0$ and the SiO_4 groups are isolated; when $P = 40\%$, $Y = 1$ and on the average SiO_4 groups appear in pairs. These glasses possess the very interesting characteristic that most properties such as viscosity pass through a minimum at $Y = 2$, i.e. 50 mol % SiO_2 . A typical example cited by Stevles is 50 mol % SiO_2 and 12.5 mol % of each of Na_2O , K_2O , Ca, BaO. Dr. Stevles explains this "anomalous" case of glass formation by saying "choosing a batch with a great number of network modifiers the 'glue' between the chains is so irregular that crystallization is prevented."

Table XXXIV

Best Glasses to Date from Cordierite-Rare Earth
and Cordierite-Beryl-Rare Earth Systems

	<u>Glass Number</u>	Young's Modulus (millions psi)	Specific Modulus (millions inches)
No BeO	125	16.1	161
	337	20.9	147
	363	19.3	150
With BeO	345	21.1	174
	344	20.3	168
	323	18.4	184
Compared with	X-2285	14.95	167
	Steel	29	103
	Molybdenum	52	141

Table XXXV

Summary of All Values for Young's Modulus Measured
on Circular Rods Formed Directly from Melt

Glass Number	Density lbs/in ³	Young's Modulus millions psi	Specific Modulus 10 ⁷ in.	Glass Number	Density lbs/in ³	Young's Modulus millions psi	Specific Modulus 10 ⁷ in.
40-3 ³	0.1076	15.5	14.5	194	0.1618	14.7	9.2
62-3 ³	0.0989	14.2	16.2	219	0.1072	14.8	13.8
67-3 ³	0.0957	14.4	15.0	222	0.1620	14.8	9.1
68-3 ³	0.0950	14.1	14.8	231 ³	0.1240	18.05	14.55
69-3 ³	0.0935	14.2	15.2	232 ³	0.1297	18.1	13.9
72-2 ³	0.1043	14.0	13.4	233 ³	0.1093	15.86	14.5
83 ²	0.1026	16.0	15.6	234 ³	0.1338	18.1	13.5
96	0.1071	16.33	15.24	235 ³	0.1203	17.4	14.4
96-2	0.1057	15.4	14.6	236 ³	0.1249	17.8	14.3
97	0.1027	15.5	15.1	237 ³	0.1203	18.3	15.2
99 ¹	0.1152	10.5	9.12	238 ³	0.1098	16.6	15.1
102 ¹	0.1050	15.0	14.3	247 ¹	0.1078	15.1	14.0
108 ¹	0.1133	14.8	13.1	248 ¹	0.1118	15.7	14.0
110 ³	0.0939	14.6	15.5	249 ¹	0.1887	15.9	14.6
114 ³	0.1163	16.7	14.4	250 ¹	0.1561	14.8	9.47
125 ³	0.1000	16.1	16.1	251 ¹	0.1108	15.9	14.3
126 ³	0.1250	16.8	13.4	252 ¹	0.1108	14.9	13.5
127 ³	0.1173	16.1	13.7	253 ¹	0.1172	12.3	10.5
129 ³	0.1193	16.5	13.8	256 ¹	0.1296	17.9	13.8
131 ³	0.1132	14.0	13.5	257 ¹	0.1347	18.4	13.7
134 ³	0.1107	15.4	13.9	258	0.0978	13.5	13.7
135 ³	0.0946	14.3	15.1	259	0.1043	13.2	12.6
136 ³	0.1012	14.4	14.2	263 ³	0.1447	14.5	10.0
137 ³	0.1113	13.3	12.0	265 ¹	0.1439	16.3	11.3
138 ³	0.1282	15.3	12.0	266 ¹	0.1153	16.7	14.5
140 ³	0.1329	15.6	11.7	267 ^{1,2}	0.0976	15.3	15.7
151	0.1175	16.9	14.4	268 ¹	0.1155	16.9	14.6
155 ³	0.1282	15.7	12.2	269 ¹	0.1242	17.2	13.8
157 ³	0.0972	13.3	13.7	270 ¹	0.1275	20.3	15.9
159 ³	0.1163	16.2	13.9	273-1 ^{1,2}	0.0988	18.4	18.6
166 ³	0.0946	12.5	13.2	273-2 ^{1,2}	0.0988	17.2	17.4
174 ³	0.1253	16.5	13.2	274 ^{1,2}	0.1077	17.2	15.9
175 ³	0.1152	16.1	14.0	275-1 ^{1,2}	0.1318	16.7	12.7
176 ³	0.1137	15.2	13.4	275-2 ^{1,2}	0.1318	16.8	12.7
179 ³	0.1553	14.9	9.6	276 ^{1,2}	0.1227	15.8	12.9

Table XXXV (Cont'd)

Glass Number	Density lbs/in. ³	Young's Modulus millions psi	Specific Modulus 10^7 in.	Glass Number	Density lbs/in. ³	Young's Modulus millions psi	Specific Modulus 10^7 in.
277 ^{1,2}	0.1413	17.9	12.6	320	0.1057	16.0	15.1
278	0.0942	13.3	13.6	321 ³	0.1313	18.7	14.2
278 ⁴	0.0942	15.2	16.1	322 ^{1,2}	0.1080	16.9	15.65
279	0.0972	12.4	12.7	323 ^{1,2}	0.0999	18.4	18.4
280	0.0742	5.56	7.5	324 ^{1,2}	0.1072	17.8	16.6
280 ⁴	0.0742	6.23	8.40	325 ^{1,2}	0.1280	20.2	15.8
281	0.0871	6.77	7.77	326 ^{1,2}	0.1115	17.0	15.3
282	0.0798	4.80	6.00	327 ¹	0.1330	18.4	13.8
282 ⁴	0.0798	6.22	7.80	328 ¹	0.1578	18.5	11.7
283 ¹	0.1313	15.5	11.8	329 ¹	0.1095	20.7	18.9
284 ¹	0.1200	14.9	12.4	330 ^{1,2}	0.1462	18.6	12.7
285 ¹	0.1322	15.1	11.4	331 ^{1,2}	0.1322	20.9	15.8
286 ¹	0.1368	15.6	11.4	331A ²	0.1310	20.07	15.35
287 ¹	0.1308	15.1	11.5	332 ¹	0.1528	17.3	11.3
288 ¹	0.1303	14.3	11.0	333 ¹	0.1338	18.9	14.1
289 ¹	0.1407	15.0	10.7	334 ¹	0.1422	17.5	12.3
290 ¹	0.1172	14.5	12.3	335 ^{1,2}	0.1392	19.0	13.6
291 ¹	0.1200	15.7	13.1	336 ^{1,2}	0.1265	21.0	16.6
292 ¹	0.1322	15.4	11.6	337 ¹	0.1423	20.9	14.7
293 ¹	0.1187	16.0	13.5	338 ¹	0.1508	----	----
294 ¹	0.1217	17.6	14.4	339 ^{1,2}	0.1500	19.4	13.0
295 ¹	0.1152	15.2	13.2	340 ^{1,2}	0.1283	20.9	16.3
296 ¹	0.1187	16.5	13.9	341 ^{1,2}	0.1413	18.9	13.4
297 ¹	0.1278	17.1	13.4	342 ^{1,2}	0.1322	----	----
299 ¹	0.1150	14.6	12.7	343 ^{1,2}	0.1383	19.4	14.0
300 ¹	0.1042	14.5	13.9	344 ^{2,3}	0.1193	20.3	17.0
302 ¹	0.1358	17.2	12.6	345 ^{2,3}	0.1208	21.1	17.45
304 ³	0.1307	19.65	15.2	346 ^{1,2}	0.1282	17.66	13.8
305 ³	0.1320	17.7	13.4	347 ^{1,2}	0.1312	21.6	16.4
306 ³	0.1322	18.9	14.3	348 ^{1,2}	0.1317	17.7	13.4
309 ^{1,2}	0.1296	16.9	13.0	349 ^{1,2}	0.1273	16.8	13.2
310 ^{1,2}	0.1327	16.7	12.6	350 ^{1,2}	0.1006	19.8	19.7
311 ^{1,2}	0.1337	15.9	11.1	351 ^{1,2}	0.1003	17.0	17.0
312 ^{1,2}	0.1183	16.5	14.0	352 ^{1,2}	0.1368	20.0	14.6
314 ¹	0.1342	17.0	12.6	353 ^{1,2}	0.1413	19.4	13.7
315 ^{1,2}	0.1293	16.6	12.8	354 ^{1,2}	0.1288	18.4	14.3
316 ^{1,2}	0.1373	16.5	12.0	355 ³	0.1365	18.1	13.2
317 ^{1,2}	0.1375	16.3	11.9	356 ³	0.1210	13.9	11.5
318 ^{1,2}	0.0978	16.0	16.4	357 ³	0.1222	17.6	14.4
319	0.1310	17.9	13.7	358 ³	0.1257	13.1	10.4
				359 ³	0.1337	17.6	13.2

Table XXXV (Cont'd)

Glass Number	Young's Modulus Specific				Glass Number	Young's Modulus Specific			
	Density gms/cm ³	Density lbs/in ³	millions psi	Modulus 10 ⁷ in.		Density gms/cm ³	Density lbs/in ³	millions psi	Modulus 10 ⁷ in.
356A	3.3158	0.1193	13.9	11.63	388	3.5767	0.1293	17.28	13.38
360	3.5183	0.1269	18.5	14.6	389	3.4540	0.1247	17.2	13.80
361	3.4989	0.1260	18.6	14.8	390B	3.3462	0.1210	16.80	13.88
362	3.4997	0.1260	18.0	14.3	391A	3.3062	0.1193	17.38	14.57
363	3.5680	0.1289	19.26	14.9	392	3.5920	0.1298	16.24	12.52
364	3.0985	0.1120	16.70	14.9	393	3.6019	0.1303	16.46	12.63
365	3.5453	0.1281	19.04	14.9	394	3.3024	0.1195	16.59	13.87
366	3.4697	0.1255	16.19	12.9	395	3.7273	0.1348	16.00	11.86
367	3.5310	0.1277	19.03	14.9	396	3.2443	0.1175	15.15	12.87
368	3.6229	0.1320	19.08	14.4	398	3.2622	0.1182	16.30	13.87
369	3.5272	0.1277	17.78	13.9	399	3.3742	0.1219	16.89	13.85
370	3.6285	0.1320	18.59	14.15	400	3.3266	0.1204	15.78	13.11
371	3.5664	0.1289	18.54	14.4	401	3.3031	0.1196	16.76	14.04
372	4.0747	0.1473	17.34	11.8	402	3.3063	0.1198	17.77	14.85
373	3.4937	0.1262	19.00	15.05	403	3.3728	0.1220	17.17	14.05
373A	3.4937	0.1262	22.0	17.35	404	3.5661	0.1292	18.13	14.04
374	3.4276	0.1238	19.00	15.45	405	3.7262	0.1350	19.74	14.63
374A	3.4276	0.1238	19.15	15.5	406	4.3956	0.1590	17.69	11.12
375	3.6819	0.1333	16.58	12.42	407	3.6398	0.1312	18.10	13.80
375A	3.6819	0.1333	15.73	11.8	408	3.8661	0.1393	18.32	13.13
376	3.6820	0.1334	15.80	11.85	409	4.0420	0.1457	19.16	13.16
376R	3.6820	0.1334	15.75	11.79	410	3.6381	0.1311	18.23	13.87
377	3.6108	0.1304	15.62	11.96	411	3.7073	0.1340	18.00	13.45
377R	3.6108	0.1304	15.02	11.53	412	4.0954	0.1477	17.92	12.13
378	3.2971	0.1192	---	---	413	3.4375	0.1239	19.13	15.43
378A	3.1701	0.1147	14.4	12.55	414	3.8764	0.1402	18.73	13.37
379	3.1448	0.1137	17.3	15.22	415	3.2899	0.1186	20.57	17.35
380	3.7107	---	15.7	---	416	3.2877	0.1193	19.61	16.4
381	2.9591	0.1063	15.87	14.9	417	3.0915	0.1121	19.35	17.25
382	3.0054	0.1082	17.7	16.32	418	3.0884	0.1121	19.31	17.18
383	3.1418	0.1136	22.75	20.02	419	3.2665	0.1185	20.15	17.0
384	3.8927	0.1407	18.62	13.23	420	3.3605	0.1220	19.50	16.13
385	2.8006	0.1011	---	---	421-spe	3.3370	0.1208	20.72	17.15
386	3.3705	0.1218	---	---	421	3.3356	0.1208	20.37	16.85
387	3.2777	0.1183	17.85	15.08	422	3.3222	0.1207	20.58	17.05

Table XXXV (Cont'd)

Glass Number	Young's Modulus Specific				Young's Modulus Specific				
	Density gms/cm ³	Density lbs/in ³	millions psi	Modulus 10 ⁷ in.	Glass Number	Density gms/cm ³	Density lbs/in ³	millions psi	Modulus 10 ⁷ in.
423	3.4505	0.1252	20.68	16.47	458	3.2094	0.1158	15.23	13.15
424	3.0401	0.1103	19.51	17.7	459	3.4538	0.1242	17.34	13.95
425	2.7355	0.0990	19.51	19.7	460	3.3785	0.1215	16.83	13.84
426	3.4378	0.1248	20.56	16.45	461	3.0354	0.1092	14.80	13.54
427	3.1550	0.1146	15.69	13.72	462	3.3294	0.1198	16.46	13.72
428	3.2284	0.1164	18.20	15.64	463	3.4296	0.1235	17.50	14.15
429	3.2496	0.1172	---	---	464	3.0700	0.1105	16.07	14.55
430	4.3482	0.1570	19.34	12.33	465	3.3184	0.1193	16.67	13.95
431	4.2720	0.1540	19.65	12.76	466	3.0731	0.1108	15.85	14.32
432	3.7345	0.1345	19.28	14.35	267A	2.7322	0.0976	16.50	---
433	3.6325	0.1308	19.12	14.65	461 cry.	3.3823	0.1218	26.0	21.3
434	3.5304	0.1273	19.43	15.35	SFS1	---	---	6.98	---
435	3.4605	0.1247	20.36	16.33	SF6	---	0.1868	6.91	3.69
436	3.4461	0.1240	19.90	16.05	LASF3	---	0.177	13.3	7.52
437	3.5067	0.1265	19.41	15.35	LASF6	---	0.2207	17.4	7.88
438	3.2348	0.1165	18.25	15.65	X-2285	---	0.0878	13.35	15.2
439	3.3510	0.1207	19.95	16.55	SiO ₂	---	0.079	10.5	13.3
440	3.3426	0.1203	19.72	16.37	"E"	---	0.092	10.5	11.4
441	3.2739	0.1181	19.52	16.52	"S"	---	0.090	12.6	14.0
442	3.5959	0.1297	20.02	15.45	Steel	---	0.280	29	10.3
443	3.6695	0.1326	20.10	15.17	Al ₂ O ₃	---	0.114	25	21.9
444	3.5011	0.1263	19.33	15.35	ZrO ₂	---	0.175	50	28.6
445	3.4488	0.1245	17.61	14.14	BN	---	0.069	13	18.8
446	3.5049	0.1263	20.01	15.85	MO	---	0.369	52	14.1
447	3.2975	0.1188	18.23	15.35					
448	3.5173	0.1268	16.91	13.34					
449	3.3944	0.1223	18.08	14.80					
450	3.3598	0.1212	17.78	14.65					
451	3.5527	0.1280	---	---					
452	3.6114	0.1302	---	---					
453	3.6837	0.1327	---	---					
454	3.6142	0.1303	18.93	14.53					
455	3.2860	0.1186	15.96	13.46					
456	3.2099	0.1158	15.02	13.00					
457	3.1765	0.1144	15.93	13.89					

¹Invert analog glasses²Contains BeO³Cordierite base glasses⁴Heat treated two phase

Table XXXVI

Summary Extended, All Values for Young's Modulus
Measured on Square Rods Cut from Plates
by Optical Equipment

<u>Glass No.</u>	<u>Young's Modulus</u> <u>millions psi</u>	<u>Glass No.</u>	<u>Young's Modulus</u> <u>millions psi</u>
1	14.86	68	15.36
4	14.94	70	15.23
14	15.07	72-2	15.15
24	10.67	72-3	15.14
26	10.18	73-2	15.13
27	11.53	76	11.51
29	14.02	77	12.16
41	10.83	93	15.72
42	10.82	96	16.30
43	10.27	97	10.86
45	11.08	98	10.62
46B	10.40	99	11.37
47	11.07	114	16.5
47B	11.62	117	16.54
48B	11.28	138	16.53
49B	10.77	191	15.35
50	11.10	192	14.06
50B	10.83		
51	11.75		
52	10.87		
63	14.71		
64	15.57		
64(rep)	14.78		
65	15.20		
66	15.14		

Using a modified version of Dr. Stevels concept, UARL has originated many glasses which we call "invert analog" glasses. In these, the UARL glasses contain only one alkali oxide usually lithia and a combination of alkaline earth oxides and trivalent and tetravalent oxides. A typical example of the UARL invert analog glass systems in UARL 270 whose composition in mole percent is 25 SiO₂, 15 Li₂O, 15 CaO, 15 ZnO, 15 MgO, 8 Al₂O₃ and 7 Y₂O₃. The best of the invert analog glasses originated to date are those shown in Table XXXVII. All such glasses are shown in Table XXXVI.

UARL experimental glass research may be summarized in a somewhat different manner. NASA contracts 1301 and 2013 have enabled UARL to prepare approximately 500 new glass compositions. Of these, a total of a dozen compositions have values for Young's modulus measured on bulk specimens greater than twenty million pounds per square inch and another two dozen have values between nineteen and twenty million pounds per square inch. The best of these has a Young' modulus for bulk specimens of 22 3/4 million psi.

A computer program for the calculation of Young's modulus on bulk glass samples. - A technique for the determination of the elastic modulus of a material in the form of a cylinder requires the determination of the resonant frequency of the specimen. This technique as discussed by Pickett (Ref. 88) has been used with a computer program to perform the calculations.

The determination of the elastic modulus simply requires the evaluation of the following expression:

$$E = (C) (\text{weight}) (\text{resonant frequency})^2.$$

The constant C is evaluated according to the expression

$$C = 0.0041632 (L/D)^3 T$$

with the parameter T evaluated for the diameter and length of the specimen according to

$$T = 1.0 + 81.79(D/2L)^2 - (1314(D/2L)^4)/(1 + 81.09(D/2L)^2) - 125(D/2L)^4.$$

For this calculation, Poisson's ratio has been taken as 1/6, and the factors T and C are those which yield an approximate solution to the differential equations for transverse vibrations as determined by Goens.

In addition to the straightforward calculation, a feature of the program used is a subroutine which can be used to sort the output data in terms of any desired parameter, such as sample diameter. With this feature, checks for systematic variations in calculated modulus values with a chosen parameter can easily be made. The program itself is written in FORTRAN IV for use with a time-shared computing system. The Research Laboratories provides this capability by either an in-house PDP-6 (Digital Equipment Corp.) computer, or by subscription to the General Electric time-shared computing system.

Table XXXVII
 Best Glasses to Date from Invert
 Analog Systems

	<u>Glass Number</u>	<u>Young's Modulus (millions psi)</u>	<u>Specific Modulus (millions inches)</u>
No BeO	383	22.75	200
	329	20.7	189
With BeO	373	22.00	173
	350	19.8	197
	331	20.9	158
Compared with	X-2285	14.95	167
	Steel	29	103
	Molybdenum	52	141

CCCC PROGRAM TO CALCULATE GLASS BULK MODULUS BY THE FORMULATION OF PICKETT
 CCC INPUT DATA GLASS IDENTIFICATION, WEIGHT IN GRAMS, DIAMETER
 CCC IN INCHES, LENGTH IN INCHES, RESONANT FREQUENCY IN KILOCYCLES
 CCC
 CCC
 DIMENSION DIA(50),WT(50),RF(50), E(50)
 DIMENSION INDEX(50)
 REAL LE
 ALPHA TITLE
 DIMENSION TITLE(10), LE(50)
 READ("PICKVAL",81)NTOT,TITLE
 81 FORMAT(5X,13,10A4)
 READ("PICKVAL",85)(WT(N),DIA(N),LE(N),RF(N), N=2,NTOT)
 85 FORMAT(5X,4F10.4)
 NN = NTOT -1
 DØ 50 N=2,NTOT
 M = N-1
 INDEX(M) = M; WT(M)=WT(N); DIA(M)=DIA(N);LE(M)=LE(N);RF(M)
 & = RF(N)
 50 CONTINUE
 DØ 55 N = 1,NN
 A = DIA(N)/(2.*LE(N))
 T=1. + 81.79*A**3 - 131.4*A**4/(1. + 81.09*A**2) -
 & 125.*A**4
 C = 0.004163/DIA(N) * (LE(N)/DIA(N))**3 * T
 E(N) = C * (WT(N)/453.59) * RF(N)**2
 55 CONTINUE
 CALL SORT(DIA, NN, INDEX)
 PRINT 123, TITLE
 123 FORMAT(1H , 10X,10A4)
 PRINT," "
 PRINT," J L DIA LENGTH WEIGHT FREQ
 & MODULUS"
 DØ 501 J=1,NN
 L = INDEX(J)
 PRINT 135,J,L,DIA(J),LE(L),WT(L),RF(L),E(L)
 501 CONTINUE
 135 FORMAT(1H ,2I3,3F10.4,2F14.4)
 STOP; END
 SUBROUTINE SORT(A, NPINTS,INDEX)
 CCC INDEX IS FILLED WITH INDEXING INTEGERS FROM 1 TO NPINTS
 CCC ARRAY IS BROUGHT IN AS A SINGLY SUBSCRIPTED ARRAY
 DIMENSION A(50),INDEX(50)
 M = NPINTS
 1 M = M/2
 IF (M .EQ. 0) RETURN
 K = NPINTS - M
 J = 1

```
2 I = J
3 IM = I + M
   IF (A(I) - A(IM)) 5,5,4
CCC SWITCH VALUES AND ARRANGE INDEX ARRAY
4 SAV = A(I); NSAV = INDEX(I)
   A(I) = A(IM); INDEX(I) = INDEX(IM)
   A(IM) = SAV ; INDEX(IM) = NSAV
   I = I - M
   IF (I .GE. 1) G0 T0 3
5 J = J+1
   IF ( J-K ) 2,2,1
END
```

CHARACTERIZATION OF EXPERIMENTAL GLASSES III.
YOUNG'S MODULUS FOR GLASS FIBERS

The Uselessness of Data Based on Hand-Drawn Fibers

Originally, it was felt that the hand-drawn fibers produced in the fiberizability test of bulk glasses could be used for the evaluation of the properties of glass fibers. It quickly became evident, however, that no matter how carefully hand-drawn fibers were prepared, they tended to show a distorted elliptical cross-section. In Fig. 56 (top) the least distorted hand-drawn fibers obtained are shown in cross-section in contrast with a 3 mil platinum wire (white) and in Fig. 58 (bottom) the most distorted hand-drawn fiber specimens encountered are shown. The distortion is so great as to make it impossible to obtain a meaningful value for the average cross-section of such fibers and this fact made the values of Young's modulus deduced by dead-weight mechanical testing procedures extremely untrustworthy. Despite this fact, many of the previous investigators have published such data leaving the available literature with a very confusing collection of data. UARL published similar data in the fifth quarterly report on this contract and we are now convinced that these values are largely meaningless.

Mechanical Drawing of Glass Fibers from An Orifice

The above problems encountered in attempting to obtain a reliable value for Young's modulus on hand-drawn fibers made it quickly obvious that it was time to switch to mechanical drawing of the experimental glass fibers. Normally this is done by purchasing massive platinum-rhodium bushings of proven design. But in our case several bushings would be necessary since the experimental glass compositions vary so widely that the lifetime of such a bushing might be very limited. Several such bushings would represent an expenditure for materials three to four times as great as the program material cost to date. Fortunately, it has proven possible using the platform furnace to substitute a relatively inexpensive 20 cc platinum crucible for the platinum bushings customarily employed. To make this substitution it was necessary to reinforce the bottom of the platinum crucible in a small central area by welding foil to the crucible until a thickness of 3/16 in. was obtained. This central area was then tapered reamed to form an orifice 0.088 in. at top, 0.063 in. at bottom and 3/16 in. long. In addition, water cooling almost directly beneath the crucible had to be introduced into the furnace as well as a ring orifice arrangement for cooling the fiber as it forms with helium jets. This equipment has now been extensively tested and proven to yield glass fiber that is very close to circular, approximately one mil in diameter when pulling speeds of 4000 ft/min are employed, and suitable for improved modulus determinations. The equipment arranged for mechanical drawing of fibers is shown in Fig. 59.

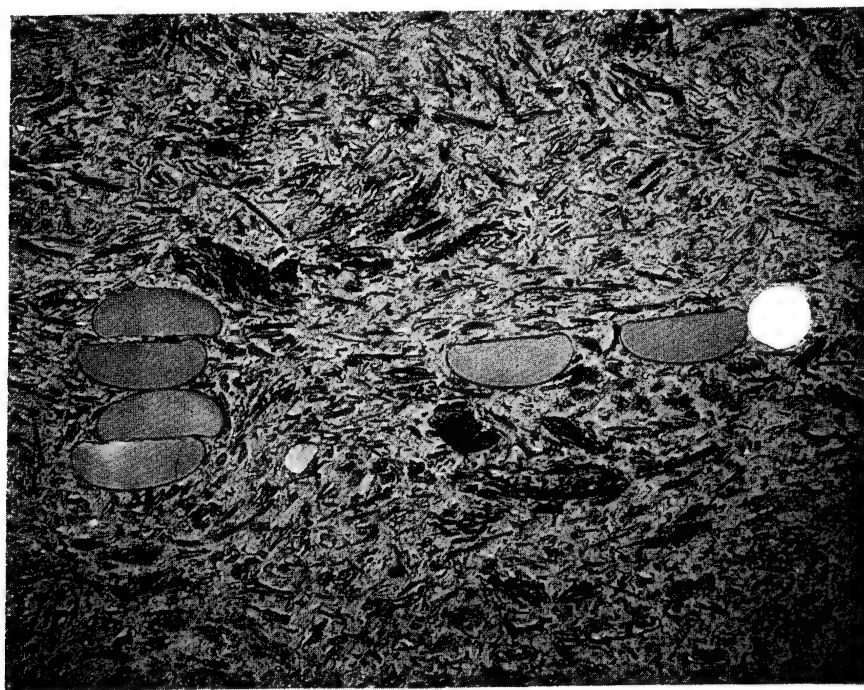
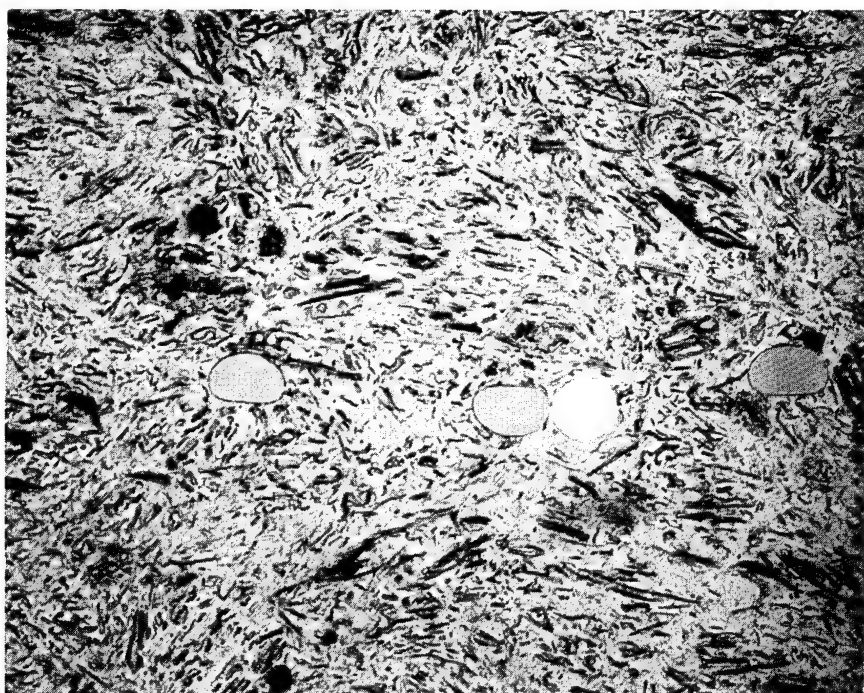
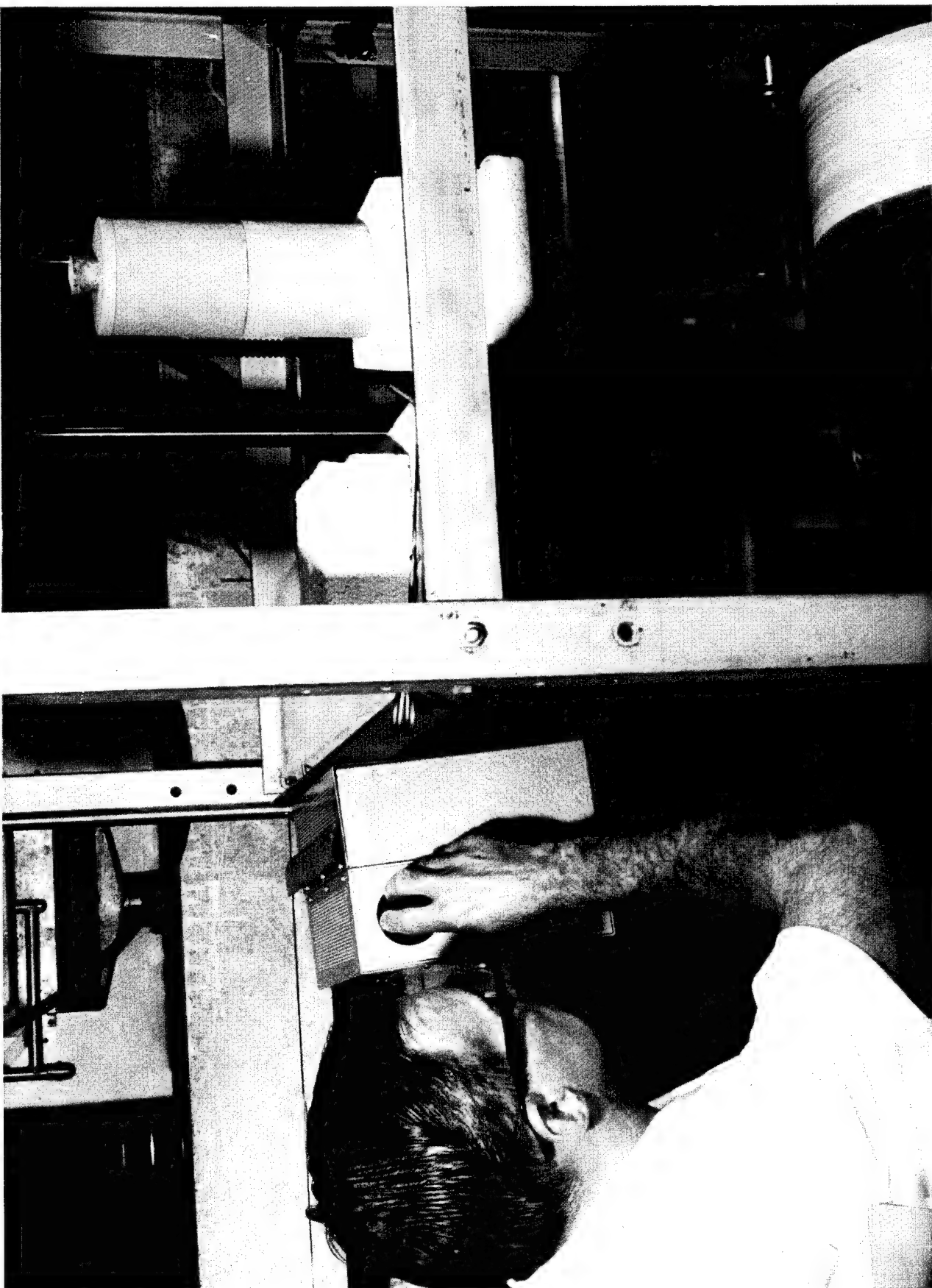


FIGURE 58. CROSS-SECTIONS OF HAND-DRAWN GLASS FIBERS SHOWING THE LEAST AND THE MOST DEPARTURE FROM CIRCULAR CROSS-SECTION COMPARED TO A PLATINUM WIRE (WHITE DOT).
100X IN ORIGINAL PHOTOGRAPH

FIGURE 59. PLATFORM KILN IN USE FOR MECHANICALLY DRAWING GLASS FIBERS



The improvement in the roundness of the glass fibers which resulted by mechanical drawing is shown in Figs. 60 and 61 where again the white specimen is a 3 mil platinum wire in cross-section. It is further obvious that much finer fibers can be drawn mechanically than were achieved by hand-drawing. The degree of circularity achieved in the mechanical drawing process is best realized by examining Table XXXVIII where typical microscopic measurements of the diameter of given samples are listed for each 45° rotation of the sample. This degree of roundness achieved is sufficient to eliminate departure from circularity as a source of error in modulus evaluation.

Young's Modulus Measurements

Young's modulus of the experimental glass fibers produced at UARL have been measured by both static and dynamic methods in general. The static or mechanical evaluations were carried out for UARL by the Lowell Institute of Technology. In carrying out these tests, Lowell Institute of Technology used an Instron CRE tester operated with a machine speed of 0.2 inches per minute, a chart speed of 20 inches per minute, a gage length of 5 inches and a full scale capacity of 1.0 pound. The specimens were held in air actuated clamps with flat rubber coated faces. For each experimental composition, a minimum of 20 fiber specimens were taken from approximately the center portion of the spool. The specimens were 8 inches long with about one yard of fiber being discarded between each specimen and in general the specimens selected represent the middle twenty yards of the fiber supplied to Lowell Institute of Technology for testing. Three fiber diameter measurements were made in the middle three-inch portion of each eight-inch specimen. The measurements were made using a monocular microscope equipped with an eyepiece reticule and operated with a magnification of 774 (18X eyepiece, 43X objective). Each reticule division was equal to 0.092 mils.

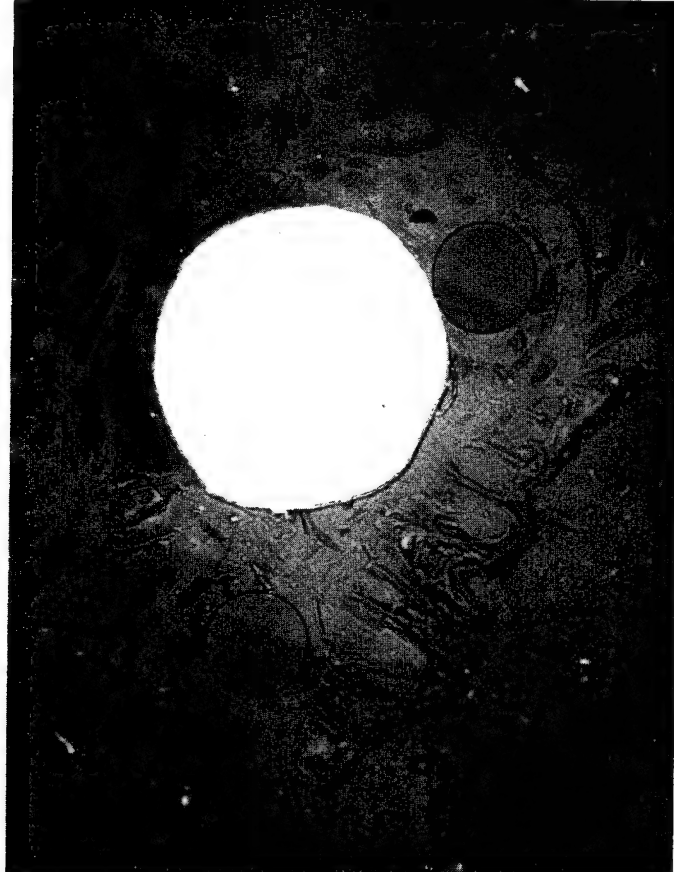
The calculation of the modulus was made by computer program. Typical standard deviations found in these measurements are shown in Table XXXIX for five glass compositions picked at random. It will be noted that the standard deviations for the dynamic method vary from 2.1 to 3.7 million pounds per square inch.

The dynamic measurements of UARL's experimental glass fibers were carried out for UARL by Panametrics, Inc., a subsidiary of the Esterline Corporation located in Waltham, Mass. To make these measurements, Mr. Kenneth Fowler of Panametrics, Inc. used a thin-line ultrasonic technique. His write-up states that "ultrasonic extensional and torsional waves are readily generated in thin-wire transmission lines by means of magnetostriction. The velocities of these two wave types are related to the elastic moduli by the formulas given in Fig. 62. A typical experimental arrangement for making modulus determinations by means of thin-line ultrasonics is shown in block form in Fig. 63 reproduced from Panametrics write-up of the method (Ref. 97). Typically, the diameter of the lead-in wire is about 20 mils. Because the diameter of the fiber is much less, in this case about 0.3 mil, then the lead-in line it is necessary to match the mechanical impedance of the two members in some way. This may be accomplished by tapering the lead-in to more



MAGNIFICATION: 500X

FIGURE 60. PRONOUNCED DECREASE IN SIZE AND IMPROVEMENT IN CIRCULARITY
OF MACHINE DRAWN FIBERS



MAGNIFICATION 500X

FIGURE 61. PRONOUNCED DECREASE IN SIZE AND IMPROVEMENT IN CIRCULARITY OF MACHINE DRAWN FIBERS

Table XXXVIII

Circularity Checks on Mechanically Drawn Glass Fibers

Specimens were checked for roundness by rotating under a microscope, readings were made approximately 45° apart. All measurements are in mils.

Glass Fiber 70-3		Glass Fiber 72-3		
<u>Specimen A</u>	<u>Specimen B</u>	<u>Specimen A</u>	<u>Specimen B</u>	<u>Specimen C</u>
1.98	1.94	1.36	2.15	4.87
1.93	1.93	1.34	2.13	4.87
1.96	1.96	1.34	2.12	4.87
1.98	1.94	1.34	2.13	4.86
1.95	1.95	1.39	2.12	4.89
1.94	1.98	1.36	2.15	4.87
1.93	1.98	1.30	2.13	4.83
1.98	1.99	1.34	2.13	4.84

Table XXXIX

Typical Standard Deviations Found in Static Tensile Measurements of Young's Modulus of Glass Fibers

<u>Glass Number</u>	<u>Average Value</u>	<u>Standard Deviation</u>
275-10	15.93	2.2
349	16.9	2.1
367	17.5	3.7
371	18.4	2.3
405	18.7	2.2

$$E = \frac{V_o^2}{K^2} \rho$$

K = A CONSTANT DEPENDENT ON UNITS SELECTED

ρ = DENSITY

V_o = EXTENSIONAL WAVE VELOCITY

E = YOUNG'S MODULUS

V_t = TORSIONAL WAVE VELOCITY

G = SHEAR MODULUS

FIGURE 62. RELATIONSHIPS EXISTING BETWEEN SOUND VELOCITY AND MODULUS

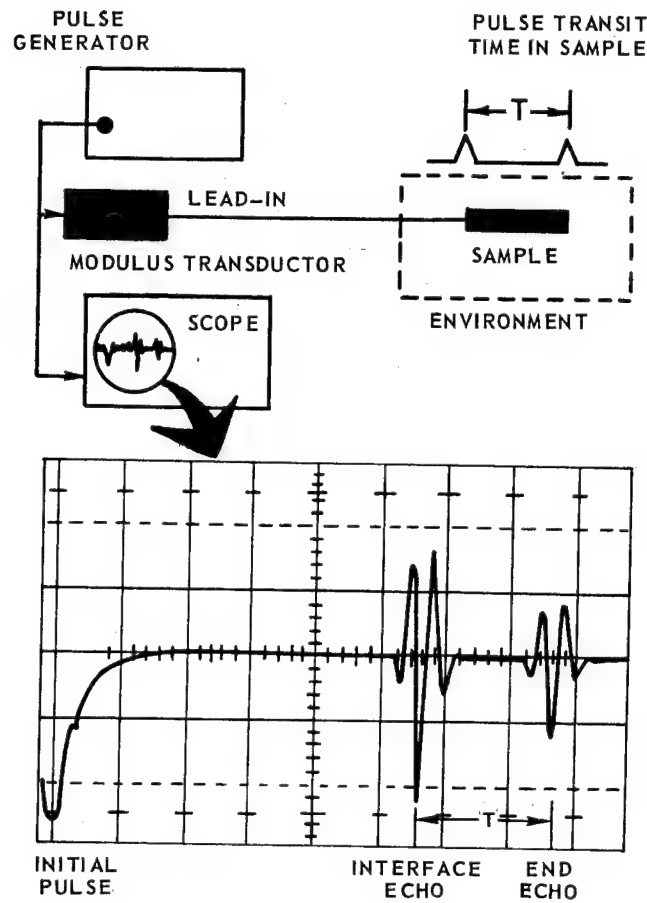


FIGURE 63. EXPERIMENTAL ARRANGEMENT FOR MAKING THIN-LINE ULTRASONIC DETERMINATIONS OF DYNAMIC ELASTIC MODULI

closely match the diameter of the fiber as indicated schematically in Fig. 64. Heating a small glass capillary tube and pulling it to reduce diameter creates the long tapered red filament. The tapered glass tubular fiber is then cut at the diameter that will closely match the impedance of the lead-in on one end and at the diameter that will yield less than a ten times impedance mismatch between the sample and the transformer section at the other end."

"If the impedance transformer element is properly constructed an echo of relatively small amplitude will occur at the junction between the lead-in and the transformer element, or the amplitude of the echoes from the beginning and end of the sample will be of the same order of magnitude. The oscillogram in Fig. 65 shows the pulse-echo signals returned from the line in the case of a single glass fiber approximately 1/2 mil in diameter. The glass fiber has been cemented in the impedance transformer with a thermoplastic or epoxy cement but for elevated temperature measurements, a fine-grained alumina cement could be used."

In Table XL, the results for glass fibers from a given glass composition and measured both by static and dynamic (thin-line ultrasonic, Panametrics, Inc.) methods are compared. It will be noted that the sixty static measurements average 15.93 million pounds per square inch and that the sixteen thin-line ultrasonic measurements of Young's modulus average 15.94 million psi, a truly remarkable agreement. It will be noted that the scatter for the dynamic method is much larger than for the thin-line ultrasonic measurement. All fibers are from UARL melt 275-10. The fibers furnished both Lowell Institute of Technology and Panametrics, Inc. varied from a diameter of 0.62 mils to 1.66 mils although each fiber sample measured was perfectly round and fairly constant in diameter.

In Table XLI, the results obtained for the more promising UARL mechanically drawglass fibers are tabulated. These values are selected from approximately one hundred UARL experimental glass compositions which have successfully been fiberized to date. In all cases where these fibers have been evaluated by both dynamic and static tests the comparative measurements are shown. It will be noted that the best fibers have a value for Young's modulus of 18.6 million psi or slightly greater. In the case of one of these fibers, namely UARL 344, more than fifty million feet of monofilament has been drawn and made into composites and the results obtained with these composites is discussed in the final section of this report. In considering the values for Young's modulus listed in this table it cannot be stressed too strongly that all of the values are measured on mechanically drawn fibers. The fiber glass literature, both publications and patents as well as our own very first reports, abounds in many higher values for Young's modulus all based on measurements made on hand-drawn fibers. Our own experience has convinced us that these values are utter nonsense since no hand-drawn fiber in general is ever round instead having more usually a flattened elliptical cross section. It is this that accounted for data like that we have shown earlier in connection with the Phillips calculations where the calculated value so violently disagrees with the published value.

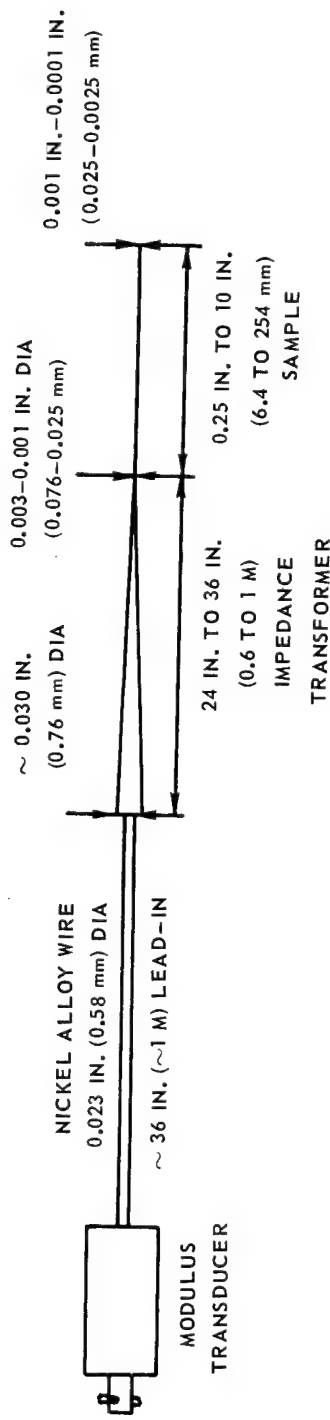


FIGURE 64. LINE CONSTRUCTION FOR THIN-LINE ULTRASONIC MEASUREMENT
 OF ELASTIC MODULI OF FIBROUS MATERIALS

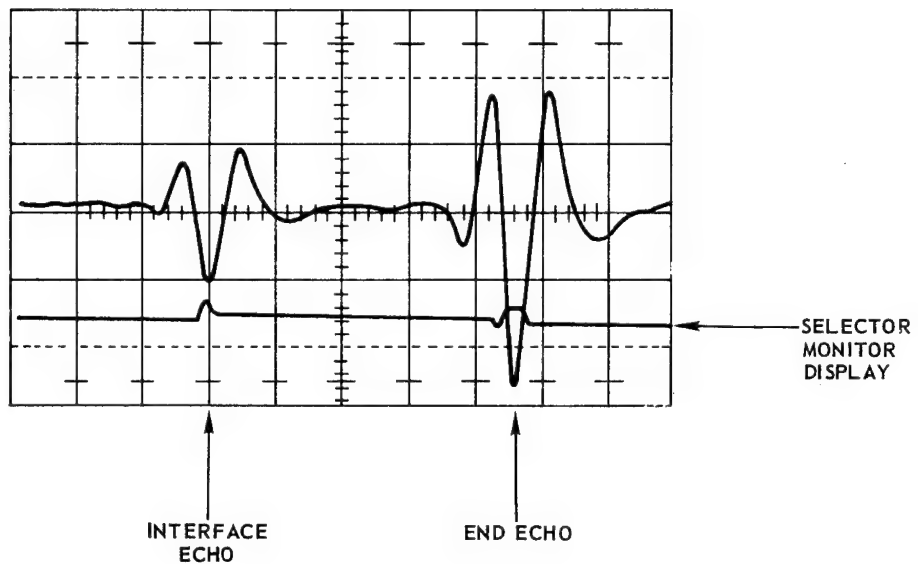


FIGURE 65. ULTRASONIC PULSE-ECHO SIGNALS FROM SINGLE GLASS FIBER

Table XL

Comparative Results on Glass Fibers of One Composition
Evaluated by Static and Dynamic Methods

Young's Modulus (millions psi)						
<u>Static Results</u>						<u>Thin-Line Ultrasonic</u>
13.8	15.6	17.2	11.3	16.8	19.9	15.77
14.5	15.6	18.2	16.4	16.7	14.8	15.96
15.5	18.5	14.8	17.4	14.7	13.1	15.5
13.2	13.9	14.8	20.1	14.3	12.1	16.27
14.1	19.4	16.9	14.3	17.3	15.4	15.67
14.2	12.1	17.9	12.2	15.9	15.4	15.77
13.2	15.0	17.0	15.9	15.7	14.6	15.98
13.7	15.0	15.2	14.0	15.7	18.3	16.33
13.7	8.2	19.8	15.1	14.1	13.4	16.00
15.4	15.5	18.3	14.7	17.6	10.4	16.09
Average 15.93						Average 15.94

Table XLI

Young's Modulus for the More Promising Mechanically
Drawn Glass Fibers

<u>Glass Number</u>	<u>Density (gms/cm³)</u>	<u>Instron Test Result Millions Psi</u>	<u>Thin-Line Ultrasonic Result Millions Psi</u>
Owens-Corning "S"	2.48	----	12.6
UARL 320	2.929	18.6	16.2
321	3.632	17.4	18.2
331	3.629	18.3	19.8
344	3.390	18.3	18.6
348	3.651	----	17.6
367	3.531	17.5	18.3
368	3.623	18.8	18.5
370	3.629	17.7	17.8
371	3.566	18.4	18.1
405	3.726	----	18.4

Finally, all the values for Young's modulus as measured on mechanically drawn fibers are assembled in Table XLII. The values for competitive glasses such as 82 and 83 as fabricated and measured using identical techniques are also shown. It will again be noted that values measured both at Panametrics using their thin-line ultrasonic technique and at Lowell Institute of Technology using an Instron test machine with air-actuated grips are in excellent agreement.

Strength Measurements on Pristine Glass Fibers

An equally important characteristic of glass fibers, however, is the strength. Because of the sensitivity of glass fiber to surface damage that can be inflicted by winding on a drum, or other contact, and by exposure to uncontrolled atmosphere for a finite length of time, it has become the practice to report so-called "virgin strength" of freshly drawn glass fiber. This is accomplished by capturing a sample of fiber between the bushing and the winding drum, and measuring the tensile strength as soon as possible and before any obvious damage has occurred to the fiber. The difference in strength measured on glass fibers shortly after capture between bushing and winding drum, and measurements on fibers off the winding drum has been shown dramatically by W. F. Thomas (Ref. 98). Figure 66 compares the strength measured by Anderegg (Ref. 99) off the winding drum with Thomas' data for virgin fibers. Thomas considers that the dependence of strength on fiber diameter shown by the data of Anderegg and many other authors is the result of the greater susceptibility of the larger fibers to damage, and that the strength of glass fiber is independent of diameter provided that care is taken to avoid damage during sampling and testing. Of particular interest in the work of Thomas is the extremely low scatter in the strength data which he obtained on virgin fibers tested within ten minutes of capture. Typically, he found that in testing 50 samples of E glass fiber produced under the same experimental conditions, all samples had strengths between 530,000 and 560,000 psi.

Preliminary Experiments

Before attempting to measure the virgin strength of UAC experimental glasses, it was considered necessary to make measurements on a known glass using testing equipment and fiber producing facilities available in these laboratories for comparison with previously published results. E glass was selected for preliminary experiments since marbles of this composition could be obtained commercially, and because E glass has been extensively studied. The fiberization equipment and technique just described in the previous section were used to produce E glass fibers varying in diameter from approximately 0.5 to 1.9 mils. In the first fiberization runs, E glass marbles were crushed to frit which was charged into the platinum crucibles. However, this procedure resulted in very seedy glass because of the many bubbles trapped in the molten glass. In subsequent runs, the as-received marbles were cleaned in an ultrasonic degreaser, rinsed several times with tap water, given a light etch with hydrofluoric acid, then rinsed and stored under distilled water until charged into the crucible. The reduction in seediness resulting from the latter procedure is shown in Fig. 67.

Table XLII

Values of Young's Modulus on Mechanically Drawn Fibers of UARL Experimental Glasses As Determined by Measurements Either on Tensile Test Equipment or Thin-Line Ultrasonics

Glass Number	Young's Modulus 10^6 psi			Young's Modulus 10^6 psi			Young's Modulus 10^6 psi		
	Standard Deviation 10^6 psi		Glass Number	Standard Deviation 10^6 psi		Glass Number	Standard Deviation 10^6 psi		Sonic
	Tensile			Tensile			Tensile		
25	12.3	1.9	83**	15.35	2.4,1.95	161	14.3	1.8	
40	16.2	4.6	97	10.4	1.7	162			
56	10.7		98	10.8	2.5	166	13.6	5.4	
62	14.0		102	13.3		175	13.1	2.9	
63	13.0		108	12.5	2.7	176	16.7	9.9	
64	14.7		110	13.8	2.2	193	13.1	4.0	
65	13.8		114	15.1		200	14.6	3.3	
66	14.6	2.0	126	16.15	1.82,1.65	201	13.2	4.3	
67	12.7		127	15.2		210	15.0	2.0	
68	13.7		129	16.7	2.7,2.6	214	12.9	1.6	
69	13.6		131	12.5		215	13.3	3.0	
70	13.4		135	13.3		233	14.6	2.3	
71	13.7		136	13.5		235	15.3	1.9	
72	12.5		137	13.9		237	18.8	7.9	
73	15.1		138	12.2		238	15.2	3.2	
74	13.8		140	15.0		260	10.4	1.5	
75	9.8		155	14.7	1.9	261	11.5	1.8	
76	10.4		157	13.1	2.8	275-10	15.93	2.2	15.94
77	11.0		159	15.7	5.0,2.2	276	17.0	6.2	
82*	13.3		160	14.6	3.0	278	11.3	1.8	

Table XLII (Cont'd)

Glass Number	Young's Modulus 10 ⁶ psi			Young's Modulus 10 ⁶ psi		
	Standard		Sonic	Glass Number	Tensile	Deviation 10 ⁶ Tensile
	Tensile	Deviation 10 ⁶ Tensile				
279	6.2	3.3		370	17.7	3.7
280	4.6	0.4		371	18.4	2.3
281	5.7	0.5		372	15.7	4.4
284	11.9	2.4		388	16.8	2.3
285	12.9	4.7		396	15.1	1.7
						16.4, 16.1
						15.1, 14.9
288-3	11.9	2.8		402	16.5	3.1
289	13.1	1.5		403	18.0	2.7
290-5	14.3	5.8		405	18.7	2.2
290-6	13.0	3.7		321A	17.4	3.6
291	13.6	3.2		E	11.8	3.9
						18.3, 18.45
						18.2
299	12.8	3.6		347	17.4	1.5
300	13.4	3.4		408	19.8	5.0
309	14.8	1.9		410	17.8	1.8
320B3	18.6	3.3	16.2	411	15.6	1.4
331	18.3	2.5	19.85	412		16.5, 16.35
						17.0, 16.65
344	18.3	3.2	18.6	416	19.8	2.7
348	17.5	3.0	17.6, 17.5	417	18.8	3.0
349	16.9	2.1	16.9, 16.7	418	18.5	1.9
367	17.5	3.7	18.4, 18.3	419	19.0	2.9
368	18.8	2.6	18.5	420	19.6	4.1
						18.4, 18.1
						17.8, 17.7

82*-Houze Glass U.S. 3,044,888
 83**-Owens Corning Glass, U.S. 3,122,277 (#4)

All tabulated observations are the average of 20
 observations except for 40, 83, 126, 129, 233, 275-10,
 320B3, 331-60

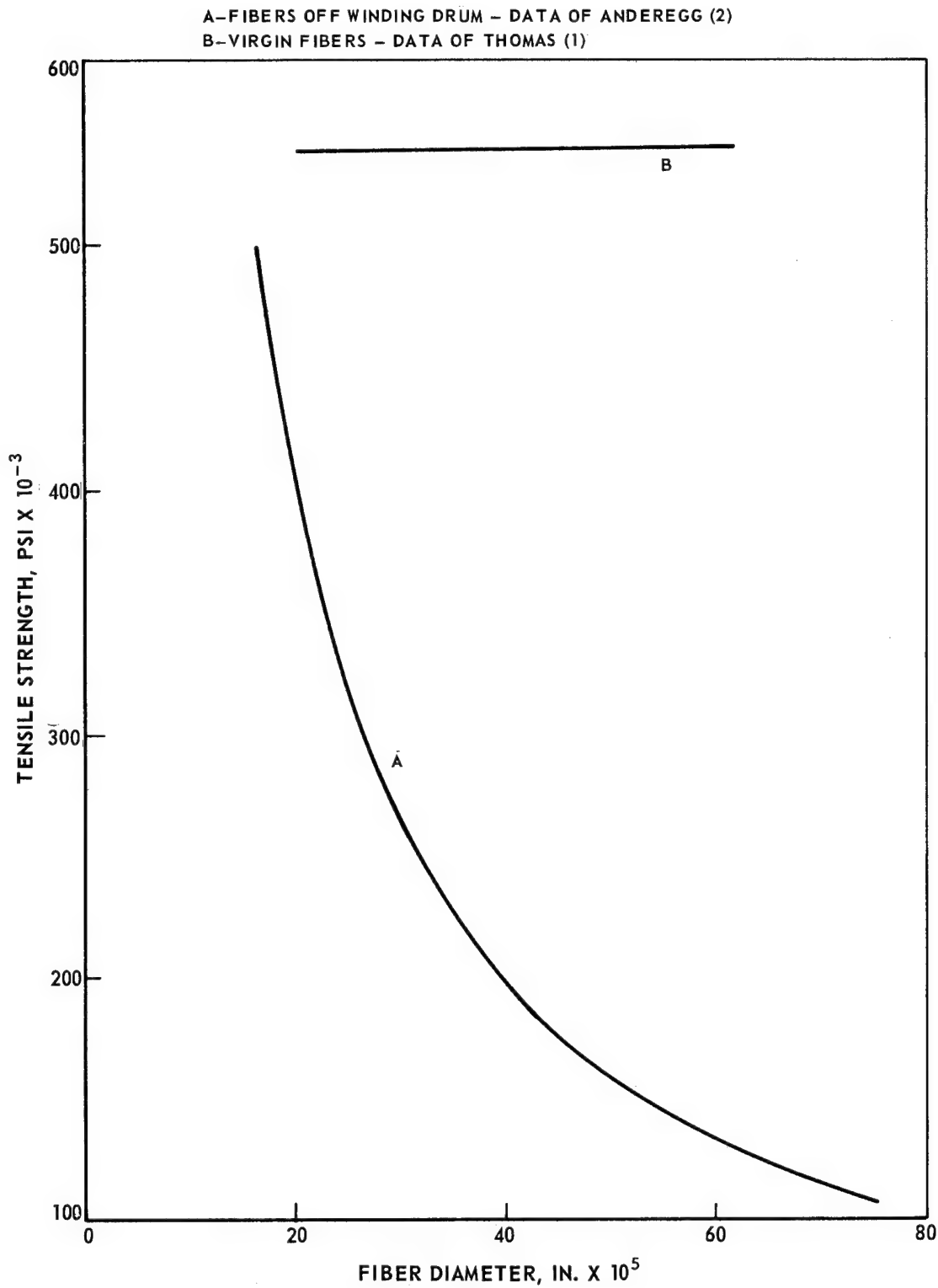
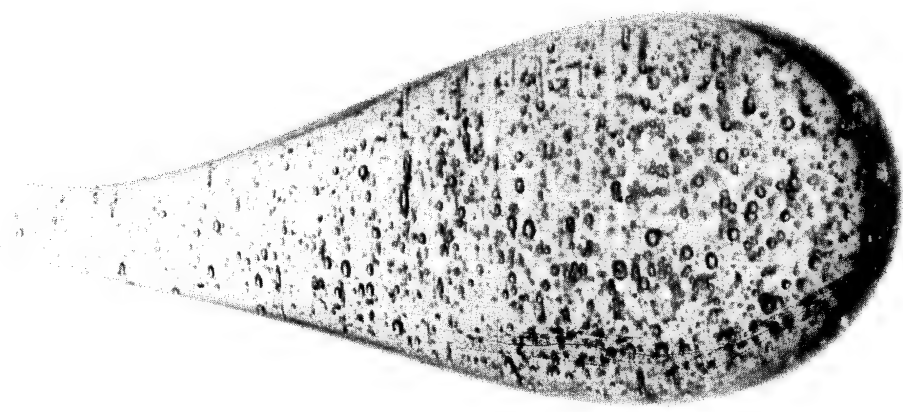


FIGURE 66. STRENGTH OF GLASS FIBER

A FROM FRIT



B FROM MARBLES

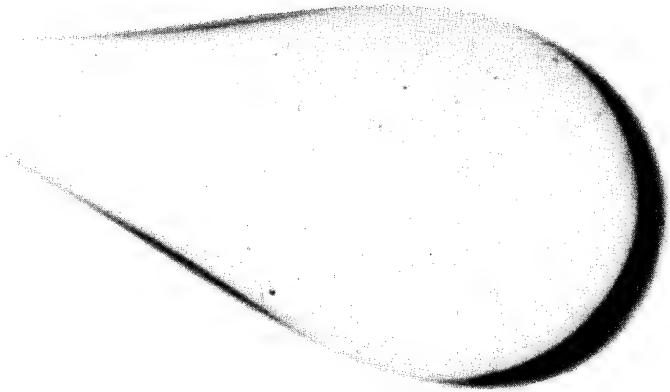


FIGURE 67. E-Glass TEAR DROPS

Fiber Capture

The capture device is shown in Fig. 68. This consists of two pairs of shears actuated by a common lever. The inner shear of each pair is made of 1/4 in. stock and the face addressing the fiber is coated with double-sided sticky tape. Attached to the outer shear of each pair is a block which presses the fiber onto the tape an instant after the fiber has been sheared. With the shears in the vertical position, the lower pair of shears is adjusted so that it cuts the fiber an instant before the upper shear closes so that the captured fiber is not in tension. After the fiber drawing process has been initiated and brought to a steady state at the desired experimental conditions, a sample is captured manually with the shears. An improved capture device is shown in Fig. 69 which because of the spring loading cuts the fiber both more cleanly and rapidly.

Fiber Testing

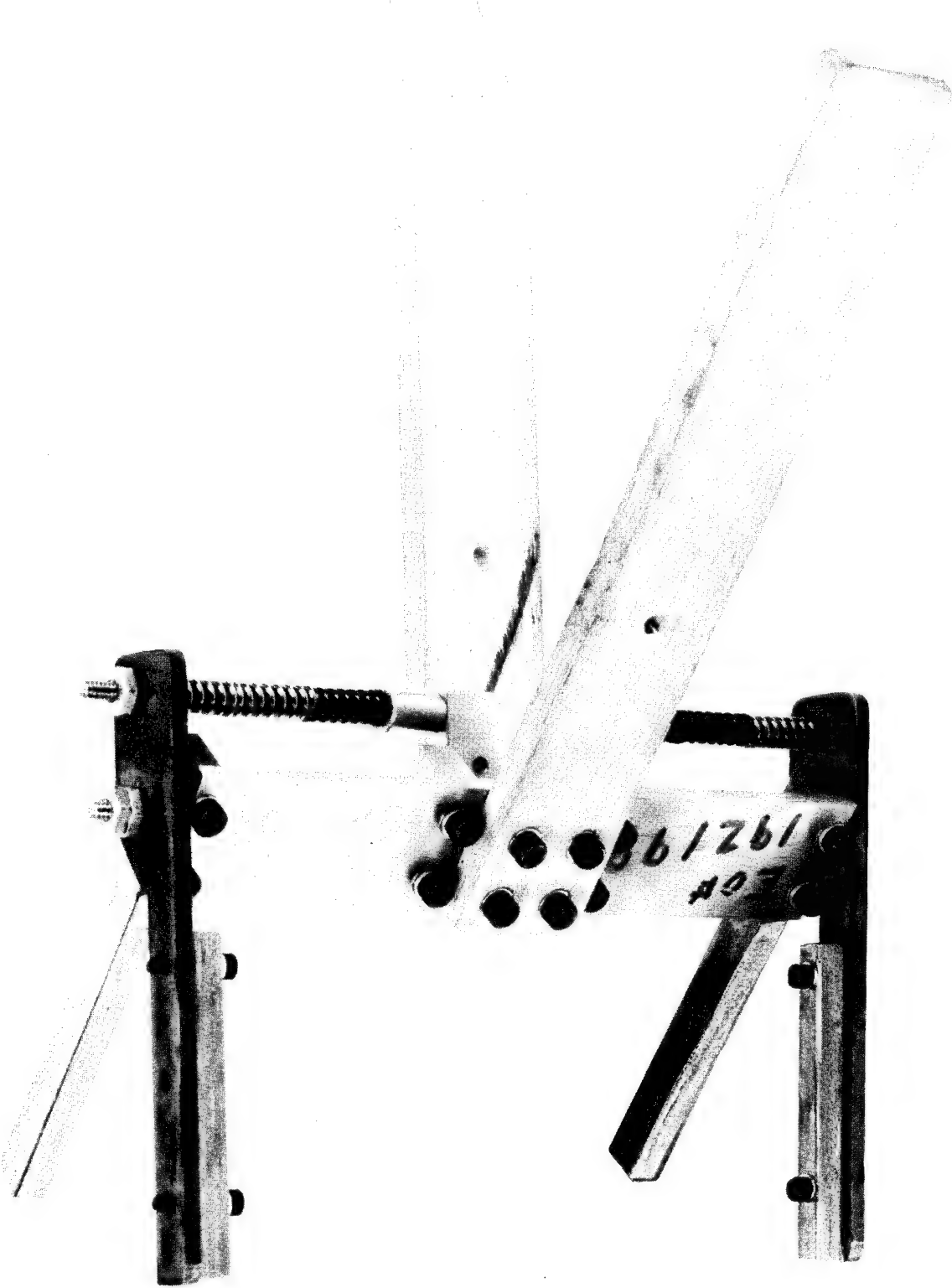
The fiber testing machine used in these preliminary experiments, shown as Fig. 70, was developed at UAC, and has been described in the literature (Ref. 100). The fiber is mounted between the moving crosshead (A) and the stationary crosshead with red sealing wax which is melted by nichrome heaters underneath the fiber mounting tabs. The crosshead moves at a constant rate of 0.77 mm/min. The load cell which is mounted on the stationary crosshead is of the strain gage type, is temperature compensated, and responds only to load components in the direction of the fiber axis. An electronic bridge circuit monitors the load cell, which is calibrated by placing the test device in the vertical position and suspending laboratory weights from the load cell. The calibration curve for the load cell used in these experiments is shown in Fig. 71. The short term drift of the bridge circuit amounts to two percent of full scale deflection.

Immediately following fiber capture the fiber, still held by the shears, is placed in position on the mounting tabs which have been preheated to melt the wax. The fiber was then cut free from the capture shears and the wax allowed to harden. Without forced cooling of the tabs, the wax would become sufficiently hard to permit testing in about fifteen minutes. Subsequently, a pair of water cooled tabs was affixed which permitted more rapid testing. A satisfactory cooling rate permitted testing about four minutes after capture. However, glass fibers mounted in the sealing wax slowly cooled or forced cooled frequently slipped, resulting in a jerky loading rather than a smooth loading rate.

As well as testing fibers captured as described above, spooled fiber was also tested after 5 days of normal laboratory storage to assess the effects of spooling and storage on fiber strength.

Two kinds of fracture were noted which we shall call "normal" and "fly-out". Low strength fibers (strength below about 300,000 psi), usually those that were measured after storage, exhibited "normal" fracture. In this case failure occurred within the guage length (approximately one inch) and the fiber ends on either side of the fracture were retained in the testing apparatus. In the case

FIGURE 68. FIBER CAPTURE SHEARS



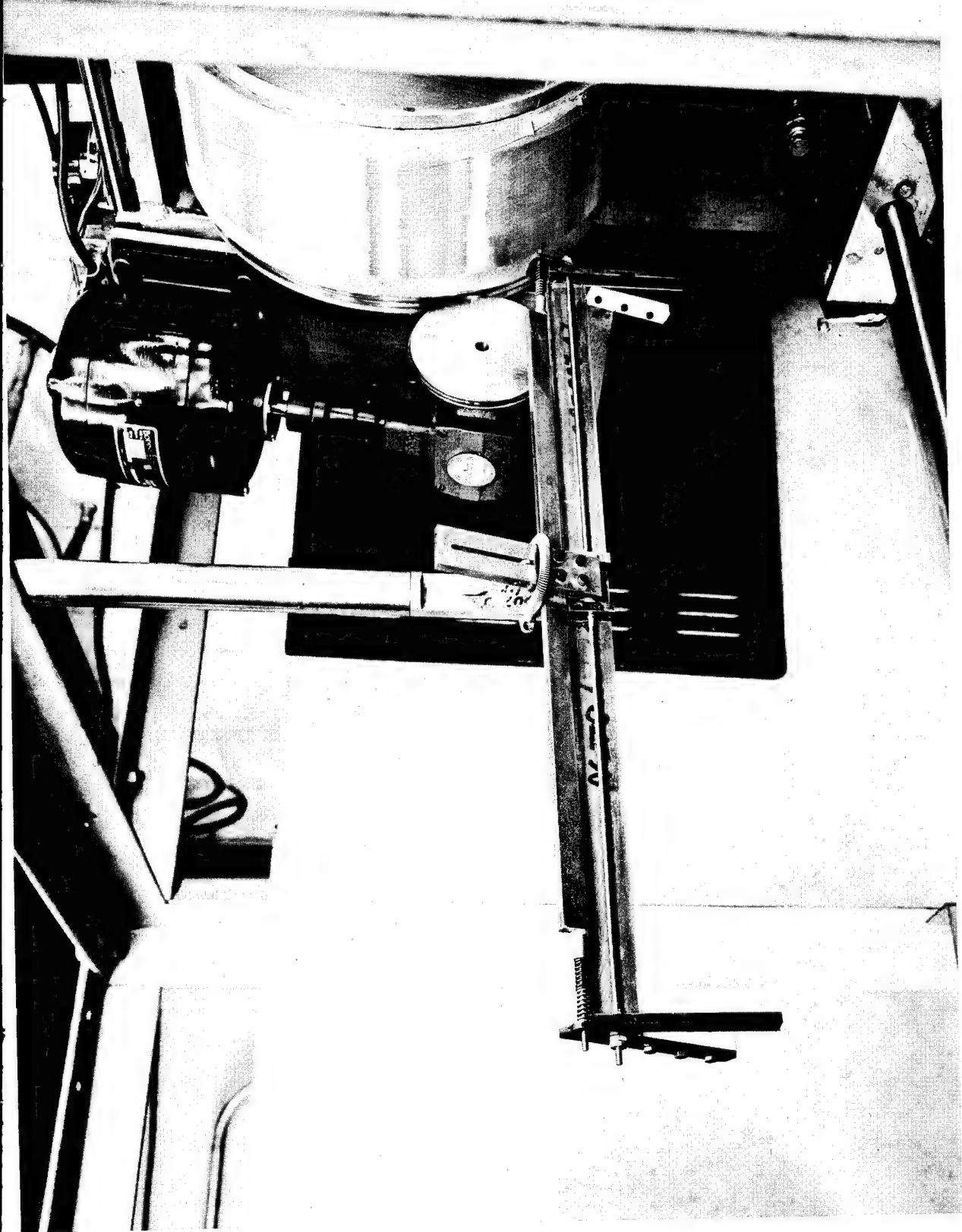


FIGURE 69. IMPROVED FIBER CAPTURE DEVICE

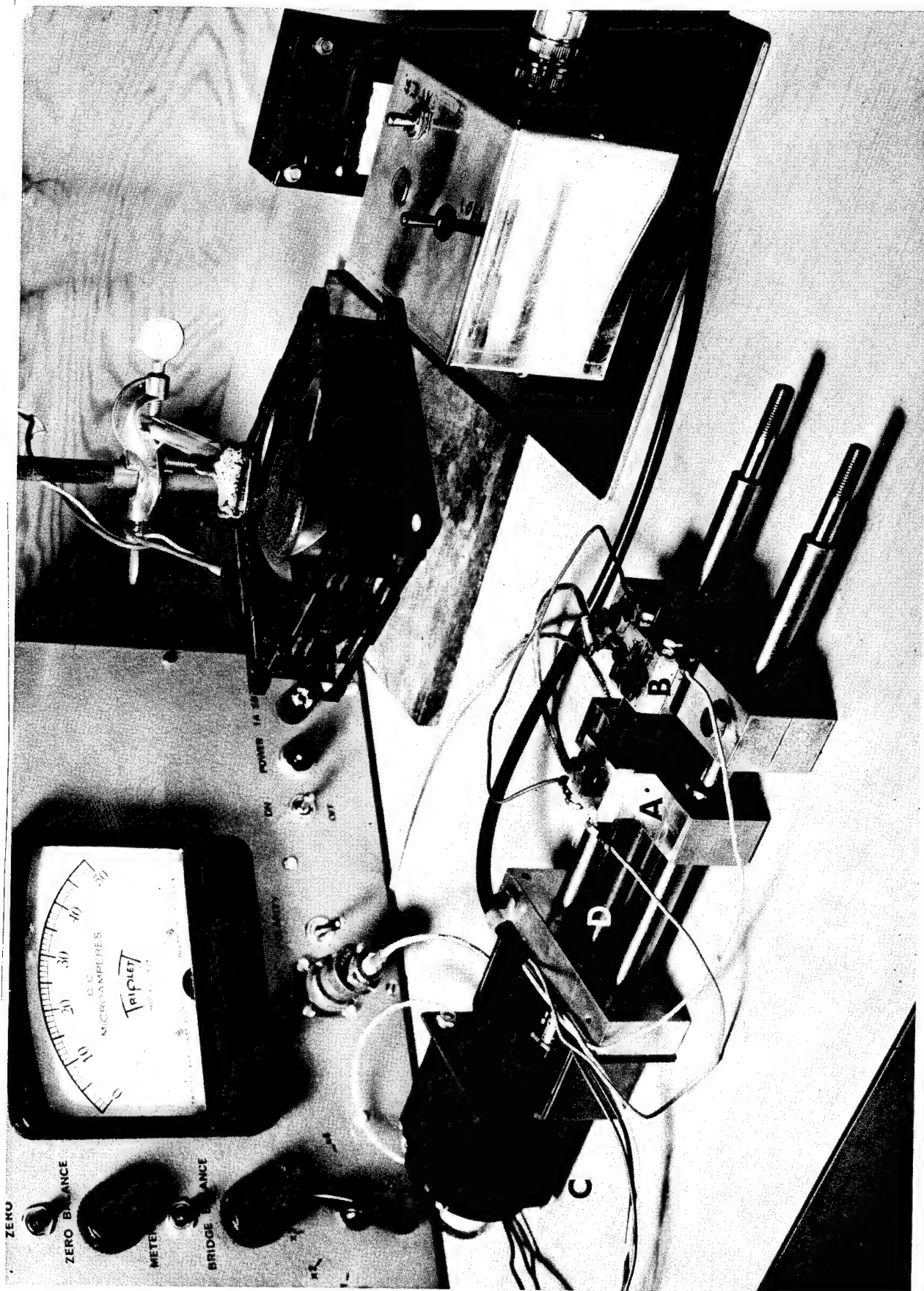


FIGURE 70. TENSII F TESTER NFVI OPEN AT HADI

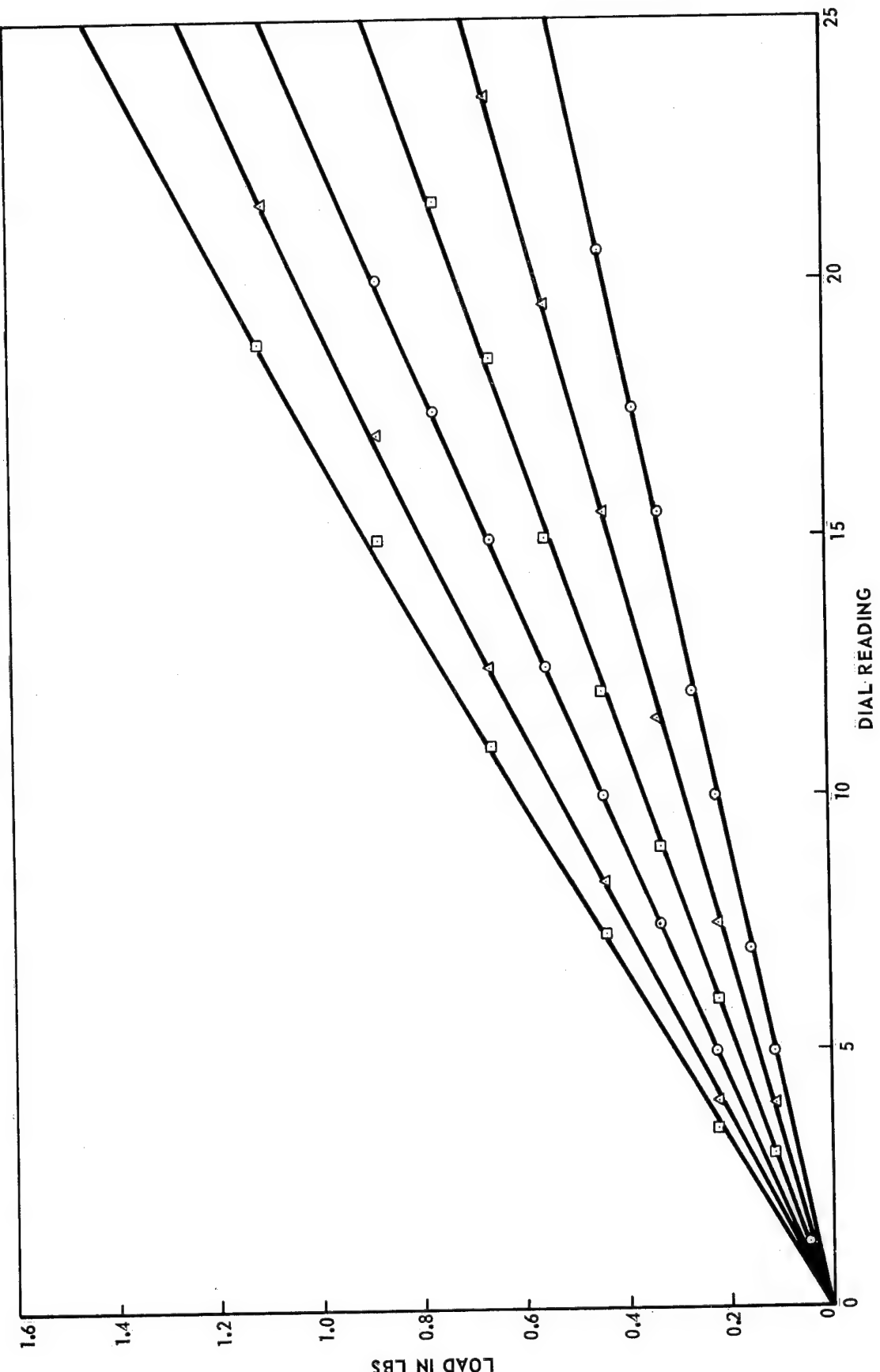


FIGURE 71. CALIBRATION CURVE FOR TENSILE TEST APPARATUS

of fibers exhibiting strengths above 300,000 psi, after fracture, it was frequently found that the fiber was broken away at either grip, or sometimes broken away at one grip while still projecting from the other. Occasionally the fiber ends would be found projecting from both grips but the center section was missing. Attempts were made to photograph this mode of fracture. The fracture event could not be recorded at 500 frames per second; one frame of a film strip would show the intact fiber mounted in the testing machine, and in the next frame the fiber would be gone.

Measurement of Fiber Diameter

Several techniques for measuring fiber diameter were investigated and the results compared. These were: (1) mechanical measurement using a Johansen dial gage, (2) scaling of high magnification photographs of the fibers, and (3) use of a Watson two color split image eye piece in conjunction with the petrographic microscope. Measurement of lengths of fiber by all three methods gave the same fiber diameter to within one half of one percent. The Watson split image eye piece was adopted as the standard diameter measuring technique because of its greater convenience. The typical variation in diameter over a two inch length of glass fiber produced in the fiberizing equipment was five percent on fibers of nominally one mil diameter.

After breaking a sample in the testing apparatus, the fiber diameter was measured adjacent to the fracture where possible. In the case of "fly-out", diameter was measured on the section of fiber that extended beyond the outside of the mounting tabs.

Experimental Results

Strength data obtained for captured and spooled E glass fibers are recorded in Table XLIII. The precision of the strength measurements S can be assessed by considering the uncertainty in the load measurement ΔL , and in the diameter measurement Δd from the equation

$$\frac{\Delta S}{S} = \frac{\Delta L}{\Delta} + 2 \frac{\Delta d}{d} \quad (1)$$

Since fly-out prevents measurement of diameter at point of fracture, the relative uncertainty in the diameter was five percent since this was found to be the variation in diameter over a two inch length. The relative uncertainty in the load at fracture varies with the load because of the short term drift in the electronics (two percent of full scale). Thus, there is a greater uncertainty in the load for fibers that failed at low loads than for fibers which failed at high loads. The uncertainty calculated for each strength value from equation (1) is recorded in Table XLIII.

Table XLIII
Strength Data.

<u>Sample Number</u>	<u>Pulling Temp. °C</u>	<u>Pulling Speed ft/sec</u>	<u>Elapsed Time from Capture to Testing (min)</u>	<u>Load at Failure (lbs)</u>	<u>Fiber Diameter (mils) $\pm 5\%$</u>	<u>Tensile Strength psix10⁻³</u>	<u>Mode of Fracture</u>	<u>Notes</u>
E-1	1237		~15	0.08 ± 0.01	1.02	90 ± 20	normal	fiber damaged, not tested
E-2	1242	4.5	~15	0.34 ± 0.01	1.06	390 ± 50	fly out	
E-3	1244		~15	0.33 ± 0.01	1.13	330 ± 43	fly out	
E-4	1246		~15	0.26 ± 0.01	0.99	340 ± 47	samples E-1 through E-10	
E-5	1248	6.2	~15	0.07 ± 0.01	0.85	120 ± 27	virgin strength measurements on glass fibers from	
E-6	1250	8.3	~15	0.22 ± 0.01	0.78	460 ± 67	seedy batch, see Fig. 7	
E-7	1252	10.5	~15	0.07 ± 0.01	0.62	230 ± 55	normal	
E-8	1267	8.8	~15	0.11 ± 0.01	0.57	440 ± 83	fly out	
E-9								fiber damaged, not tested
E-10								
E-11				0.11 ± 0.01	1.11	114 ± 22	normal	
E-12				0.27 ± 0.01	1.97	89 ± 11	samples E-11 through E-21	
E-13				0.41 ± 0.01	1.28	318 ± 40	tested after storage on	
E-14				0.10 ± 0.01	1.05	115 ± 30	winding drum for five days	
E-15				0.18 ± 0.01	1.06	204 ± 32		
E-16				0.15 ± 0.01	1.11	155 ± 26		
E-17				0.06 ± 0.01	0.605	208 ± 55		
E-18				0.52 ± 0.01	1.41	333 ± 40		
E-19				0.10 ± 0.01	1.05	116 ± 32		
E-20				0.27 ± 0.01	1.37	184 ± 25		
E-21				0.12 ± 0.01	1.28	93 ± 17		
E-22	1247	4.5	~15	0.465 ± 0.01	1.32	337 ± 41	samples E-22 through E-43	
E-23	1245	4.5	~15	0.465 ± 0.01	1.21	405 ± 49	are virgin measurements	
E-24	1252	4.5	~15	0.77 ± 0.02	1.68	348 ± 44	on relatively seed-free	
								glass

Table XLIII (Cont'd)

Sample Number	Pulling Temp. °C	Pulling Speed ft/sec	Elapsed Time from Capture to Testing (min)	Load at Failure (lbs)	Fiber Diameter (mils) +5%	Tensile Strength $\times 10^{-3}$ psi	Mode of Fracture	Notes
E-25	1264	4.5	~15	0.515+0.02	1.52	285+40	fly out	
E-26	1268	4.5	~4	0.88+0.025	1.45	532+68	fly out	
E-27	1268	4.5	~4	0.66+0.025	1.61	336+46	fly out	
E-28	1266	4.5	~4	0.64+0.025	1.36	441+61	fly out	
E-29	1262	4.5	~4	0.75+0.025	1.45	454+60	fly out	
E-30	1266	4.5	~4	0.75+0.025	1.76	308+41	fly out	
E-31	1267	4.5	~4	0.86+0.025	1.56	448+60	fly out	
E-32	1267	4.5	~4	0.77+0.025	1.42	484+64	fly out	
E-33	1255	4.5		0.66+0.025	1.38	4442+61	fly out	
E-34	1264	4.5		0.73+0.025	1.42	460+62	fly out	
E-35	1281	4.5	~15	0.73+0.025	1.39	480+64	fly out	
E-36	1280	4.5	~15	0.64+0.025	1.52	353+49	fly out	
E-37	1270	4.5	~15	0.60+0.025	1.49	343+47	fly out	
E-38	1266	4.5	~15	0.73+0.025	1.33	525+70	fly out	
E-39	1251	16.3	~4	0.12+0.01	0.720	296+54	fly out	
E-40	1250	16.3	~4	0.14+0.01	0.635	452+77	fly out	
E-41	1252	16.3	~4	0.12+0.01	0.727	290+53	fly out	
E-42	1252	16.3	~4	0.14+0.01	0.645	430+73	fly out	
E-43	1252	16.3	~4	0.15+0.01	0.560	607+110	fly out	

Except for 3 measurements (E-1, E-6, and E-8) all virgin fibers exhibited fly out fracture and had strengths above about 300,000 psi. The three low values were obtained on fibers pulled from the seedy melt and presumably resulted from entrained bubbles. The remaining virgin strength measurements are plotted as a function of fiber diameter, with drawing temperature and elapsed time before testing as parameters in Fig. 72. Fibers tested from the winding drum after five days are plotted in Fig. 73.

Possible sources of scatter and low strength values for E glass fibers tested as described above have been investigated. Considerable uncertainty as to the validity of a given strength measurement exists when the fiber failed in the "fly out" mode described previously. This is because of the impossibility of measuring the fiber diameter at the point of failure, and because it is not possible to assess whether initial failure was in the gage length. In order to assess the prevalence of grip failures occurring with fly out, a series of E glass specimens were taken from a spool and tested. Alternate specimens were tested in air, or damped with oil in order to prevent fly out. The method of accomplishing the damping is shown in Fig. 74. A microscope slide is positioned just below the mounted fiber, and a drop of oil is placed on the slide so as to cover the fiber over most of the guage length. Of ten samples broken without damping, five failures were fly-out, four were normal (i.e. a single fracture within the guage length) and one was a grip failure. Of eleven samples broken with oil damping, none were fly-outs, five were normal failures and six were grip failures, i.e. fracture occurred immediately adjacent to the wax, or under the wax. Thus, about half of undamped tests were fly-out, and where fly-out was prevented it was disclosed that about half the failures were grip failures and cannot be considered as valid data.

Consider now the strength data for virgin E glass fibers presented in the previous progress report. This data is replotted as a histogram in Fig. 75a. The mode of failure in all instances was fly-out. A bimodal distribution of strength values is observed. It seems reasonable that the low strength values centered around 300 to 350×10^3 psi represent grip failures possibly resulting from misalignment, and that high values centered around 450×10^3 psi are valid guage length failures.

Based on these observations, it was decided to change to a paper tab fiber mounting system for tensile specimens, because such a system would provide a degree of self-alignment for the tensile specimens, and because it was thought that the paper mounts would absorb energy from fiber whiplash thus tending to damp fly-out. Also, because several tensile specimens can be prepared simultaneously from a captured fiber, testing can be speeded up. The capture device was modified so as to capture eighteen inch lengths of fiber between the bushing and the take-up spool. The modified capture device, mounted on the fiberization furnace, was shown in Fig. 69. The captured fiber is picked off the capture device using a bent wire frame to which the fiber is temporarily glued, and transferred to a pre-cut paper tape consisting of five (5) paper mounting tabs. The fiber is attached to the tabs with de Khotinsky cement applied with a pencil type

▲ TESTED AFTER 15 MIN
 ○ TESTED AFTER 4 MIN
 I $1240 < T \leq 1250$
 II $1250 < T \leq 1260$
 III $1260 < T \leq 1270$
 IIII $1270 < T \leq 1280$

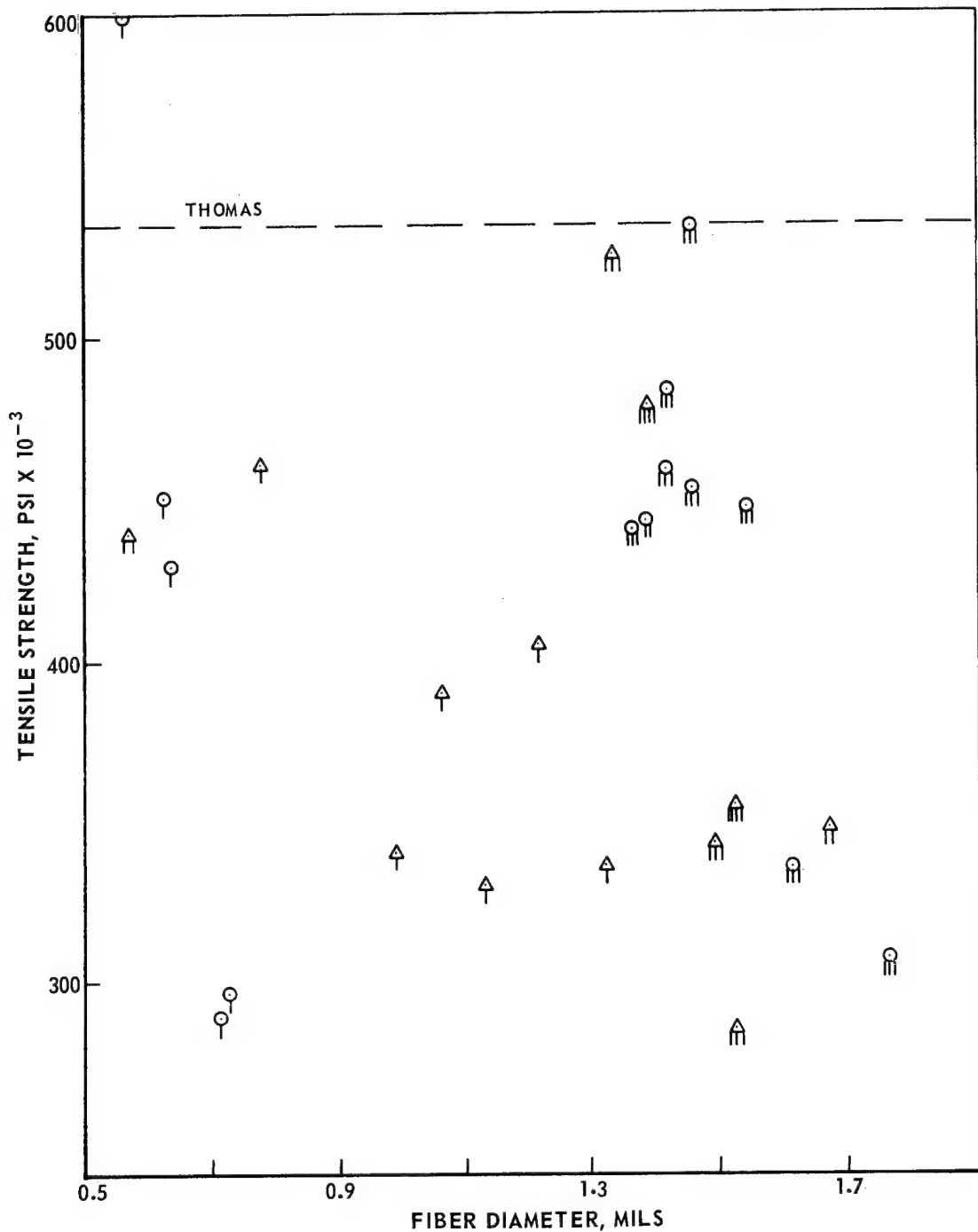


FIGURE 72. VIRGIN STRENGTH OF E-Glass FIBERS

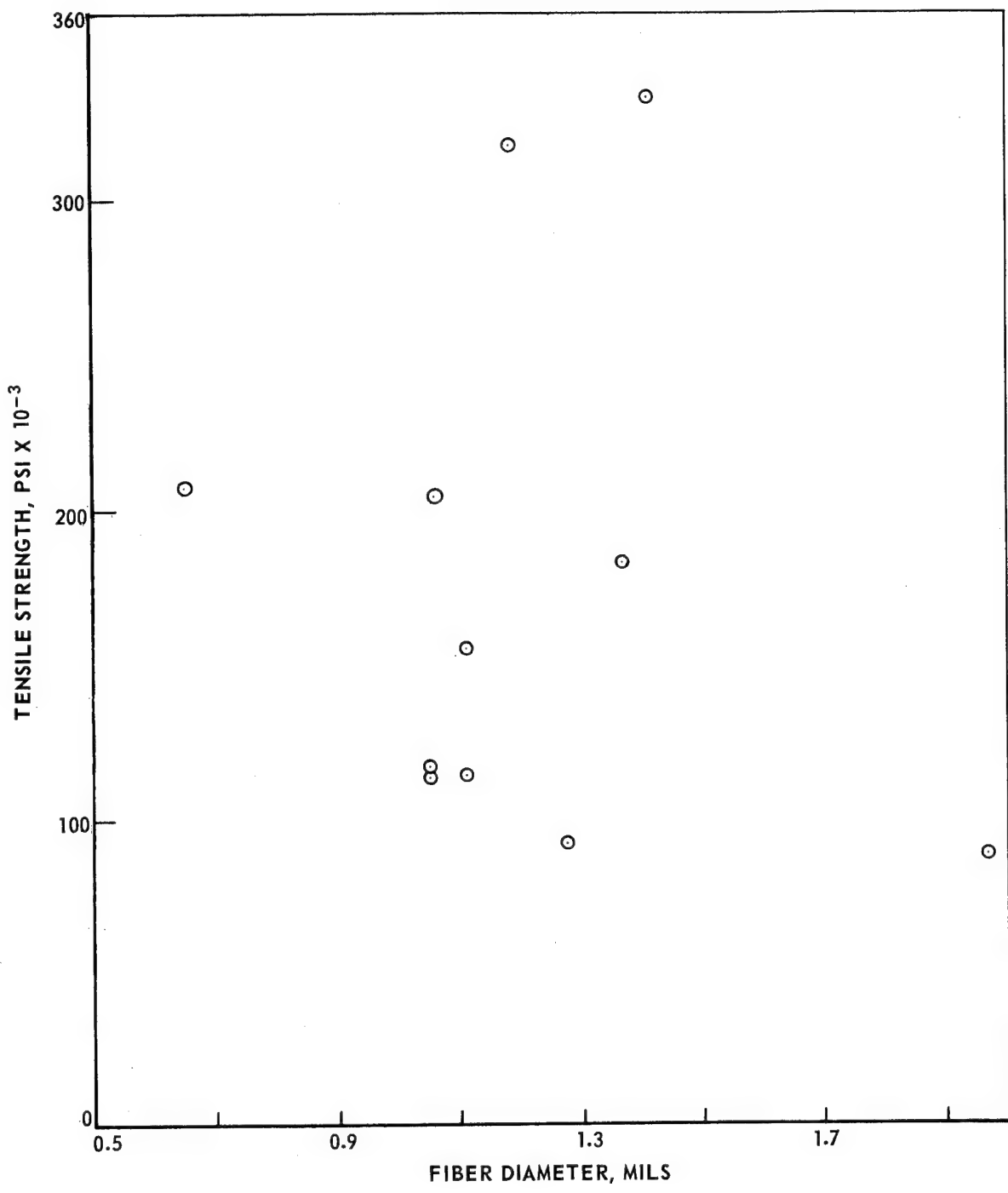


FIGURE 73. STRENGTH OF E-GLASS FIBERS TAKEN OFF WINDING DRUM

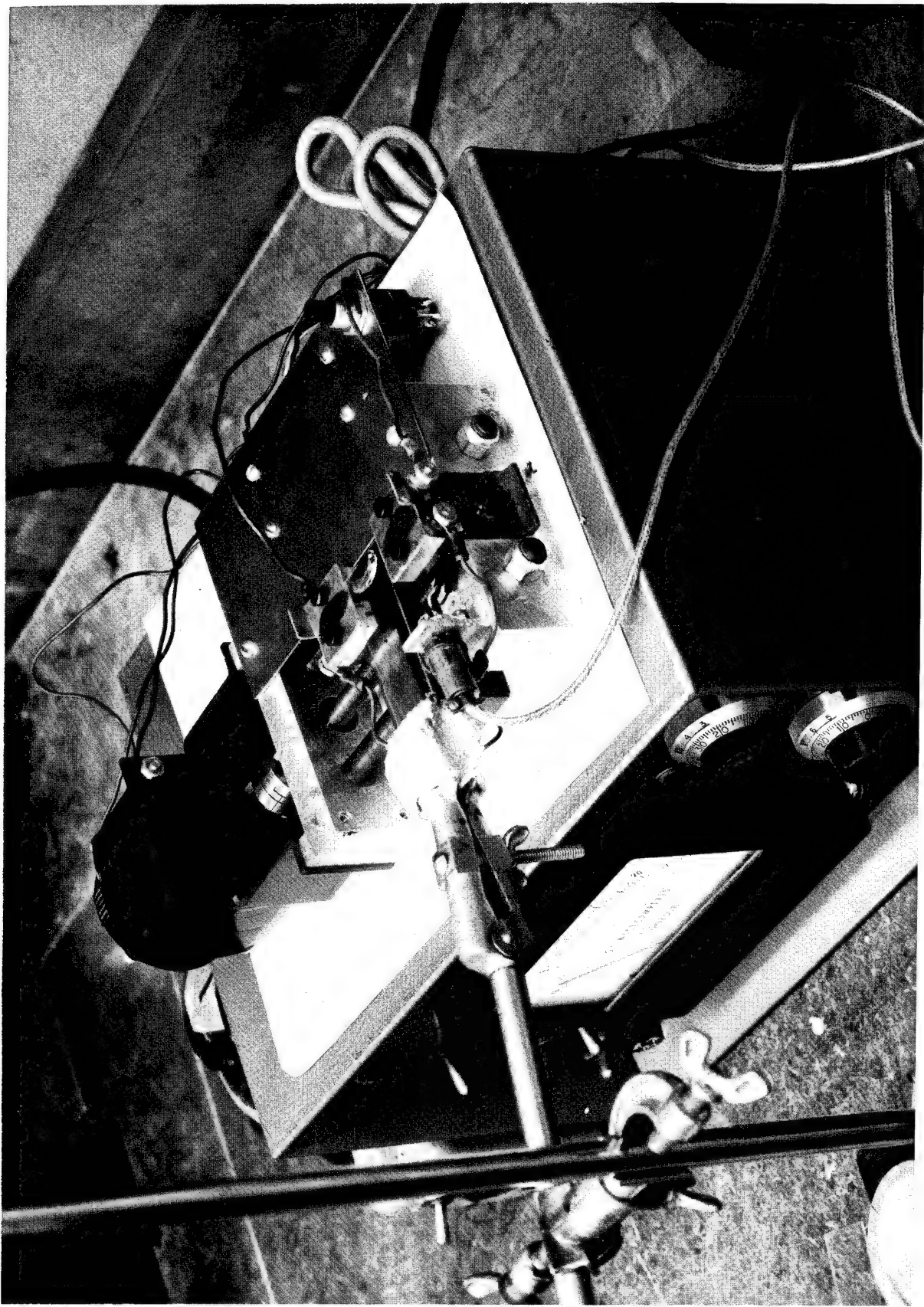
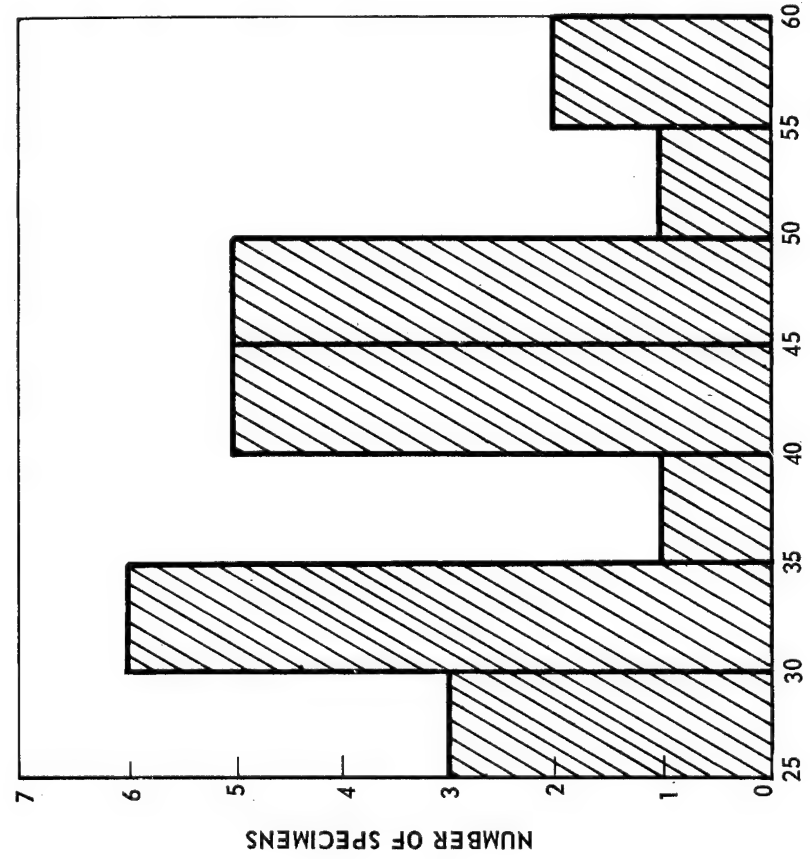


FIGURE 74. METHOD OF DAMPING TENSILE TEST SPECIMEN

A. MEASURED WITH RIGID MOUNT



B. MEASURED WITH PAPER MOUNTS

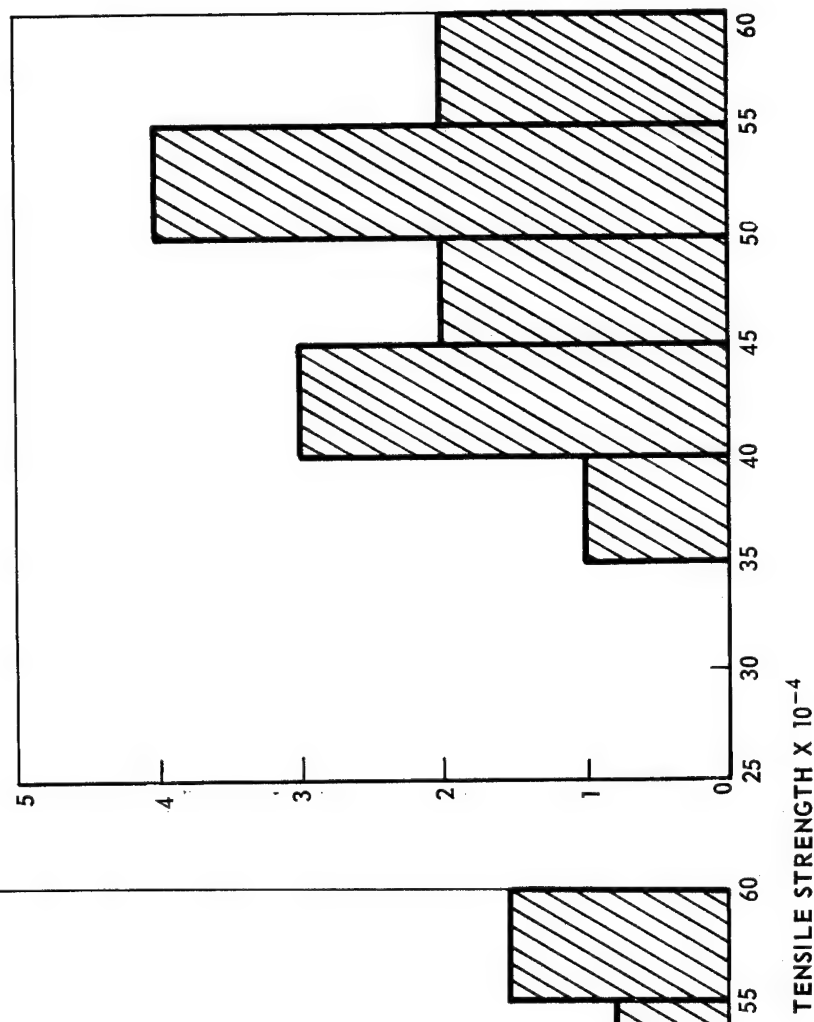


FIGURE 75. STRENGTH OF PRISTINE E GLASS FIBERS

soldering iron. A tensile specimen is then cut from the tape, mounted on the testing machine with spring clips, and the mounting tab cut so as to permit loading the fiber. A tensile specimen mounted on the testing machine in this fashion is shown in Fig. 76.

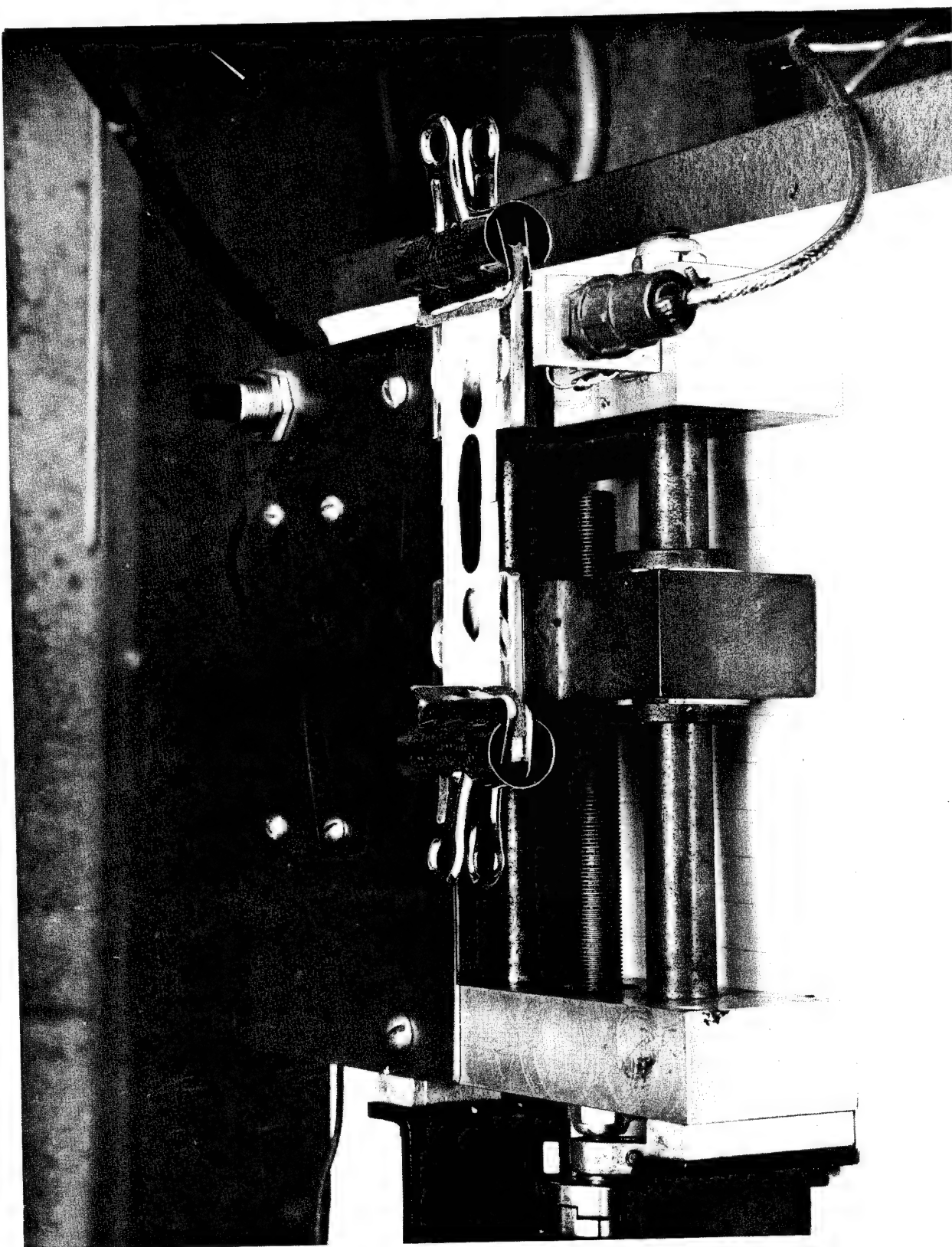
Virgin E glass fibers were captured and tensile strength measured using the above procedure. These strength data are shown in Fig. 75b. Comparison with the strength data obtained using the original mounting system indicates that a major source of low strength values has been eliminated. However, samples still failed with fly-out making accurate diameter measurements at points of fracture impossible. Diameters used in strength calculations are therefore averages of values measured some distance from the point of fracture. Variations in diameter along a captured eighteen inch length of fiber were found to be as high as twenty percent. Thus, uncertainty in diameter is possibly the greatest remaining source of scatter in the virgin strength data measured for E glass. Further effort should thus be directed toward producing defect-free fiber of uniform diameter.

Testing experimental fibers. - Representative glass compositions that had previously been fiberized in the UAC apparatus and for which modulus data had been obtained were selected, and virgin strength measured by the method described. These data are recorded on Fig. 77. The values fall roughly on a single curve of strength versus diameter. Such behavior is typical of fibers containing flaws and probably indicates that the fiberization process variables which control the quality of the fiber rather than any variation in glass composition are determining the strength. Fibers of these experimental glasses were examined under the microscope, and in all instances were found to contain crystalline inclusions, examples of which are shown in Fig. 78. The lowest strength values were seldom accompanied by fly-out and so the point of fracture could be observed. This was found frequently to be at such inclusions.

In order to assess qualitatively the possibility of continuously pulling good quality fibers of a short-working range high modulus glasses such as UAC-114, 135, 6, 7, 8, 126, 129 etc., the behavior of 126 glass was examined in the microfurnace. The liquidus temperature was found to be approximately 1460°C. A qualitative measure of the viscosity could be obtained by microscopic observation of the flow of glass as the thermocouple was withdrawn from the glass surface. By correlating observations on UAC 126 glass and E glass it was concluded that in the temperature range 1200-1250°C, viscosity was in the proper range to permit fiber drawing. This is in agreement with previous experience in fiberizing this composition. However, after being held at 1200°C for several minutes, crystals could be discerned growing in the glass at an appreciable rate. After 10 min the sample in the microfurnace was filled with crystalline material.

In order to confirm that these results were indeed characteristic of 126 glass in bulk and not specific to the particular environment and high relative surface conditions of the microfurnace the following experiments were performed. A 50 ml platinum crucible was charged with 126 glass buttons, and a thermocouple arranged so as to be immersed when the glass became liquid. The crucible was

FIGURE 76. PAPER TAB FIBER MOUNTING SYSTEM



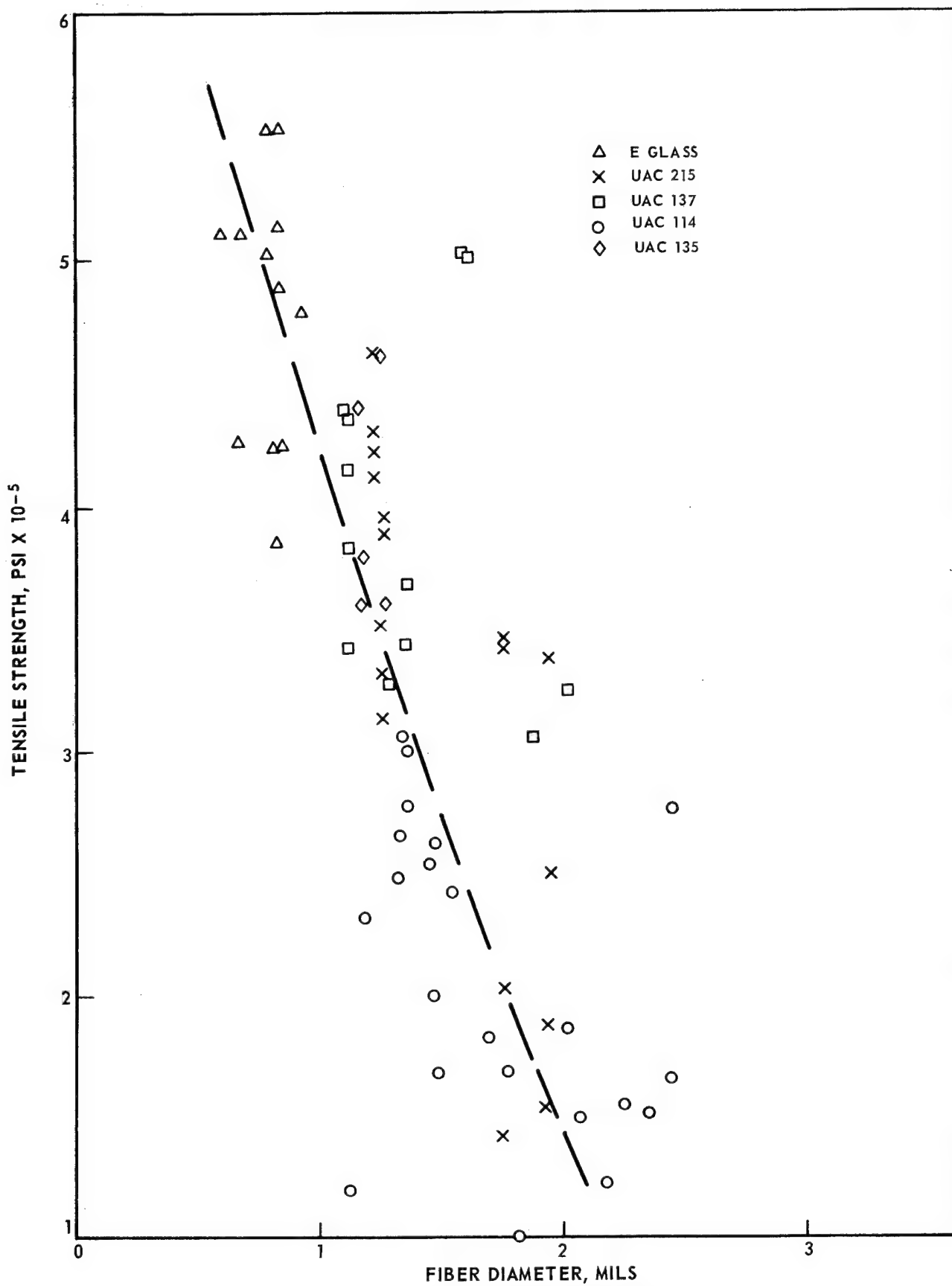


FIGURE 77. STRENGTH OF EXPERIMENTAL GLASS FIBERS

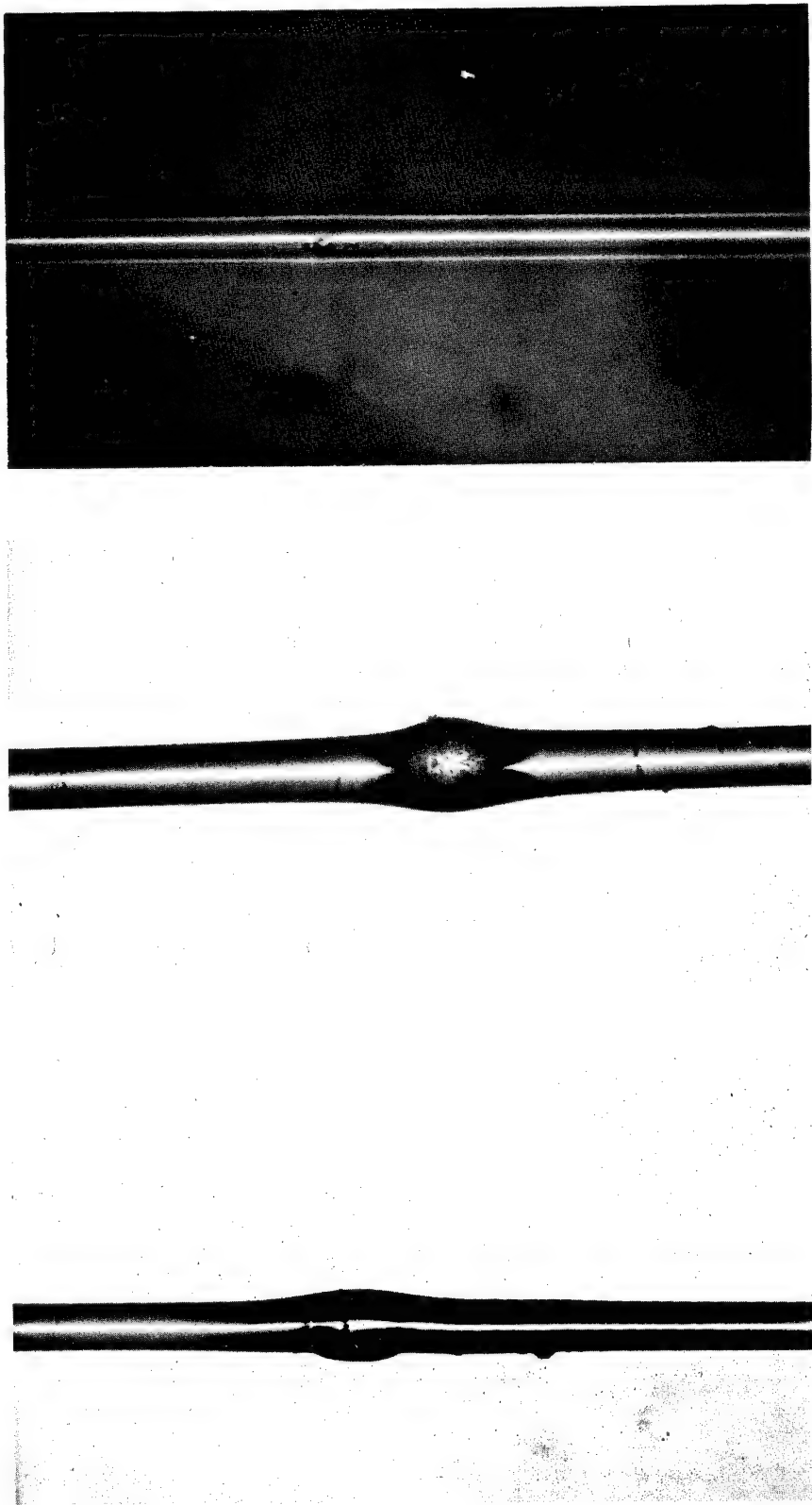


FIGURE 78. TYPICAL INCLUSIONS IN FIBERS

heated to 1560°C, i.e. 100°C above the liquidus, for one hour, then removed from the furnace and cooled to room temperature. No crystalline material was observed in the glass. The crucible was returned to 1560°C for an hour then moved to a cooler portion of the furnace where the temperature fell to 1200°C in about 5 min. The glass was maintained at this temperature an additional twenty minutes, then removed from the furnace. It was found that a considerable amount of crystalline material had formed as shown in Fig. 79. It can be concluded that, at least for this glass, microfurnace observations can be considered to apply to bulk conditions as well. Assuming that microfurnace observations on other glass could equally well be translated to bulk conditions, glasses 114, 129, 136 and 138 were examined in the microfurnace. Qualitative observation of crystal growth rate at temperatures in the fiberization range are given below.

Qualitative Observations on the Crystallization
of Experimental Glasses

Glass	Approximate Liquidus	Approximate Fiberization Range	Relative Crystallization Rate
114	1375	1200-1250	rapid
126	1460	1200-1250	rapid
129	1355	1200-1250	relatively slowly
136	1315	1200-1250	relatively slowly
138	1325	1200-1250	quite slowly

These qualitative observations are in agreement with quantitative kinetic studies which showed the greater effectiveness of La₂O₃ (glasses 136 and 138) in reducing the crystallization rate of cordierite in similar glasses compared to Y₂O₃ (glasses 114, 126, 129). The La₂O₃ bearing glass compositions should be more adaptable to a continuous fiberization process.

Recently, strength measurement procedures have been only slightly modified by using Banker's Wax (a hard red sealing wax) applied with a pencil-sized soldering iron to fasten the specimen to the paper tabs in place of the Khotinsky cement originally employed.

Using these procedures, the strength measurements shown in Table XLIV were obtained. The twenty-two consecutive measurements listed in this table gave an average tensile strength of 772,000 pounds per square inch and discarding the three lowest and three highest values the values range from 600,000 lbs/in.² to 1,000,000 psi. It will be noted also that there is a considerable variation in diameter. The range in strength values may be due to gas trapped in the glass or local lack of uniformity in chemical composition or variation in orifice temperature or in the level of molten glass present in the bushing. Until the effects of such variables are understood and eliminated, we cannot say with certainty what the strength of the UARL 344 glass actually is and the average value of 772,000 psi obtained should be regarded as the lower limit of strength likely to be obtained.



MAGNIFICATION 50x

FIGURE 79. CRYSTAL GROWN IN UAC 126 GLASS AT 1200 C FOR 20 MINUTES

Table XLIV
Assessment of Strength of UARL 344 Glass Fiber

<u>Diameter (mils)</u>	<u>Area (square mils)</u>	<u>Breaking Load (pounds)</u>	<u>UTS (#/in.²)</u>
0.202	0.032	0.02381	743,000
0.302	0.072	0.04938	689,000
0.199	0.031	0.03748	1,205,000
0.265	0.055	0.03307	600,000
0.190	0.028	0.03086	1,089,000
0.262	0.054	0.03307	613,000
0.226	0.040	0.03307	824,000
0.223	0.039	0.03086	790,000
0.181	0.026	0.01543	600,000
0.160	0.020	0.01984	987,000
0.199	0.031	0.02205	709,000
0.175	0.024	0.02425	1,008,000
0.199	0.031	0.01543	496,000
0.163	0.021	0.01984	951,000
0.154	0.019	0.01984	1,065,000
0.320	0.080	0.04321	537,000
0.280	0.062	0.05115	831,000
0.335	0.088	0.05379	610,000
0.323	0.082	0.04321	527,000
0.247	0.048	0.04057	847,000
0.247	0.048	0.02910	607,000
0.253	0.050	0.03263	649,000

Mean UTS 771,730 \pm 204,000 lbs/in.²

EVALUATION OF EPOXY RESIN-GLASS FIBER COMPOSITES
MADE WITH UARL GLASS FIBERS

Preliminary Research on Sizing UARL Glass
Fibers, Especially UARL 344

A preliminary evaluation of UARL 344 glass fiber in an epoxy matrix indicated that this glass has excellent strength and modulus characteristics (Table XLV). The room temperature non-aged tensile and shear strength of UARL 344 glass-epoxy composites were equivalent to composites made from "S" glass with HTS finish. However, boiling water treatment (2 hrs) of composites made from unsized UARL 344 glass caused a large reduction in shear strength from 12,000 psi to 2970 psi, indicating that a sizing or coating was required to protect the glass from abrasive deterioration and a coupling agent to prevent moisture degradation of the fiber-resin interface.

A literature and patent search was made to determine the materials that have been successful in protecting glass fiber from mechanical deterioration and glass fiber-resin composites from moisture degradation. This survey indicated that the essential components of a good surface finish consisted of a wetting agent having antistatic, lubricant, and surfactant properties and a coupling agent having hydrophobic properties, but fiber and resin bonding capabilities. With these properties under consideration, a series of formulations were prepared and evaluated using UARL 344 glass fibers. The data on the effect of two hour water boil on the short beam strength retention are given in Table XLVI. Data for unsized UARL fiber are given for comparison. The encouraging results experienced with several of the finish formulations suggested that these formulations being evaluated after exposure to more stringent conditions, namely for 24 hrs and 168 hrs (1 week) in boiling water.

The results of these studies are shown in Table XLVII. The data indicate that finishes UARL 237B, D, and C have protected the fiber-resin interface from severe degradation due to boiling water treatment for 1 week. The results are further tabulated in the form of percent retention of shear strength after exposure to boiling water for 1 week (Table XLVIII). The results of these studies show that UARL fiber, when properly protected by a surface finish, exhibits excellent shear and flexural strength and stiffness properties in a composite, even when exposed to a boiling water environment.

Comments on Composite Preparation and Properties

A series of glass-epoxy composites was fabricated and tested in order to obtain some preliminary information on the translation of fiber properties into composite properties. In addition it was anticipated that some insight would be gained in potential problem areas such as ease of fabrication, the need for coupling agents, etc. A total of ten composites was initially fabricated using ERL-2256 epoxy as the matrix and glass compositions 344 and 347 as reinforcement. It must be emphasized that the data reported below are not considered to be

Table XLV
Glass Fiber 2256-0820 Epoxy Resin Composites

UARI 344 Glass	Surface Treatment	% Void	Fiber Volume %	Density g/cc	Flexural Properties			Flexural Properties		
					Shear Strength psi	Strength 10 ³ psi	Modulus 10 ⁶ psi	Fiber Strength 10 ³ psi	Modulus 10 ⁶ psi	Norm. to 50 vol % Fiber
344-0	none	---	51	2.32	---	127 ^a	8.67	125	8.50	
344-1	none	---	74	2.61	12,000	---	12.1	---	8.20	
625	none	3.7	73	2.75	11,710	192	11.9	131	8.2	
636	none	2.6	59	2.41	14,800	264	11.6	225	9.85	
638	none	5.5	63	2.52	16,070	241	10.8	192	8.60	
<hr/>										
S-glass										
456 A	HTS	---	---	1.99	10,330	---	---	91.5	---	
SG-1	HTS	---	77	2.16	5,990 ^b	141	10.1	6.5	6.5	
634	HTS	0.6	67	5,310 ^b	---	---	---	---	---	
635	HTS	0.6	59	2.07	15,200	150	7.5	124	6.35	
637	HTS	2.9	53	1.96	14,950	150	7.4	148	7.0	

^afailed in shear, S/D = 20/1; other flex tests run at S/D = 32/1

^bstrength at room temperature after 2 hrs water boil

Table XLVI

UARL 344 Glass Fiber-Epoxy Resin Laminates - Effect of UARL Glass Finish

Composite No.	Finish ^e	Laminate Properties					
		Short Beam Shear Strength			Flex. Properties		
		Void Vol %	Fiber Vol %	Dry ^a psi	Wet ^b psi	% Retention	Strength 10 ³ psi
344-1	none	---	74	12,000	2,970	25	---
636	none	2.6	59	14,800	3,913	26	12.1
703	none	4.9	45	14,042	7,733	55	11.6
704	none	2.8	65	11,683	7,610	65	---
344-C7	3% A-1100 in acetone	---	64	12,475	8,157	65	---
706	UARL 237B	1.4	45	12,770	11,650	91	245c
707	UARL 237B	4.5	43	13,700	11,660	86	---
710	UARL 237D	1.9	59	15,650	14,580	93	10.4
711	UARL 237C	3.3	49	12,750	11,300	89	---
689	231A-1 + 231B-2	2.1	56	13,000	11,750	90	297d
690	235D + 231B-1	3.5	64	13,930	12,550	90	266c
694	231A-1 + 231B-2	3.3	54	16,350	14,850	91	239c
695	235D + 231B-2	2.5	60	16,690	15,133	91	290c
691	231A-1 + 231B-2	1.9	41	12,570	12,860	102	11.2
							157d
							8.0

^a strength at room temperature^b strength at RT after 2 hr water boil^c 4-point flexural test, measured at a span-to-depth ratio of 20/1^d 4-point flexural test measured at a span-to-depth ratio of 32/1^e this is a UARL proprietary treatment developed on UARL Corporate funds

Table XLVII

UARL 344 Glass Fiber-Epoxy Resin Laminates - Effect of UARL Glass Finish

Composite No.	Surface Treatment	Void %	Fiber Vol %	Shear Strength, psi				Flexural Properties			
				Wet ^b		Wet ^b		Strength 10 ³ psi		Modulus 10 ⁶ psi	
				Dry ^a	hrs	After	hrs	After	hrs	Wet	After
634(S-glass)	HTS ^d	0.6	67	13,920	13,820	12,230	11,800	11,750	215 ^c	---	---
689	237A + 231B-2	2.1	56	13,000	11,750	---	---	9,750	297 ^c	---	14.3
691	231A-1+231B-2	1.9	41	12,570	12,860	---	---	---	157 ^c	---	---
706	237B	1.4	45	12,770	10,650	---	---	10,680	---	---	8.0
710	237D	1.9	59	15,650	14,580	---	10,250	10,600	---	---	---
711	237C	3.3	49	12,750	11,300	---	9,730	8,420	---	190	10.9

^astrength at room temperature^bstrength at RT after the indicated no. of hrs in boiling water^c4-point flexural test measured at a span-to-depth ratio of 32/1^dthis is a UARL proprietary treatment developed on UARL Corporate funds

Table XLVIII

Shear Strength Retention of UARL 344 Glass-Epoxy Resin Composites

Composite No. & Glass	Fiber Finish ^e	Shear Strength, psi					
		Dry ^a	Wet ^b 2 hrs	% Retention	Wet ^c 72 hrs	% Retention	1 Week ^d
634(S-glass)	HHS	13,920	13,820	99	11,800	85	11,750
689	237A + 231B-2	13,000	11,750	91	---	---	9,750
691	231A + 231B-2	12,570	12,860	102	---	---	75
706	237B	12,770	10,650	86	---	---	---
710	237D	15,650	14,580	93	10,250	66	10,600
711	237C	13,750	11,300	89	9,730	76	8,420
							66

^aStrength at room temperature^bStrength at RT after 2 hr water boil^cStrength at RT after 72 hr water boil^dStrength at RT after 168 hr (1 week) water boil^eThis is a UARL proprietary treatment developed on UARL Corporate funds

representative of the best which can be obtained from high modulus glass composites for two reasons: first, the glass compositions used were those which were readily fiberized; no attempt was made to use compositions having maximum modulus; second, composite quality was not optimum due to inexperience in working with the fibers, and to the method necessary to prepare the composites.

Glass filament was drawn from a single-hole bushing and wound on a drum which had been previously covered with a sheet of mylar film. By traversing the drum from side to side during the drawing operation, a unidirectional layer of glass filaments approximately three inches wide was obtained. The "thickness" of the layer in terms of the number of filaments was dependent on the total length of filament drawn.

Impregnation of the filaments with epoxy resin was accomplished by simply brushing on a 60% solids solution of ERL-2256/acetone. The impregnated "tape" and mylar backing were then cut from the drum and b-staged in an air circulating oven for approximately 15 minutes at 100°C. The tape was next cut into pieces of the desired size, the mylar backings were removed, and the layers were stacked in a mold. The cure and post cure cycles were as follows:

<u>Time</u>	<u>Temperature</u>	<u>Pressure</u>
10 min	80°C	contact
2 hrs	80°C	200 psi
2 hrs	150°C	post cure in oven

Four point flexure tests ($S/D = 32/1$) and short beam shear tests ($S/D = 5/1$) were carried out on the composites. Fiber volume fraction was determined by a standard burn-off technique. The results of the tests are presented in Table XLV along with some comparative data for HTS-901 glass/epoxy obtained from a composite made and tested by UARL. Properties in the table are averages of three tests.

Considering the flexural modulus data, it can be seen that there was fairly good translation of fiber modulus into composite modulus. Back calculating the modulus of composition 344 using a netting analysis for the first three composites in the table results in a fiber modulus of 16.6×10^6 psi. This value is approximately 2×10^6 psi less than that determined by fiber testing. The data for the composites reinforced with 347 glass indicate that the fiber modulus is approximately 2.5×10^6 psi less than that of 344 glass, but no fiber data were available for 347 for direct comparison.

The flexural strength data must be considered in light of the failure mode of the composites. As indicated in Table XLV, three of the composites failed in shear, so in those cases the calculated flexural strengths have no relation to the tensile or compressive properties of the composite. Consequently, the values of 245×10^3 psi and 224×10^3 psi are considered to be more representative of the flexural strengths of composites reinforced with 344 and 347 glasses, respectively. The shear strengths of the composites reinforced with filaments which had no coupling agent were quite good.

It will be noted that the epoxy-resin composite with UARL glass fiber shows a modulus forty percent higher than that achievable with the most common type of competitive glass fiber, and twenty percent higher than that obtainable with the best available grade of competitive fiber. Specimens have been subjected to flexural stresses as high as 277,000 psi at which point shear failure occurred. Composite tensile strengths in excess of 300,000 psi appear likely with the UARL 344 glass fiber. Even further increases in composite strength may be realized by applying a surface finish during the preparation of the fiber although this investigation is still in the preliminary stage. Shear strengths are greater than 16,000 psi.

Micrographs of three UARL 344 glass fiber-epoxy resin composites recently prepared in our laboratory are shown in Fig. 80. While we cannot claim that these composites are as uniformly filled as similar commercial composites, it should be noted that there is virtually no glass-to-glass contact, that variation in glass size is relatively small, and that all the glass fibers are at least as round as the very best grades of tungsten or stainless steel or copper wires. It is believed, accordingly, that measurements made on these and similar composites give a valid picture of the properties of such composites.

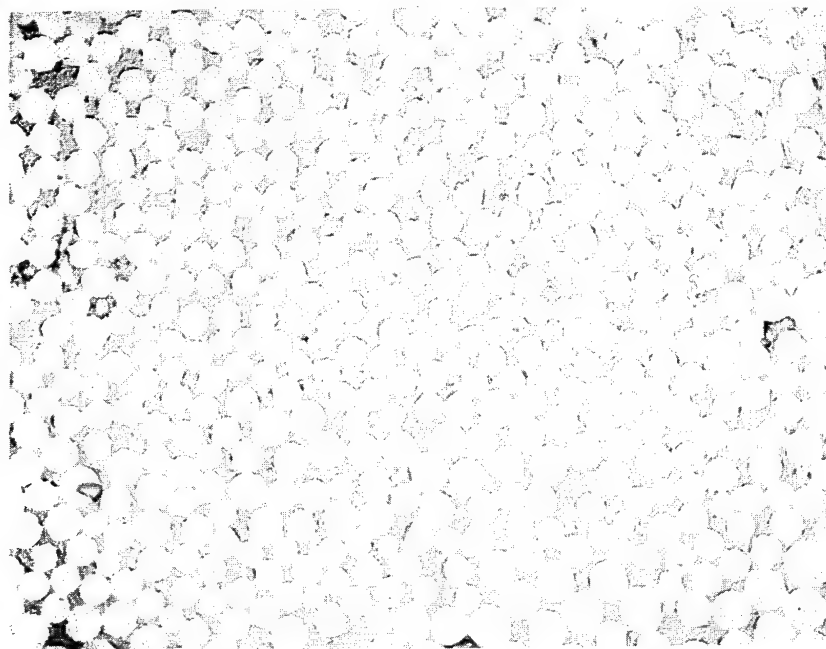
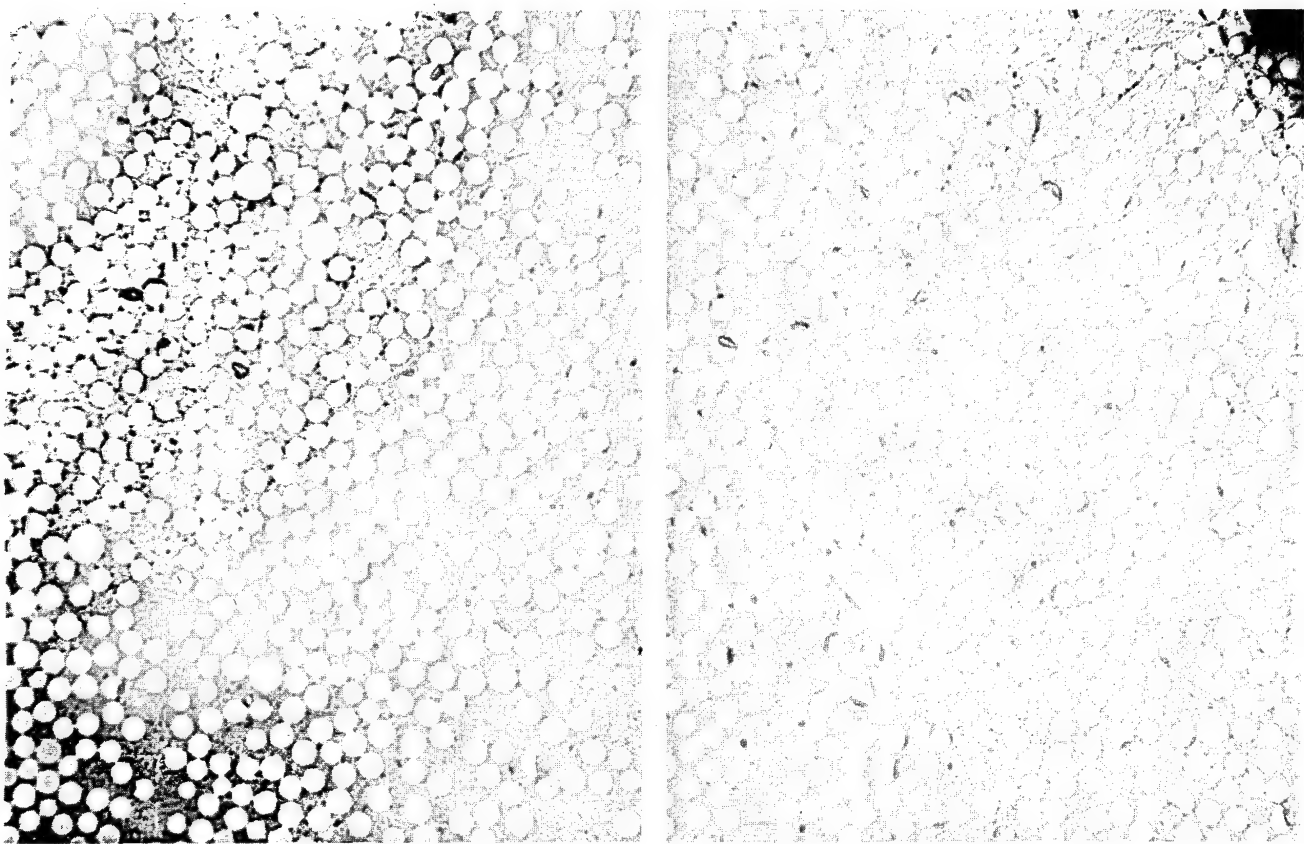
Polyimide-Fiber Glass Composites

The objective of the current work was to determine the effectiveness of the new high modulus glass as a reinforcing filament for a high temperature resin matrix as compared to conventional "S" glass.

The composites, 1 1/2 in. x 5 in. - 16 ply, were fabricated by compression molding techniques using Monsanto RS-6228 polyimide resin. The only difference in fabricating the two types of glass filament was the method used to apply the resin solution. The high modulus glass was received wound on a mandrel and the resin solution was simply painted over the wound fibers. By this technique it is difficult to achieve uniform resin thickness and fiber spacing. The "S" glass roving was coated by first drawing the tow through a dip tank of resin solution followed by drum winding, similar to graphite filament.

The composites, after post cure, were tested in flexure both at room and elevated temperature. The results are listed in Table XLIX.

In spite of the low flexural strengths obtained with the new glass filament, the high modulus, 13.65×10^6 at room temperature, indicates the excellent potential this type of glass exhibits as a reinforcing fiber in high temperature resin matrices. The poor fiber spacing as seen in Fig. 81 which shows a considerable number of fibers touching as well as the absence of a sizing or coupling agent normally employed on glass to improve bonding between fiber and resin are two factors which would account for the initial strength results obtained. Use of coupling agents as well as improved fabrication techniques will provide composites of more optimum mechanical properties.



500X ENLARGEMENT

FIGURE 80. UARL 344 FIBER GLASS-EPOXY RESIN COMPOSITES

Table XLIX
RS-6228 Polyimide/Glass Reinforced Composites

High Modulus Glass

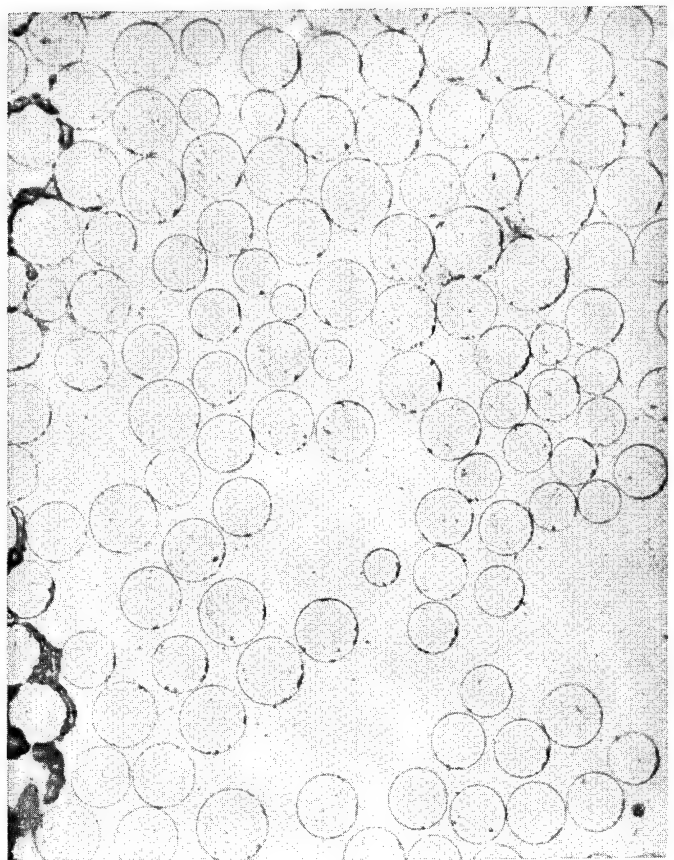
	R.T.	500°F	600°F
v/o fiber	56		
Flexural strength (psi)	85,750 ^a	58,000 ^b	38,000 ^b
Flexural modulus (psi x 10 ⁶)	13.65	10.9	6.46

"S" Glass

	R.T.	277°F	600°F
v/o fiber	67		
Flexural strength (psi)	186,000 ^a	240,000 ^b	60,000 ^b
Flexural modulus (psi x 10 ⁶)	8.26	7.6	5.85

^aMeasured by 4-point flexural test

^bMeasured by 3-point flexural test



500X

FIGURE 81. HIGH MODULUS GLASS REINFORCED POLYIMIDE COMPOSITE

Improvement in Specific Modulus of Epoxy-Glass Fiber
Composites as Fiber Modulus Increases

Calculations by Mr. R. Novak of this laboratory of the modulus of a 70 vol % glass fiber epoxy resin composition with a layup $\pm 45^\circ$ shows the marked advantage of UARL 344 glass fibers in modulus limited applications:

<u>Fiber</u>	<u>Density lbs/in.³</u>	<u>Modulus million psi</u>	<u>Specific Modulus ten million inches</u>
E	0.0776	3.27	4.21
S	0.0762	4.12	5.41
UARL 344	0.0951	6.08	6.39

These results are examined graphically in Fig. 82 as well where the results have first been normalized to 50 percent glass fiber fill.

Comparative Evaluation of UARL 344 Glass
Fiber-Epoxy Resin Impact Specimens

Full-size notched Charpy specimens were prepared from graphite fiber-epoxy resin, UARL boron fiber-epoxy resin, UARL 344 fiber glass-epoxy resin, and fully sized Owens-Corning "S" fiber glass-epoxy resin and subjected to impact in an impact testing machine. The results of the test are shown below. It will be noted that the UARL 344 glass-epoxy resin composite has a value greater than seven times that of graphite fiber-epoxy resin and three times that of boron fiber-epoxy resin. However, apparently the higher modulus of UARL 344 glass compared to Owens-Corning "S" results in a lower impact value for UARL 344 glass fiber composite at least in this case where unsized and unprotected UARL 344 glass fiber was incorporated in the composite in contrast to fully sized and protected "S" glass roving. The test, of course, will be repeated using sized specimens of UARL 344 glass fiber.

Preliminary Data on Comparative Impact Tests of Some
of the Newer Fiber-Epoxy Resin Composites

<u>Type of Sample</u>	<u>% Fiber</u>	<u>Impact Value (ft lbs)</u>	<u>Young's Modulus millions psi</u>
		<u>Full Size Notched Charpy</u>	
Graphite fiber-epoxy	55	4	50
Boron fiber-epoxy	55	10	58.5
UARL 344 glass-epoxy	63.3	30	18.6
Owens-Corning "S" glass-epoxy	65	54	12.4

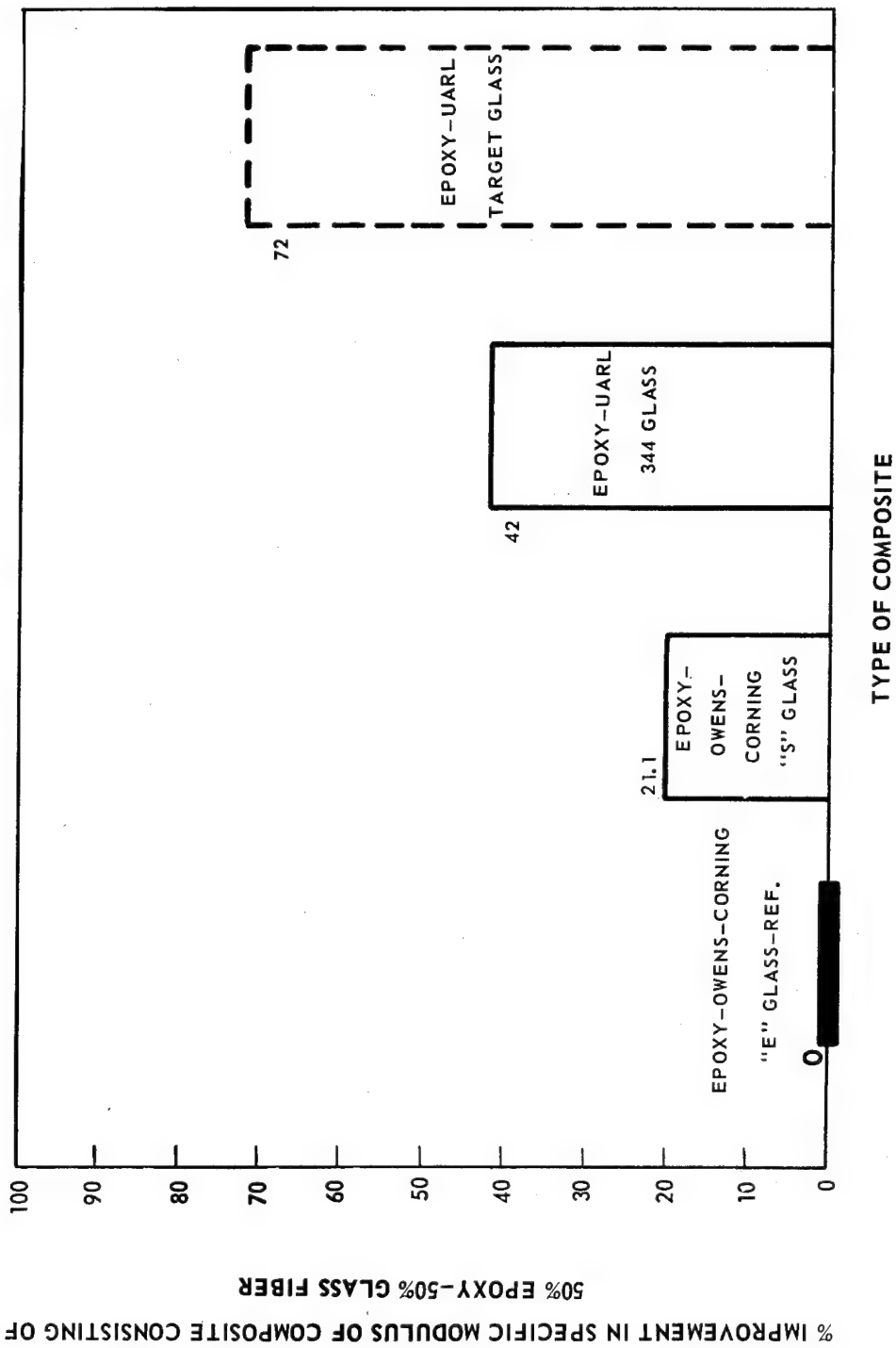
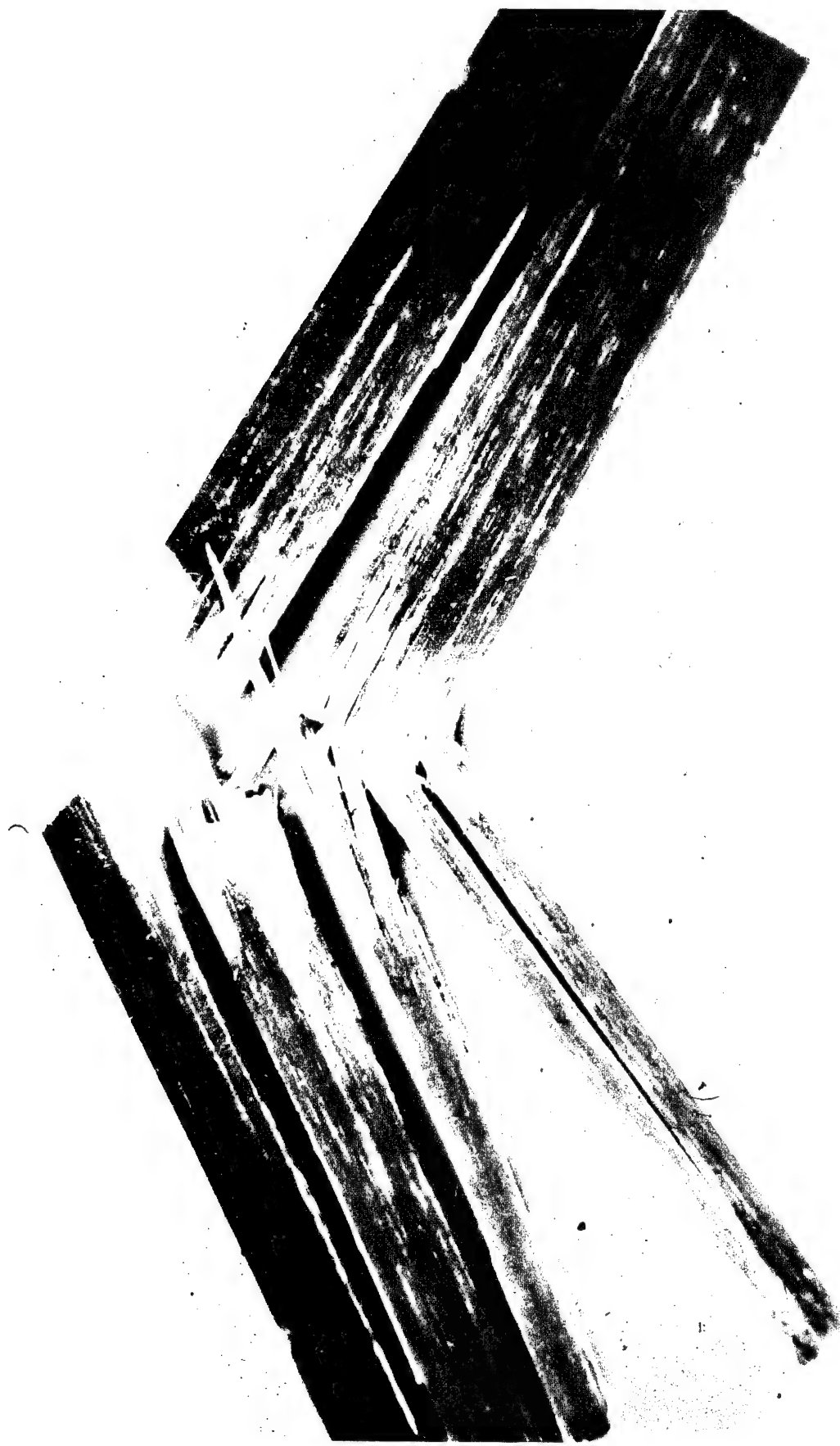


**FIGURE 82. IMPROVEMENT IN THE SPECIFIC MODULUS OF
EPOXY-50% GLASS FIBERS COMPOSITE AS
MODULUS OF GLASS FIBER IS INCREASED**

The machine used for these tests is the Tinius Olsen Testing Machine Company's "Model 64 Universal Impact Testing Machine." The hammer weighing 60 lbs undergoes a 4.4 ft drop and strikes the specimen with a velocity of 16.8 ft per second and an energy of 264 ft lbs.

The values for the fiber glass-epoxy resin composites suggests that spar propellers, for example, should be made with 3 layers of boron fiber and one of glass fiber for optimum impact resistance to form a composite-composite. The manner in which the full-sized notched Charpy impact sample fails on impact is shown in Fig. 83.

FIGURE 83. NOTCHED CHARPY IMPACT SAMPLE UARL 344E FIBER GLASS-EPOXY COMPOSITE



PRELIMINARY MANUFACTURING RESEARCH

The "poor-man's bushing" in use at UARL throughout most of the contract and described in detail in an earlier section failed to yield sufficiently uniform and defect-free fiber suitable for strength measurements. UARL has, therefore, purchased two platinum-20% rhodium single hole glass bushings of the more conventional type as shown in Fig. 84a. This design, which is a UARL design, hopefully combines the best features of single-hole bushings described by Tiede (Refs. 87,101) and the National Bureau of Standards (Ref. 102). The two bushings have now been tested and installed and one of these was used to form the large amounts of "E" glass fiber for the strength measurements already described.

In attempting to form the UARL 344 glass fiber by means of this original design single-hole bushing, the glass itself was first remelted to form a shaped slug that would fit the platinum-rhodium single-hole bushing shown in the engineering sketch as 84a. The bushing itself was insulated and heated by a massive current (1000 amperes at 1.3 volts, 60 cycle a.c.) supplied through water-cooled copper electrodes. Trouble quickly developed since with this original design bushing of Fig. 84a, the temperature at the top of the platinum bushing was approximately 350°C cooler than the temperature on the side of the bushing and just a quarter inch above the orifice. As a consequence of the lack of sufficient heat at the top of the bushing to prevent nucleation of UARL glass 344, the glass bridged across the top and interfered with the continuity of operation by making it impossible to charge a second shaped slug of glass. As a temporary expedient to alleviate this condition the installation of a gas-oxygen ring burner around the top of the bushing was suggested, but instead it seemed simpler to place a hollowed-out refractory brick carrying two silicon carbide heating element on top of the bushing with the platinum lid removed. This device proved satisfactory and allowed the necessary temperature distribution to be obtained, i.e. the top of the furnace approximately 45°C hotter than the bottom.

Even with this auxiliary top heater, no glass fibers were made initially because the glass did not form the proper shape drop close enough to the orifice. At the suggestion of Dr. W. N. Otto who was visiting UARL on other business, a water cooler was installed directly below the orifice to replace the argon jet cooling originally used and this worked satisfactorily. It was possible to carry out fiberization runs lasting several hours with this apparatus and more than five million feet of 0.4 mil fiber was prepared from the slugs of UARL 344. In the meantime, the original design of glass fiber bushing shown in Fig. 84a has been twice changed as may be seen from Figs. 84b & 84c. The resultant bushing appears as shown in the photograph of Fig. 85. Using this version of the bushing more than one hundred million feet of UARL glass fiber has been made without any serious interruptions or down time. Operating variables have included a variation in orifice temperature from 1260°C to 1310°C, a variation in the head of molten glass from 1 1/2 in. to 3/8 in., a variation in winding rates from 4000 to 8000 ft/min.

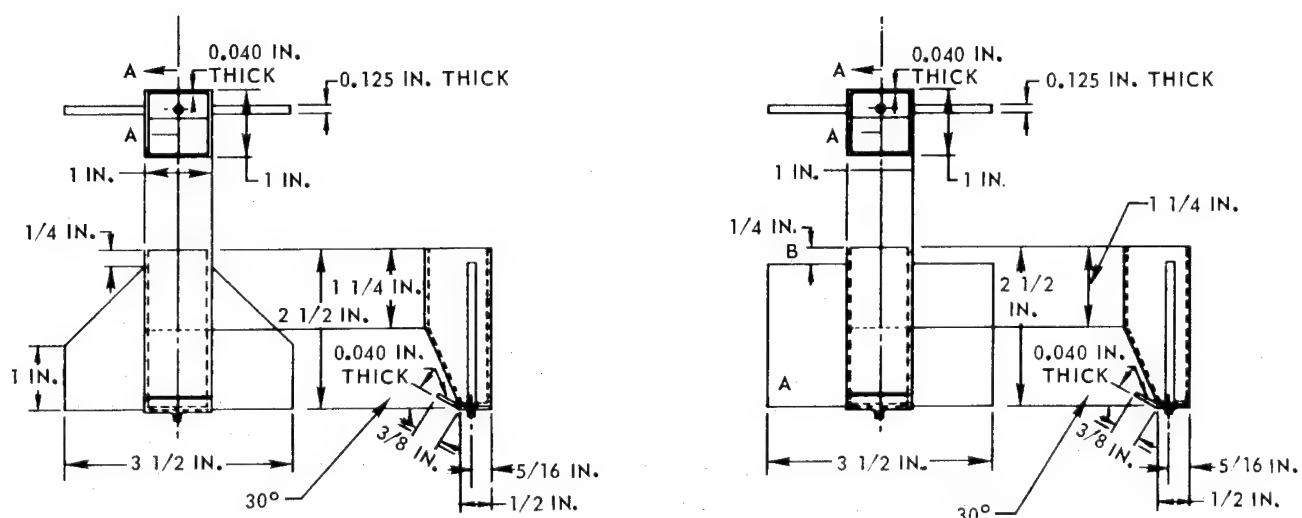
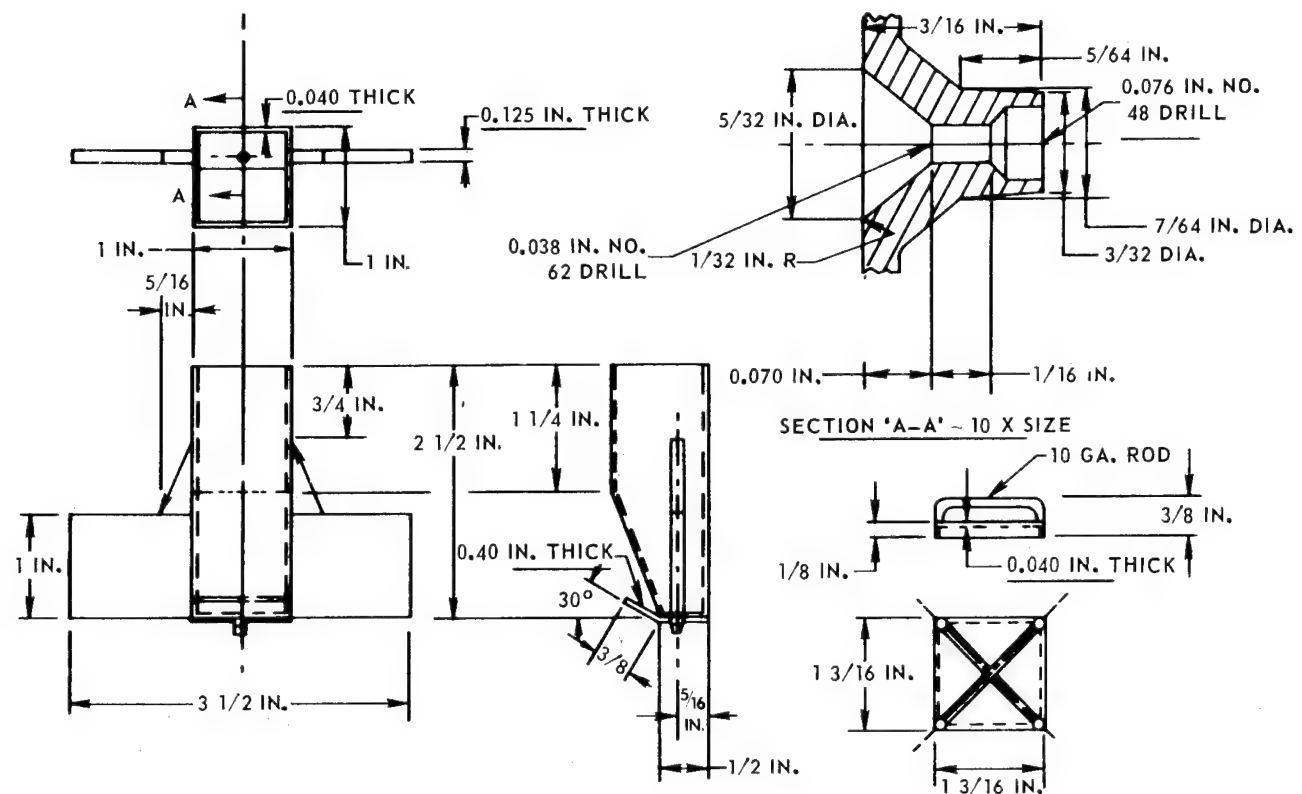


FIGURE 84. EVOLUTION OF UARL DESIGN FOR SINGLE-HOLE BUSHING

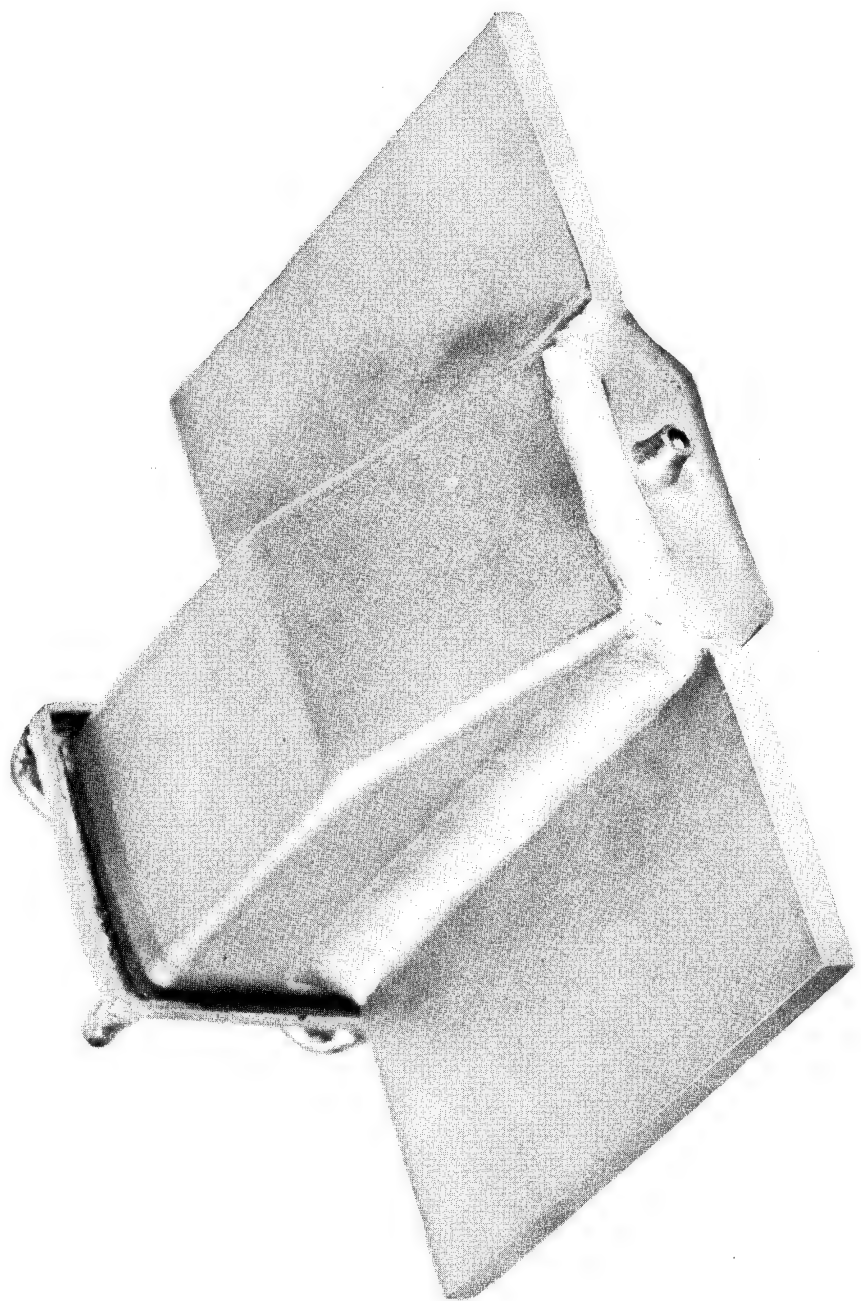


FIGURE 85. FINAL DESIGN UARL PLATINUM-RHODIUM BUSHING

The mode of operation most successful with the single-hole bushing design sketched in Fig. 84c and photographed in Fig. 85 is to completely fill the bushing with a previously prepared glass slug, heat the mold to give the desired orifice temperature, allow the drop to form and fall to the 45° deflection plate near the winder with the winder running slowly and to gradually accelerate the winder until the desired winding rates are achieved. Glass is then added at the rate of about one 3/8 in. thick slug slice every hour. The winding can be continued indefinitely in this manner or started and stopped at will. Single lengths of several million feet in one piece can be obtained during the single working shift that we normally operate. No top heater is needed with this design.

Multihole (6-hole) Bushing Operations

Recently the first attempts to draw fibers from UARL 344 glass composition through the use of a multihole bushing were made. Figure 86 shows a photograph of the six-hole bushing actually used. Figure 87 shows six glass fibers being drawn simultaneously from this bushing. Although several large-scale glass fiber manufacturers indicated that they did not think multihole operations with the UARL 344 glass composition would be feasible, actually UARL has found no problem in drawing fibers from the six-hole platinum-rhodium bushing. A typical temperature profile for the bushing during successful six-hole operation is a reading of 1315 to 1360°C for the thermocouple on the edge of the bottom weld and 1480°C for the thermocouple an inch and a quarter up from the bottom weld and on the opposite side. Hole size for this bushing is 0.038 in. diameter in marked contrast to the much larger hole size employed in most commercial bushings. The holes are placed on quarter-inch centers in two rows. Drawing speeds for successful operation have so far been in the range of 3000 ft/min to 6000 ft/min. Original trials using a water-ring cooler of the type employed in our monofilament operations showed the necessity of using alternate cooling schemes. Replacement of the water-ring with a system of small air jets for cooling proved to be satisfactory. More recently a simplified version of the air jet system comprised of only two air jets seems to be even better.

No composite samples have as yet been fabricated from UARL 344 glass fiber using the 6-hole bushing and no measurements have as yet been made on the fiber itself. Therefore, the effects of multihole operation on the properties of this glass are completely unknown at this time.

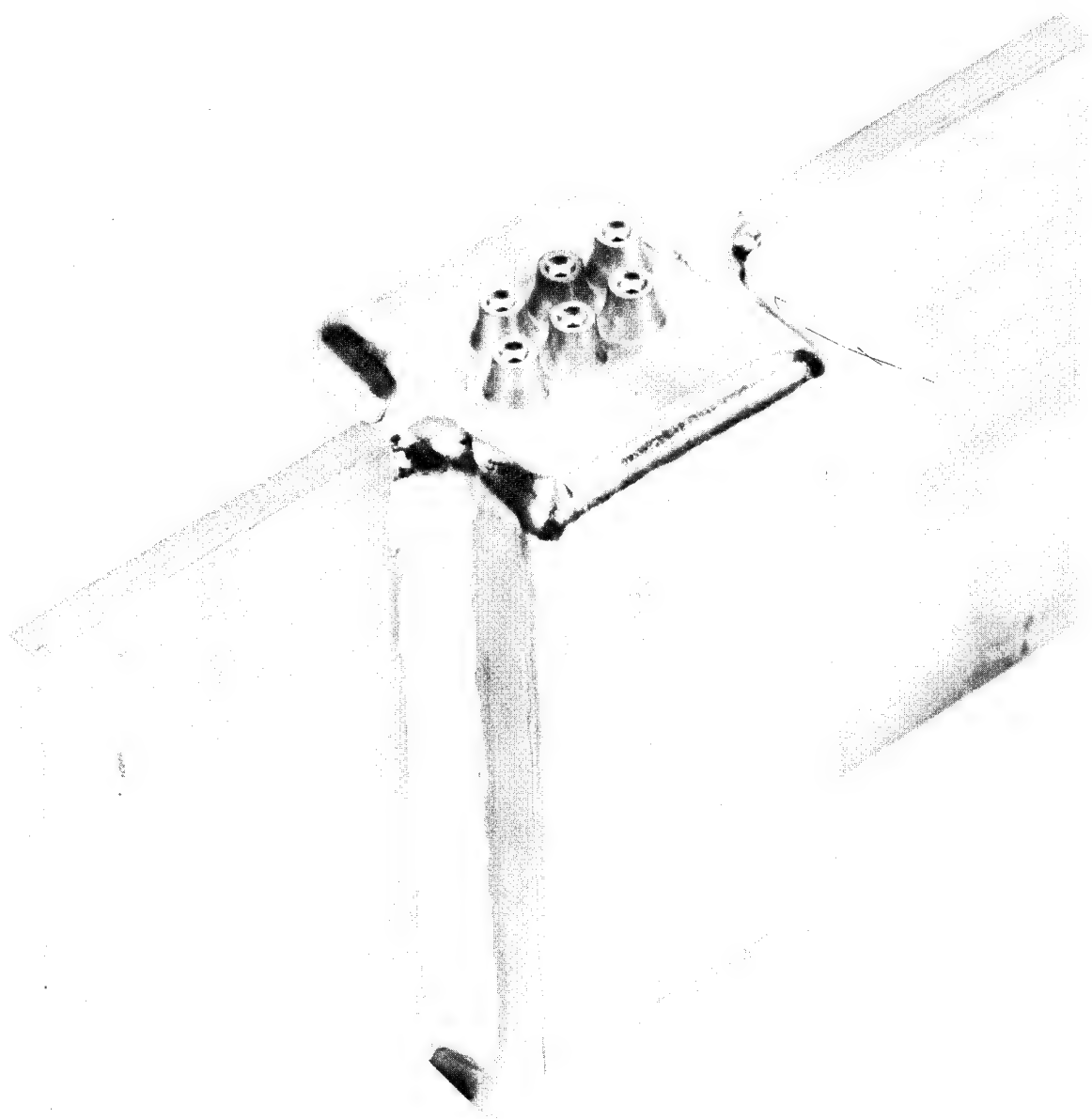


FIGURE 86. UARL DESIGN 6-HOLE PLATINUM-RHODIUM BUSHING

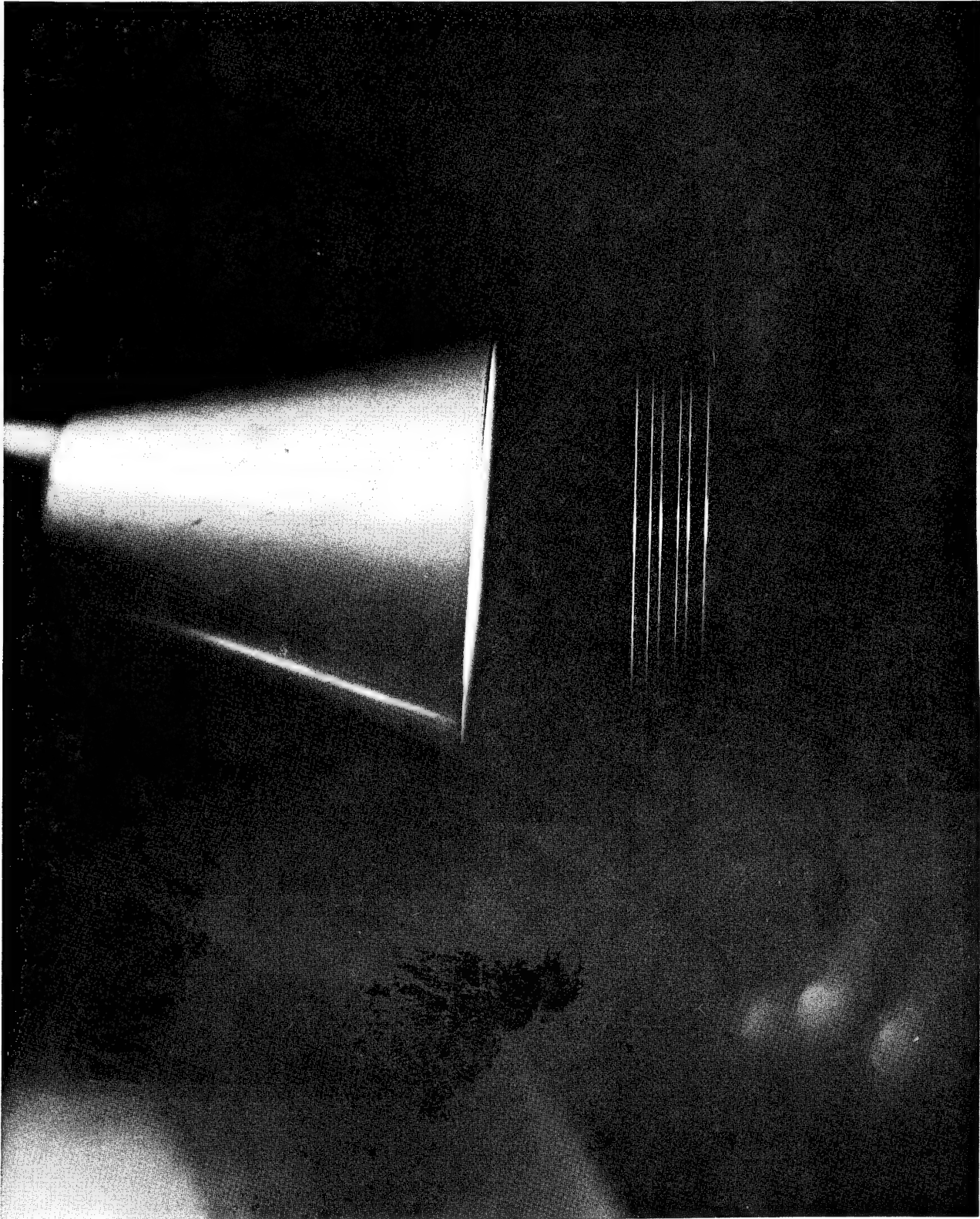


FIGURE 87. UARL 344 GLASS FIBERS ARE SIMULTANEOUSLY DRAWN FROM EXPERIMENTAL 6-HOLE BUSHING

CONCLUSIONS

1. This contract to date has produced three promising directions in which to move in search of high-modulus high-strength glass fibers.

a. The cordierite glass system with rare earths and/or zirconia as major constituents has yielded bulk glass specimens with values for Young's modulus as high as 21.1 million psi and a specific modulus of 174 million inches.

b. The UARL development of invert analog glass systems has produced bulk glass specimens with values for Young's modulus of 22.75 million psi and specific moduli of 200 million inches.

c. A preliminary exploration of two phase glass systems has indicated that the second phase develops so rapidly that it can be produced as the glass fiber is drawn with subsequent pronounced improvement in modulus. Very little research in this area has produced glasses with moduli as high as 15 million psi. These systems offer a most promising new and unexplored approach.

2. One of these compositions, UARL 344, has been used to produce more than 100 million feet of monofilament and has recently been successfully processed in a multihole (six-hole) platinum-rhodium bushing to produce continuous glass fibers at reasonable rates of speed such as 5000 ft/min. Coupled with the facts that these glass fibers in monofilament form showed a Young's modulus of 18.6 million psi, a specific modulus of 157 million inches, and a probable strength of around 770,000 psi, this glass should offer an attractive commercial product. Additional tests with UARL 344 glass fiber-epoxy resin composites including tensile strength, compressibility, static-fatigue, and boiling water tests on composites fabricated with experimental sizes should fill in the picture of the usefulness of this glass.

3. The directions in which we are altering the compositions of our non-beryllia containing glasses have sufficiently modified the working characteristics of such glasses so as to support the hope that a nonberyllia glass composition at least as useful as the UARL 344 composition will evolve.

4. Preliminary examination of the impact characteristics of the UARL glasses and epoxy resin-UARL glass fiber composites indicate that a much more careful examination of all our prior glass compositions is in order since the glasses examined showed enhanced impact resistance. These studies also indicate that our highest modulus glasses are probably not our strongest and additional studies of the strength of some of the earlier UARL compositions are clearly needed.

5. The making of glass fiber sufficiently free of defects to provide consistent strength measurements requires a conventional type single-hole glass bushing.

6. For glass fibers of nonconstant diameter due to occasional crystalline inclusions an ultrasonic pulse technique of modulus measurement is capable of yielding consistent data.

REFERENCES

1. Phillips, C. J.: Calculation of Young's Modulus of Elasticity from Composition of Simple and Complex Silicate Glasses. *Glass Technology*, Vol. 5, No. 6, Dec. 1964, pp 216-223.
2. Machlan, G. R., Owens-Corning Fiberglas Corp., Newark, Ohio: The Development of Fibrous Glasses Having High Elastic Moduli. WADC TR55-290, Nov. 1955.
3. Waugh, J. F., V. E. J. Chiochetti, H. I. Glaser, and R. Z. Schreffler, Owens-Corning Fiberglas Corp., Newark, Ohio: The Development of Fibrous Glasses Having High Elastic Moduli, Part II. WADC TR55-290, May 1958.
4. Frickert, P. J., R. L. Tiede, H. I. Glaser, and A. B. Isham, Owens-Corning Fiberglas Corp., Newark, Ohio: High Modulus, High Temperature Glass Fibers for Reinforced Plastics. WADD TR60-24, Nov. 1960.
5. Machlan, G. R., C. J. Stalego, R. L. Tiede, A. B. Isham, and D. E. Caromente, Owens-Corning Fiberglas Corp., Newark, Ohio: High Modulus, High Temperature Glass Fibers for Reinforced Plastics, Supplement 1. WADD TR60-24, March 1961.
6. McMartin, R. M., R. L. Tiede, F. M. Veazie, Owens-Corning Fiberglas Corp., Newark, Ohio: High Strength-High Modulus Glass Fibers, Part I. AFML-TR-65-90, March 1965.
7. Lambertson, W. A., D. B. Aiken, and E. H. Girard, The Carborundum Company, Res. & Dev. Div.: Continuous Filament Ceramic Fibers. WADD TR60-244, June 1960.
8. Girard, E. H., The Carborundum Company, Res. & Dev. Div.: Continuous Filament Ceramic Fibers, Part II. WADD TR60-244, Feb. 1961.
9. Drummond, W. W. and B. A. Cash, Bjorksten Res. Labs., Inc., Madison, Wis.: Development of Textile Type Vitreous Silica Yarns. WADC 59-699, Final Report, March 1960.
10. Nagler, R. T., Bjorksten Res. Labs., Inc., Madison, Wis.: High Viscosity Refractory Fibers, Quarterly Report No. 1. Contract NOrd-18492, AD 209137, July 1 - Sept. 30, 1958.
11. Drummond, W. W., Bjorksten Res. Labs., Inc., Madison, Wis.: High Viscosity Refractory Fibers, Quarterly Report No. 2. Contract NOrd-18492, AD 210948, Oct. 1 - Dec. 31, 1958.
12. Dunn, S. A. and W. P. Roth, Bjorksten Res. Labs., Inc., Madison, Wis.: High Viscosity Refractory Fibers, Quarterly Report No. 3. Contract NOrd-19100, AD 242218, Apr. 20 - July 20, 1960.

REFERENCES (Cont'd)

13. Dunn, S. A. and W. P. Roth, Bjorksten Res. Labs., Inc., Madison, Wis.: High Viscosity Refractory Fibers, Quarterly Report No. 5. Contract NOrd-19100, Oct. 30 - Jan. 31, 1961.
14. Rowe, E., D. Silvey, and G. Thomas, B. F. Goodrich Research Center, Brecksville, Ohio: New High-Strength Glasses. Paper presented at Sect. 4-C, 18th Annual Conference, Tech. and Management, Reinforced Plastic Division, pp 1-8, Feb. 5-7, 1963. Chicago, Ill., The Society of the Plastics Industry, Inc.
15. Kroenke, W. J., E. H. Rowe, and G. L. Thomas, B. F. Goodrich Research Center, Brecksville, Ohio: Structured Glasses Patterned After Asbestos, Part I. Contract AF33(657)8905, RTD-TDR-63-4043, Apr. 30, 1963.
16. Kroenke, W. J., B. F. Goodrich Research Center, Brecksville, Ohio: Linear Structured Glass Fibers, Quarterly Progress Report. AF33(657)8905, Sept. 1 - Nov. 30, 1964.
17. Kroenke, W. J., B. F. Goodrich Research Center, Brecksville, Ohio: Flexible Glass Fibers. Contract AF33(657)8905, Project 7320- Task No. 732001, TDR-ML-TDR-64-119, March 1964.
18. Kroenke, W. J., B. F. Goodrich Research Center, Brecksville, Ohio: Isotropic Glass Fibers and Property-Composition Relationships. Contract AF33(657)8905, AFML-TR-65-189, Project 7320, Task No. 732001, 1965.
19. Otto, W. H., Narmco Res. & Dev. Div., San Diego, Calif.: Silica Fiber Forming and Core Sheath Composite Fiber Development, Final Summary Technical Report. Navy, BuWeps N600(19)59607, Jan. 3, 1964.
20. Otto, W. H., Narmco Res. & Dev. Div., Whittaker Corp., San Diego, Calif.: Silica Fiber/Core-Sheath Fiber, Quarterly Progress Report No. 1. BuWeps N600(19)61810, May 30, 1964.
21. Otto, W. H., Narmco Res. & Dev. Div., Whittaker Corp., San Diego, Calif.: Silica Fiber/Core-Sheath Fiber, Quarterly Progress Report No. 2, BuWeps N600(19)61810, Aug. 31, 1964.
22. Otto, W. H., Narmco Res. & Dev. Div., Whittaker Corp., San Diego, Calif.: Silica Fiber/Core-Sheath Fiber/High-Temperature Oxide Fibers, Quarterly Progress Report No. 4. BuWeps N600(19)61810, Feb. 10, 1965.
23. Otto, W. H., D. Plaskon, and D. Bradford, Narmco Res. & Dev. Div., Whittaker Corp., San Diego, Calif.: Silica Fiber/Core-Sheath Fiber, Final Tech. Report. Navy, BuWeps Contract N600(19)61810, June 15, 1965.

REFERENCES (Cont'd)

24. Schmitz, G. K. and A. G. Metcalfe, Solar, Subsidiary of International Harvester Co., San Diego, Calif.: Exploration and Evaluation of New Glasses in Fiber Form, Final Report. NRL Project 62 R05 19A, RDR 1266-7, Apr. 12, 1963.
25. Schmitz, G. K., Solar, Subsidiary of International Harvester Co., San Diego, Calif.: Exploration and Evaluation of New Glasses in Fiber Form, Bimonthly Progress Report No. 2. RDR 1343-2, June 24, 1963.
26. Schmitz, G. K. and A. G. Metcalfe, Solar, Subsidiary of International Harvester Co., San Diego, Calif.: Exploration and Evaluation of New Glasses in Fiber Form, Bimonthly Progress Report No. 6. NRL Project 62 R05 19A, Contract NONR 3654(00) (X), Jan. 15, 1965.
27. Davies, L. G. and J. C. Withers, Materials Div., General Technologies Corp., Alexandria, Va.: A Study of High Modulus, High Strength Filament Materials by Deposition Techniques, 1st Bimonthly Report. Contract N0W 64-0176-E N64 14676, Unclassified, Code 3, Jan. 15, 1964.
- 28 through 35. Capps, W., D. H. Blackburn, M. H. Black, H. F. Shermer, and A. A. Edwards: The Development of Glass Fibers Having High Young's Moduli of Elasticity. Nat. Bur. of Standards Reports 3978, 4176, 4318, 4417, 4572, 4699, 4850, 5188. Bur. Ord., U. S. Navy Contract IPR N0rd 03046, NBS Project 0902-20-4464, Dec. 1954 - Apr. 1, 1957.
36. Lasday, A. H., Houze Glass Corp.: Development of High Modulus Fibers from Heat Resistant Materials. WADC TR 58-285, ASTIA Doc. No. 202500, Contract AF33(616)-5263, Project 7340, Oct. 1958.
37. Brossy, J. F. and J. D. Provance, Houze Glass Corp.: Development of High Modulus Fibers from Heat Resistant Materials, Part II. WADC TR58-285, ASTIA Doc. 236991, Contract AF33(616)-5263, Project 7340, March 1960.
38. Lewis, A. and D. L. Robbins, Glass Technology Section, Von Karman Res. Center, Aerojet-General Corp., Azusa, Calif.: High-Strength, High-Modulus Glass Filaments, Part I. AFML-TR-65-132, April 1965.
39. Fleming, J. D., Engineering Experiment Station, Georgia Inst. of Technology, Atlanta, Ga.: Fused Silica Manual, Final Report. Contract AT-(40-1)-2483, Sept. 1, 1964.
40. Phillips, B. and R. Roy, Pennsylvania State University: Studies Related to The Crystallization of Glasses: Controlled Phase Separation Due to Meta-stable Liquid Immiscibility in Simple Silicate Systems, Tech. Report No. 2, Contract NONR 4089(00), Metallurgy Branch, ONR, May 15, 1964.

REFERENCES (Cont'd)

41. Frechette, V. D. (Editor): Non-Crystalline Solids. John Wiley and Sons, Inc., New York, 1960. Douglas, R. W., Chapter 16, pp 378, 405.
42. Charles, R. J.: Article on The Nature of Glasses. Scientific American, Vol. 217, No. 3, pp 127-136, Sept. 1967.
43. Wells, A. F.: Structural Inorganic Chemistry, Third Edition, Oxford University Press, London, 1962.
44. Klingsberg, C. (Editor): The Physics and Chemistry of Ceramics. Gilman, J. J.: The Strength of Ceramic Crystals. Gordon & Breach, New York, pp 246-274, 1963.
45. Bacon, James. F., R. B. Graf, G. K. Layden: Investigation of the Kinetics of Crystallization of Molten Binary and Ternary Oxide Systems, Summary and Quarterly Status Report No. 10, Contract NASW-1301, Apr. 1, 1968.
46. Kuan-Han Sun: U.S. Patent 2,456,033, issued Dec. 14, 1948.
47. Weissenberg, Gustav and Otto Ungemach: U.S. Patent 2,764,492, issued Sept. 25, 1956.
48. Morey, George W.: U.S. Patent 2,150,694, issued Mar. 14, 1939.
49. DePaoli, Paul F.: U.S. Patent 2,787,554, issued Apr. 2, 1957.
50. Weyl, W. A. and E. C. Marbox: The Constitution of Glasses, Vol. II - Constitution and Properties of Some Representative Glasses, Interscience Publ., New York, p 820, 1964.
51. Hafner, H. C., N. J. Kreidl, and R. A. Weidel: Optical and Physical Properties of Some Calcium Aluminate Glasses. Journ. of the Amer. Ceramic Society, Vol. 41, No. 8, pp 315-323, Aug. 1958.
52. Rawson, H.: Inorganic Glass-Forming Systems. Academic Press, London and New York, 1967.
53. Weyl, W. A. and E. C. Marboe: The Constitution of Glasses, Vol. II: Constitution and Properties of Some Representative Glasses, Part I. Interscience Publishers (John Wiley & Sons), New York, pp 757-790 and Section 5, p 531, 1964.
54. Ram, Atma, S. N. Prasad, and K. P. Srivastava: Viscosity of Copper Ruby Glass in and Below the Striking Range of Temperature. Glass Technology, Vol. 9, No. 1, pp 1-4, Feb. 1968.

REFERENCES (Cont'd)

55. Weyl, W. A. and E. C. Marboe: The Constitution of Glasses, Vol. I. Interscience Publishers (John Wiley & Sons), New York, pp 245-248, 1962.
56. Krebs, H.: The Structure of Glasses. Angew. Chem., International Edition, Vol. 5, No. 6, pp 544-554, 1966.
57. Argyle, J. F. and F. A. Hummel: Liquid Immiscibility in the System BaO-SiO₂. Physics and Chem. of Glasses 4, pp 103-105, 1963.
58. Cahn, J. W. and R. J. Charles: The Initial Stages of Phase Separation in Glasses. Physics and Chem. of Glasses 6, 5, 181-191, October 1965.
59. Charles, R. J.: Phase Separation in Borosilicate Glasses. Journ. Am. Cer. Soc., Vol. 47, No. 11, pp. 559-563, November 1964.
60. Herczog, A.: Microcrystalline BaTiO₃ by Crystallization from Glass. Journ. Am. Cer. Soc. 47, 107-115.
61. Hummel, F. A., T. Y. Tien and K. H. Kim: Studies in Lithium Oxide Systems: VIII, Application of Silicate Liquid Immiscibility to Development of Opaque Glazes. Journ. Amer. Cer. Soc., Vol. 43, No. 4, pp- 192-197, April 1960.
62. Johnson, D. W. and F. A. Hummel: Phase Equilibria and Liquid Immiscibility in the System PbO-B₂O₃-SiO₂. J. Amer. Cer. Soc., Vol. 31, 4, 196-201, April 1968.
63. Levin, E. M. and G. W. Cleek: Shape of Liquid Immiscibility Volume in the System Barium Oxide-Boric Oxide-Silica. J. Amer. Cer. Soc., Vol. 41, No. 5, pp. 175-179, May 1958.
64. Ohlberg, S. M., H. R. Golob, C. M. Hollabaugh: Fractography of Glasses Evidencing Liquid-in-Liquid Colloidal Immiscibility. J. Am. Cer. Soc., Vol. 45, No. 1, 1-4, January 1962.
65. Ohlberg, S. M., J. J. Hammel and H. R. Golob: Phenomenology of Non-Crystalline Microphase Separation in Glass. J. Am. Cer. Soc., Vol. 48, No. 4, pp. 178-180, April 1965.
66. Rindone, G. E.: Further Studies of the Crystallization of a Lithium Silicate Glass. Jour. Am. Cer. Soc., Vol. 45, 1, 7-12, January 1962.
67. Rockett, T. J., W. R. Foster and R. G. Ferguson, Jr.: Metastable Liquid Immiscibility in the System Silica-Sodium Tetraborate. J. Am. Cer. Soc. 48, 6, 329-332, June 1965.
68. Roy, R.: Metastable Liquid Immiscibility and Nucleation Subsolidus. J. Am. Cer. Soc. 43, 670-671.

REFERENCES (Cont'd)

69. Sastry, B. S. R. and F. A. Hummel: Studies in Lithium Oxide Systems: III, Liquid Immiscibility in the System Li_2O - B_2O_3 - SiO_2 . *J. Am. Cer. Soc.*, Vol. 42, 2, pp 81-88, Feb. 1959.
70. Tichane, R. M. and G. B. Carrier: Microstructure of a Soda-Lime Glass Surface. *J. Am. Cer. Soc.*, Vol. 44, No. 12, pp 606-610, Dec. 1961.
71. Tran, T. L.: Study of Phase Separation and Devitrification Products in Glasses of the Binary System, Na_2O - SiO_2 .
72. Watanabe, M., H. Noake and T. Aiba: Electron Micrographs of Some Borosilicate Glasses and Their Internal Structure. *J. Am. Cer. Soc.*, Vol. 42, No. 12, pp 593-599.
73. Janakiramarao, Bh. V.: Neo-Ceramic Glasses and Their Structure. *Glass Technology*, Vol. 5, No. 2, pp 67-77, Apr. 1964.
74. Stanworth, J. E.: *Physical Properties of Glass*. Oxford Univ. Press, London, 1950.
75. Tiede, R. L.: U.S. 3,127,277; 2,640,784; 2,571,074; 3,132,033; 2,640,784.
76. Armistead, W. H.: U.S. 2,517,459 and 2,433,883.
77. Bastian, R. R. and A. C. Ottojon: U.S. 2,978,341.
78. Labino, D.: U.S. 2,685,526.
79. Shartsis, Leo and Sam Spinner: Viscosity and Density of Molten Optical Glasses. *J. Res. N.B.S.*, Vol. 46, No. 3, R. P. 2190, pp 176-194, March 1951.
80. Bacon, James. F., A. A. Hasapis, and J. W. Wholley, Jr.: Viscosity and Density of Molten Silica and High Silica Content Glasses. *Physics and Chemistry of Glasses*, Vol. 1, No. 3, pp 90-98, June 1960.
81. Morley, J. G.: Crystallization Kinetics in Some Silicate Glasses, Part I, Apparatus for the Direct Measurement of Crystal Growth at High Temperatures. *Glass Technology*, Vol. 6, No. 3, pp 69-76.
82. Meiling, G. S. and D. R. Uhlmann: Paper 33-G-67, 69th Annual Meeting, American Ceramic Society, New York; Abstract, *Am. Cer. Soc. Bull.*, 46, No. 4, p 397, 1967.
83. Keith, M. L. and J. F. Schairer: *Jour. Geol.*, 60, p 181, 1952.
84. Schreyer, W. and J. F. Schairer: *Jour. Petrology*, 2, Part 3, p 324, 1961.

REFERENCES (Cont'd)

85. Swift, H. R.: J. Am. Cer. Soc., 30, pp 165-169, 1947.
86. Milne, A. J.: J. Soc. Glass Tech., 36, p 275, 1952.
87. Tiede, R. L.: Improved Apparatus for Rapid Measurement of Viscosity of Glass at High Temperature. J. Amer. Ceramic Soc., Vol. 42, pp 537-541, 1959.
88. Pickett, Gerald: Equations for Computing Elastic Constants from Flexural and Torsional Resonant Frequencies of Vibration of Prisms and Cylinders. Proceedings ASTM 45, 846, 1945.
89. Lowenstein, K. L.: Studies in the Composition and Structure of Glasses Possessing High Young's Moduli, Part I. The Composition of High Young's Modulus Glass and the Function of Individual Ions in the Glass Structure. Physics & Chemistry of Glasses, Vol. 2, No. 3, pp 69-82, June 1961.
90. Weyl, W. A. and E. C. Marboe: The Constitution of Glasses, Vol. 2, Part I. Constitution and Properties of Some Representative Glasses, Chapter XVII, Sect. 5, p 531, Interscience Publishers, John Wiley and Sons, Inc., New York, 1964.
91. Bacon, James F.: Investigation of the Kinetics of Crystallization of Molten Binary and Ternary Oxide Systems, Summary & Quarterly Status Report No. 4. Contract NASW-1301, Sept. 30, 1966.
92. Brown, S. D. and G. Y. Onoda, Jr.: High Modulus Glasses Based on Ceramic Oxides, Final Report. Contract N0w-65-0426-d, Rocketdyne with Bureau of Naval Weapons, AD 642 259 (R-6692), Oct. 1966.
93. Burke, J. E.: Progress in Ceramic Science, Vol. 1, Chapter 5.
R. W. Douglas: The Properties and Structure of Glasses. Pergamon Press, New York, pp 203-204, 1961.
94. Robbins, D. L. and A. Lewis: High-Strength, High-Modulus Glass Filaments. Aerojet General Corp. Technical Report AFML-TR-65-132, Part II, May 1966; Air Force Materials Laboratory, Research and Technology Div., Air Force Systems Command, Wright-Patterson Air Force Base, Ohio.
95. Provance, Jason D.: U.S. 3,044,888, patented July 17, 1962.
96. Pauling, L.: Nature of the Chemical Bond. Cornell University Press, Ithaca, New York, 1945.
97. Fowler, K. A.: Elastic Moduli of Thin Filaments and Fibers by Thin Line Ultrasonics. Technical Memorandum No. 2, Panametrics, Inc., Nov. 1969.

REFERENCES (Cont'd)

98. Thomas, W. F.: Phys. & Chem. Glass, Vol. 1, pp 4-18, 1960.
99. Anderegg, F. O.: Ind. & Eng. Chem., Vol. 31, pp 290-298, 1939.
100. Schile, R. D. and G. A. Rosica: Rev. Sci. Instruments, Vol. 38, pp 1103-1104, 1967.
101. Tiede, R. L.: Viscometer for Measuring Glass Viscosity by Means of Flow Through An Orifice. J. Amer. Cer. Soc., Vol. 38, No. 5, pp 183-186, May 1955.
102. Capps, Webster and Douglas H. Blackburn: The Development of Glass Fibers Having Young's Moduli of Elasticity. Nat. Bur. Standards No. 5188, April 1957.

ABSTRACTS OF THREE PAPERS PRESENTED DURING
THE CONTRACTUAL PERIODS

We enclose, for completeness, the abstracts of three papers presented at the meetings during the course of the contract. The first of these papers will be published shortly as part of the proceedings of the 1969 Annual Meeting of the International Commission on Glass.

Paper presented at Joint Meeting of International Commission on Glass and The Canadian Ceramic Society, Toronto, Canada, Sept. 3-6, 1969

Studies of the Young's Modulus of Magnesia-Alumina-Silica-Rare Earth Glass Systems with Respect to their Composition and Crystallization Kinetics

Glasses prepared from mixtures of magnesia-alumina-silica in such proportions that their primary crystal phase on devitrification is either sapphirine or cordierite, and to which either a rare earth oxide or zirconia have been added have been found to have unusually high values of Young's modulus. After preparation these glasses are characterized by measurement of their density, modulus, and fiberizability. Examination of the results obtained showed that the moduli of these glasses can be successfully calculated by the methods of C. J. Phillips (Ref. 1) and that the molar coefficients for the rare-earths ceria, lanthana, and yttria as well as for zirconia are as large or larger than the corrected Phillips' molar coefficient for beryllia.

Direct microscopic observations of the kinetics of crystallization of the MgO-Al₂O₃-SiO₂-rare earth systems showed that the rare-earths added to increase Young's modulus also had the beneficial result of actively delaying the onset of devitrification.

The techniques used in preparing these high melting glass compositions, in determining their fiberizability, in studying their crystallization rates, and in preparing and evaluating the samples used for modulus measurement are sketched briefly. (The results of the several experiments are tabulated.) These results show that the most favorable non-toxic composition found had a value for Young's modulus of slightly more than 20 million pounds per square inch while cordierite base compositions to which beryllia was intentionally added yielded glasses with Young's modulus as high as twenty-two million pounds per square inch.

Paper presented at the Symposium of New England Section of the American Ceramic Society "Ceramic Spectrum in New England", Massachusetts Institute of Technology, Cambridge, Mass., October 21, 1970

Recent Developments of High Modulus Glass Fibers

The Research Laboratories of the United Aircraft Corporation under Contract NASW-1301 and its successor, NASW-2013 by James J. Gangler of NASA/OART Washington Headquarters, have originated more than 450 new glass compositions. These compositions can most readily be discussed in three categories: high modulus glasses containing beryllia as a constituent, high modulus glasses without beryllia, and two-phase glasses. Alternately, the discussion can be carried out under three other headings; namely, cordierite base glasses with and without beryllia, invert-analog glasses with and without beryllia, and two-phase glass systems. The talk today will use this second set of headings as most illustrative of the mode of approach employed in originating the new glasses.

In the case of the cordierite base glasses, i.e. magnesia-alumina-silica-rare earth glasses, it was found by studying the glass crystallization kinetics that the rare earth oxides delayed the onset of devitrification so that such compositions proved suitable for the production of rapidly chilled bulk glasses and glass fibers having high elastic moduli. It was also found possible to calculate the Young's modulus of the cordierite or beryl base glasses by the methods of C. J. Phillips (Ref. 1). Experimental determination of the molar coefficients for elements such as yttria, lanthana, and ceria not only showed their molar contributions to Young's modulus to be as great or greater than the corrected molar contribution of beryllia but also increased the range of compositions to which Phillips-type calculations could be applied.

New glasses of the invert analog-rare earth glass systems proved to have even higher moduli than the cordierite or beryl base glasses but were not as readily fiberizable. The best of these glasses is UARL 383 which has a value for Young's modulus in the bulk state of 22.8 million psi and a specific modulus of 200 million inches and is free of beryllia. It is not yet possible, however, to predict the Young's modulus of these glasses by Phillips-type calculations.

One particular UARL glass, namely, UARL 344, has been studied extensively. This glass in bulk state has a Young's modulus of 20.3 million psi and a specific modulus of 168 million inches. As fiber, UARL 344 has a Young's modulus of 18.6 million psi, a specific strength of 161 million inches, a probable strength of around 770,000 psi. It can readily be fiberized both in a single-hole bushing (over 50,000,000 lineal feet) and a multi-hole or six-hole bushing and can be easily made into fiber glass-epoxy resin composites. The results of evaluation of such composites proved that a UARL 344 glass fiber-epoxy resin composite has a modulus 40 percent better than that achievable using the more common grade of competitive glass fiber and 20 percent better than that obtainable with the best available grade of competitive glass fiber. In addition, UARL 344 glass fiber-epoxy resin composites have an impact resistance seven times greater than similar composites made with graphite fiber.

The mode of fracture of UARL 344 glass in the bulk state is interesting and has caused us to start examining some of our other glasses for impact resistance and mode of fracture. Extremely preliminary research indicates that some of the UARL high modulus glasses with lower moduli may have much greater strength. In conclusion, some of the problems in measuring moduli, strength, and impact resistance are briefly discussed.

Paper presented at ASTM Symposium on "High Performance Fibers-Properties, Applications and Test Methods", Williamsburg, Va., Nov. 17-18, 1970

The Origination and Testing of New High-Modulus Glass Fibers

Contract NASW-1301 and its successor, NASW-2013 monitored by J. J. Gangler of NASA Headquarters and carried out by the United Aircraft Research Laboratories, is almost at the end of its fifth year. In this time, approximately 500 new glass compositions have been prepared. Of these, a total of a dozen glass compositions have values for Young's modulus measured on bulk specimens greater than twenty million pounds per square inch and another dozen have values between nineteen and twenty million pounds per square inch as bulk specimens. The glasses originated belong either to the magnesia-alumina-silica-rare earth glass family having as their primary crystal phase on devitrification either sapphirine or cordierite or to the invert analog-rare earth glass system.

In the case of the magnesia-alumina-silica-rare earth glasses, it was found by studying their crystallization kinetics that the rare earth oxides delay the onset of devitrification so that such compositions prove suitable for the production of rapidly chilled bulk glasses and glass fibers having high elastic moduli. It has also been found possible to calculate the Young's modulus of the magnesia-alumina-silica-rare earth glasses by the methods of C. J. Phillips (Ref. 1). These calculation procedures proved to be readily extendable to a greater range of glass compositions by determining experimentally the molar coefficients for elements such as yttria, lanthana, and ceria. When these experimental values were obtained, it was found that the molar contributions to Young's modulus of these elements were as great or greater than the corrected molar contribution for beryllia.

From the new glasses of the magnesia-alumina-silica-rare earth family and the invert analog-rare earth glass system, eighty-seven of the compositions proved suitable for the production of mechanically-drawn fibers on a laboratory basis, although this is not the same as saying that they are readily fiberizable on a commercial scale. At this time, the best of these UARL glass fibers has a Young's modulus of 19.8 million pounds per square inch. Another of these fibers which is undoubtedly producible on a commercial scale judged from the viscosity-temperature relationships is UARL 344. This glass, in the fiber state, has a modulus of 18.6 million pounds per square inch, a specific modulus of 157 million inches, and has already been produced in quantities greater than 25 million lineal feet of 0.2 to 0.4 mil diameter monofilament at rates up to 10,000 ft per minute.

Not only has the UARL glass been studied as a monofilament, but it has been successfully incorporated in several plastic matrices. The results of the evaluation of these composites proved that a UARL 344 glass fiber-epoxy resin composite has a modulus 40 percent better than that achievable using the more common grade of competitive glass fiber and 20 percent better than that obtainable with the best available grade of competitive glass fiber.

SUMMARY OF PATENT APPLICATIONS

In connection with the contract and in agreement with NASA procedures, four patent applications have been filed and NASA waivers received on the same. These applications are UARL code numbers R-1156, R-1333, R-1335, R-1480 respectively. Their summaries are as follows:

R-1156. Glass Compositions with A High Modulus of Elasticity

Summary of the invention. - The glass compositions of the present invention comprise silica, alumina and magnesia together with at least 5% by weight of one or more uncommon oxides such as lanthana, ceria, or yttria. In some cases certain other glass forming ingredients may be included in the formulation either in the nature of partial substitutions or as additions to the basic elements.

R-1333. Nontoxic Invert Analog Glass Compositions of High Modulus

Summary of the invention. - The glass compositions of the present invention are an invert glass which, in their preferred form, comprise a combination of silica, the monovalent oxide of lithium, two or more bivalent oxides, at least one trivalent oxide, and one or more tetravalent oxides. More particularly, the glass compositions preferably comprise a combination of silica, the monovalent oxide of lithium, two or more bivalent oxides selected from the group consisting of CaO, ZnO, MgO, and CuO, at least one trivalent oxide selected from the group consisting of Al₂O₃, Y₂O₃, La₂O₃, B₂O₃, Sm₂O₃ and the mixed rare earth oxides (which average out as a trivalent oxide) and from 0-15 mol % of one or more tetravalent oxides selected from the group consisting of CeO₂, ZrO₂, and TiO₂. It will be noted that while the glasses are comprised substantially of only one alkali oxide and a combination of alkaline earth oxides and trivalent and tetravalent oxides, the glass compositions may also contain certain additional minor amounts of tetravalent or sesquivalent oxides or fluorides commonly employed in optical glass making such as tantalum pentoxide or tungsten trioxide.

R-1335. Cordierite-Uncommon Oxide Glasses Containing Beryllia

Summary of the invention. - The glass compositions of the present invention generally comprise silica, alumina, magnesia and beryllia together with at least 5% by weight of one or more uncommon oxides such as lanthana, ceria, yttria, samaria, zirconia or mixed rare earth oxides. In some cases certain other glass forming ingredients may be included in the formulation either in the nature of partial substitutions or as additions to the basic elements. In all cases, however, beryllia is present, when compared to the uncommon oxides on a molal basis, in a ratio of from 1/2 to 3/1.

R-1480. High Modulus Invert Analog Compositions Containing Beryllia

Summary of the invention. - The glass compositions of the present invention preferably comprise a combination of silica, the monovalent oxide of lithium, two or more bivalent oxides, at least one trivalent oxide, and one or more tetravalent oxides. More particularly, the glass compositions comprise a combination of silica, the monovalent oxide of lithium, two or more bivalent oxides one being beryllia and the others being selected from the group consisting of CaO, ZnO, MgO, and CuO, at least one trivalent oxide selected from the group consisting of Al_2O_3 , Y_2O_3 , La_2O_3 , B_2O_3 , Sm_2O_3 and mixed rare earth oxides (which average out as trivalent) and from 0-12 mol % of one or more tetravalent oxides selected from the group consisting of CeO_2 , ZrO_2 , and TiO_2 . It will be noted that the glasses are comprised of only one alkali oxide and a combination of alkaline earth oxides and trivalent and tetravalent oxides. Of course, the glass compositions may contain certain additional minor amounts of tetravalent or sesquivalent oxides of fluorides commonly employed in optical glass making such as tantalum pentoxide or tungsten trioxide.

The glass compositions described have been made the subject of patent applications filed by United Aircraft Corporation. Instruments of Waiver have been executed by the Administrator of the National Aeronautics and Space Administration for the inventions in appropriate cases.

NATIONAL AERONAUTICS AND SPACE ADMINISTRATION
WASHINGTON, D.C. 20546

OFFICIAL BUSINESS
PENALTY FOR PRIVATE USE \$300

FIRST CLASS MAIL

POSTAGE AND FEES PAID
NATIONAL AERONAUTICS AND
SPACE ADMINISTRATION



002 001 CI U 18 711124 S00942DS
DEPT OF THE ARMY
PICATINNY ARSENAL
PLASTICS TECHNICAL EVALUATION CENTER
ATTN: SMUPA-VP3
DOVER NJ 07801

POSTMASTER: If Undeliverable (Section 158
Postal Manual) Do Not Return

"The aeronautical and space activities of the United States shall be conducted so as to contribute . . . to the expansion of human knowledge of phenomena in the atmosphere and space. The Administration shall provide for the widest practicable and appropriate dissemination of information concerning its activities and the results thereof."

— NATIONAL AERONAUTICS AND SPACE ACT OF 1958

NASA SCIENTIFIC AND TECHNICAL PUBLICATIONS

TECHNICAL REPORTS: Scientific and technical information considered important, complete, and a lasting contribution to existing knowledge.

TECHNICAL NOTES: Information less broad in scope but nevertheless of importance as a contribution to existing knowledge.

TECHNICAL MEMORANDUMS: Information receiving limited distribution because of preliminary data, security classification, or other reasons.

CONTRACTOR REPORTS: Scientific and technical information generated under a NASA contract or grant and considered an important contribution to existing knowledge.

TECHNICAL TRANSLATIONS: Information published in a foreign language considered to merit NASA distribution in English.

SPECIAL PUBLICATIONS: Information derived from or of value to NASA activities. Publications include conference proceedings, monographs, data compilations, handbooks, sourcebooks, and special bibliographies.

TECHNOLOGY UTILIZATION PUBLICATIONS: Information on technology used by NASA that may be of particular interest in commercial and other non-aerospace applications. Publications include Tech Briefs, Technology Utilization Reports and Technology Surveys.

Details on the availability of these publications may be obtained from:

SCIENTIFIC AND TECHNICAL INFORMATION OFFICE

NATIONAL AERONAUTICS AND SPACE ADMINISTRATION

Washington, D.C. 20546